WETLAND BIOGEOCHEMISTRY: RESPONSE TO ENVIRONMENTAL CHANGE

EDITED BY: Fereidoun Rezanezhad, Bernd Lennartz and Colin McCarter
PUBLISHED IN: Frontiers in Environmental Science

frontiers Research Topics

frontiers

ISSN 1664-8714
ISBN 978-2-88963-845-1
DOI 10.3389/978-2-88963-845-1

About Frontiers

Frontiers is more than just an open-access publisher of scholarly articles: it is a pioneering approach to the world of academia, radically improving the way scholarly research is managed. The grand vision of Frontiers is a world where all people have an equal opportunity to seek, share and generate knowledge. Frontiers provides immediate and permanent online open access to all its publications, but this alone is not enough to realize our grand goals.

Frontiers Journal Series

The Frontiers Journal Series is a multi-tier and interdisciplinary set of open-access, online journals, promising a paradigm shift from the current review, selection and dissemination processes in academic publishing. All Frontiers journals are driven by researchers for researchers; therefore, they constitute a service to the scholarly community. At the same time, the Frontiers Journal Series operates on a revolutionary invention, the tiered publishing system, initially addressing specific communities of scholars, and gradually climbing up to broader public understanding, thus serving the interests of the lay society, too.

Dedication to Quality

Each Frontiers article is a landmark of the highest quality, thanks to genuinely collaborative interactions between authors and review editors, who include some of the world's best academicians. Research must be certified by peers before entering a stream of knowledge that may eventually reach the public - and shape society; therefore, Frontiers only applies the most rigorous and unbiased reviews.
Frontiers revolutionizes research publishing by freely delivering the most outstanding research, evaluated with no bias from both the academic and social point of view. By applying the most advanced information technologies, Frontiers is catapulting scholarly publishing into a new generation.

What are Frontiers Research Topics?

Frontiers Research Topics are very popular trademarks of the Frontiers Journals Series: they are collections of at least ten articles, all centered on a particular subject. With their unique mix of varied contributions from Original Research to Review Articles, Frontiers Research Topics unify the most influential researchers, the latest key findings and historical advances in a hot research area! Find out more on how to host your own Frontiers Research Topic or contribute to one as an author by contacting the Frontiers Editorial Office: researchtopics@frontiersin.org

WETLAND BIOGEOCHEMISTRY: RESPONSE TO ENVIRONMENTAL CHANGE

Topic Editors:
Fereidoun Rezanezhad, University of Waterloo, Canada
Bernd Lennartz, University of Rostock, Germany
Colin McCarter, University of Toronto Scarborough, Canada

Citation: Rezanezhad, F., Lennartz, B., McCarter, C., eds. (2020). Wetland Biogeochemistry: Response to Environmental Change. Lausanne: Frontiers Media SA. doi: 10.3389/978-2-88963-845-1

Table of Contents

frontiers in Environmental Science

EDITORIAL
published: 29 May 2020
doi: 10.3389/fenvs.2020.00055

Editorial: Wetland Biogeochemistry: Response to Environmental Change

Fereidoun Rezanezhad[1]*, *Colin P. R. McCarter*[2] *and Bernd Lennartz*[3]

[1] Ecohydrology Research Group, Water Institute and Department of Earth and Environmental Sciences, University of Waterloo, 200 University Avenue West, N2L 3G1, Waterloo, ON, Canada, [2] Department of Physical and Environmental Sciences, University of Toronto, Scarborough, ON, Canada, [3] Faculty of Agricultural and Environmental Sciences, University of Rostock, Justus-von-Liebig-Weg 6, 18059, Rostock, Germany

Keywords: wetlands, biogeochemical cycling, climate change, peatlands, hydrological processes

Editorial on the Research Topic

Wetland Biogeochemistry: Response to Environmental Change

Wetlands around the world are increasingly impacted by a shift in environmental conditions due to climate change, land use development, resource extraction, urbanization, and sea level rise, to name a few external pressures (Meng et al., 2016; Walpole and Davidson, 2018). These environmental changes can alter the hydrological regime, impacting the biogeochemical processes that govern important wetland ecosystem services, such as carbon sequestration and water storage. Biogeochemical processes in wetlands are highly dynamic (Reddy et al., 2010; Jackson et al., 2014) and involve complex interactions between hydrological processes, mineralogical transformations, bacterial and vegetation communities, and soil stores of carbon and nutrients (Cherry, 2011; U.S. EPA, 2015). Currently, our understanding of biogeochemical properties of wetlands are derived from mechanistic and statistical links between biological, geological, and chemical processes. However, how climatic and hydrological processes interact with wetland biogeochemical functions is still not well-understood.

Wetland ecosystems maintain a fragile balance between soil, water, plant, microbial, and atmospheric processes, which regulates water flow and water quality (Reddy and Delaune, 2008). Even minor gradients (naturally or anthropogenically induced) in hydrological and climatic parameters (e.g., wetting and drying, flooding, freezing, and thawing, groundwater-surface water interactions, etc.) can change the ecology and (bio)geochemistry of wetlands. These changes can have profound impacts on globally important processes, such as greenhouse gas emissions. Within a wetland, there is a high degree of spatial and temporal heterogeneity of chemical properties, temperature, and water-saturation that regulates the transport and transformation of carbon, nutrients, and redox-active elements (Reddy et al., 2010; Cherry, 2011; Jackson et al., 2014). The heterogeneity results in both spatial and temporal pulses of biogeochemical activity, primarily associated with aerobic or anaerobic microbial respiration. Thus, wetlands are considered "biogeochemical hotspots" in the landscape, with an enhanced cycling of nutrients, carbon and trace metals (Megonigal, 2008; Reddy et al., 2010; Cherry, 2011). Quantifying the variability in process intensity remains challenging but is, however, critical to unravel the linkages between forcing environmental boundary conditions and biogeochemical responses.

This Research Topic brings together wetland (bio)geochemists, hydrologists, biologists, ecologists, and soil scientists to share research in various areas of wetland biogeochemistry

OPEN ACCESS

Edited by:
Vera I. Slaveykova,
Université de Genève, Switzerland

Reviewed by:
Adrien Mestrot,
University of Bern, Switzerland

***Correspondence:**
Fereidoun Rezanezhad
frezanez@uwaterloo.ca

Specialty section:
This article was submitted to Biogeochemical Dynamics, a section of the journal Frontiers in Environmental Science

Received: *08 April 2020*
Accepted: *27 April 2020*
Published: *29 May 2020*

Citation:
Rezanezhad F, McCarter CPR and Lennartz B (2020) Editorial: Wetland Biogeochemistry: Response to Environmental Change. Front. Environ. Sci. 8:55. doi: 10.3389/fenvs.2020.00055

that addresses how current and future hydroclimatic conditions and land use change modulate (bio)geochemical processes in wetlands. The resultant collection of papers covers a broad snapshot of our understanding of how biogeochemical transformations and the movement of water in wetlands impacts the concentration and mobility of nutrients and contaminants, microbial community dynamics, greenhouse gas emissions, carbon cycling, and sequestration. The studies cover a range of freshwater wetland classifications (i.e., marsh, peatland, etc.) in natural, disturbed, and restored environments. The assembled papers provide important new information that addresses critical knowledge gaps on how wetland biogeochemistry is impacted by environmental change.

The impact of environmental change on vegetation and subsequent impacts on biogeochemical cycling are apparent and several papers in this Research Topic showcase the interconnected nature of wetland biogeochemistry, ecology, and carbon cycling. Yuckin and Rooney quantified the effect of Phragmites *australis* invasion on carbon and macronutrient standing stocks in a freshwater coastal marsh, highlighting that plant invasions may create trade-offs between ecosystem processes. Yavitt et al. examined the importance of leaf litter in carbon cycling in peatlands and why vegetation, plant species composition, and peatland type must be determined to put peatland ecosystems into the context of global carbon budgets. Turner et al. demonstrated how wind sheltering influences land-atmosphere fluxes of carbon in wetlands and plays an important role on wetland ecosystem characteristics and energy balance. Koop-Jakobsen and Gutbrod observed distinctive spatio-temporal oxygen dynamics in an open tidal marsh that differs from the surrounding shaded vegetated marsh. The authors highlight the role of vascular plant canopies for biogeochemical processes in wetlands. It is evident from these papers that the feedbacks between vegetation and biogeochemical processes in wetlands provide an important mechanism that regulates essential ecosystem services.

Several authors highlighted the complex controls and interactions between microbiological communities, biogeochemical processes, and hydrological setting. In coastal peatlands, Gosch et al. assessed the change in the decomposition of organic matter and releasing organic and inorganic solutes from peat under seawater intrusion. While in inland peatlands, Negassa et al. discussed the lack of empirical data on the high variability of chemical and biochemical properties in rewetted peatlands. Zak et al. examined if long-term peat mineralization during decades of drainage in minerotrophic fens causes an enrichment or a decline of enzyme-inhibiting polyphenols. While, Alshehri et al. evaluated the potential of adding phenolic compounds to peatland soils to inhibit extracellular enzyme activities in order to reduce the flux of CO_2 from peatlands; the authors recommend phenolic enrichment as a potential peatland restoration strategy. Limpert et al. examined the CO_2 and CH_4 emissions and microbial community diversity during a wetland rehabilitation process (rewetting) and observed a clear succession of microbial communities during the dry-wet phases, suggesting that wetland hydrology plays a significant role in the microbial community structure. All of the publications in this Research Topic elucidate strong linkages between the hydro-physical setting and biogeochemical processes and recognized that understanding the feedbacks associated with these linkages requires further studies.

With 42 authors from six countries in Europe, North America, and Australia/Oceania this Research Topic identifies key priorities for future research in wetlands biogeochemical transformation and processes. This Research Topic highlights the need for a more detailed understanding of interactions between and cycling of carbon, oxygen, nitrogen, phosphorus, and sulfur. The authors emphasize the role of redox-pH conditions, organic matter, microbial-mediated processes that drive nutrient and carbon transformations in wetlands, plant responses, and adaptation to wetland soil conditions. Importantly, the contributions emphasize the need for more integrated research efforts into the physical, hydrological and climatic processes that regulate wetland biogeochemical processes. The further development of interdisciplinary linkages is considered essential for a process-based understanding of wetland functions and the successful restoration and management of wetland ecosystems.

AUTHOR CONTRIBUTIONS

All authors listed have made a substantial, direct and intellectual contribution to the work, and approved it for publication.

ACKNOWLEDGMENTS

FR acknowledged funding supports from the Canada Excellence Research Chair program in Ecohydrology and the Global Water Futures funded by the Canada First Excellence Research Fund. CM acknowledged funding provided by the Natural Sciences and Engineering Research Council of Canada Postdoctoral Fellowship. BL is grateful for the support by the Research Training Group Baltic TRANSCOAST program, funded by the DFG under grant number DFG-GRK 2000/1, and the WETSCAPES project (ESF/14-BM-A55-0028/16).

REFERENCES

Cherry, J. A. (2011). Ecology of wetland ecosystems: water, substrate, and life. *Nat. Educ. Knowl.* 3:16.

Jackson, C. R., Thompson, J. A., and Kolka, R. K. (2014). "Wetland soils, hydrology and geomorphology, Chapter 2," in *Ecology of Freshwater and Estuarine Wetlands*, eds D. Batzer and R. Sharitz (Berkeley: University of California Press), 23–60.

Megonigal, J. P. (2008). Frontiers in wetland biogeochemistry. *Arch. Agron. Soil Sci.* 54, 237–238.

Meng, L., Roulet, N., Zhuang, Q., Christensen, T. R., and Frolking, S. (2016). Focus on the impact of climate change on wetland ecosystems and carbon dynamics. *Environ. Res. Lett.* 11:100201. doi: 10.1088/1748-9326/11/10/100201

Reddy, K. R., DeLaune, R., and Craft, C. B. (2010). Nutrients in wetlands: implications to water quality under changing climatic conditions. *Final Report*

submitted to U. S. Environmental Protection Agency. EPA Contract No. EP-C-09-001.

Reddy, K. R., and Delaune, R. D. (2008). *Biogeochemistry of Wetlands: Science and Applications*. Boca Raton, FL: CRC Press.

U.S. EPA. (2015). *Connectivity Of Streams And Wetlands To Downstream Waters: A Review And Synthesis Of The Scientific Evidence (Final Report)*. (Washington, DC: U.S. Environmental Protection Agency), EPA/600/R-14/475F.

Walpole, M., and Davidson, N. (2018). Stop draining the swamp: it's time to tackle wetland loss. *Oryx* 52, 595–596.

Conflict of Interest: The authors declare that the research was conducted in the absence of any commercial or financial relationships that could be construed as a potential conflict of interest.

frontiers in Environmental Science

ORIGINAL RESEARCH
published: 11 July 2019
doi: 10.3389/fenvs.2019.00112

Significant Increase in Nutrient Stocks Following *Phragmites australis* Invasion of Freshwater Meadow Marsh but Not of Cattail Marsh

*Sarah Yuckin and Rebecca Rooney**

Department of Biology, University of Waterloo, Waterloo, ON, Canada

Invasive species are a threat to biodiversity and can cause ecological degradation, however, well-established invasive species may serve valuable ecological functions. For example, in the Laurentian Great Lakes, where nutrient pollution is a major issue, highly productive *Phragmites australis* (European Common Reed) may provide a nutrient retention service. Yet there is a lack of research comparing carbon and macronutrient stocks in *P. australis* with resident plant communities, such as cattail and meadow marsh. We quantified the effect of *P. australis* invasion on carbon and macronutrient standing stocks in a freshwater coastal marsh by comparing the above- and belowground biomass, tissue nutrient concentrations, and annual nutrient standing stocks in marsh invaded by *P. australis* with cattail marsh (dominated by *Typha* spp.) and meadow marsh (dominated by *Calamagrostis canadensis*), which are being displaced by *P. australis* in Lake Erie coastal marsh. We conclude that the effect of *P. australis* invasion on carbon and macronutrient standing stocks is dependent on the plant community being replaced. The annual standing stock of carbon, nitrogen, phosphorus, and potassium are consistent between cattail marsh and *P. australis*-invaded marsh, though cattail marsh contains more magnesium (112% mean increase) and calcium (364% mean increase). In contrast, when *P. australis* replaces meadow marsh, the standing stocks of all measured nutrients and carbon increase significantly (103–188% mean increase). Our study highlights that plant invasions may create trade-offs between ecosystem services. In our case, the increase in nutrient standing stocks when *P. australis* invades meadow marsh should be weighed against the documented reductions in biodiversity and habitat value.

Keywords: Canada bluejoint, cattail marsh, common reed, exotic species, invasive species, meadow marsh, nutrient retention, nutrient stocks

OPEN ACCESS

Edited by:
Colin McCarter, University of Toronto Scarborough, Canada

Reviewed by:
Md Nazim Uddin, Saitama University, Japan
Peng Lin, Texas A&M University at Galveston, United States

****Correspondence:***
Rebecca Rooney
rrooney@uwaterloo.ca

Specialty section:
This article was submitted to Biogeochemical Dynamics, a section of the journal Frontiers in Environmental Science

Received: *12 March 2019*
Accepted: *26 June 2019*
Published: *11 July 2019*

Citation:
Yuckin S and Rooney R (2019) Significant Increase in Nutrient Stocks Following Phragmites australis Invasion of Freshwater Meadow Marsh but Not of Cattail Marsh. Front. Environ. Sci. 7:112. doi: 10.3389/fenvs.2019.00112

INTRODUCTION

Invasive species are considered a major threat to biodiversity and a driver of ecological degradation (Zedler and Kercher, 2005; Simberloff, 2011). Recent research, however, has found evidence that invasive species can provide ecological functions equal to or greater than those provided by native species (Norkko et al., 2012; Bertness and Coverdale, 2013; Grutters et al., 2015) and may even lead

to increased local and regional biodiversity (Sax and Gaines, 2003). Recognition of the potential for invasive species to provide ecological functions has led to debate about whether conservation objectives should include the eradication of all invasive species (Schlaepfer et al., 2011, 2012; Vitule et al., 2012). It has been proposed that the decision to control invasive species should be made on a case-by-case basis through evaluation of the impact of a given invasive species on ecological function (Hershner and Havens, 2008; Hobbs et al., 2009; Davis et al., 2011).

Throughout North America, the invasive lineage of *Phragmites australis* (hereafter *P. australis*) is increasing in abundance and distribution (Catling and Mitrow, 2011). For example, in Lake Erie coastal marsh, *P. australis* took advantage of historically low lake levels during the 1990s (Tulbure et al., 2007; Tulbure and Johnston, 2010) and increased nutrient loading in the watershed (Croft and Chow-Fraser, 2007) to rapidly expand, primarily replacing cattail marsh (dominated by *Typha* spp.) and rare "Graminoid Coastal Meadow Marsh" (Imperiled [S2]; Ministry of Natural Resources Forestry, 2018; dominated by *Calamagrostis canadensis*) (Wilcox et al., 2003). These resident plant communities are naturally stratified by water depth with cattail marsh in deeper water (11–52 cm) and meadow marsh in shallower water (0–27 cm; **Supplementary Materials 1**), indicating the relatively broader niche of invasive *P. australis*.

Phragmites australis forms dense monocultures that replace resident plant communities (Keller, 2000; Mal and Narine, 2004; Tulbure et al., 2007) and can negatively affect wetland birds (Robichaud and Rooney, 2017), amphibians (Greenberg and Green, 2013), and turtles (Bolton and Brooks, 2010; Markle et al., 2018). The stem density of *P. australis* typically increases with age (Rooth et al., 2003), and while these negative effects on wildlife are reported from dense, established *P. australis* stands (e.g., 100 live stems m^{-2}), some research suggests that at lower densities *P. australis* can provide habitat value (Meyer et al., 2010; Kiviat, 2013).

There is also evidence that *P. australis* invasion may affect nutrient and carbon cycling (Rothman and Bouchard, 2007; Windham and Ehrenfeld, 2013) as a result of high net primary production (Windham, 2001; Rothman and Bouchard, 2007; Duke et al., 2015), high rates of carbon assimilation (Farnsworth and Meyerson, 2003; Tho et al., 2016) and high nitrogen content in its foliar tissues (Findlay et al., 2002; Hirtreiter and Potts, 2012). Indeed, in its native range, *P. australis* is often used in constructed wetlands to remove nutrient pollution (Gumbricht, 1993; Bhatia and Goyal, 2014), suggesting it could provide an important water quality improvement function where it has invaded. Yet, despite the importance of carbon and macronutrients phosphorus, potassium, calcium, and magnesium (Ehrenfeld, 2010), research on *P. australis* invasion and its effects on nutrient stocks in freshwater coastal marsh has primarily focused on nitrogen (but see Findlay et al., 2002; Ouellet-Plamondon et al., 2004). In addition, prior work has focused on differences between *Typha* spp. and *P. australis* (e.g., Findlay et al., 2002; Farnsworth and Meyerson, 2003; Hirtreiter and Potts, 2012), ignoring critically imperiled meadow marsh, which differs markedly in vegetation diversity and physical structure from stands of *P. australis* and *Typha* spp.

Given that climate change and eutrophication are two immense environmental threats facing Lake Erie (Watson et al., 2016; Environment and Climate Change Canada and the U.S. Environmental Protection Agency, 2017; Jarvie et al., 2017) the capacity of a marsh plant, regardless of its origin, to take up and store carbon and macronutrients represents a critically important ecosystem function. With the limited success (Lombard et al., 2012; Quirion et al., 2018) and high costs (Martin and Blossey, 2013) of *P. australis* control in North America, quantifying the ecosystem functions provided by *P. australis* should inform decision makers considering whether to attempt its eradication.

We therefore sought to evaluate the influence of *P. australis* invasion on carbon and macronutrient standing stocks, including nitrogen, phosphorus, calcium, magnesium, and potassium. Further, we aimed to contrast this effect in areas where *P. australis* is displacing cattail marsh with areas where meadow marsh is being displaced. Thus, we compared standing crop above- and belowground biomass, tissue nutrient concentrations, and annual nutrient standing stocks in marsh invaded by *P. australis* with marsh dominated by *Typha* spp. or by *C. canadensis* (Canadian bluejoint grass). Because wetland plants can carry out luxury consumption of nutrients (Gumbricht, 1993 and references therein), we contrasted the three vegetation communities in two adjacent marshes, one with higher soil nutrients than the other. Because emergent vegetation may allocate more resources to aboveground biomass in deeper water (Wetzel and van der Valk, 2005; Duke et al., 2015), we also evaluated sites spanning a range in water depth. We hypothesized that, due to the high net primary production, foliar chlorophyll and nitrogen content of *P. australis* (Windham, 2001; Rothman and Bouchard, 2007; Duke et al., 2015), invaded areas would support higher carbon and nutrient standing stocks and tissue carbon and nutrient concentrations (Findlay et al., 2002; Hirtreiter and Potts, 2012). We also hypothesized that tissue concentrations and standing crop biomass would be greater in areas with more plentiful soil nutrients. Lastly, we hypothesized that standing crop biomass would be greater in deeper water.

METHODS

Study Area

We conducted the study in freshwater coastal marshes within the Long Point peninsula (42° 34′ N, 80° 24′ W), a 35 km long sandspit formation located on the north shore of Lake Erie, Ontario. We sampled in the Big Creek National Wildlife Area and Long Point Provincial Park management units (**Figure 1**). The Long Point peninsula constitutes more than 70% of the remaining intact coastal marsh on the north shore of Lake Erie (Ball et al., 2003) and is designated as a Ramsar wetland and an UNESCO World Biosphere Reserve. Over the past 30 years, resident coastal marsh communities in this area have been increasingly replaced by invasive *P. australis* (Wilcox et al., 2003; Jung et al., 2017).

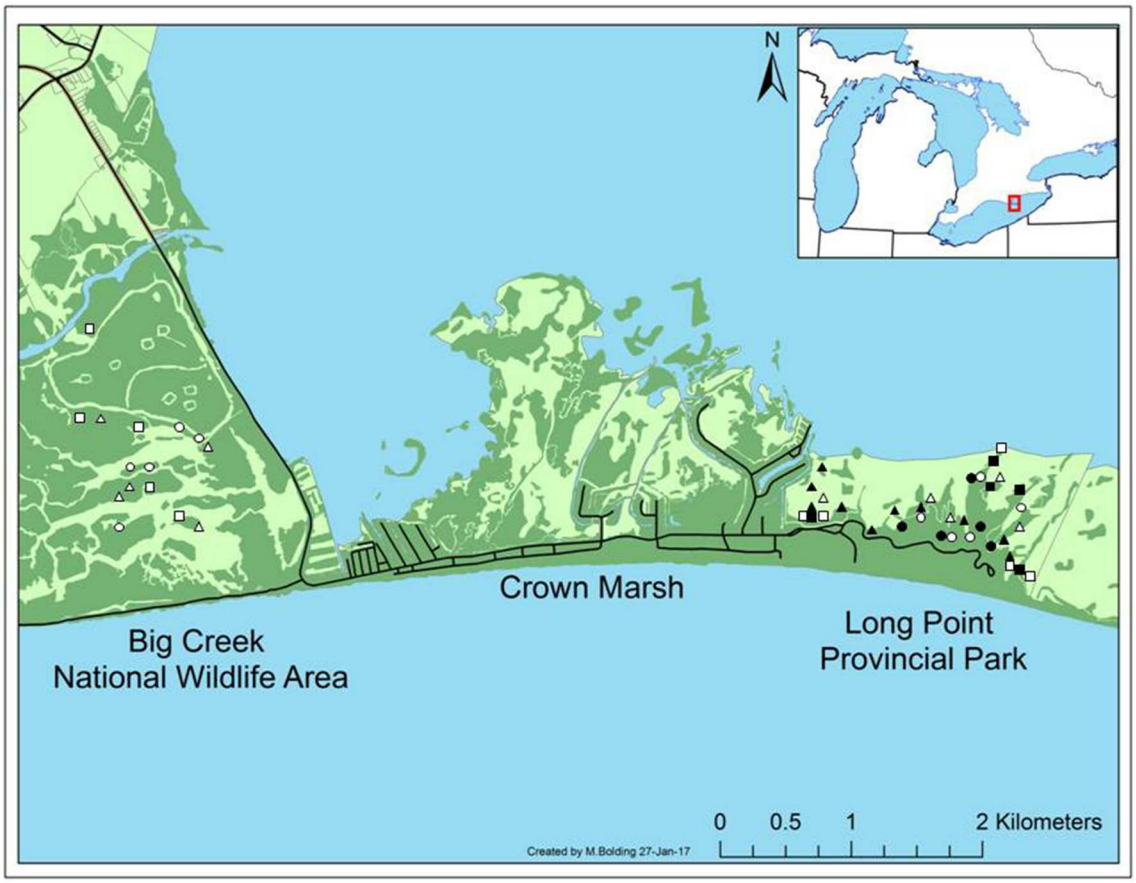

FIGURE 1 | Study location in the Big Creek National Wildlife Area (42° 35′ N, 80° 27′ W) and Long Point Provincial Park (42° 34′ N, 80° 22′ W) management units of the Long Point peninsula. Circles are meadow marsh sites, squares are cattail marsh sites, and triangles are *P. australis*-invaded sites. Black symbols were sampled in 2017, white symbols were sampled in 2016.

Experimental Design

In 2016, we evaluated the influence of soil nutrient conditions by comparing carbon and macronutrient pools and tissue concentrations among three vegetation community types (*P. australis*-invaded marsh, cattail marsh and meadow marsh) between two regions of the Long Point peninsula that have differing soil nutrient levels (**Table 1**, **Supplementary Materials 1**). In this experiment, we measured nutrient concentrations in plant tissues, as well as above and belowground biomass from 15 sites in the Big Creek National Wildlife Area (higher nutrient environment) and 15 sites in the Long Point Provincial Park (lower nutrient environment; **Figure 1**). The Big Creek National Wildlife Area is located in a drainage basin that is 71.1% agricultural land cover (Essex Region Conservation Authority, 2013) and receives substantial amounts of phosphorus and nitrate from the Big Creek tributary; phosphorus levels within the marsh were above the Provincial Water Quality Objectives (>0.03 mg/L) although nitrate levels were below the Canadian Environmental Quality Guidelines (<2.93 mg/L; Essex Region Conservation Authority, 2013). In contrast, Long Point Provincial Park, which is approximately four kilometers away, is located on nutrient poor sand substrate. Regardless of vegetation community type, sites in the Big Creek National Wildlife Area consisted of taller, lower diversity plant communities growing in deeper water than sites in the Long Point Provincial Park (**Table 1**).

In 2017, we evaluated the influence of water depth by comparing carbon and macronutrient pools and tissue concentrations among the same three vegetation community types spanning a gradient in lake water depth. In this experiment, we measured plant tissue levels and plant biomass in 20 sites in the Long Point Provincial Park (10 *P. australis*-invaded sites and 10 uninvaded sites: 5 shallower meadow marsh sites and 5 deeper cattail marsh sites). The invaded and uninvaded sites were selected to be paired by May water depth to span a common gradient (14–56 cm). Note we also measured water depth at each site in July because seasonal water depth changes could differ among vegetation community types.

In both experiments, we selected a focal species to represent each community to characterize nutrient stocks in the three vegetation community types. These focal species were *P. australis*, *C. canadensis*, and *Typha* spp. for the *P. australis*-invaded,

TABLE 1 | Average site characteristics of meadow, cattail, and *P. australis*-invaded marsh, based on measurements from three quadrats per site.

Site characteristic	Plant community type	#Sites	July water depth (cm)	Canopy height (cm)	Living (stems/m^2)	Living (% cover)	Species richness
2016 Big Creek National Wildlife Area	Meadow	5	20.5 (±6.0)	178 (±13)	837 (±165)	81 (±8)	3.2 (±5.7)
	Cattail	5	15.5 (±3.0)	276 (±30)	47 (±6)	74 (±10)	3.0 (±2.1)
	P. australis	5	20.5 (±2.0)	409 (±29)	59 (±18)	81 (±6)	2.6 (±2.2)
2016 Long Point Provincial Park	Meadow	5	2.5 (±3.5)	101 (±16)	802 (±284)	65 (±3)	14.4 (±1.1)
	Cattail	5	14.5 (±3.5)	265 (±7)	71 (±45)	70 (±7)	3.4 (±1.0)
	P. australis	5	15.5 (±9.0)	319 (±27)	125 (±53)	78 (±7)	5.8 (±1.8)
2017 Long Point Provincial Park	Meadow	5	17.5 (±7.0)	102 (±26)	776 (±160)	59 (±14)	11.4 (±4.4)
	Cattail	5	41.0 (±8.5)	266 (±14)	83 (±66)	63 (±9)	3.0 (±1.9)
	P. australis	10	36.0 (±10.5)	350 (±48)	91 (±48)	80 (±9)	3.7 (±2.5)

Sites sampled in 2016 contrasted a higher (Big Creek National Wildlife Area) and lower nutrient environment (Long Point Provincial Park). Sites sampled in 2017 captured a water depth gradient in the lower nutrient environment. Standard deviation in brackets.

meadow marsh and cattail marsh communities, respectively. This approach is justified by the low evenness of these communities, wherein 50% or more of total plant cover comes from the selected focal species (**Figure 2**). Notably, evenness in meadow marsh in the Big Creek National Wildlife Area was lower than in meadow marsh from the Long Point Provincial Park, with the *C. canadensis* comprising 80% or more of total plant cover in Big Creek vs. 59–65% in Long Point (**Table 1**).

Typha latifolia, *Typha angustifolia*, and *Typha* × *glauca* are known to occur in the Long Point area (Freeland et al., 2013), but due to hybridization and extensive back-crossing with parental species, they are not reliably separable in the field (Kirk et al., 2011). Based on morphological characteristics and growth form (Swearingen et al., 2012), we determined that the *P. australis* in our study was all the non-native European lineage rather than the native North American lineage. This assessment was supported by prior genetics work in our study area, which concluded that 90% of the *P. australis* stands tested were the non-native lineage (Wilcox et al., 2003).

Measuring Biomass and Leaf:Shoot Mass Ratios

To standardize the vegetation sampling time, we sampled above and belowground biomass during the period of peak seasonal aboveground biomass. Because this can vary year to year, we established the timing of peak aboveground biomass in 2016 and 2017 independently. To determine the timing of peak aboveground biomass we clipped all live rametes from three replicate 0.25 m^2 quadrats in meadow, cattail and *P. australis*-invaded sites every 10 days during the growing season. Clipped tissues were air dried for 48 h and then weighed. Biomass plateaued around 16 August in 2016 and 22 July in 2017. At this time, we carried out extensive sampling of aboveground and belowground standing crop biomass.

Because all three focal species are rhizomatous perennials, we employed a modified soil ingrowth method (Neill, 1992) to restrict belowground biomass collection to the current season's growth. We removed soil cores (11.3 cm deep by 4.8 cm diameter) and replaced them with an artificial growth medium at each sampling location (**Figure 1**). This depth was selected to capture the peak rooting depth for each of the vegetation communities, though it likely did not capture all root and rhizome growth. Belowground biomass measurements in our study thus reflect the annual belowground biomass production within the upper 11.3 cm of soil.

In 2016, to compare the higher (Big Creek) and lower (Long Point Provincial Park) nutrient environments, we installed 5 replicate cores made of a mixture of sand and peat in early May at each site and retrieved them during peak aboveground biomass (August 16–19) for a 91–99 day incubation period. We then removed all roots, rhizomes, and shoots (live and dead) from the cores and oven dried them at 100°C for 48 h before weighing them to the nearest 0.01 g (Advanced Balance PB602-S, Mettler Toledo, ON, Canada).

In 2017 to evaluate the influence of water depth, we installed 7 replicate cores made of vermiculite at each sample site in Long Point Provincial Park, and then retrieved them during peak aboveground biomass (July 22–25) for a 60–65 day incubation period. This shorter incubation period was due to earlier onset of peak aboveground biomass in 2017. As in 2016, we removed, dried and weighed all roots, rhizomes, and shoots from the cores, but due to oven availability, the drying temperature in 2017 was reduced to 80°C. Though the 2 years were not directly compared, we note that the differences in incubation period and drying oven temperature did not result in a significant difference in belowground biomass when we compared Long Point Provincial Park samples collected in 2016 with those from 2017 (**Tables S2a,b**).

We measured the aboveground biomass from each vegetation community type following the same schedule as ingrowth core retrieval. At each site (**Figure 1**), we randomly deployed three 0.25 m^2 quadrats and harvested all aboveground living tissues by clipping vegetation just above the sediment (including all plant species in a quadrat, not simply the focal species). We then dried

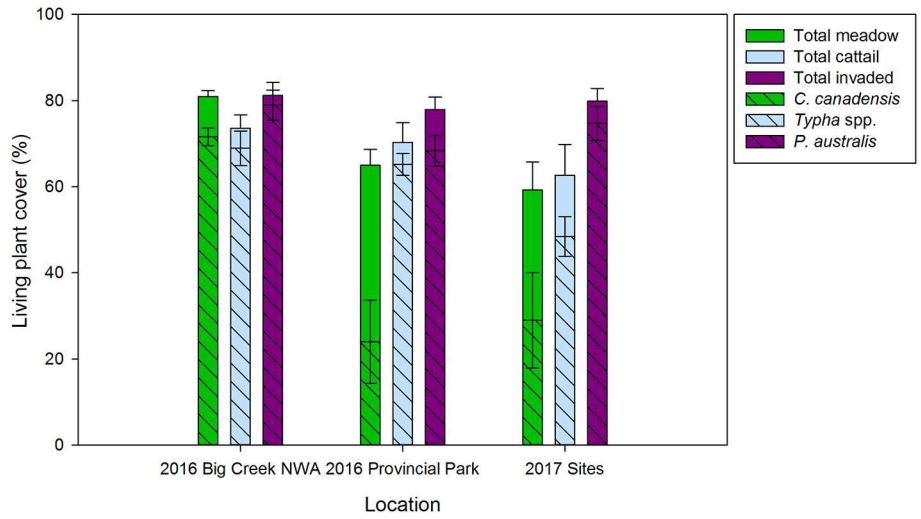

FIGURE 2 | Comparison of mean total living plant cover and mean cover of the dominant focal species (*C. canadensis*, *Typha* spp., and *P. australis*, in meadow marsh, cattail marsh, and *P. australis* invaded marsh, respectively) in a higher nutrient (Big Creek) and lower nutrient (Long Point) environment. Bars from July 2016 average across five sites per nutrient environment, whereas sampling in 2017 in the Long Point Provincial Park covered a common gradient in water depth between resident communities [meadow ($n = 5$) and cattail ($n = 5$)] and *P. australis* invaded marsh ($n = 10$). Standard error bars shown.

and weighed all aboveground tissues following the same protocol as for belowground tissues.

In addition, in 2017, we determined the mass ratio of leaf tissues to stem tissues for the focal species at each sample site. Deploying a fourth 0.25 m^2 quadrat randomly at each site, we harvested all the *P. australis* rametes from *P. australis* invaded sites, the *Typha* spp. rametes from cattail marsh sites, and the *C. canadensis* rametes from meadow marsh sites. We then separated the leaf and shoot tissues and dried these for 48 h at 80°C before weighing them to the nearest 0.01 g (Advanced Balance PB602-S, Mettler Toledo, ON, Canada). From the resulting data, we calculated the average leaf to stem mass ratio for each focal species.

Plant and Soil Nutrients

In August 2017, we revisited the 2016 sample sites that had the highest, median, and lowest total biomass from each plant community in Big Creek and Long Point ($n = 18$) and collected soil samples using a 11.3 cm deep corer. We dried the samples at 35°C for 1 week, and then sieved samples through a 2 mm screen to remove roots. We sent the sieved soil samples to the Agriculture and Food analytical services laboratory at the University of Guelph for determination of total nitrogen, total carbon, and plant available phosphorus, potassium, magnesium and calcium. Total nitrogen and carbon were measured using thermal conductivity detection, plant available phosphorus was extracted using sodium bicarbonate (Reid, 1998), and the other nutrients were extracted using ammonium acetate prior to measurement with mass spectrometry (Simard, 1993; Agriculture and Food Laboratory University of Guelph, 2017).

In July 2016, during peak aboveground biomass, we collected leaf, stem, and below ground tissues from our focal species in ten sites from each of the meadow marsh, cattail marsh, and *P. australis*-invaded marsh communities in Big Creek and Long Point Provincial Park. We oven-dried the tissues at 100°C for 48 h, homogenized and then submitted them to the Agriculture and Food Laboratory at the University of Guelph for measurement of total nitrogen and carbon (% dry weight), using thermal conductivity detection (Reid, 1998) and total phosphorus, potassium, magnesium and calcium (% dry weight), using mass spectrometry.

Nutrient Standing Stocks

Using the carbon and macronutrient concentrations for different tissue types, we estimated annual nutrient standing stocks (in g m^{-2}) characteristic of the *P. australis*-invaded, cattail, and meadow marsh community types. To achieve this, we multiplied tissue nutrient concentrations (% dry weight) by the above and belowground biomass weights of the total community (g m^{-2} dry weight) and the leaf: stem and root: shoot mass ratios for the focal species. Note that this approach assumes all the plant biomass in a community has the same tissue nutrient levels and tissue mass ratios as the focal species. The validity of this assumption is greater for cattail marsh and *P. australis*-invaded marsh than for meadow marsh in Long Point Provincial Park (**Figure 2**). As a sensitivity analysis, we also estimated nutrient standing stocks (g m^{-2}) of only the focal species in their respective communities, excluding biomass attributable to other co-occurring species. Based on this comparison, the assumption that all biomass in our samples came from the focal species did not sway our conclusions.

Statistical Analysis

To test for differences in aboveground biomass, belowground biomass, total biomass, and root: shoot mass ratios among *P. australis*-invaded, emergent cattail and meadow marsh habitats,

we used general linear models. All the model forms we tested are defined in **Table 2**. To meet normality assumptions, we square-root transformed belowground biomass (g m^{-2}) and root: shoot ratio, and log-transformed magnesium (g m^{-2}) and calcium (g m^{-2}). All general linear models were calculated using the "lm" function from the "stats" package (R Core Team, 2016). Even if interaction terms were non-significant, we retained them in our final models if the model itself had a good fit. To determine the best fit for the 2017 biomass response variable, we used the "AICc" function in the "MuMIn" package (Barton, 2018). Significant differences in response variable among treatments were determined at $p < 0.05$, and we performed all statistical tests using R Studio (R Core Team, 2016). We interpreted the model fit to be strong at the arbitrary threshold where $R^2 \geq 0.6$.

To test for the effect of soil nutrient availability on any differences in these response variables among vegetation community types, we used the 2016 samples to cross vegetation community type with soil nutrient level, comparing the high nutrient (Big Creek NWA) and low nutrient (Long Point Provincial Park) environments and included their interaction (**Table 3**).

To test for an effect of water depth on any differences in these response variables among vegetation community types, we used the 2017 samples from Long Point Provincial Park to include water depth as a covariate (**Table 4**). Because the water depths measured at each site in May differed from the July measurements, we tested general linear models for each response variable using both measurement dates and selected the measurement date generating the lowest Akaike's Information Criterion (corrected for small sample size) as our final model.

Next, we used a general linear model to test whether soil nutrients differed significantly between the Big Creek NWA and the Long Point Provincial Park, combining the three vegetation community types (**Table 2**). We also used general linear models to test whether differences in nutrient concentrations (% dry weight) among focal species (*P. australis*, *Typha* spp., and *C. canadensis*), plant tissue types (leaf, stem, and belowground tissue), and their interaction were significant (**Table 2**). Similarly, we used general linear models to test whether nutrient standing stocks (g m^{-2}) differed among vegetation communities (meadow, cattail, and *P. australis*-invaded; **Table 2**).

TABLE 2 | General linear model fit tests for 2016 and 2017 biomass response variables (g m^{-2} aboveground, belowground, total biomass, root: shoot), soil nutrient concentration (total carbon, total nitrogen and plant available phosphorus, potassium, magnesium, and calcium), tissue carbon and macronutrient concentrations (% dry weight of carbon, nitrogen, phosphorus, potassium, magnesium, and calcium), and carbon and macronutrient standing stock (g m^{-2} of carbon, nitrogen, phosphorus, potassium, magnesium, and calcium).

Response variable	Model
2016 Biomass	y = β0 + β1 plant community + β2 nutrient environment + β3 (plant community * nutrient environment)
2017 Biomass	y = β0 + β1 plant community + β2 water depth gradient + β3 (plant community * water depth gradient).
Soil nutrient concentration	y = β0 + β1 plant community + β2 nutrient environment + β3 (plant community * nutrient environment)
Tissue nutrient concentration	y = β0 + β1 plant species+ β2 tissue type + β3 (plant species * tissue type)
Nutrient standing stock	y = β0 + β1 plant community

Plant community type refers to meadow, cattail and P. australis-invaded marsh. Nutrient environment refers to high nutrient (Big Creek National Wildlife Area) or low nutrient (Long Point Provincial Park). Plant species refers to C. canadensis, Typha spp., or P. australis. Tissue type refers to belowground, stems, or leaves.

RESULTS

Biomass

The models predicting biomass measurements based on plant community (meadow, cattail and *P. australis*-invaded), nutrient environment (low and high) and their interaction provided a statistically significant fit (**Table 3**). There was no significant interaction between the effect of nutrient environment and plant community on any biomass response variable (**Supplementary Materials 2**). The higher nutrient environment produced significantly greater aboveground

TABLE 3 | Results of general linear model fit tests for the response variables aboveground, belowground, and total live biomass, as well as root:shoot ratio.

Response variable	*F*-test (d.f.)	*p*-value	R^2
Aboveground biomass	23.340 (5, 24)	< 0.001	0.829
SQRT (Belowground biomass)	4.252 (5, 24)	0.007	0.470
Total live biomass	15.200 (5, 24)	< 0.001	0.760
SQRT (Root:shoot)	6.017 (5, 24)	0.001	0.556

*The general model form is $y = \beta_0 + \beta_1$ plant community + β_2 nutrient environment + β_3 (plant community *nutrient environment), wherein plant community refers to meadow marsh (n = 10), emergent cattail (n = 10) or P. australis-invaded marsh (n = 10), and nutrient environment refers to the Big Creek National Wildlife Area (higher nutrients) or the Long Point Provincial Park (lower nutrients). Belowground biomass and root to shoot ratio were square-root transformed to meet the assumption of normality (see **Supplementary Materials 2** for more details).*

TABLE 4 | Results of general linear model fit tests for biomass response variables, as predicted by $y = \beta_0 + \beta_1$ plant community + β_2 water depth gradient + β_3 (plant community * water depth gradient).

Response variable	Water measurement	*F*-test (d.f.)	*p*-value	R^2
Aboveground biomass	July	5.250 (5, 14)	0.006	0.652
SQRT (Belowground biomass)	May	10.080 (5, 14)	< 0.001	0.783
Total live biomass	July	5.770 (5, 14)	0.004	0.673
SQRT (Root:shoot)	May	4.190 (5, 14)	0.015	0.599

*Plant community refers to meadow marsh (n = 5), emergent cattail (n = 5), or P. australis-invaded marsh (n = 10). Water depth measurement date (May or July 2017) was determined from the glm producing the lower AICc value (**Supplementary Materials 2**). Belowground biomass and root: shoot were square root transformed to meet the assumption of normality. See **Supplementary Materials 2** for detailed results and AICc values.*

and total biomass, though nutrient environment evidenced no significant effect on belowground biomass or root:shoot ratio (**Tables S2a–f**). Regardless of the nutrient environment, aboveground and total biomass were greatest in *P. australis*-invaded communities, intermediate in cattail marsh, and lowest in meadow marsh (**Figure 3**). Differences in belowground biomass and root:shoot ratio among plant communities were not statistically significant (**Tables S2d,f**), though cattail marsh produced more belowground biomass on average than the other two communities (**Figure 3**).

The models predicting biomass response variables based on plant community type (meadow, cattail and *P. australis* invaded), water depth, and their interaction all provided a reasonable fit with $R^2 \geq 0.6$ (**Table 4**). Interestingly, both aboveground and total biomass were best predicted by July 2017 water depth measurements, tending to increase with water depth, whereas the model fit for belowground biomass and root:shoot ratio was best using May 2017 water depths (**Tables S2g–n**). Both belowground biomass and root:shoot ratio evidenced a significant interaction effect for cattail marsh (**Tables S2i–j,m,n**). In water depths above 40 cm, cattail had significantly greater belowground biomass than *P. australis* invaded sites (**Figure S3a**), while meadow sites had the lowest belowground biomass at all water depths. Similarly, the root:shoot ratio of cattail sites was greater than the root:shoot of *P. australis* invaded sites at water depths >40 cm.

Given that *P. australis* invaded and resident plant community plots established in May 2017 were intentionally paired by water depth, it is not surprising that average May water depths were similar (36 cm ± 12 SD in *P. australis*-invaded, 37 cm ± 11 SD in resident plant communities; **Figure S1a**). Yet, when remeasured in July 2017, the average water depth of resident plant community sites had decreased to an average 29 cm (± 14 SD), whereas the average water depth for *P. australis*-invaded sites was unchanged from May values (36 cm ± 11 SD in July; **Table S1a**; **Figure S1a**).

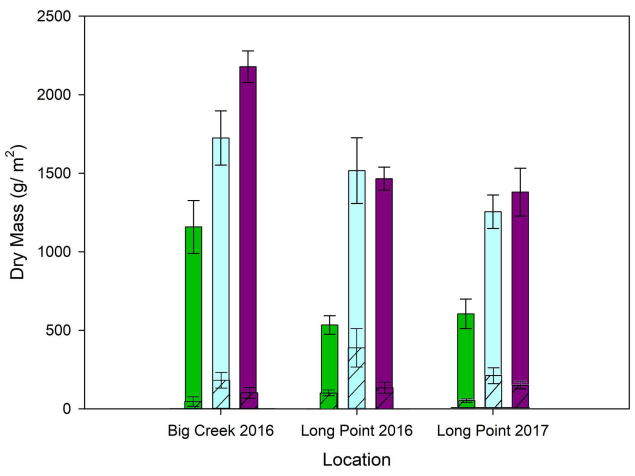

FIGURE 3 | Stacked bar graph indicating annual production as total live biomass, partitioned into aboveground (solid bars) and belowground (stripped bars) components. Bars contrast meadow marsh (green), cattail (blue) and *P. australis*-invaded plant communities (purple) in a higher nutrient (Big Creek NWA 2016) and lower nutrient (Long Point Provincial Park 2016) environment. Bars from Long Point Provincial Park 2017 average across a water depth gradient (14–56 cm water depth). Standard error bars shown. Note that belowground biomass is one growing season's production within the upper 11.3 cm of soil.

Plant Morphology

Overall, there was little difference in leaf:stem ratio between *P. australis* (0.36 ± 0.10 SD) and *C. canadensis* (0.33 ± 0.08 SD). *Typha* spp., however, had a much higher leaf:stem ratio (0.90 ± 0.33 SD).

Soil and Plant Tissue Nutrient Concentrations

The models predicting soil carbon and macronutrient levels based on plant community (meadow, cattail and *P. australis*-invaded), the nutrient environment (low and high), and their interaction all provided a good fit with $R^2 \geq 0.7$ (**Table 5**). There were no significant interactions between the influence of wetland and plant community on any of the measured soil carbon and macronutrients (**Supplementary Materials 2**). All measured soil carbon and macronutrients, except potassium, were significantly higher in Big Creek NWA than in Long Point Provincial Park, regardless of plant community (**Supplementary Materials 2**). Averaging the two nutrient environments, for the most part we detected no significant difference in soil carbon or macronutrients among the plant community types (**Supplementary Materials 2**), although meadow marsh in the Long Point Provincial Park generally had the lowest levels (**Supplementary Materials 4**). Plant available calcium was an exception, being significantly higher in the soil collected from cattail marsh than meadow marsh in Long Point Provincial Park (**Supplementary Materials 4**).

The models predicting plant tissue carbon and macronutrient concentrations based on plant species (*C. canadensis*, *Typha* spp., or *P. australis*), tissue type (leave, stem, or roots and rhizomes) and their interaction provided a strong fit ($R^2 \geq 0.8$) for all macronutrients but not for total carbon (**Table 6**). This model also failed to predict nitrogen to phosphorus ratios (**Table 6**).

TABLE 5 | Results of general linear model fit tests for soil nutrient content in the higher nutrient Big Creek National Wildlife Area and the lower nutrient Long Point Provincial Park sites.

Soil carbon or macronutrient		*F*-test (d.f.)	*p*-value	R^2
Total	Nitrogen	11.370 (5, 12)	<0.001	0.826
	Carbon	9.490 (5, 12)	<0.001	0.798
Plant available	Phosphorus	7.943 (5, 12)	0.002	0.768
	Potassium	5.866 (5, 12)	0.006	0.710
	Magnesium	11.920 (5, 12)	<0.001	0.832
	Calcium	10.090 (5, 12)	<0.001	0.808

*The general model form is predicted soil carbon and macronutrient concentration = $\beta 0 + \beta_1$ plant community + β_2 nutrient environment + β_3 (plant community *nutrient environment). Plant community refers to meadow marsh (n = 6), emergent cattail (n = 6), or P. australis-invaded marsh (n = 6) (see* ***Supplementary Materials 2*** *for detailed results).*

Generally, phosphorus, potassium and magnesium in plant tissues exhibited no interaction between plant species and tissue type (**Supplementary Materials 2**). These were lowest in the stem tissues and higher in the leaf and belowground tissues (**Figure 4**). Specifically, leaf tissue contained significantly higher phosphorus and potassium, while belowground tissues had significantly higher magnesium. In addition, phosphorus and potassium concentrations differed among plant species (**Supplementary Materials 2**). Phosphorus and potassium levels in plant tissues also differed among species: *P. australis* tissues contained significantly more phosphorus and potassium than *C. canadensis* and significantly more potassium than *Typha* spp. (**Figure 4**, **Supplementary Materials 2**).

Trends with carbon, nitrogen and calcium were more complex as they exhibited significant interactions between plant species and tissue type (**Supplementary Materials 2**). For example, *Typha* spp. contained significantly more carbon in its roots and rhizomes than its leaves, whereas the other species did not exhibit differences in carbon content among tissues (**Figure 4**). Nitrogen was much higher in *P. australis* leaf tissue than in *C. canadensis* or *Typha* spp. leaves, but there were no differences in the nitrogen concentration of stems and belowground tissue among species (**Figure 4**). Calcium concentrations in *Typha* spp. stem tissue was much higher than in *C. canadensis* or *P. australis*, but similar calcium concentrations were present in *P. australis* and *Typha* spp. foliar tissue and *C. canadensis* and *Typha* spp. belowground tissue (**Figure 4**).

TABLE 6 | General linear model fit test results for carbon and macronutrients in plant tissue and estimated standing stocks.

Carbon or Macronutrient	Units	*F*-test (d.f.)	*p*-value	R^2
Tissue carbon	% dry weight	2.288 (8, 21)	0.062	0.466
Tissue nitrogen		51.480 (8, 21)	<0.001	0.952
Tissue carbon:nitrogen		32.020 (8, 21)	<0.001	0.924
Tissue phosphorus		10.380 (8, 21)	<0.001	0.798
Tissue nitrogen:phosphorus		1.381 (8, 21)	0.261	0.345
Tissue potassium		16.240 (8, 21)	<0.001	0.861
Tissue magnesium		13.490 (8, 21)	<0.001	0.837
Tissue calcium		112.500 (8, 21)	<0.001	0.977
Standing stock carbon	g m^{-2}	16.450 (2, 47)	<0.001	0.412
Standing stock nitroge		14.840 (2, 47)	<0.001	0.387
Standing stock phosphorus		14.330 (2, 47)	<0.001	0.379
Standing stock potassium		29.760 (2, 47)	<0.001	0.559
Log_{10} (Standing stock magnesium)		35.760 (2, 47)	<0.001	0.604
Log_{10} (Standing stock calcium)		150.000 (2, 47)	<0.001	0.865

The general model form for plant tissue nutrient concentration (% dry weight) is $y = \beta_0 + \beta_1$ *plant species* $+ \beta_2$ *tissue type* $+ \beta_3$ *(plant species *tissue type). Tissue types were leaf, stem or belowground tissues. Plant species were either C. canadensis, Typha spp., or P. australis. The general model form for carbon and macronutrient standing stocks (g* m^{-2}*) is* $y = \beta_0 + \beta_1$ *plant community. Plant community refers to meadow marsh (n = 15), cattail marsh (n = 15), or P. australis-invaded marsh (n = 20). Standing stocks (g* m^{-2}*) of magnesium and calcium were log-transformed to meet the normality assumption (see* ***Supplementary Materials 2*** *for detailed results).*

Nutrient Standing Stocks

The models predicting annual nutrient standing stock (g m^{-2}) for carbon and the five macronutrients based on plant community type (meadow, cattail, or *P. australis*-invaded marsh) provided a statistically significant fit (**Table 6**). Overall, the stocks of carbon, nitrogen, phosphorus and potassium were lower in meadow marsh, but were equivalent in *P. australis*-invaded and emergent cattail (**Figure 5**, **Supplementary Materials 2**). Stocks of calcium and magnesium were also lowest in meadow marsh but were lower in P. *australis*-invaded marsh than in cattail marsh (**Figure 5**). We compared analyses wherein carbon and nutrient standing stocks were estimated by assuming that all species in the plot were the focal species with estimates considering only the fraction of total biomass attributable to the focal species itself (estimates in **Supplementary Materials 5**), but the model results were unchanged.

DISCUSSION

Invasive species may provide valuable ecological services in invaded ecosystems (Kopf et al., 2017). In the Great Lakes, where nearshore eutrophication and climate change are two of the most pressing environmental threats, a wetland plant that enhances carbon and other macronutrient assimilation could be an asset, even if it is non-native in origin. Decisions about *P. australis* control should weigh the ecological costs and benefits of invasion (Hershner and Havens, 2008; Hobbs et al., 2009; Davis et al., 2011), but a lack of research comparing nutrient pools and fluxes in habitat invaded by *P. australis* with those in the cattail and meadow marsh that *P. australis* is replacing prevents such calculations. Our research addressed this gap, comparing annual plant production (above and belowground) and carbon and nutrient standing stocks in *P. australis* invaded marsh with values typical of the marsh types *P. australis* is replacing. Importantly, we also examined the effects of environmental conditions like nutrient availability and water depth, which can influence plant production and nutrient assimilation.

Outcome of Invasion Contingent on Community Being Replaced

Our most important result is arguably that when rare meadow marsh is replaced by *P. australis*, we see a major increase in plant biomass, carbon and macronutrient standing stocks. Yet, when *P. australis* replaces cattail marsh, little change in biomass, carbon or nutrient standing stocks takes place, despite significantly higher nitrogen and marginally higher phosphorus and potassium in *P. australis* leaves than in *Typha* spp. leaves. Indeed, the only significant difference in standing stocks between cattail marsh and *P. australis*-invaded marsh was that *P. australis*-invaded marsh had lower calcium and magnesium stocks. Our research thus emphasizes that the magnitude and direction of change in carbon and macronutrient standing stocks caused by plant invasion is contingent on the vegetation community that is being replaced. *Phragmites australis* invasion cannot simply be assumed to increase carbon and macronutrient assimilation in invaded coastal marsh, even on the basis of differences in tissue carbon and macronutrient concentrations.

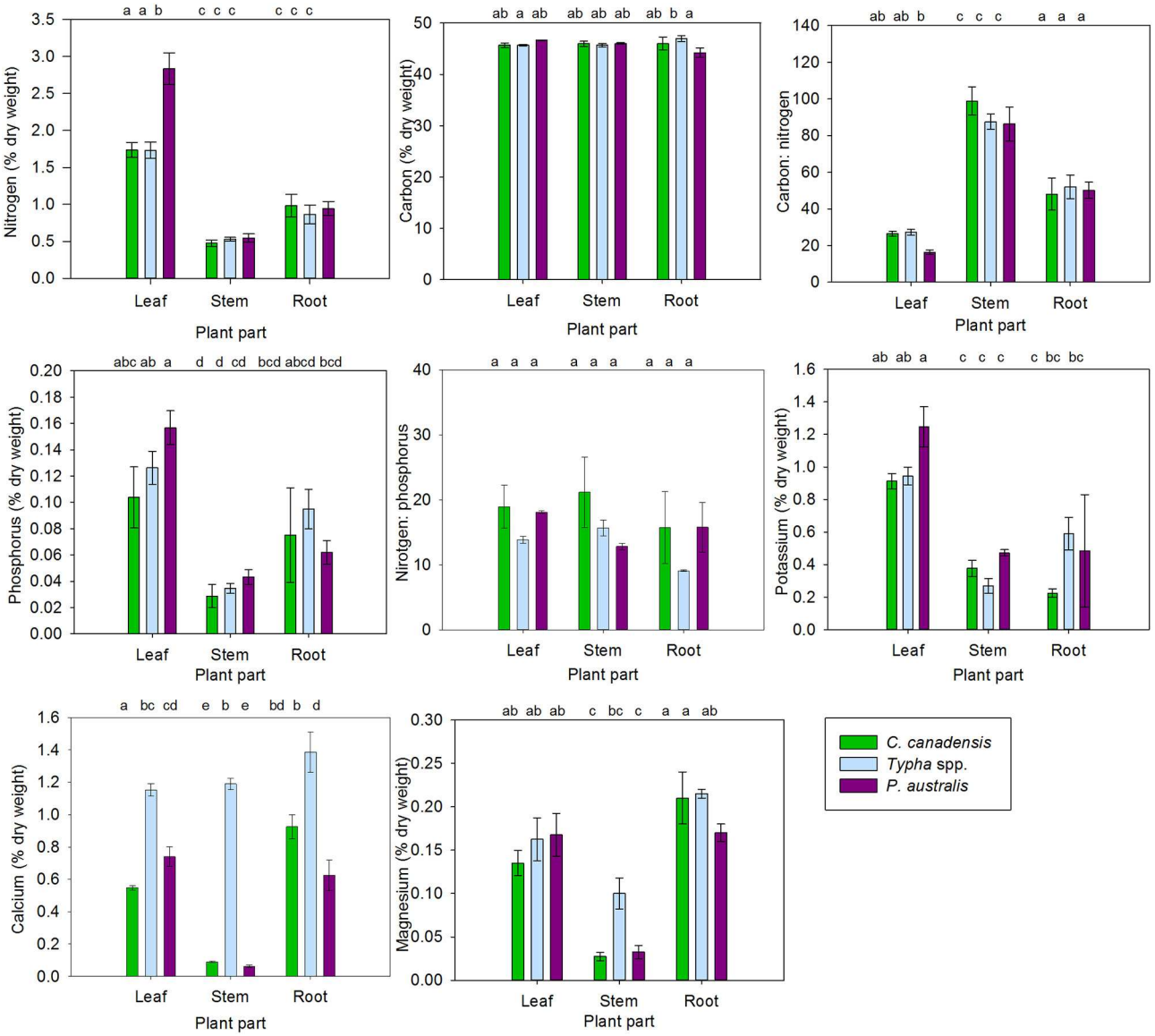

FIGURE 4 | Carbon and nutrients (% dry-weight) in *C. canadensis*, *Typha* spp., and *P. australis* leaves, stems, and belowground tissues (called "Root" in plots for simplicity). Samples collected from meadow ($n = 5$/wetland), cattail ($n = 5$/wetland) and *P. australis*-invaded marsh ($n = 5$/wetland) in the Big Creek National Wildlife Area ($n = 15$) and the Long Point Provincial Park ($n = 15$) in August 2016. Note that this averages tissues from a relatively high nutrient environment (Big Creek) with tissues from a relatively low nutrient environment (Long Point). Error bars represent standard error. Letters above bars indicate significant differences in nutrient content between plant species and tissue type at $p < 0.05$ (**Supplementary Materials 2**).

To our knowledge, no other field studies have compared *C. canadensis* carbon and macronutrient concentrations to *Typha* spp. or *P. australis* tissues, nor carbon and macronutrient stocks in meadow, with those in cattail and *P. australis*-invaded marsh. A study by Kao et al. (2003) established that *C. canadensis* had a low ability to assimilate nitrogen and phosphorus pollutants compared to other wetland macrophytes ($\sim$7 g m^{-2} N, $\sim$1 g m^{-2} P), suggesting that nutrient stocks may increase following *P. australis* invasion of *C. canadensis* dominated meadow marsh. Based on equivalent concentrations of carbon, phosphorus, and potassium in the tissues of *C. canadensis* and those of *Typha* spp. and *P. australis* measured in our study, this inferior nutrient assimilation is likely attributable to lower standing crop biomass in meadow marsh. Indeed, the aboveground biomass in meadow marsh reported in our study is similar to that reported in a greenhouse experiment (1,057 $\pm$ 12 g/m^2; Ouellet-Plamondon et al., 2004), and lies well below the standing crop biomass values for cattail marsh and *P. australis*-invaded marsh.

Our conclusion that *P. australis* invasion in cattail marsh does not increase nutrient stocks conflicts with some published studies. For example, Findlay et al. (2002) reported that *P. australis* retained almost two times more nitrogen than *Typha*

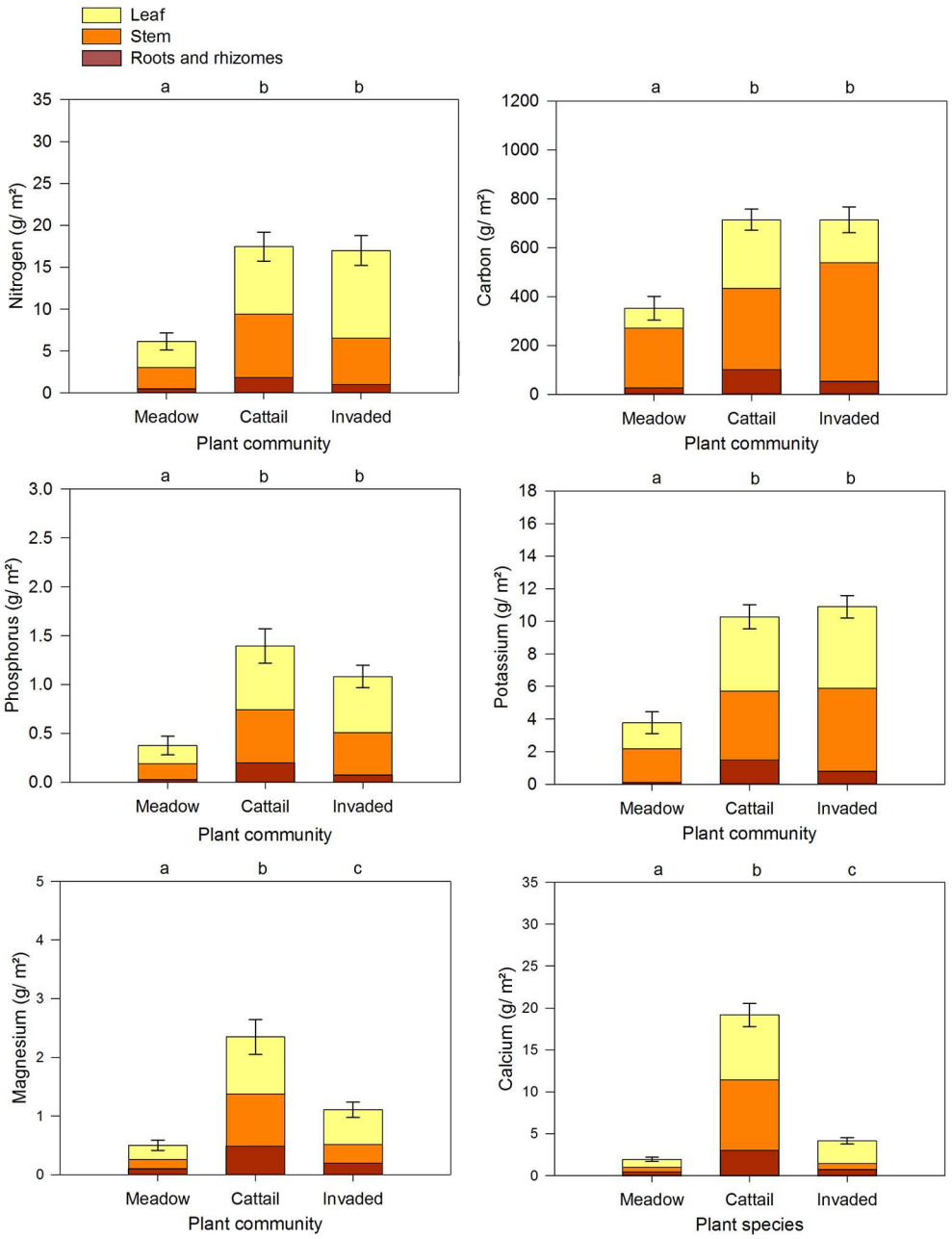

FIGURE 5 | Estimated annual carbon and nutrient standing stocks in the three plant community types broken down by tissue type. The values combine 2016 samples from the Big Creek National Wildlife Area ($n = 5$ each from meadow, cattail, and *P. australis*-invaded marsh) and the Long Point Provincial Park ($n = 5$ each from meadow, cattail, and *P. australis*-invaded marsh) with the 2017 samples from Long Point Provincial Park ($n = 5$ meadow, $n = 5$ cattail, and $n = 10$ *P. australis* invaded sites). Error bars reflect standard error in total nutrient standing stock, summed from all tissues. Letters above bars indicate significant differences among plant community types at $p < 0.05$ (**Supplementary Materials 2**).

angustifolia in living aboveground biomass (Findlay et al., 2002). They concluded that *P. australis* had both a higher nitrogen tissue concentration and 50% more biomass production than *T. angustifolia* (Findlay et al., 2002). The discrepancy between Findlay et al. (2002)'s results and ours is likely due to a focus on different species of *Typha*. The *Typha* spp. dominating cattail marsh in our study could not be identified to species by their morphology and most likely comprised the hybrid *Typha* × *glauca* with varying degrees of backcrossing to parental *T. angustifolia* and *T. latifolia* (Freeland et al., 2013). *Typha* × *glauca*, like *P. australis,* is a highly productive, tall, clonal, non-native monocot that forms monocultures and can have a negative impact on native species diversity (Larkin et al., 2012). Consequently, the difference in nutrient assimilation by *P. australis* and cattail marsh reported by other authors might occur in study areas where *T. angustifolia* or *T. latifolia* are

more common or when only foliar nitrogen stocks are examined (Findlay et al., 2002; Farnsworth and Meyerson, 2003; Hirtreiter and Potts, 2012).

Yet our conclusion regarding *P. australis* invasion of cattail marsh agrees with some recent field studies in the Great Lakes region (Rothman and Bouchard, 2007; Duke et al., 2015), potentially because the *Typha* spp. in these studies likely also included *Typha* × *glauca*. These studies reported wide ranges in aboveground biomass values that were similar to our observations (cattail: 1,661–2,930 g/m^2 and *P. australis*-invaded: 1,522–3,378 g/m^2; Rothman and Bouchard, 2007; Duke et al., 2015). This variation in aboveground biomass may be due to differences in water or nutrient regimes, which is why we repeated our comparisons in higher and lower nutrient environments as well as along a water depth gradient.

Outcome of Invasion Depends on Nutrient Environment and Water Depth

Invasive *P. australis* has been noted to allocate more resources to aboveground biomass in high nitrogen environments, which is believed to facilitate its spread in disturbed environments (Minchinton and Bertness, 2003). Such a response could contribute to its nutrient retention service: higher loading would trigger higher uptake, a desirable property. However, we observed that all focal species exhibited lower root:shoot ratios and higher biomass and nutrient tissue concentrations in the more nutrient rich Big Creek compared to the lower nutrient Long Point Provincial Park. This agrees with widespread studies concluding that increasing nutrient loads led to increased total biomass of vegetation, foliar nitrogen and phosphorus, and decreased root: shoot ratios (e.g., Powelson and Lieffers, 1992; Kvet et al., 2008; Rong et al., 2014; Caplan et al., 2015; Graham and Mendelssohn, 2016; Li et al., 2016). In fact, the largest difference in annual production between nutrient environments was observed in meadow marsh, not *P. australis* invaded marsh. Consequently, any nutrient retention benefit of *P. australis* invasion of meadow marsh would be minimized under high nutrient loading environments, which are the conditions under which increased nutrient stocks would be desirable. The difference in nutrient tissue concentrations between higher and lower nutrient environments could be due to either nutrient limitation in Long Point Provincial Park or luxury consumption in Big Creek NWA (e.g., Gumbricht, 1993). Regardless of mechanism, clearly nutrient loading will influence the degree to which *P. australis* invasion alters carbon and macronutrient pools in coastal marsh.

Water depth may also influence plant production and resource allocation to different tissue types, with consequences for carbon and macronutrient standing stocks. Depending on the plant species, standing crop biomass may increase, decrease or not change with water depth (e.g., Fraser and Karnezis, 2005; Miller and Zedler, 2013; Middleton et al., 2015). In a greenhouse experiment, Wetzel and van der Valk (2005) reported higher *C. canadensis* aboveground biomass in flooded conditions compared to well-watered and dry conditions, leading to our prediction that standing crop biomass for our focal species would increase with water depth. The response of *P. australis* biomass to water depth has been reviewed by Engloner (2009) who reported inconsistency that might be attributable to differences in water depth stability. In our study, the total biomass of *P. australis* and *C. canadensis* both increased with water depth, though a natural community turnover takes places between 30 and 40 cm of standing water (May measurements), where higher biomass cattail marsh replaces lower biomass meadow marsh. The relationship between cattail marsh standing crop biomass and water depth in our study is less clear, with aboveground biomass decreasing with water depth and belowground biomass increasing. In contrast, Duke et al. (2015) reported that *Typha* spp. aboveground biomass was positively related to water depth in a Great Lakes wetland. Our results also differ from previous studies that did not find a difference in belowground biomass between cattail and *P. australis*-invaded communities (Ouellet-Plamondon et al., 2004; Rothman and Bouchard, 2007). A major difference between our study and others examining below ground biomass in *P. australis*-invaded marhes (e.g., Farnsworth and Meyerson, 2003; Rothman and Bouchard, 2007) is that we used the in-growth core technique because our interest was in annual standing stocks, whereas other field studies typically used traditional soil core methods to measure total belowground standing crop biomass. Our approach would exclude any roots and rhizomes produced during previous seasons, and consequently yields lower estimates of belowground biomass than many other studies (e.g., Farnsworth and Meyerson, 2003; Ouellet-Plamondon et al., 2004; Rothman and Bouchard, 2007).

The mechanism driving the relationships between plant production and water depth are uncertain. Some studies suggest that differences in biomass allocation above or belowground may occur because of increased oxygen demands in rooting systems, greater availability of some nutrients in saturated soil, or higher nutrient uptake within the roots due to increased root length: root mass ratios (Rubio et al., 1995; Rubio and Lavado, 1999). It is also possible that plants may grow taller in deeper water to increase structural support or to access light. Regardless, we recommend that future studies examining nutrient stocks of wetland plants consider nutrient availability and water depths explicitly, as the total biomass production and allocation among tissues types is contingent on these two factors.

Less Well-Studied Nutrients: Calcium and Magnesium

A novel contribution of our work is that we considered elements beyond the commonly studied carbon, nitrogen and phosphorus. For example, calcium, and magnesium, despite their potential importance in nutrient cycling, receive much less attention in the literature (Ehrenfeld, 2010). *Typha* spp. had a higher concentration of calcium than the other focal species in all tissues and a higher concentration of magnesium in its stems. Consequently, the annual cattail nutrient standing stock of calcium and magnesium was significantly greater than in *P. australis*-invaded or meadow marsh. Though the difference in

terms of magnesium was only one to two grams per meter squared, the difference in calcium standing stock was more pronounced: nearly 10-fold higher in cattail marsh than meadow marsh, for example. One possible explanation is that *Typha* spp. produces calcium oxalate raphide crystal bundles (Borrelli et al., 2011), which may be used for structural support, defense against herbivores, or produced as a metabolic end-product (Franceschi and Horner, 1980). In general, it appears that *Typha* spp. often accumulates high levels of calcium and magnesium (Olivares et al., 2002; Parzych et al., 2015). However, based on the similarity in soil calcium and magnesium concentrations, the activity of *Typha* spp. is not sufficient to deplete soil levels to a detectable degree. Nor is the distribution of *Typha* spp. restricted to areas with higher calcium or magnesium levels in the soil. This is somewhat surprising for calcium, as 19.2 g m^{-2} ± 4.5 SD calcium in standing stock in cattail marsh is not an insignificant concentration, given the soil concentration of 6.1 g kg^{-1} ± 2.0 SD (**Supplementary Materials 4**). The ecological consequences of these macronutrient differences between *P. australis*-invaded and cattail marsh communities require further study.

Scaling Up

Our study scaled up from carbon and macronutrient concentrations at the tissue-level to estimate annual vegetative standing stocks per meter-squared of wetland habitat. It is important not to base assessments of carbon assimilation and nutrient retention services solely on tissue concentrations, as different tissue types typically support different carbon and nutrient levels and the ratio of tissue types can vary substantially among species. This is exemplified in our work by the higher concentration of nitrogen in *P. australis* leaves being offset by the greater proportion of leaf tissues in *Typha* spp. such that their nitrogen standing stock estimates are equivalent. If we had relied only on tissue concentrations, we would have drawn the erroneous conclusion that *P. australis* invasion provided enhanced nitrogen and phosphorus assimilation, regardless of which community was being replaced.

Scaling-up from tissues to standing stocks does introduce uncertainty. In our study, *C. canadensis* is a less dominant component of its community compared with *Typha* spp. and *P. australis* (**Table 1**). Consequently, when scaling up from tissue concentrations to marsh-level annual standing stocks, meadow marsh estimates have greater uncertainty than estimates for the cattail and *P. australis*-invaded marsh. We do not believe that this assumption undermines our conclusions, however, as recalculating carbon and macronutrient stocks based only on biomass contributed by the focal species (i.e., excluding biomass contributed by non-focal species) did not change our general conclusions. Moreover, our conclusions are supported by obvious differences in relative canopy heights and total biomass, which were significantly lower in meadow marsh than in cattail and *P. australis*-invaded marsh.

The difference in carbon, nitrogen and phosphorus assimilation between meadow marsh and invaded marsh is not negligible. Scaled up to metric tons per hectare of invaded wetland, *P. australis*-invaded marsh has an annual standing stock of carbon that is 3.87 T ha^{-1} greater than meadow marsh (a 2-fold increase). Canada is implementing a carbon pricing system beginning in 2019 that would price one ton of CO_2 or equivalent at $16 USD, and by 2,022 plans to increase that price to $39 USD/T CO_2 (Goyal et al., 2018). After converting tons of carbon to CO_2, every conversion of one hectare of meadow marsh to *P. australis*-invaded marsh would be worth $227.32 in 2019 and $554.10 in 2022. Currently, large portions of Lake Erie are invaded by *P. australis*, with invasion estimates ranging from 2,553 ha within Lake Erie coastal wetlands (Carson et al., 2018) to 8,233 ha invaded within 10 km of the American side of Lake Erie (Bourgeau-Chavez et al., 2013). Where *P. australis* replaced cattail marsh, this would yield no change in annual carbon stocks, but where it replaced the much rarer and biodiverse meadow marsh, we may have experienced a significant increase in carbon uptake.

While the overall amount of phosphorus in the annual vegetative standing stock of *P. australis*-invaded marshes is much smaller than the annual carbon standing stock, it still represents an almost 3-fold increase compared to meadow marsh (a difference of 0.01 T ha^{-1}). If we assumed that 10% of the Lake Erie coastal marsh considered *P. australis*-invaded by Carson et al. (2018) and Bourgeau-Chavez et al. (2013) was formerly meadow marsh, the annual standing stock of phosphorus would only have increased by 2.0–6.4 T in total. This is notably less than the phosphorus output from smaller tributaries; for example, phosphorus output from Big Creek is about 19 T phosphorus $year^{-1}$ (OMECC, 2017). Cleary, even a 3-fold increase in annual phosphorus stock is insufficient to make a meaningful contribution toward Lake Erie phoshorus load reduction targets, given that the current Great Lakes Water Quality Agreement between Canada and the United States of America has an interim target load for phosphorus of 11,000 T $year^{-1}$ for Lake Erie (United States-Canada, 2013).

Phragmites australis invaded marshes also incorporate 3-fold more nitrogen into the annual vegetative standing stock than meadow marsh (an increase of 0.12 T N ha^{-1}). Scaled up to the Lake Erie basin using the same estimates for the area of invasion, invasion of meadow marsh by *P. australis* would result in an 30.7–99.0 T increase in annual nitrogen standing stock. As with phosphorus, this is merely a drop in the bucket: nitrogen loading in Lake Erie was estimated at 136,000 T in 2002 (Robertson and Saad, 2013). Overall, despite extensive invasion by *P. australis*, increases in annual standing stocks of nitrogen and phosphorus are likely inconsequential for Lake Erie.

Nutrient Retention vs. Nutrient Standing Stocks

Importantly, our study focuses on the assimilation of nutrients into the vegetative standing stock of different plant communities during a single growing season but does not examine their long-term storage, which should ultimately determine nutrient retention services. In wetlands, nutrients taken up by macrophytes are quickly cycled by decomposition (Maltby and Barker, 2009). Long term retention of nutrients in plants

varies by species and by nutrient. For example, *P. australis* litter and standing dead stems can decrease in nitrogen by approximately 40–60% and in phosphorus by 75–85% compared to the living tissue (Findlay et al., 2002). In contrast, *T. angustifolia* litter nitrogen concentration exceeds that of living tissues, whereas phosphorus in litter is 0–25% lower than in living tissues (Findlay et al., 2002). *Calamagrostis canadensis* litter can retain 70% of the nitrogen and 51% of the phosphorus it assimilated (Kao et al., 2003). This litter, typically shed by the plant each fall, then decomposes in the wetland at a rate usually dependent on the ratio of carbon to nitrogen and nitrogen to phosphorus (Enriquez et al., 1993). Because the fraction of carbon, nitrogen, and phosphorus retrieved by the plant from senescing tissues before they are shed as litter can vary among species, there could be differences in litter decomposition rates among our focal species, even though we observed no differences in carbon: nitrogen or nitrogen: phosphorus ratios among our focal species for any of the plant tissues. Importantly, our study did not address the speciation of carbon or nutrients in plant tissues. Obviously, differences in the extent or proportion of bioavailable inorganic fractions will have important ecological and biogeochemical ramifications. For example, Judd and Franceour (2019) found that ammonium in surface and pore water increased but nitrate did not change in marshes where invasive *P. australis* was controlled with herbicide. Though both of these forms of nitrogen are bioavailable to plants, increasing the dominance of ammonium over nitrate can lead to ammonium toxicity in plants and changes in soil pH. More, if nutrient storage in invasive *P. australis* is only temporary, all the nutrients assimilated by *P. australis* may be released back into the watershed during natural senescence and decomposition in the same manner as following herbicide-caused mortality, unless plant biomass is harvested and removed for disposal by wetland managers (Carson et al., 2018). We recommend that future work establish decomposition rates and nutrient fluxes from decomposing plant litter of our three focal species to further investigate the effects of *P. australis* invasion on carbon and nutrient cycling and retention services. This future work should partition total carbon and nutrient values into organic and inorganic fractions to better inform the biogeochemical consequences of changes in stock and tissue concentrations due to *P. australis* invasion.

CONCLUSION

Phragmites australis has the capacity to assimilate carbon and nutrients at an amount and rate equal to or greater than meadow marsh communities though not more than cattail marsh. In the case of carbon stocks, invasion may even yield an economic benefit, though increases in nitrogen or phosphorus stocks where meadow marsh was invaded were negligible compared to overall nutrient loading rates and are unlikely to ameliorate nearshore eutrophication. It is also important to recognize that annual carbon and nutrient stocks offer temporary storage, and an unknown proportion will be released following senescence and decomposition of plant litter.

We caution that, as suggested by Alldred et al. (2016), invasion by *P. australis* triggers a variety of opposing changes in wetland ecosystem services that reflect trade-offs among service types. A net assessment of the effects of *P. australis* invasion must also account for the resulting loss of plant biodiversity (Keller, 2000; Tulbure et al., 2007) and associated degradation of bird (Robichaud and Rooney, 2017) and turtle habitat (Markle and Chow-Fraser, 2018). In economic terms, replacing biodiverse and rare meadow marsh habitat with *P. australis*-invaded marsh could increase carbon stocks by 3.87 T ha^{-1} and under future carbon pricing could reflect about $550 USD ha^{-1} in carbon savings. Yet, *P. australis* invasion is a recognized threat to 25% of the 217 species at risk in Ontario (Bickerton, 2015), which exerts a much larger economic cost. For example, between 2012 and 2017, the Ontario Ministry of Natural Resources and Forestry, through the Species at Risk Stewardship Program, spent $89,826 USD on the threatened eastern hog-nosed snake (*Heterodon platirhinos*) alone, which makes use of meadow marsh habitat, but not *P. australis*-invaded marsh in our study area (Ministry of Natural Resources and Forestry, 2017). Thus, the funds allocated to species at risk conservation likely dwarf any benefits in increased carbon and nutrient stocks resulting from *P. australis* invasion. These trade-offs in ecosystem services need to be weighed to arrive at effective management decisions regarding species at risk (Hershner and Havens, 2008; Hobbs et al., 2009; Davis et al., 2011), but such a comprehensive analysis is too frequently impaired by knowledge gaps like the ones we addressed in this study.

DATA AVAILABILITY

The datasets generated for this study are available on request to the corresponding author.

AUTHOR CONTRIBUTIONS

RR and SY designed the study. SY conducted the field and lab work. SY and RR analyzed the data and co-authored the manuscript.

FUNDING

This work was supported by NSERC Discovery 03846, the Ontario Ministry of Natural Resources and Forestry MNRF-W-(12)6-17, and Mitacs Accelerate IT07466 73027 in partnership with the Nature Conservancy of Canada. Funders had no role in study design, analysis, interpretation or reporting.

ACKNOWLEDGMENTS

This work could not have been completed without help from many volunteers and lab technicians; thank you Jacob Basso, Bailey Dhanani, Megan Jordan, Madison Brook, Taylor Blackwell, Lauren Koiter, and Calvin Lei. Map of our study

area was created by Mathew Bolding and is used with permission. Thanks to Dr. Janice Gilbert, Dr. Merrin Macrae, Dr. Roland Hall, and Dr. Marcel Pinero for feedback on an early draft. Thanks also to two reviewers for their constructive comments.

SUPPLEMENTARY MATERIAL

The Supplementary Material for this article can be found online at: https://www.frontiersin.org/articles/10.3389/fenvs.2019.00112/full#supplementary-material

REFERENCES

Agriculture and Food Laboratory University of Guelph (2017). *Soil and Nutrient Laboratory Service List*. Soil and Plant Nutrient Testing Laboratory, 1–4.

Alldred, M., Baines, S. B., and Findlay, S. (2016). Effects of invasive-plant management on nitrogen-removal services in freshwater tidal marshes. *PLoS ONE* 11:e0149813. doi: 10.1371/journal.pone.0149813

Ball, H., Jalava, J., King, T., Maynard, L., Potter, B., and Pulfer, T. (2003). *The Ontario Great Lakes Coastal Weltand Atlas: A Summary of information (1983–1997)*. Available online at: http://longpointbiosphere.com/download/Environment/Ontario.Great_.Lakes_.Coastal.Wetland.Atlas-2003.pdf (accessed February 14, 2018).

Barton, K. (2018). *MuMIn: Multi-Model Inference. R Package Version 1.40.4*. Available online at: https://cran.r-project.org/package=MuMIn

Bertness, M. D., and Coverdale, T. C. (2013). An invasive species facilitates the recovery of salt marsh ecosystems on Cape Cod. *Ecology* 94, 1937–1943. doi: 10.1890/12-2150.1

Bhatia, M., and Goyal, D. (2014). Analyzing remediation potential of wastewater through wetland plants: a review. *Environ. Prog. Sustain. Energy* 33, 9–27. doi: 10.1002/ep.11822

Bickerton, H. (2015). *Extent of European Common Reed (Phragmites australis ssp. australis) as a Threat to Species at Risk in Ontario*. Report prepared for Natural Heritage Section Ontario Ministry of Natural Resources and Forestry. Peterborough, ON.

Bolton, R. M., and Brooks, R. J. (2010). Impact of the seasonal invasion of *Phragmites australis* (Common Reed) on turtle reproductive success. *Chelonian Conserv. Biol.* 9, 238–243. doi: 10.2744/CCB-0793.1

Borrelli, N., Fernández Honaine, M., Altamirano, S. M., and Osterrieth, M. (2011). Calcium and silica biomineralizations in leaves of eleven aquatic species of the Pampean Plain, Argentina. *Aquat. Bot.* 94, 29–36. doi: 10.1016/j.aquabot.2010.10.003

Bourgeau-Chavez, L. L., Kowalski, K. P., Carlson Mazur, M. L., Scarbrough, K. A., Powell, R. B., Brooks, C. N., et al. (2013). Mapping invasive *Phragmites australis* in the coastal Great Lakes with ALOS PALSAR satellite imagery for decision support. *J. Great Lakes Res.* 39, 65–77. doi: 10.1016/j.jglr.2012.11.001

Caplan, J. S., Hager, R. N., Megonigal, J. P., and Mozdzer, T. J. (2015). Global change accelerates carbon assimilation by a wetland ecosystem engineer. *Environ. Res. Lett.* 10, 1–12. doi: 10.1088/1748-9326/10/11/115006

Carson, B. D., Lishawa, S. C., Tuchman, N. C., Monks, A. M., Lawrence, B. A., and Albert, D. A. (2018). Harvesting invasive plants to reduce nutrient loads and produce bioenergy: an assessment of Great Lakes coastal wetlands. *Ecosphere* 9:e02320. doi: 10.1002/ecs2.2320

Catling, P. M., and Mitrow, G. (2011). The recent spread and potential distribution of *Phragmites australis* subsp. *australis* in Canada. *Can. Field-Naturalist* 125, 95–104. doi: 10.22621/cfn.v125i2.1187

Croft, M. V., and Chow-Fraser, P. (2007). Use and development of the wetland macrophyte index to detect water quality impairment in fish habitat of Great Lakes coastal marshes. *J. Great Lakes Res.* 33, 172–197. doi: 10.3394/0380-1330(2007)33[172:UADOTW]2.0.CO;2

Davis, M. A., Chew, M. K., Hobbs, R. J., Lugo, A. E., Ewel, J. J., Vermeij, G. J., et al. (2011). Don't judge species on their origins. *Nature* 474, 153–154. doi: 10.1038/474153a

Duke, S. T., Francoeur, S. N., and Judd, K. E. (2015). Effects of *Phragmites australis* invasion on carbon dynamics in a freshwater marsh. *Wetlands* 35, 311–321. doi: 10.1007/s13157-014-0619-x

Ehrenfeld, J. G. (2010). Ecosystem consequences of biological invasions. *Annu. Rev. Ecol. Evol. Syst.* 41, 59–80. doi: 10.1146/annurev-ecolsys-102209-144650

Engloner, A. I. (2009). Structure, growth dynamics and biomass of reed (*Phragmites australis*)—a review. *Flora Morphol. Distrib. Funct. Ecol. Plants* 204, 331–346. doi: 10.1016/j.flora.2008.05.001

Enriquez, S., Duarte, C., and Sand-Jensen, K. (1993). Patterns in decomposition rates among photosynthetic organisms: the importance of detritus C: N: P content. *Oecologia* 94, 457–471. doi: 10.1007/BF00566960

Environment and Climate Change Canada and the U.S. Environmental Protection Agency (2017). *State of the Great Lakes 2017 Technical Report: Indicators to Assess the Status and Trends of the Great Lakes Ecosystem*. Available online at: https://binational.net/wp-content/uploads/2017/09/SOGL_2017_Technical_Report-EN.pdf (accessed May 29, 2018).

Essex Region Conservation Authority (2013). *Big Creek Watershed Plan*. Available online at: https://essexregionconservation.ca/wp-content/uploads/2018/03/BigCreekWatershedPlan_Final_Complete_Dec6-13.pdf (accessed July 31, 2018).

Farnsworth, E. J., and Meyerson, L. A. (2003). Comparative ecophysiology of four wetland plant species along a continuum of invasiveness. *Wetlands* 23, 750–762. doi: 10.1672/0277-5212(2003)023[0750:CEOFWP]2.0.CO;2

Findlay, S. E. G., Dye, S., and Kuehn, K. A. (2002). Microbial growth and nitrogen retention in litter of *Phragmites australis* compared to *Typha angustifolia*. *Wetlands* 22, 616–625. doi: 10.1672/0277-5212(2002)022[0616:MGANRI]2.0.CO;2

Franceschi, V. R., and Horner, H. T. (1980). Calcium oxalate crystals in plants. *Bot. Rev.* 46, 361–427. doi: 10.1007/BF02860532

Fraser, L. H., and Karnezis, J. P. (2005). A comparative assessment of seedling survival and biomass accumulation for fourteen wetland plant species grown under minor water-depth differences. *Wetlands* 25, 520–530. doi: 10.1672/0277-5212(2005)025[0520:ACAOSS]2.0.CO;2

Freeland, J., Ciotir, C., and Kirk, H. (2013). Regional differences in the abundance of native, introduced, and hybrid *Typha* spp. in northeastern North America influence wetland invasions. *Biol. Invasions* 15, 2651–2665. doi: 10.1007/s10530-013-0481-4

Goyal, R., Gray, S., Churie Kallhauge, A., Nierop, S., Berg, T., and Leuschner, P. (2018). *State and Trends of Carbon Pricing 2018*.

Graham, S. A., and Mendelssohn, I. A. (2016). Contrasting effects of nutrient enrichment on below-ground biomass in coastal wetlands. *J. Ecol.* 104, 249–260. doi: 10.1111/1365-2745.12498

Greenberg, D. A., and Green, D. M. (2013). Effects of an invasive plant on population dynamics in toads. *J. Soc. Conserv. Biol.* 27, 1049–1057. doi: 10.1111/cobi.12078

Grutters, B. M. C., Pollux, B. J. A., Verberk, W. C. E. P., and Bakker, E. S. (2015). Native and non-native plants provide similar refuge to invertebrate prey, but less than artificial plants. *PLoS ONE* 10:e0124455. doi: 10.1371/journal.pone.0124455

Gumbricht, T. (1993). Nutrient removal processes in freshwater submersed macrophyte systems. *Ecol. Eng.* 2, 1–30. doi: 10.1016/0925-8574(93)90024-A

Hershner, C., and Havens, K. J. (2008). Managing invasive aquatic plants in a changing system: strategic consideration of ecosystem services. *Conserv. Biol.* 22, 544–550. doi: 10.1111/j.1523-1739.2008.00957.x

Hirtreiter, J. N., and Potts, D. L. (2012). Canopy structure, photosynthetic capacity and nitrogen distribution in adjacent mixed and monospecific stands of *Phragmites australis* and *Typha latifolia*. *Plant Ecol.* 213, 821–829. doi: 10.1007/s11258-012-0044-2

Hobbs, R. J., Higgs, E., and Harris, J. A. (2009). Novel ecosystems: implications for conservation and restoration. *Trends Ecol. Evol.* 24, 599–605. doi: 10.1016/j.tree.2009.05.012

Jarvie, H. P., Johnson, L. T., Sharpley, A. N., Smith, D. R., Baker, D. B., Bruulsema, T. W., et al. (2017). Increased soluble phosphorus loads to Lake

Erie: unintended consequences of conservation practices? *J. Environ. Qual.* 46, 123–132. doi: 10.2134/jeq2016.07.0248

Judd, K., and Franceour, S. N. (2019). Short-term impacts of Phragmites management on nutrient budgets and plant communities in Great Lakes coastal freshwater marshes. *Wetlands Ecol. Manag.* 27, 55–74. doi: 10.1007/s11273-018-9643-6

Jung, J. A., Rokitnicki-Wojcik, D., and Midwood, J. D. (2017). Characterizing past and modelling future spread of *Phragmites australis* ssp. australis at Long Point Peninsula, Ontario, Canada. *Wetlands* 37, 961–973. doi: 10.1007/s13157-017-0931-3

Kao, J. T., Titus, J. E., and Zhu, W.-X. (2003). Differential nitrogen and phosphorus retention by five wetland plant species. *Wetlands* 23, 979–987. doi: 10.1672/0277-5212(2003)023[0979:DNAPRB]2.0.CO;2

Keller, B. E. M. (2000). Plant diversity in *Lythrum*, *Phragmites*, and *Typha* marshes, Massachusetts, U.S.A. *Wetl. Ecol. Manag.* 8, 391–401. doi: 10.1023/A:1026505817409

Kirk, H., Connolly, C., and Freeland, J. R. (2011). Molecular genetic data reveal hybridization between *Typha angustifolia* and *Typha latifolia* across a broad spatial scale in eastern North America. *Aquat. Bot.* 95, 189–193. doi: 10.1016/j.aquabot.2011.05.007

Kiviat, E. (2013). Ecosystem services of *Phragmites* in North America with emphasis on habitat functions. *AoB Plants* 5:plt008. doi: 10.1093/aobpla/plt008

Kopf, R. K., Nimmo, D. G., Humphries, P., Baumgartner, L. J., Bode, M., Bond, N. R., et al. (2017). Confronting the risks of large-scale invasive species control. *Nat. Ecol. Evol.* 1, 172. doi: 10.1038/s41559-017-0172

Kvet, J., Pokorny, J., and Cizkova, H. (2008). Carbon accumulation by macrophytes of aquatic and wetland habitats with standing water. *Proc. Natl. Acad. Sci. India Sect. B Biological Sci.* 78, 91–98. Available online at: https://www.researchgate.net/publication/282684167

Larkin, D. J., Freyman, M. J., Lishawa, S. C., Geddes, P., and Tuchman, N. C. (2012). Mechanisms of dominance by the invasive hybrid cattail *Typha* × *glauca*. *Biol. Invasions* 14, 65–77. doi: 10.1007/s10530-011-0059-y

Li, H., Liu, Y., Li, J., Zhou, X., and Li, B. (2016). Dynamics of litter decomposition of dieback *Phragmites* in *Spartina*-invaded salt marshes. *Ecol. Eng.* 90, 459–465. doi: 10.1016/j.ecoleng.2016.01.012

Lombard, K. B., Tomassi, D., and Ebersole, J. (2012). Long-term management of an invasive plant: lessons from seven years of *Phragmites australis* control. *Northeast Nat.* 19, 181–193. doi: 10.1656/045.019.s614

Mal, T. K., and Narine, L. (2004). The biology of Canadian weeds. 129. *Phragmites australis* (Cav.) Trin. ex Steud. *Can. J. Plant Sci.* 84, 365–396. doi: 10.4141/P01-172

Maltby, E., and Barker, T. (2009). *The Wetlands Handbook. 1st Edn*. West Sussex: Wiley-Blackwell. Available online at: https://www.amazon.ca/Wetlands-Handbook-Edward-Maltby/dp/0632052554

Markle, C. E., Chow-fraser, G., and Chow-fraser, P. (2018). Long-term habitat changes in a protected area: implications for herpetofauna habitat management and restoration. *PLoS ONE* 13, 1–15. doi: 10.1371/journal.pone.0192134

Markle, C. E., and Chow-Fraser, P. (2018). Effects of European common reed on Blanding's turtle spatial ecology. *J. Wildl. Manag.* 82, 857–864. doi: 10.1002/jwmg.21435

Martin, L. J., and Blossey, B. (2013). The runaway weed: costs and failures of *Phragmites australis* management in the USA. *Estuar. Coasts* 36, 626–632. doi: 10.1007/s12237-013-9593-4

Meyer, S. W., Badzinski, S. S., Petrie, S. A., and Ankney, C. D. (2010). Seasonal abundance and species richness of birds in Common Reed habitats in Lake Erie. *J. Wildl. Manage.* 74, 1559–1567. doi: 10.1111/j.1937-2817.2010.tb01284.x

Middleton, B. A., Van Der Valk, A. G., and Davis, C. B. (2015). Responses to water depth and clipping of twenty-three plant species in an Indian monsoonal wetland. *Aquat. Bot.* 126, 38–47. doi: 10.1016/j.aquabot.2015.06.004

Miller, R. C., and Zedler, J. B. (2013). Responses depth of native and invasive wetland plants to hydroperiod and water. *Plant Ecol.* 167, 57–69. doi: 10.1023/A:1023918619073

Minchinton, T. E., and Bertness, M. D. (2003). Disturbance-mediated competition and the spread of *Phragmites australis* in a coastal marsh. *Ecol. Appl.* 13, 1400–1416. doi: 10.1890/02-5136

Ministry of Natural Resources and Forestry (2017). *Five-year Review of Progress towards the Protection and Recovery of Ontario's Species at Risk 2017*. Available online at: https://files.ontario.ca/2017_5yrsummary_final-22-02-18.pdf (accessed September 13, 2018).

Ministry of Natural Resources and Forestry (2018). *Get Natural Heritage Information. Queen's Print. Ontario, 2012–17*. Available online at: https://www.ontario.ca/page/get-natural-heritage-information (accessed January 10, 2017).

Neill, C. (1992). Comparison of soil coring and ingrowth methods for measuring belowground production. *Ecology* 73, 1918–1921. doi: 10.2307/1940044

Norkko, J., Reed, D. C., Timmermann, K., Norkko, A., Gustafsson, B. G., Bonsdorff, E., et al. (2012). A welcome can of worms? Hypoxia mitigation by an invasive species. *Glob. Chang. Biol.* 18, 422–434. doi: 10.1111/j.1365-2486.2011.02513.x

Olivares, E., Vizcaíno, D., and Gamboa, A. (2002). Mineral nutrition of three aquatic emergent macrophytes in a managed wetland in Venezuela. *J. Plant Nutr.* 25, 475–496. doi: 10.1081/PLN-120003377

OMECC (2017). *Partnering in Phosphorus Control: Achieving Phosphorus Reductions in Lake Erie from Canadian sources*. The Canada-Ontario Draft Action Plan. Available online at: http://www.downloads.ene.gov.on.ca/envision/env_reg/er/documents/2017/012-9971~ENG.pdf

Ouellet-Plamondon, C. M., Brisson, J., Comeau, Y. (2004). "Effect of macrophyte species on subsurface flow wetland performance in cold climate," in *Proceedings of the 2004 Self-Sustaining Solutions for Streams, Wetlands, and Watersheds Conference*, 8–15. Available online at: http://www.scopus.com/inward/record.url?eid=2-s2.0-27844525643&partnerID=40&md5=2eb4c1676aeeb9934759e44e05506efb

Parzych, A. E., Cymer, M., Jonczak, J., and Szymczyk, S. (2015). The ability of leaves and rhizomes of aquatic plants to accumulate macro- and micronutrients. *J. Ecol. Eng.* 16, 198–205. doi: 10.12911/22998993/2956

Powelson, R. A., and Lieffers, V. J. (1992). Effect of light and nutrients on biomass allocation in *Calamagrostis canadensis*. *Ecography* 15, 31–36. doi: 10.1111/j.1600-0587.1992.tb00005.x

Quirion, B., Simek, Z., Dávalos, A., and Blossey, B. (2018). Management of invasive *Phragmites australis* in the Adirondacks: a cautionary tale about prospects of eradication. *Biol. Invasions* 20, 59–73. doi: 10.1007/s10530-017-1513-2

R Core Team (2016). *R: A Language and Environment for Statistical Computing*. Available online at: https://www.r-project.org/

Reid, K. (1998). *Soil Fertility Handbook*. OMAFRA Publication. Available online at: http://www.omafra.gov.on.ca/english/crops/pub611/pub611.pdf (accessed May 29, 2018).

Robertson, D. M., and Saad, D. A. (2013). Nutrient inputs to the Laurentian Great Lakes by source and watershed estimated using SPARROW watershed models. *J. Am. Water Resour. Assoc.* 49, 725–734. doi: 10.1111/jawr.12060

Robichaud, C. D., and Rooney, R. C. (2017). Long-term effects of a Phragmites australis invasion on birds in a Lake Erie coastal marsh. *J. Great Lakes Res.* 43, 141–149. doi: 10.1016/j.jglr.2017.03.018

Rong, M., Xinhou, Z., and Changchun, S. (2014). Effects of nitrogen addition on plant functional traits in freshwater wetland of Sanjiang Plain, Northeast China. *Chin. Geogr. Sci.* 24, 674–681. doi: 10.1007/s11769-014-0691-4

Rooth, J. E., Stevenson, J. C., and Cornwell, J. C. (2003). Increased sediment accretion rates following invasion by *Phragmites australis*: the role of litter. *Estuaries* 26, 475–483. doi: 10.1007/BF02823724

Rothman, E., and Bouchard, V. (2007). Regulation of carbon processes by macrophyte species in a Great Lakes coastal wetland. *Wetlands* 27, 1134–1143. doi: 10.1672/0277-5212(2007)27[1134:ROCPBM]2.0.CO;2

Rubio, G., Casasola, G., and Lavado, R. S. (1995). Adaptations and biomass production of two grasses in response to waterlogging and soil nutrient enrichment. *Oecologia* 102, 102–105. doi: 10.1007/BF00333316

Rubio, G., and Lavado, R. S. (1999). Acquisition and allocation of resources in two waterlogging-tolerant grasses. *New Phytol.* 143, 539–546. doi: 10.1046/j.1469-8137.1999.00482.x

Sax, D. F., and Gaines, S. D. (2003). Species diversity: from global decreases to local increases. *Trends Ecol. Evol.* 18, 561–566. doi: 10.1016/S0169-5347(03)00224-6

Schlaepfer, M. A., Sax, D. F., and Olden, J. D. (2011). The potential conservation value of non-native species. *Conserv. Biol.* 25, 428–437. doi: 10.1111/j.1523-1739.2010.01646.x

Schlaepfer, M. A., Sax, D. F., and Olden, J. D. (2012). Toward a more balanced view of non-native species. *Conserv. Biol.* 26, 1156–1158. doi: 10.1111/j.1523-1739.2012.01948.x

Simard, R. (1993). "Ammonium acetate-extractable elements," in *Soil Sampling and Methods of Analysis, Canadian Society of Soil Science*, ed M. R. Carter (Boca Raton, FL: Lewis Publishers), 39–42.

Simberloff, D. (2011). How common are invasion-induced ecosystem impacts? *Biol. Invasions* 13, 1255–1268. doi: 10.1007/s10530-011-9956-3

Swearingen, J., Saltonstall, K., and Tilley, D. (2012). *Phragmites Field Guide: Distinguishing Native and Exotic Forms of Common Reed (Phragmites australis) in the United States*. USDA Natural Resources Conservation Service Technical Note TN Plant Materials No. 56. Available online at: https://www.nrcs.usda.gov/Internet/FSE_PLANTMATERIALS/publications/idpmctn11494.pdf

Tho, B. T., Sorrell, B. K., Lambertini, C., Eller, F., and Brix, H. (2016). Phragmites australis: how do genotypes of different phylogeographic origins differ from their invasive genotypes in growth, nitrogen allocation and gas exchange? *Biol. Invasions* 18, 2563–2576. doi: 10.1007/s10530-016-1158-6

Tulbure, M. G., and Johnston, C. A. (2010). Environmental conditions promoting non-native *Phragmites australis* expansion in Great Lakes coastal wetlands. *Wetlands* 30, 577–587. doi: 10.1007/s13157-010-0054-6

Tulbure, M. G., Johnston, C. A., and Auger, D. L. (2007). Rapid invasion of a Great Lakes coastal wetland by non-native *Phragmites australis* and *Typha*. *J. Great Lakes Res.* 33, 269–279. doi: 10.3394/0380-1330(2007)33[269:RIOAGL]2.0.CO;2

United States-Canada (2013). *Great Lakes Water Quality Agreement*. Available online at: http://ijc.org/files/tinymce/uploaded/GLWQA2012.pdf (accessed August 1, 2018).

Vitule, J. R. S., Freire, C. A., Vazquez, D. P., Nuñez, M. A., and Simberloff, D. (2012). Revisiting the potential conservation value of non-native species. *Conserv. Biol.* 26, 1153–1155. doi: 10.1111/j.1523-1739.2012.01950.x

Watson, S. B., Miller, C., Arhonditsis, G., Boyer, G. L., Carmichael, W., Charlton, M. N., et al. (2016). The re-eutrophication of Lake Erie: harmful algal blooms and hypoxia. *Harmful Algae* 56, 44–66. doi: 10.1016/j.hal.2016.04.010

Wetzel, P. R., and van der Valk, A. G. (2005). The biomass and nutrient levels of *Calamagrostis canadensis* and *Carex stricta* under different hydrologic and fungicide regimes. *Can. J. Bot.* 83, 124–130. doi: 10.1139/b04-142

Wilcox, K. L., Petrie, S. A., Maynard, L. A., and Meyer, S. W. (2003). Historical distribution and abundance of *Phragmites australis* at Long Point, Lake Erie, Ontario. *J. Great Lakes Res.* 29, 664–680. doi: 10.1016/S0380-1330(03)70469-9

Windham, L. (2001). Comparison of biomass production and decomposition between *Phragmites australis* (Common Reed) and *Spartina patens* (Salt Hay Grass) in brackish tidal marshes of New Jersey, USA. *Wetlands* 21, 179–188. doi: 10.1672/0277-5212(2001)021[0179:COBPAD]2.0.CO;2

Windham, L., and Ehrenfeld, J. G. (2013). Net impact of a plant invasion on nitrogen-cycling processes within a brackish tidal marsh. *Ecol. Appl.* 13, 883–897. doi: 10.1890/02-5005

Zedler, J. B., and Kercher, S. (2005). Wetland resources: status, trends, ecosystem services, and restorability. *Annu. Rev. Environ. Resour.* 30, 39–74. doi: 10.1146/annurev.energy.30.050504.144248

Conflict of Interest Statement: The authors declare that the research was conducted in the absence of any commercial or financial relationships that could be construed as a potential conflict of interest.

frontiers in Environmental Science

ORIGINAL RESEARCH
published: 19 July 2019
doi: 10.3389/fenvs.2019.00116

Small-Scale Spatial Variability of Soil Chemical and Biochemical Properties in a Rewetted Degraded Peatland

Wakene Negassa, Christel Baum, Andre Schlichting, Jürgen Müller and Peter Leinweber*

Faculty of Agricultural and Environmental Sciences, University of Rostock, Rostock, Germany

There is indication in the literature that degradation of natural peatlands reduced spatial variability of soil chemical and biochemical properties. However, we lack empirical data on the impact of rewetting peatland on the spatial variability of these properties. We investigated the spatial variability of the soil properties of a peatland that has been used for extensive and intensive grazing from 1400 to 1970. The peatland has been rewetted since 1970, and we collected 50 soil samples from 50 grid cells of 0–10, and 10–20 cm soil depths in October 2001. We measured 33 important soil chemical and biochemical properties and evaluated the data with descriptive and geospatial statistical analyses. The concentrations of most plant available nutrients were low with high coefficients of variation (CV) that ranged from 15 to 117%, whereas the CV of most of the total and oxalate extracted elements was ≤15% CV. The degree of phosphorus (P) saturation (DPS) and P saturation ratio (PSR) were 11% and 0.05, which were low as compared to the threshold levels of 25% DPS and 0.11 PSR for mineral and wetland soils. The microbial biomass C and N ranged from 389 to 2,463 mg kg^{-1} and 32 to 215 mg kg^{-1} at the depth of 0–10 cm and from 343 to 1570 mg kg^{-1} and 14 to 160 mg kg^{-1} at the depth of 10–20 cm, respectively. Similarly, the dehydrogenase and β-glucosidase activities were lower by 76 and 61% at the soil depth of 10–20 cm compared to the upper 10 cm. The geospatial statistical analysis revealed that 87% of the soil chemical properties were spatially correlated and 85% of the spatial correlation was strong with <0.20 nugget to sill ratio at 5 to 12 m ranges. Similarly, 86 and 71% of the biochemical properties were strongly spatially correlated at the depth of 0–10, and 10–20 cm, respectively, with ≤0.16 nugget to sill ratio at the short ranges (4 to 6 m). The strong spatial correlation of most of the soil chemical and biochemical properties at short ranges indicate the high variability of the rewetted peatland.

Keywords: biochemical properties, oxalate extractable soil nutrients, soil variability, spatial correlation, nugget

OPEN ACCESS

Edited by:
Fereidoun Rezanezhad, University of Waterloo, Canada

Reviewed by:
Tim Moore, McGill University, Canada
Dominik Zak, Aarhus University, Denmark

****Correspondence:***
Wakene Negassa
wakene.chewaka@uni-rostock.de

Specialty section:
This article was submitted to Biogeochemical Dynamics, a section of the journal Frontiers in Environmental Science

Received: *10 April 2019*
Accepted: *08 July 2019*
Published: *19 July 2019*

Citation:
Negassa W, Baum C, Schlichting A, Müller J and Leinweber P (2019) Small-Scale Spatial Variability of Soil Chemical and Biochemical Properties in a Rewetted Degraded Peatland. Front. Environ. Sci. 7:116. doi: 10.3389/fenvs.2019.00116

INTRODUCTION

Soil chemical and biochemical properties may vary strongly from small scale to large scale that influence services and functions obtained from peatland ecosystems (Jenerette and Wu, 2004). The heterogeneity is apparent in peatlands at landscape, habitat, and microscales (Larkin, 2016). A previous study showed that spatial heterogeneity of soil chemical and biochemical properties can be

reduced after degradation of natural peatlands (Brooks et al., 2005). However, rewetting degraded peatlands could create spatially heterogeneous soil properties (Gallardo, 2003). For instance, alternation of water loads to peatlands can alter soil chemical and biochemical properties (Kercher and Zedler, 2004) and plant community composition (Mentzer et al., 2006) thereby nutrient transformations and release not only at the landscape scale but also at small scale. The success of restoration of degraded peatland by rewetting can depend on the type of peatland, intensity of initial degradation, peat characteristic, biota community, and climatic condition (Joosten and Clarke, 2002; Höper, 2007). These important biotic and abiotic factors can cause spatial variability that could influence the biogeochemistry of natural and rewetted peatland ecosystems (Whiting and Chanton, 2001; Bubier et al., 2003).

Most European countries, including Germany, have degraded more than 85% of their original peatlands (Joosten, 1997; Lamers et al., 2015; Joosten et al., 2017). It has been estimated that 930 000 ha of peatlands have been drained to increase the area available for agriculture in Germany and about one-third of the degraded peatlands is located in Mecklenburg–West Pomerania, northern Germany (Förster, 2009). However, considerable efforts have been undertaken to restore the degraded peatlands since 2000. Between 2000 and 2008, about 10% of the degraded peatlands was rewetted (Förster, 2009). Although the biogeochemistry of peatlands has been researched intensively (Reddy and DeLaune, 2008; Strack, 2008; Landry and Rochefort, 2012), no information is available on the influence of rewetting degraded peatlands on spatial variability of soil chemical and biochemical properties.

A number of studies have been conducted to understand the effects of peatland restoration on chemical properties and greenhouse gas emissions (Höper et al., 2008; Couwenberg, 2009; Haapalehto et al., 2011; Krüger et al., 2015; Karki et al., 2016; Herzsprung et al., 2017), bioavailable nutrients (Dietrich and MacKenzie, 2018), water table depth and vegetation composition (Bantilan-Smith et al., 2009; Haapalehto et al., 2011; Görn and Fischer, 2015). Most previous studies investigated chemical and biochemical properties in contrasting peatland management systems (Groffman et al., 1996; Bruland et al., 2006; Dick and Gilliam, 2007; Nkheloane et al., 2012), microbial colonization, and activities in constructed wetlands (Hunt et al., 1997; Truu et al., 2009), rewetted (Baum et al., 2003; Andersen et al., 2006), and natural peatlands (Gutknecht et al., 2006). Studies conducted in rewetted peatlands also mostly focused on methane, nitrous oxide, and carbon dioxide emissions (e.g., Waddington and Roulet, 1996; Dasselaar et al., 1998; Krohn et al., 2017). A few studies also investigated the phosphorus status in degraded peatland and wetland soils (Litaor et al., 2003; Zak et al., 2008; Nair, 2014; Emsens et al., 2017).

Soil spatial variability can develop from uneven litter decomposition, vegetation composition, soil moisture content, topographic position, and historical land use, and soil management practice (Baldrian, 2014). These factors could influence chemical and biochemical processes differently in different peatlands. For example, dehydrogenase enzyme mostly operates under anaerobic soil conditions (Wolinska and Stepniewska, 2012), whereas protease and acid phosphatase activities decline as soils become more anaerobic (Reddy and DeLaune, 2008). Furthermore, the rate of synthesis, release and stability of phosphatase depends on soil pH, and soil organic matter (SOM) (Tabatabai, 1994; Baldrian, 2014). The sensitivity of a soil enzyme to pH changes is variable from one soil enzyme to another (Acosta-Martínez and Tabatabai, 2000). A few studies conducted on soils in mountain forest indicated that acid phosphatase and β-glucosidase activities were spatially correlated at the range of 3 m (Yang et al., 2018), whereas, microbial biomass showed spatial variability within 6 m (Štursová et al., 2016). Similarly, soil pH and total N showed strong spatial correlation in the range of ∼0.4 m to a few meters because of variations in soil moisture, vegetation, soil, and management practices (Baldrian, 2014).

Vegetation composition and distribution can significantly influence soil chemical and biochemical properties, and thereby restoration of rewetted degraded peatlands (Borga et al., 1994; Boon et al., 1996; Dick and Gilliam, 2007; Wiedermann et al., 2017). For instance, restoration of a degraded peatland depends on the recolonization of the original flora, and fauna that play a leading role in peat accumulation and nutrient cycle. Understanding the plant community composition and distribution is particularly important in a rewetted peatland for monitoring a success of a degraded peatland restoration process (Zerbe et al., 2013).

Employing conventional soil sampling and statistical analysis such as composite sampling with the assumptions of sample independent, normal sample distribution, and a randomized experimental design have less power in detecting spatial variability of soil properties than geospatial analysis (Rossi et al., 1992; Kravchenko et al., 2006; Nkheloane et al., 2012). Suitable geospatial analysis can help detect spatial variability of soil chemical and biochemical properties. The geospatial analysis has been also used successfully in detecting spatial distributions of SOM (Kravchenko et al., 2006; Kumar, 2015; Liu et al., 2015). The results of many studies indicated that correlation, linear regression and regression kriging captured spatial variability of mineral soils (Kumar et al., 2012; Wang et al., 2013). However, only a few studies used such a statistical tool to understand spatial correlation of soil chemical and biochemical properties in peatlands (Nkheloane et al., 2012; Marton et al., 2015).

The scale at which samples are collected to study spatial variability of soil chemical and biochemical properties can influence interpretations of biogeochemical processes in peatlands (Hunt et al., 1997; Gutknecht et al., 2006). To understand spatial variability in rewetted peatland, small-scale soil sampling is required as the soil environments could be heterogeneous depending on management practices and historical land uses (Klironomos et al., 1999; Truu et al., 2009). However, little information is available on spatial variability of soil chemical, and chemical properties at small scale in rewetted peatlands. Therefore, the objective of the present study was to investigate the spatial variability of selected soil chemical and biochemical properties and vegetation composition of a rewetted degraded fen peatland.

MATERIALS AND METHODS

Site Description and Soil Sampling

The study site is located in a telmatic peatland of Warnow Valley, Northern Germany (**Figure 1A**). The site is part of about 250,000 hectares of peatlands in the Federal State of Mecklenburg-Western Pomerania, Northeast Germany. Historically, the first references to any agricultural use of these fens near Rostock date back to 1471, and the use has been very extensive for more than 400 years (Hanschke, 1996). Nearby the sampling site, there are ponds originating from peat excavation after the mid-Nineteenth century; however, the most intensive of the peatland has been started immediately after the WW2 (1945–59). Lowering of groundwater level to enable peat excavation concurrently allowed a stepwise intensification of the previously only occasional agricultural use of the peatland, which however remained only moderately intensive until the 1960s. In almost all similar fen peatlands in Northern Germany, drainage, and agricultural use have been intensified from the early 1970s on by digging deeper drainage ditches that enabled heavy machinery for compacting meadows, fertilizer application, and grass harvest to travel at the fen peatland. Two to three cuts for silage and intermitted mineral fertilizer applications became the common management regime, which essentially led to peat subsidence and mineralization, nutrient transfers into waterways (Warnow River). The intensive uses degraded the site so severely and the meadows became unproductive, cleaning of drainage ditches was given up (end 1950s). Finally, the areas were taken out of a regular agricultural use (end 1970s) and gradually rewetted passively because the drainage ditches get closed by sediment accumulation (Hanschke, 1996). The degradation of the fenland probably resulted in a more heterogeneous soil structure because of stamping through from the undulated mineral ground beneath the peat. The passive rewetting of the degraded fenland likely reduced further peat oxidation although the surface soil of the peatland usually dries for at least 2 months during summer season (June to August).

The climate is characterized by annual means of 592 mm precipitation and 8.4°C temperature. The thickness of the peat layer is about 2.7 m and classified as Eutri-Ombric Histosol and Hemic Haplofibrist according to the World Reference Base for Soil Resources (IUSS Working Group WRB, 2015), and Soil Survey Staff (1999), respectively.

The soil samples were collected from the upper 0–10 and 10–20 cm depths after 20 years of rewetting the degraded peatland in October 2001. Samples from both depths were used for the analyses of pH, water content, and biochemical properties. Since the contents of SOM, plant available, total and oxalate-extracted elements were similar in both depths, we used only the data generated from the 0 to 10 cm depths for these soil variables. The soil samples were collected from 50 grid cells with an individual grid cell size of 3 m × 3 m (**Figure 1B**). A soil sample was collected from each grid cell using a Macauley sampler. After the sampling, the plant roots were removed, and the samples were homogenized. Soil water content at sampling was determined by gravimetry, whereas SOM was determined by loss-on-ignition method. Field moist samples were used for the biochemical analysis immediately after sampling or stored in a freezer until required for analysis. Separate subsamples were air dried at 35°C for the determination of selected soil chemical properties.

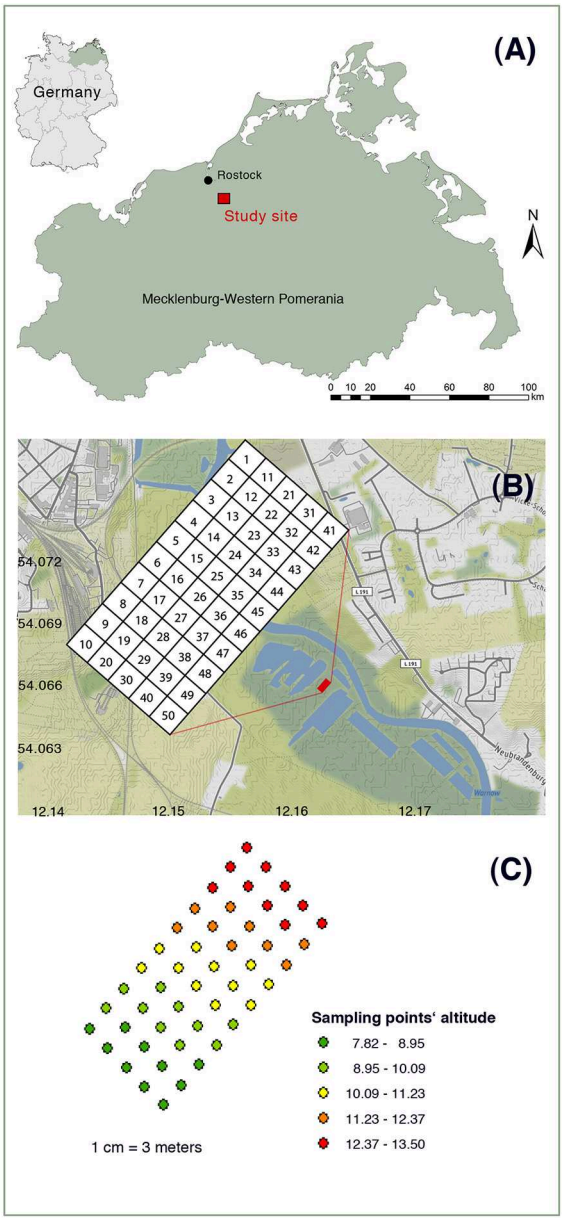

FIGURE 1 | Location of the study site **(A)**, plot arrangement **(B)**, and elevations **(C)** of peat sampling plots.

Chemical and Biochemical Analyses

The soil pH was determined by suspending the samples in 0.01 M $CaCl_2$-solution with 1:2 ratio of sample to solution using a glass electrode and pH-meter. The Al, Fe, Mn, and P associated with non-crystalline minerals were extracted by acid ammonium oxalate (Schwertmann, 1964; Courchesne et al., 2008), whereas the P was extracted by sodium hypobromide (P_{hyp}), and microwave assisted acid digestion (total P) (Dick

and Tabatabai, 1977). The concentration of oxalate extracted elements and total P were determined by inductively coupled plasma-optical emission spectroscopy (ICP-OES) (Jobin Yvon 238 Ultrace, Instruments S.A. GmbH, D-85630 Grasbrunn, Germany). Furthermore, the degree of P saturation (DPS) was calculated using the following formula as suggested for wetland soils by Nair and Reddy (2013):

$$DPS = \frac{Pox}{\alpha\ [Feox\ +\ Alox]}$$

where P_{ox}, Fe_{ox}, and Al_{ox} were oxalate extracted P, Fe, and Al in molar concentrations. α is an empirical factor to account for the fraction of Fe and Al responsible for P sorption and researchers usually use 0.5 (Litaor et al., 2003; Nair, 2014). When the corrective factor α is omitted, the P saturation ratio (PSR) can be used which is a simple ratio of molar P_{ox} to molar (Fe_{ox} + Al_{ox}) (Nair, 2014).

The amounts of C_{org} and total N were determined by dry combustion using a CNS analyzer (Vario EL, Elementar Analysensysteme GmbH, D-63452 Hanau, Germany). The plant

TABLE 1 | Gravimetric water (GW) content and pH in the surface and subsurface soil of a rewetted peatland.

0–10 cm soil depth	Mean	Median	Minimum	Maximum	Skewness	Kurtosis	SD	CV%
GW (%)	78	79	66	83	−1.18	0.55	4	6
pH_{H2O}	6.54	6.52	6.06	7.20	0.00	0.00	0.26	4
pH_{CaCl2}	5.98	5.97	5.60	6.74	1.05	1.80	0.24	4
10-20 cm SOIL DEPTH								
GW (%)	72	73	63	79	−0.79	0.42	4	5
pH_{H2O}	6.22	6.20	5.77	6.75	0.00	0.00	0.22	4
pH_{CaCl2}	5.82	5.81	5.56	6.17	0.00	0.00	0.13	2

TABLE 2 | Selected plant available nutrients (mg kg^{-1} dry soil) in the surface soil of a rewetted peatland.

	Mean	Median	Minimum	Maximum	Skewness	Kurtosis	SD	CV%
P	1.3	1.33	0.4	2	−0.1	0.5	0.4	28
Mg	17	171	113	234	0.1	0.0	26	15
S	113	109	55	229	0.9	0.9	37	33
Fe	1.7	1.38	0.5	5	1.5	2.4	0.9	55
Mn	5.6	2.50	0.6	27	1.6	2.2	7	117

TABLE 3 | Soil organic matter, total, and ammonium oxalate extractable elements concentrations in the surface soil of a rewetted peatland.

(g kg^{-1} dry soil)	Mean	Median	Minimum	Maximum	Skewness	Kurtosis	SD	CV%
SOM	640	660	490	760	−0.52	−0.68	70.0	11
C_{org}	320	330	250	360	−0.52	−0.46	30.0	9
N	30	30	20	30	−0.67	−0.30	2.0	9
S	6	6	5	8	0.23	−0.80	1.0	12
P	1.5	1.5	1.4	1.8	−0.37	0.04	0.1	10
P_{hypo}	1.28	1.28	0.98	1.52	−0.20	−0.26	0.13	10
P_{ox}	0.44	0.44	0.32	0.58	0.11	−0.73	0.07	15
K	0.50	0.49	0.32	0.65	0.23	0.32	0.07	14
Ca	25	25	17	29	−0.63	−0.44	3.0	13
Mg	1.1	1.1	1.0	1.3	−0.27	0.07	0.1	7
Fe	16	16	11	20	−0.12	0.84	1.7	11
Fe_{ox}	13	13	9	16	−0.63	0.05	1.7	14
Al	8	8	6	10	−0.43	0.69	0.8	11
Al_{ox}	1.14	1.17	0.85	1.53	0.20	1.43	0.12	10
Mn	0.6	0.6	0.3	0.8	−0.20	−0.54	0.1	22
Mn_{ox}	0.4	0.4	0.2	0.7	−0.04	−0.52	0.1	24
DSP	10.57	10.75	7.47	13.16	−0.28	0.06	1.17	11
PSR	0.05	0.05	0.04	0.07	0.09	−0.03	0.01	13

hypo, hypobromite extractable P; ox, oxalate extractable P; Fe, Al, and Mn; DPS, degree of P saturation in percent; and PSR, P saturation ratio; SOM, soil organic matter.

available nutrients were extracted by 0.01 M $CaCl_2$ and measured by ICP-OES. The total K, Ca, Mg, Al, Fe, and Mn were extracted by aqua regia digestion after calcination of the soil samples and ICP- OES was used to determine their concentrations.

The microbial biomass carbon and nitrogen were extracted by 0.5 M K_2SO_4 solution after fumigation following the method recommended by Vance et al. (1987) and modified by Joergensen (1995). The biomass carbon was estimated using the following formula:

$$Microbial\ biomass\ C = EC\ ^{*}KEC \quad (1)$$

$$Microbial\ biomass\ N = EN\ ^{*}KEN \quad (2)$$

Where EC is the organic C extracted from fumigated soil sample minus the organic C extracted from non-fumigated soil sample, KEC = 0.45 is the proportionality factor to convert EC to microbial biomass C. EN: the flush of NH_4^+-N due to fumigation, KEN = 0.57 was the proportionality factor to convert EN to microbial biomass N (Jenkinson, 1988). The dehydrogenase, acid phosphatase and β-glucosidase activities were determined following the procedures outlined by Tabatabai (1994), whereas the protease activity by the method of Ladd and Buttler (1972).

Vegetation Analysis

We recorded species compositions of each of grid cell in August 2008, and the percent of the vegetation cover of each 50 grid cell was estimated by the "vegan" version 2.4-5 (Oksanen et al., 2017) using the R environment version 3.3.2. (R Development Core Team 2016). The vegetation data were analyzed for species diversity using the Shannon and the Simpson indices and for grid cell vegetation composition's dissimilarity by the Bray-Curtis and the Gower indices. The multivariate ordination methods "detrended correspondence analysis" (DCA) and "non-metric multidimensional scaling" (NMDS) were used to explore compositional gradients in vegetation patterns across the grid cells. Soil chemical and biological parameters were fitted to NMDS ordination to analyze soil-vegetation-relationships. Goodness of fit was tested by permutation ($n = 999$). Only traits with a marked correlation to the ordination matrix at the $p < 0.1$ level were plotted as vectors into the ordination frame.

Statistical Analysis

The descriptive statistics, correlation matrix and principal component analysis of the gravimetric water content, chemical, and biochemical properties such pH, SOM, plant available nutrients, oxalate extractable, and total elements, soil microbial biomass, and enzymes activities were analyzed using SAS version 9.4 (SAS Institute Inc., 2013). However, the spatial correlation was analyzed by Geostatistical software GS^{+TM} version 7 (Gamma Design Software, Plainwell, Michigan, USA). We run a semivariogram analysis to evaluate the spatial correlation of soil chemical and biochemical properties. A typical semivariogram can be described by nugget effect, range and sill. Nugget represents micro-scale variation at $h = 0$, range is the distance at which data are no longer correlated, and sill is the plateau where the semivariogram reaches at the range (Berry, 2005). The soil chemical and biochemical properties were fitted to linear, spherical, exponential, and Gaussian models to obtain best fit based on the lowest residual sum of squares (RSS). The semivariogram was interpreted based on nugget: sill ratio. The nugget to sill ratio indicates what percent of the overall variance is found at a distance smaller than the smallest lag interval, and it gives a sense of how much variance was accounted for in the model. The nugget: sill ratio can be interpreted as strong spatial correlation (<0.25), and moderate (0.25–0.75), and no spatial correlation (>0.75) (Cambardella et al., 1994). The low nugget: sill ratio (<0.25) indicates a large part of the variance is introduced spatially that implying a strong spatial dependence and vice versa for the large nugget: sill ratio.

TABLE 4 | Soil microbial biomass and enzyme activities in surface and subsurface soil of a rewetted peatland.

0–10 cm soil depth	Mean	Median	Min.	Max.	Skewness	Kurtosis	SD	CV%
Biomass C (mg kg^{-1})	1,277	1,210	389	2,463	0.68	0.90	402	31
Biomass N (mg kg^{-1})	120	122	32	215	−0.08	−0.72	45	37
MBC: MBN	11	10	4	23	1.30	1.54	4	36
Dehydrogenase (μg TPF g $soil^{-1}$)	3,044	2,876	513	7,910	0.84	1.49	1,483	49
APA (μg p-Nitrophenol g $soil^{-1}$ h^{-1})	851	862	539	1,106	−0.59	−0.26	138	16
β-Glu (μg p-Nitrophenol g $soil^{-1}$ h-1)	3,533	3,670	1,405	5,747	0.03	−0.16	993	28
Protease (μg Amino-N g $soil^{-1}$ 15 h^{-1})	301	295	130	462	0.06	−0.32	76	25
10–20 cm SOIL DEPTH								
Microbial biomass C (mg kg^{-1})	689	640	343	1,570	1.60	3.66	240	35
Microbial biomass N (mg kg^{-1})	54	47	14	160	1.52	4.14	26	48
MBC: MBN	14	13	6	30	1.34	2.06	5	36
Dehydrogenase (μg TPF g $soil^{-1}$)	717	633	211	2,016	1.24	1.19	415	58
APA (μg p-Nitrophenol g $soil^{-1}$ h^{-1})	652	662	476	911	0.33	−0.25	105	16
β-Glu (μg p-Nitrophenol g $soil^{-1}$ h^{-1})	1,379	1,354	639	2,294	0.52	1.49	286	21
Protease (μg Amino-N g $soil^{-1}$ 15 h^{-1})	283	266	147	501	0.56	0.04	79	28

MBC, microbial biomass C; MBN, microbial biomass N; APA, acid phosphatase; β-Glu, β-glucosidase; Min, minimum; Max, maximum. All concentrations were kg^{-1} dry soil.

RESULTS

Gravimetric Water Content, and Plant Nutrient Elements

The gravimetric water content and pH were slightly higher at the soil depth of 0–10 than at the 10–20 cm (**Table 1**), and the water content was in the range of 66 to 83% for the 0–10 cm depth, and 63 to 79% for the 10–20 cm soil depth. However, depths did not change pH_{H2O} and pH_{CaCl2}, but the pH_{H2O} was slightly higher than pH_{CaCl2} at both depths. The coefficient of variation (CV) of the water content at the 0–10 cm soil depth was higher than at the 10–20 cm soil depth. Concentration of the selected plant available nutrients were low except for sulfur (S) and magnesium (Mg) (**Table 2**). Furthermore, the CV of most plant available nutrients were high and ranged from 15 to 117%. The CV of plant available Mn was particularly very high (117%) followed by plant available Fe (55%).

TABLE 5 | Pearson correlation coefficient among biochemical activities and plant available nutrients in surface of a rewetted peatland.

	C_{mic}	N_{mic}	DHA	APA	Mg	Mn
N_{mic}	0.75***					
APA	0.34*	0.48**	0.28*			
GLU	0.33*	0.23	0.28*	0.36**		
PTA	−0.09	−0.08	−0.27	−0.39		
Fe	0.17	0.13	0.14	0.11		
Mg	0.13	0.23	−0.41	−0.03		
Mn	0.17	0.22	−0.03	0.02	0.42*	
P	0.11	0.33*	−0.05	0.05	0.50***	0.45**

*Number of observations: 50, *, **, and *** indicate significant correlation coefficient at $P < 0.05$, $P < 0.01$, and $P < 0.001$, respectively. C_{mic}, microbial biomass C; N_{mic}, Microbial biomass N; DHA, Dehydrogenase; APA, Acid phosphatase; GLU, β-Glucosidase.*

SOM, Oxalate Extracted, and Total Elements

The concentrations of SOM, oxalate-extracted, and total elements are presented in **Table 3**. The SOM, C_{org} and total N were in the range of 490 to 760, 250 to 360, and 20 to 30 g kg^{-1}, respectively, with CV in the range of 9 to 11%. Similarly, the concentration of total P and S were in the range of 1.4 to 1.8, and 5 to 8 g kg^{-1}, respectively, and their CVs were in the range of 10 and 12%. The mean mass ratios of C: N, C: P, and C: S calculated from the **Table 3** were 11, 213 and 53, respectively. Similarly, the N: P, and N: S ratios were 20 and 5, respectively. The hypobromide-extracted P (P_{hyp}) was 85% of the total P extracted by aqua regia, whereas the P_{ox} was about 29% of the total P (**Table 3**). The concentration of Ca was the highest followed by total Fe and Al excluding C_{org} and total N, whereas the concentrations of total K and Mn were the lowest.

The oxalate-extracted elements were in the ranges of 0.32 to 0.58 g kg^{-1} for P_{ox}, 9 to 16 g kg^{-1} for Fe_{ox}, 0.85 to 1.53 g kg^{-1} for Al_{ox}, and 0.2 to 0.7 g kg^{-1} for Mn_{ox} (**Table 3**). These were 29, 81, 14, and 67% of the total concentrations of P, Fe, Al, and Mn, respectively. The CV of the oxalate extracted elements were in the range of 10 to 24%, and the CV of Al_{ox} was the lowest, whereas the CV of Mn_{ox} was the highest. Furthermore, the DPS, and PSR were in the range of 7.47 to 13.16% and 0.04 to 0.07, respectively

TABLE 6 | Pearson correlation coefficients among soil organic matter, selected available plant nutrients and total element concentrations in surface soil of a rewetted peatland.

	S_t	N_t	C_{org}	SOM	P_t	P_{pyro}	P_{ox}	Mn_t	Mn_{ox}	Mg_t	Fe_t	Fe_{ox}	Ca_t	Al_t
N_t	0.74***													
C_{org}	0.77***	0.93***												
SOM	0.72***	0.93**	0.94***											
P_t	0.30	0.68***	0.59***	0.73***										
P_{pyro}	0.75***	0.85***	0.85***	−0.74***	0.50***									
P_{ox}	−0.86***	−0.85***	−0.85***	0.99***	0.01	−0.79***								
Mn_t	−0.1	0.51***	0.40**	0.53***	0.73**	0.39**	−0.03							
Mn_{ox}	−0.20	0.07	0.00	0.18	0.55***	0.18	0.13	0.76***						
Fe_t	−0.1	0.25	0.24	0.28	0.38**	0.26	−0.10	0.57***	0.58***	0.12				
Fe_{ox}	0.08	0.29*	0.24	0.06	0.57***	0.29*	−0.01	0.71***	0.72***	−0.22	0.82***			
Ca_t	0.47***	0.85***	0.80***	0.90***	0.83***	0.32*	0.11	0.77***	0.60***	−0.11	0.46***	0.69***		
Al_t	0.00	0.36**	0.35*	0.40**	0.48***	0.25	−0.01	0.64***	0.66***	0.03	0.95***	0.89***	0.55***	
Al_{ox}	−0.02	−0.02	0.00	−0.09	−0.10	0.00	−0.06	−0.28	0.01	0.14	−0.03	−0.18	−0.27	−013
S_a	0.52***	0.11	0.1	0.12	−0.14	−0.22	0.23	−0.36**	−0.30*	0.11	−0.24	−0.11	−0.05	−0.16
P_a	0.45***	0.42**	0.40**	0.45***	0.21	−0.14	0.23	0.02	−0.16	0.19	−0.01	0.13	0.30*	0.05
Mn_a	0.36*	0.16	0.19	0.09	−0.1	−0.23	0.19	−0.27	−0.24	0.42**	−0.03	−0.11	−0.05	−0.05
Mg_a	0.81***	0.66***	0.73***	0.70***	0.23	−0.13	0.29*	−0.07	−0.10	0.34*	−0.09	0.13	0.46***	0.00
Fe_a	0.12	0.01	−0.05	−0.02	0.04	−0.12	0.18	−0.12	−0.11	0.05	−0.34*	−0.29*	−0.01	−0.35

*Number of observations: 50, *, **, and *** indicate significant correlation coefficient at $P < 0.05$, $P < 0.01$, and $P < 0.001$, respectively, t, total element; a, plant vailable nutrient; ox, oxalate extracted, hypo, hypobromite extractable P; See **Tables 2**, **3** for the unit of each parameter.*

(**Table 3**). The CV of DPS and PSR were similar to the CV of total and oxalate extracted elements.

Biochemical Properties

The microbial biomass C ranged from 389 to 2,463 mg kg^{-1} (0–10 cm) and 343 to 1,570 mg kg^{-1} (10–20 cm). Furthermore, the microbial biomass N was in the ranges of 32 to 215 mg kg^{-1} (0–10 cm) and 14 to 160 mg kg^{-1} (10–20 cm). This resulted in microbial biomass C: N ratios of 11 (0–10 cm) and 14 (10–20 cm) (**Table 4**). The microbial biomass C and N were low by 46 and 55% at the 10–20 cm soil depth, respectively, as compared to that of the 0–10 cm soil depth. Similarly, the dehydrogenase and β-glucosidase activities was low by 76 and 61%, and the acid phosphatase and protease activities were low by about 23 and 6% at the depth of 10–20 cm as compared to that of the 0–10 cm soil depth, respectively.

Relationships of Chemical and Biochemical Properties

The soil microbial biomass C was significantly ($P < 0.05$) correlated with the microbial biomass N, β-glucosidase, and acid phosphatase activities, whereas microbial biomass N was significantly correlated with the acid phosphatase activity (**Table 5**). Similarly, β-glucosidase activity was significantly correlated with dehydrogenase and acid phosphatase activities. However, there were no significant correlations between the biochemical activities and plant available nutrients except for the available P and microbial biomass N. We also observed a few significant correlations among the plant available elements. For instance, the plant available Mg was significantly correlated with plant available Mn and P.

The correlation of biochemical properties with the concentration of SOM, total and oxalate extracted elements were not significant ($P > 0.05$) except for the dehydrogenase activity which was significantly negatively correlated with total Ca, SOM, C_{org}, total N, and S (data not shown). However, the correlations among the SOM, total N, total S, total P, P_{hyp}, and P_{ox} and total Mn were highly significant ($P < 0.001$) (**Table 6**). These parameters were also strongly correlated with concentrations of most of the plant available nutrients. Similarly, the concentration of total Ca was strongly correlated with the concentration of SOM and most of the total elements. Furthermore, the concentration of total P was highly significantly correlated ($P < 0.001$) with P_{hyp}, Mn_{ox}, and Fe_{ox}, total Al, Ca, and total Fe. The concentration of total Mn was also strongly correlated with Mn_{ox}, total Fe, Fe_{ox}, total Ca, and total Al. The correlation among the concentration of some plant available nutrients and total elements were positive; however, the P_{ox} was significantly negatively correlated with the C_{org}, total S, total N, and P_{hyp}.

principal component analysis separated the biochemical properties in two depths in which the biochemical properties at the 0–10 cm depths mostly contributed to PC1 and those at the 10–20 cm mostly contributed to the PC2 (**Figure 2**). The PC1 explained about 23% of the total variance with the positive loading of microbial biomass C and N, acid phosphatase, β-glucosidase, dehydrogenase, and with the negative loading of protease of the 0–10 cm depth and β-glucosidase of 10–20 cm depth. On the other hand, PC2 explained 20% of the total variance with the positive loading of microbial biomass C and N, acid phosphatase, β-glucosidase, dehydrogenase, and negative loading of the protease at the depth of 10–20 cm. Furthermore, the principal component analysis separated the chemical properties into four main groups depending on their contribution to the total variance with positive and negative loadings where the PC1 explained 51 % and PC2 14% of the total variance (**Figure 3**). The high positive loading came from C_{org}, total N, DSP, hypobromide extracted P and water content, whereas total S, PSR, SOM, P_{ox}, Al_{ox}, Mn_{ox}, and pH-$CaCl_2$ contributed to the high negative loading.

Spatial Correlation of Chemical and Biochemical Properties

The nugget to sill ratio of soil pH_{H2O} and pH_{Cal2} were 0.07 and 0.16 at 6 and 10 m ranges, respectively, at the 0–10 cm soil depth (**Table 7**). All of the biochemical properties showed strong spatial correlation at the depths of 0–10 cm except for protease activity (**Table 7** and **Figure 4**). The strong spatial correlation was revealed by the lowest nugget to sill ratio, which was ≤0.07 except for microbial biomass C where the nugget to sill ratio was 0.27. At 10–20 cm peat depth, pH_{H2O}, pH_{Calcl2}, microbial biomass C had no spatial correlation since they were fitted best to the linear model. However, the microbial biomass and enzymes activities were strongly spatially correlated at the soil depth of 10–20 cm except for the microbial biomass C and dehydrogenase activity. The biochemical properties were not only spatially correlated but also the spatial correlation appeared at the shortest range of 4 to 9 m (**Table 7**). Overall, about 86, and 71% of the biochemical properties were strongly spatial correlated at the depth of 0–10 cm, and 10–20 cm, respectively.

The gravimetric water content, plant available nutrients, total and oxalate extracted elements showed strong spatial correlations (**Table 8**). In general, the nugget to sill ratio of 15 of the 24 soil properties were ≤0.1 at the ranges of 5 to 10 m which indicated the plant available and total elements were strongly spatially correlated at the short distance interval. Similarly, the DPS and PSR were strongly spatially correlated with the nugget to sill ratio of 0.17 and 0.16 at the range of 8 and 5 m, respectively. Among the 23 soil chemical properties, only Fe_{ox}, total Al, and Fe lacked spatial correlation, whereas plant available Mn and S, and total K showed moderate spatial correlation with the nugget to sill ratio of 0.32, 0.32, and 0.41, respectively (**Table 8**).

Vegetation Composition

The vegetation composition indicated the transition from wet grassland to extensive reed (*Phragmitis australis*) dominated vegetation (**Figure 4**). Turquois colored dots in the DCA-plot indicate the plot positions as arranged according to their similarity in plant composition. The position of the single species in the ordination space is given by the brown colored BCI-name, an abbreviation of their Latin names. Five plots differed markedly in their composition of the vegetation from the conglomerated rest. NMDS was based on a Bray & Curtis

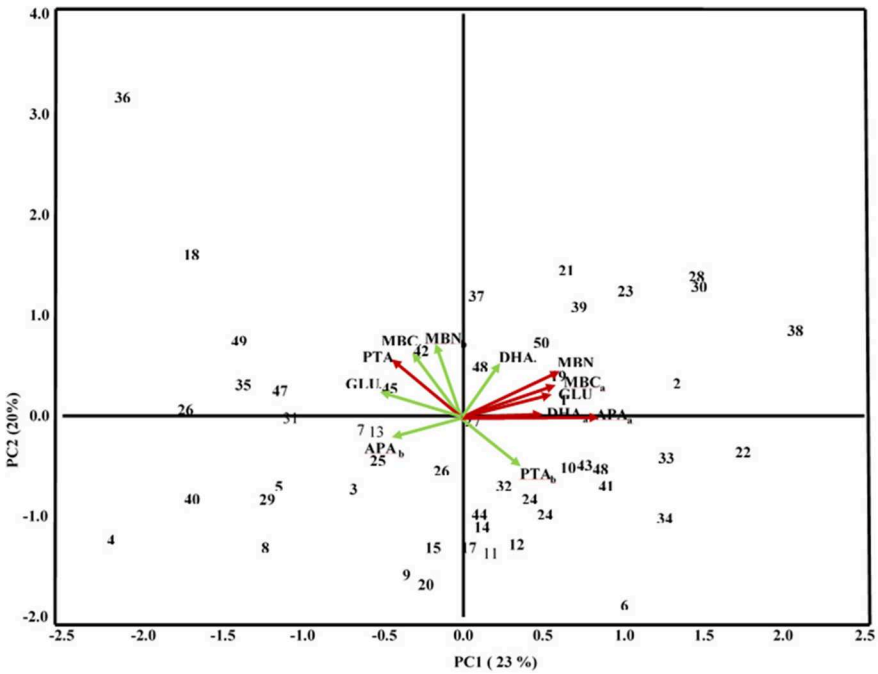

Loading values of PC1 and PC2

Properties	Factor1	Factor2
BMCa	**0.60**	0.36
BMNa	**0.58**	0.45
DHAa	**0.50**	0.04
APAa	**0.78**	0.01
GLUa	**0.57**	0.24
PTAa	**-0.42**	-0.20
BMCb	-0.33	**0.66**
BMNb	-0.16	**0.74**
DHAb	0.25	**0.55**
APAb	-0.42	**0.60**
GLUb	**-0.47**	0.26
PTAb	0.34	**-0.46**

FIGURE 2 | PCA of soil biochemical properties in a rewetted peatland. MBC, microbial biomass C; MBN, Microbial biomass N; DHA, Dehydrogenase; APA, Acid phosphatase; GLU, β-Glucosidase; PTA, Protease. The subscript "a" and "b" represent samples of 0–10 and 10–20 cm depths, respectively. Numbers in the Figure stand for the number of sampling grid cells.

dissimilarity matrix and allows a gradient analysis to explore possible soil-vegetation-relationships. Fitting of all analyzed soil-chemical and soil-biological traits as environmental variables and use them for gradient analyses was successful for N_{mic}, Al_{ox}, and Fe_{ox} (**Figure 4**).

DISCUSSION

Chemical and Biochemical Properties

The pH-H_2O and pH-$CaCl_2$ remained constant around 6 which can be attributed to the buffering capacity of CO_2 in the saturated peat soil (Reddy and DeLaune, 2008). Furthermore, the low CV of pH (**Table 1**) can be attributed to pH is the log transformed H^+ concentration. Different studies also reported ls ow CV for pH from the tropical wetlands (Nkheloane et al., 2012) and temperate bog and fens (Ulanowski and Branfireun, 2013; Barrett and Watmough, 2015).

The low concentrations of some plant available nutrients agreed with the results of previous study that indicated 0.01 M $CaCl_2$ recovered the lowest plant available P among 14 soil P extraction methods (Wuenscher et al., 2015). This is also true for the proportion of plant available P, Fe, and Mn to their respective concentrations of total elements that were in the range of 0.01 to 1% (**Tables 2**, **3**). We explain the low concentrations and proportions of 0.01 M $CaCl_2$ extracted plant available nutrients by the weak extractant and/or existence of the elements in stable organic and inorganic complex forms (**Table 2**). Such low concentrations of plant available nutrients could jeopardize the growth and development of plant communities adapted to the drained peatlands, although plants grown in anoxic soil conditions have their own mechanisms to adapt to low plant available nutrients (Elzenga and van Veen, 2010). The highest CV of the plant available Mn followed by Fe indicated the highest variability of these plant available nutrient elements in the studied peatland.

In contrast to the plant available nutrients, the CV of the total concentrations of most elements and SOM were low (**Table 3**) which indicates that the rewetting and drying cycles of peats did not influence the variability of these soil constituents. Similarly, low CV was reported for SOM from restored temperate peatland and tropical wetlands (Bruland et al., 2006; Nkheloane et al., 2012).

The Fe_{ox} was 81% of the total Fe that indicated the major proportion of total Fe existed in poorly crystalline mineral form (**Table 3**) (Courchesne et al., 2008). The higher concentration of Fe_{ox} than Al_{ox} and Mn_{ox} also showed the non-crystalline Fe in the rewetted peatland could control P solubility (Nair, 2014). However, the mean of (DPS 10.6%) and PSR (0.05) in the present study were very low as compared to the threshold level of P leaching which are 25% DPS in degraded peatland (Litaor et al., 2003) and 0.11 PSR for wetland soil (Nair and Reddy, 2013). This implies that potential loss of P to the ground and drainage water could be low. Although oxalate could recover some P associated with SOM, the proportion of P_{ox}, 29% of the total P, was comparable to the proportion of sum of inorganic P fractions in peat soils of northern Germany

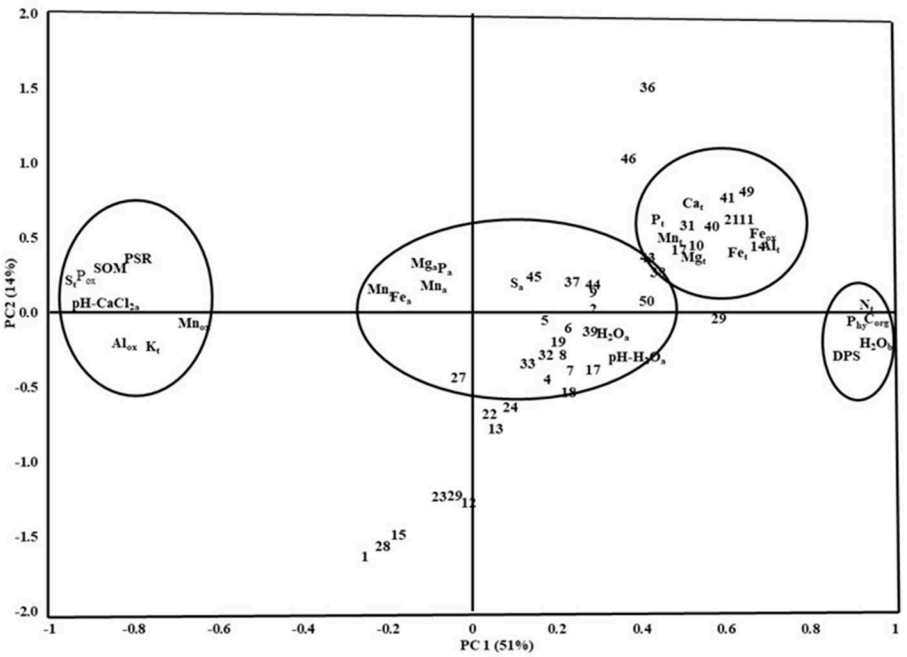

FIGURE 3 | PCA of soil chemical properties in a rewetted peatland. Subscript: "a": plant available elements, "t": total element, ox, oxalate extracted elements; Phy, hypobromide extracted P; H2Oa, water content of 0–10 cm soil depth; H2Ob, water content of 10–20 cm soil depth; DPS, degree of P saturation; PSR, P saturation ratio, numbers in the Figure stand for the number of sampling grid cells.

TABLE 7 | Spatial correlation of soil pH and biochemical properties in the surface and subsurface soil of a rewetted peatland.

0–10 cm soil depth	Model	Nugget	Sill	Range (m)	Nugget: Sill ratio	RSS	R^2
pH_{H2O}	Spherical	0.0056	0.0755	6	0.07	7.60×10^{-5}	0.66
pH_{CaCl2}	Exponential	0.011	0.0682	10	0.16	1.94×10^{-5}	0.92
Microbial C	Exponential	200	10,800	5	0.05	5.65×10^{8}	0.33
Microbial N	Spherical	662	2,429	13	0.27	3.50×10^{3}	0.99
Mic-C : Mic-N	Exponential	0.63	14.32	6	0.04	2.49	0.64
Dehydrogenase	Spherical	52,000	2,085,000	5	0.02	1.25×10^{11}	0.39
Acid phosphatase	Spherical	310	19,070	5	0.02	8.23×105	0.83
β- Glucosidase	Spherical	47,000	1,035,000	5	0.05	3.06×10^{9}	0.79
Protease	Linear						
10–20 cm SOIL DEPTH							
pH_{H2O}	Linear						
pH_{CaCl2}	Linear						
Microbial C	Linear						
Microbial N	Exponential	92	742	4	0.12	6.03×10^{2}	0.53
Mic-C : Mic-N	Exponential	0.015	0.099	10	0.15	5.37×10^{-4}	0.44
Dehydrogenase	Linear						
Acid phosphatase	Exponential	1,040	11,390	4	0.09	1.91×10^{6}	0.2
β-Glucosidase	Spherical	6,800	88,510	4	0.05	3.91×10^{7}	0.00
Protease	Spherical	10	5,712	4	0.0018	6.60×10^{5}	0.00

(Schlichting et al., 2002). According to these authors, 75–80% of the total P were organic P in the peat soils. Since more than 75% of the total P existed in organic P form, maintaining and/or improving the SOM content of peatlands by rewetting not only sequestrates C but also stores P in unavailable organic P form.

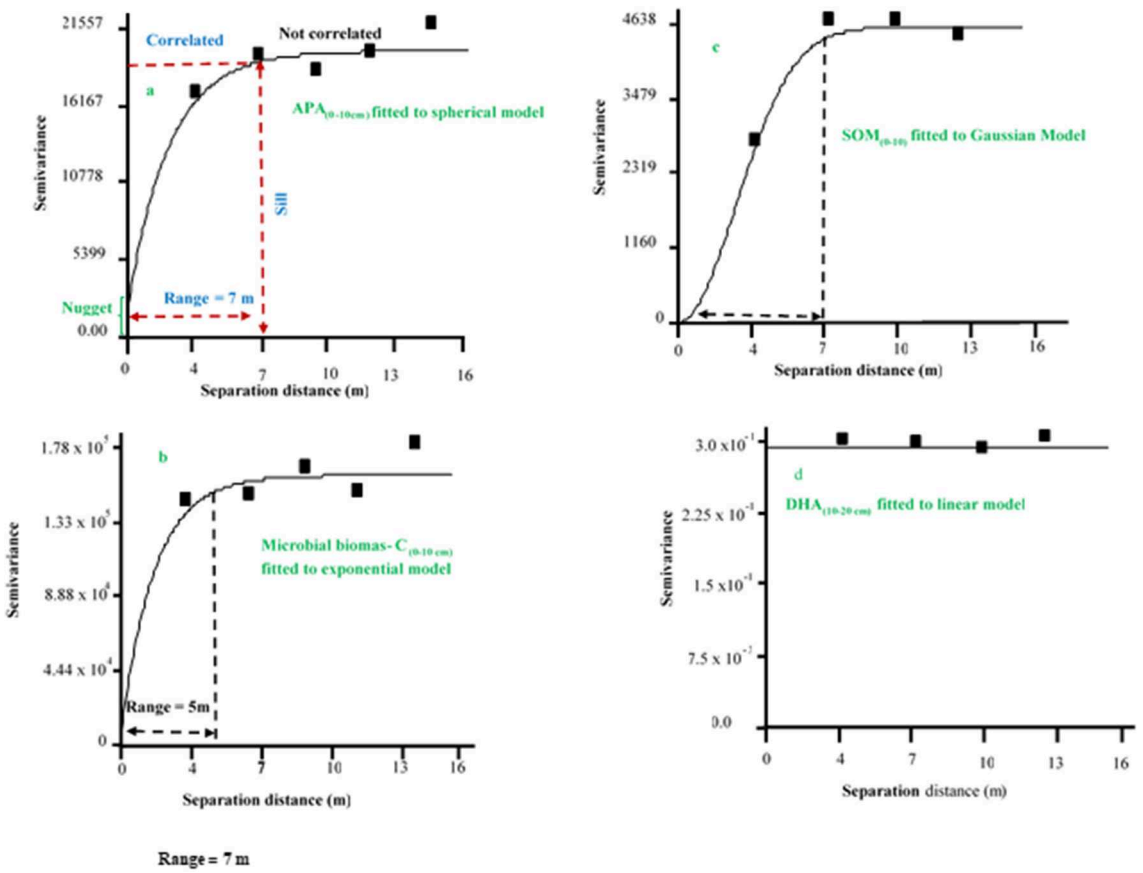

FIGURE 4 | Example of semivariogram of soil chemical and biochemical properties fitted to spherical, exponential, Gaussian, and linear models. APA, acid phosphatase activity; SOM, soil organic matter; DHA, dehydrogenase.

The higher biochemical activities at the soil depths of 0–10 cm than at the soil depth of 10–20 cm (**Table 4**) indicated the presence of enough aeration particularly during the summer season and rooting which together can increase microbial activities and transformations of organic matter (Tokarz and Urban, 2015). On the other hand, the highest dehydrogenase activity confirmed the significance of oxidoreductases under anaerobic soil conditions (Salazar et al., 2011; Wolinska and Stepniewska, 2012). Furthermore, the C_{org}, microbial biomass C and N of the present study were considerably lower than that reported for a rewetted peatland of Trebel valley, northern Germany (Baum et al., 2003). Similarly, the acid phosphatase activity in the current study was less than that of the Trebel valley by 3 to 4-folds. Such a great variation in enzyme activity can be attributed to seasonal and site-specific effects rewetting degraded peatland. Dehydrogenases are intracellular enzymes with indicator value for the soil microbial activity, but also for fine root activity (Zhang et al., 2010). The discrepancy of high dehydrogenase activity but low protease and acid phosphatase activities at both peat depths (0–10 and 10–20 cm) can be attributed to low aeration, since the activities of these enzymes are favored in aerobic soil conditions (Kang et al., 2005; Reddy and DeLaune, 2008; Romanowicz et al., 2015).

Correlations Among Soil Properties

The significant positive correction between soil microbial biomass C and N (**Table 5**) proved the well-established facts of their strong association. Similarly, the significant positive correlation between microbial biomass C and acid phosphatase activity, and microbial biomass C and β-glucosidase activity indicated that SOM and hydrology regulate the microbial biomass and enzyme activity in peat soils (Groffman et al., 1996). However, none of the content of plant available nutrients was correlated with the microbial biomass and enzyme activity, which can be attributed to less decomposition of peats because of high gravimetric water content at sampling (**Table 1**). The significant positive correlation of plant available P with the plant available Mg and Mn could be attributed to the pH and gravimetric water content that influenced the plant availability of these nutrient elements in the same direction.

The significant positive correlations among the SOM, C_{org}, total S, total N, total P and P_{hyp}, and most plant available elements (**Table 6**) indicated the major source of the elements was the SOM in peat soil. However, the lack of significant correlation among microbial biomass C and C_{org}, microbial biomass N and total N (data not shown), can be explained by high variations between

TABLE 8 | Spatial correlation of gravimetric water content (GW), soil organic matter, available plant nutrients, total and oxalate extractable elements in the surface of a rewetted peatland.

	Model	Nugget	Sill	Range (m)	Nugget: Sill ratio	RSS	R^2
GW	Spherical	0.63	6.32	10	0.10	0.689	0.89
SOM	Gaussian	10	4592	6	0.0022	6.68×10^{4}	0.97
C_{org}	Spherical	30	836	7	0.04	3879	0.94
N_t	Gaussian	0.01	4.819	7	0.0021	0.0132	0.99
P_t	exponential	0.00001	0.01822	6	0.0005	9.00×10^{-7}	0.87
P_{ox}	Gaussian	0.0002	0.00432	6	0.05	3.06×10^{-5}	0.74
P_{pyro}	Spherical	0.00001	0.01455	9	0.0007	2.55×10^{-6}	0.77
S_t	Spherical	0.001	0.704	12	0.001	3.75×10^{-4}	1.00
Al_{ox}	Exponential	0.00001	0.013320	6	0.0008	5.44×10^{-7}	0.85
Fe_a	Spherical	0.04	0.908	5	0.04	6.38×10^{-1}	0.14
Fe_{ox}	Linear						
Mg_a	Spherical	1.00	854.8	10	0.00	1.45×10^{3}	0.92
Mn_a	Spherical	19.60	60.93	23	0.32	3.29	0.99
Mn_{ox}	Spherical	0.00032	0.01184	5	0.03	1.40×10^{-5}	0.05
P_a	Spherical	0.0125	0.1650	10	0.08	2.32×10^{-4}	0.95
S_a	Spherical	757	2,318	53	0.32	6.69×10^{4}	0.69
Al_t	linear						
Ca_t	Spherical	0.28	8.818	6	0.03	2.04	0.49
Fe_t	Linear						
K_t	Exponential	0.00346	0.00838	69	0.41	1.62×10^{-7}	0.87
Mg_t	Exponential	0.0003	0.00594	9	0.05	7.53×10^{-8}	0.96
Mn_t	Spherical	0.00068	0.01546	7	0.04	1.75×10^{-5}	0.41
DPS	Exponential	0.27	1.556	8	0.17	1.16×10^{-1}	0.13
PSR	Exponential	0.000008	0.00005	5	0.16	7.03×10^{-11}	0.17

DPS, degree of P saturation; PSR, P saturation ratio.

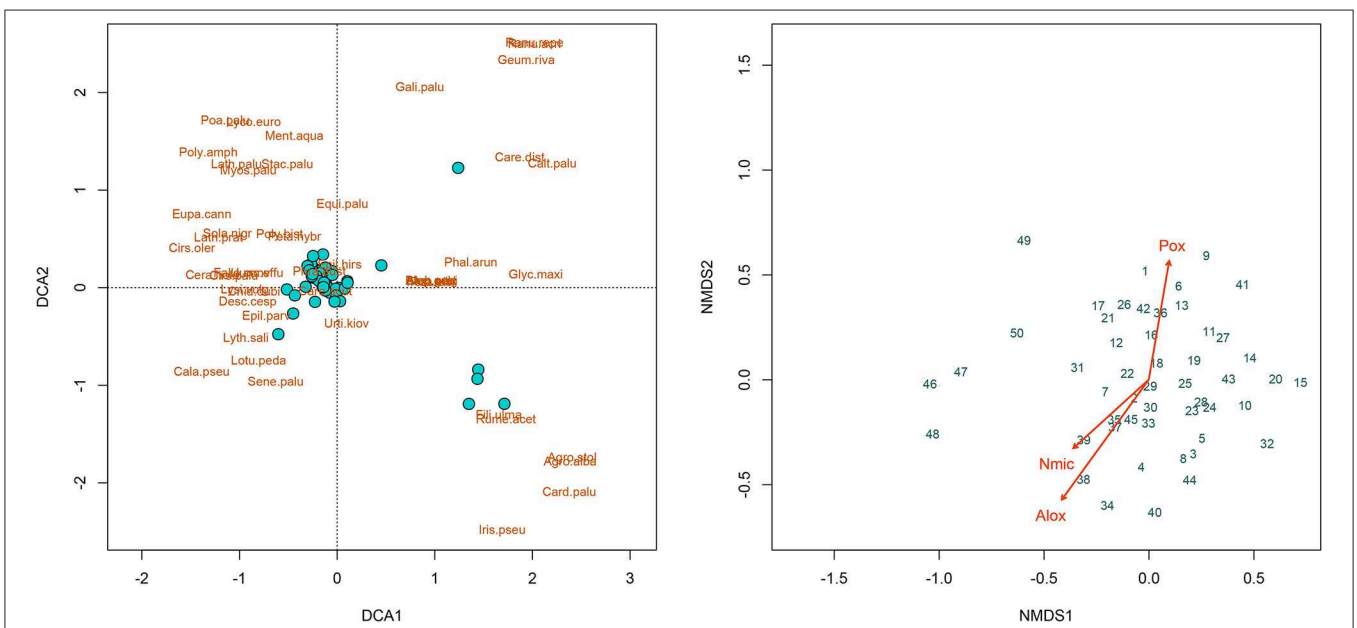

FIGURE 5 | Ordination plots of the detrended correspondence analysis (DCA, left) and of the non-metric multidimensional scaling (NMDS, right), Numbers in the Figure stand for the number of sampling grid cells.

the concentration of microbial biomass and the concentration of C_{org} and total N. A previous study also reported that the linearity of C_{org} to microbial biomass C association was achieved when C_{org} was below 2.5% (Anderson and Domsch, 1989). However, the C_{org} concentration in the present study was about 14 times higher than the critical level of C_{org} (2.5%) to detect a significant correlation between C_{org} and C_{mic}. Furthermore, high concentration of dissolved organic carbon and permanent flooding can contribute to lack of significant correlation between microbial biomass C with C_{org}, and microbial biomass N with total N (Reddy and DeLaune, 2008).

Spatial Correlation

The nugget to sill ratio is a good indicator whether a given soil variable is strongly spatially correlated (<0.25), moderately spatially correlated (0.25–0.75) or weakly spatially correlated (>0.75) (Cambardella et al., 1994; Iqbal et al., 2005; Ruffo et al., 2005). Accordingly, most of the biochemical properties were not only strongly spatially correlated, but also the spatial correlation was apparent at the shortest ranges (**Table 7** and **Figure 4**). The shortest range indicated a strong spatial variability of the soil variable under consideration. The highest spatial correlation particularly of the dehydrogenase activity was a good indicator of the overall microbial diversity in the rewetted peatland. Previous study also indicated that soil microbial activities showed strong spatial correlation below 0.25 m separation distance (Stark et al., 2004). This unequivocally indicated that a small-scale sampling is required to study biochemical properties in the rewetted degraded peatland. However, the lack of spatial correlation for the protease at the 0–10 cm soil depth and for the pH, microbial biomass C, and dehydrogenase activity at the depth of 10–20 cm can be attributed to the wet-dry cycles that could enhance variations from point to point in the rewetted degraded peatland. When a soil parameter lacks spatial correlation, reducing the sampling scale of the current study could exhibit spatial correlation (Cambardella et al., 1994) or a classic randomization block design could be used to handle the spatial variability (Kravchenko et al., 2006). The strong spatial correlation of most of the soil chemical properties could indicate the soil variables may be controlled by intrinsic soil variation (Cambardella and Karlen, 1999). Furthermore, extrinsic factors such as drainage, rewetting, historical land use and similar vegetation composition can contribute to strong spatial correlation. The vegetation composition is linked to the soil microbial colonization via rhizosphere effects and litter quality (Eisenhauer et al., 2010), and this is confirmed in our data set by the significant correlation with N_{mic} (**Figure 5**). The vegetation composition was assumed to represent a relative stable "summary" of the effects of multiple drivers, like the soil chemical properties, over time and, thus, a good predictor of the soil microbial community (Mitchell et al., 2010).

In conclusion, the combined use of the descriptive and geospatial spatial statistical analyses have paramount importance in disclosing the spatial variability pattern of soil chemical and biochemical properties in a rewetted degraded peatland at the small scale. Among 33 soil chemical and biochemical properties investigated in the present study, the CV of plant available nutrients were the highest. Similarly, soil biochemical activities were higher by many folds at the depth of 0–10 cm than 10–20 cm because of aeration during dry periods. Furthermore, about 88% of the soil chemical and biochemical properties were spatially correlated and 83% of the spatial correlation was strong at the ≤8 m range. The strong spatial correlation at such short range clearly indicated a small-scale spatial variability of the rewetted peatland. Those soil chemical and biochemical properties lacking spatial correlation were also spatially heterogeneously distributed because they varied from point to point. The main causes of such spatial variability can be attributed to slight variations in topography (**Figure 1C**) which are enhanced by peat degradation and subsidence. This essentially influence the soil moisture distribution and almost all biogeochemical processes that are related to moisture and redox conditions. Furthermore, direct anthropogenic influences like uneven distributions of formerly applied fertilizers have added to the spatial variability of the soil properties. Thus, small-scale sampling is required to understand the influence of rewetting degraded peatland on biogeochemistry and restoration processes thereby avoiding undesirable effects on environment.

DATA AVAILABILITY

All datasets generated for this study are included in the manuscript and/or the supplementary files.

AUTHOR CONTRIBUTIONS

WN statistical data analysis and writing the manuscript. CB and AS design of the study and editing the manuscript. PL conception of the research and editing the manuscript. JM collected vegetation composition data, data analysis, and editing the manuscript.

FUNDING

The European Social Fund (ESF) and the Ministry of Education, Science, and Culture of Mecklenburg-Western Pomerania funded this work within the scope of the project WETSCAPES (ESF/14-BM-A55-0029/16-64160025).

ACKNOWLEDGMENTS

The authors are grateful to Prof. R. Bill, University of Rostock, for his comments on the first draft of this manuscript and the technical assistances received from F. Beyer, W. Schomann, and M. Naumann.

REFERENCES

Acosta-Martínez, V., and Tabatabai, M. A. (2000). Enzyme activities in a limed agricultural soil. *Biol. Fert. Soils* 31, 85–91. doi: 10.1007/s003740050628

Andersen, R., Francez, A.-J., and Rochefort, L. (2006). The physicochemical and microbial status of a restored bog in québec: identification of relevant criteria to monitor success. *Soil Biol. Biochem*. 38, 1375–1387. doi: 10.1016/j.soilbio.2005.10.012

Anderson, T., and Domsch, K. H. (1989). Ratios of microbial biomass carbon to total organic carbon in arable soils. *Soil Biol. Biochem*. 21, 471–479. doi: 10.1016/0038-0717(89)90117-X

Baldrian, P. (2014). Distribution of extracellular enzymes in soils: spatial heterogeneity and determining factors at various scales. *Soil Sci. Soc. Am. J.* 78, 11–18. doi: 10.2136/sssaj2013.04.0155dgs

Bantilan-Smith, M., Bruland, G. L., MacKenzie, R. A., Henry, A. R., and Ryder, C. R. (2009). A comparison of the vegetation and soils of natural, restored, and created coastal lowland wetlands in Hawai'i. *Wetlands* 29, 1023–1035. doi: 10.1672/08-127.1

Barrett, S. E., and Watmough, S. A. (2015). Factors controlling peat chemistry and vegetation composition in sudbury peatlands after 30 years of pollution emission reductions. *Environ. Pollut.* 206, 122–132. doi: 10.1016/j.envpol.2015.06.021

Baum, C., Leinweber, P., and Schlichting, A. (2003). Effects of chemical conditions in re-wetted peats on temporal variation in microbial biomass and acid phosphatase activity within the growing season. *Appl. Soil Ecol*. 22, 167–174. doi: 10.1016/S0929-1393(02)00129-4

Berry, J. K. (2005). *Analyzing Geo-Spatial Resource Data: A Hands-on Case Study in Spatial Analysis and Data Mining*. Denver, CO: University of University of Denver.

Boon, P. I., Virtue, P., and Nichols, P. D. (1996). Microbial consortia in wetland sediments: a biomarker analysis of the effects of hydrological regime, vegetation and season on benthic microorganisms. *Mar. Freshwater Res.* 47, 27–41. doi: 10.1071/MF9960027

Borga, P., Nilsson, M., and Tunlid, A. (1994). Bacterial communities in peat in relation to botanical composition as revealed by phospholipid fatty acid analysis. *Soil Biol. Biochem.* 26, 841–848. doi: 10.1016/0038-0717(94)90300-X

Brooks, R. P., Wardrop, D. H., Cole, C. A., and Campbell, D. A. (2005). Are we purveyors of wetland homogeneity? A model of degradation and restoration to improve wetland mitigation performance. *Ecol. Eng.* 24, 331–340. doi: 10.1016/j.ecoleng.2004.07.009

Bruland, G. L., Richardson, C. J., and Whalen, S. C. (2006). Spatial variability of denitrification potential and related soil properties in created, restored, and paired natural wetlands. *Wetlands* 26, 042–1056. doi: 10.1672/0277-5212(2006)26[1042:SVODPA]2.0.CO;2

Bubier, J. L., Bhatia, G., Moore, T. R., Roulet, N. T., and Lafleur, P. M. (2003). Spatial and temporal variability in growing-season net ecosystem carbon dioxide exchange at a large peatland in Ontario, Canada. *Ecosystems* 6, 353–367. doi: 10.1007/s10021-003-0125-0

Cambardella, C. A., and Karlen, D. L. (1999). Spatial analysis of soil fertility parameters. *Precis. Agric.* 1, 5–14. doi: 10.1023/A:1009925919134

Cambardella, C. A., Moorman, T. B., Novak, J. M., Parkin, T. B., Karlen, D. L., Turco R. F., et al. (1994). Field-scale variability of soil properties in Central Iowa soils. *Soil Sci. Soc. Am. J.* 58, 1501–1511. doi: 10.2136/sssaj1994.03615995005800050033x

Courchesne, F., Cloutier-Hurteau, B., and Turmel, M.-C. (2008). Relevance of rhizosphere research to the ecological risk assessment of trace metals in soils. *Hum. Ecol. Risk Assess*. 14, 54–72. doi: 10.1080/10807030701790306

Couwenberg, J. (2009). "Methane emissions from peat soils," in *August 2009 produced for the UN-FCCC meetings in Bonn, Germany*. Ede: Greifswald University; Wetlands International. Available online at: www.wetlands.org

Dasselaar, A. D. P-V., Corre, W. J., Prieme, A., Klemedtsson, A. K., Weslien, P., Stein, A., et al. (1998). Spatial variability of methane, nitrous oxide, and carbon dioxide emissions from drained grasslands. *Soil Sci. Soc. Am. J.* 62, 810–817. doi: 10.2136/sssaj1998.03615995006200030039x

Dick, D. A., and Gilliam, F. S. (2007). Spatial heterogeneity and dependence of soils and herbaceous plant communities in adjacent seasonal wetland and pasture sites. *Wetlands* 27, 951–963. doi: 10.1672/0277-5212(2007)27[951:SHADOS]2.0.CO;2

Dick, W. A., and Tabatabai, M. A. (1977). An alkaline oxidation method for determination of total phosphorus in soils. *Soil Sci. Soc. Am. J.* 41, 511–514. doi: 10.2136/sssaj1977.03615995004100030015x

Dietrich, S. T., and MacKenzie, M. D. (2018). Comparing spatial heterogeneity of bioavailable nutrients and soil respiration in boreal sites recovering from natural and anthropogenic disturbance. *Front. Environ. Sci.* 6:126. doi: 10.3389/fenvs.2018.00126

Eisenhauer, N., Beßler, H., Engels, C., Gleixner, G., Habekost, M., Milcu, A., et al. (2010). Plant diversity effects on soil microorganisms support the singular hypothesis. *Ecology* 91, 485–496. doi: 10.1890/08-2338.1

Elzenga, J. T. M., and van Veen, H. (2010). "Waterlogging and Plant Nutrient Uptake," in *Waterlogging Signalling and Tolerance in Plants*, eds S. Mancuso and S. Shabala (Berlin: Springer-Verlag), 23–35.

Emsens, W.-J., Aggenbach, C. J. S., Smolders, A. J. P., Zak, D., and van Diggelen, R. (2017). Restoration of endangered fen communities: the ambiguity of iron–phosphorus binding and phosphorus limitation. *J. Appl. Ecol*. 54, 1755–1764. doi: 10.1111/1365-2664.12915

Förster, J. (2009). *Peatlands Restoration in Germany: a Potential Win-Win-Win Solution for Climate Protection, Biodiversity Conservation and Land Use*. Ministerium für Landwirtschaft, Umwelt und Verbraucherschutz Mecklenburg-Vorpommern. Available online at: http://doc.teebweb.org/wp-content/uploads/2013/01/Peatlands-restoration-for-carbon-sequestration-Germany.pdf (accessed November 26, 2018).

Gallardo, A. (2003). Spatial variability of soil properties in a floodplain forest in northwest Spain. *Ecosystems* 6, 564–576. doi: 10.1007/s10021-003-0198-9

Görn, S., and Fischer, K. (2015). Measuring the efficiency of fen restoration on carabid beetles and vascular plants: a case study from north-eastern Germany. *Restor. Ecol.* 23, 413–420. doi: 10.1111/rec.12203

Groffman, P. M., Hanson, G., Kiviat, E., and Stevens, G. (1996). Variation in microbial biomass and activity in four different wetland types. *Soil. Sci. Soc. Am. J.* 60, 622–629. doi: 10.2136/sssaj1996.03615995006000020041x

Gutknecht, J. L. M., Goodman, R. M., and Balser, T. C. (2006). Linking soil process and microbial ecology in freshwater wetland ecosystems. *Plant Soil* 289, 17–34. doi: 10.1007/s11104-006-9105-4

Haapalehto, T. O., Vasander, H., Jauhiainen, S., Tahvanainen, T., and Kotiaho, J. S. (2011). The effects of peatland restoration on water-table depth, elemental concentrations and vegetation: 10 years of changes. *Restor. Ecol.* 19, 587–598. doi: 10.1111/j.1526-100X.2010.00704.x

Hanschke, T. (1996). *Erfassung und bewertung der hydrologischen verhältnisse im niedermoor bei gragetopshof* (Diploma Dissertation). University of Rostock, Rostock, Germany, 116.

Herzsprung, P., Osterloh, K., von Tümpling, W., Harir, M., Hertkorn, N., Schmitt-Kopplin, P. et al. (2017). Differences in DOM of rewetted and natural peatlands - Results from high-field FT-ICR-MS and bulk optical parameters. *Sci. Total Environ.* 586, 770–781. doi: 10.1016/j.scitotenv.2017.02.054

Höper, H. (2007). Freisetzung von Treibhausgasen aus deutschen Mooren. *TELMA* 37, 85–116. doi: 10.23689/fidgeo-3035

Höper, H., Augustin, J., Cagampan, J. P., Drösler, M., Lundin, L., Moors, E., et al. (2008). "Restoration of peatlands and greenhouse gas balances," in *Peatlands and Climate Change*, ed M. Strack (Wageningen: International Peat Society), 182–210.

Hunt, R. J., Krabbenhoft, D. P., and Anderson, M. P. (1997). Assessing hydrogeochemical heterogeneity in natural and constructed wetlands. *Biogeochemistry* 39, 271–293. doi: 10.1023/A:1005889319205

Iqbal, J., Thomasson, J. A., Jenkins, J. N., Owens, P. R., and Whisler, F. D. (2005). Spatial variability analysis of soil physical properties of alluvial soils. *Soil. Sci. Soc. Am. J.* 69, 1–14. doi: 10.2136/sssaj2004.0154

IUSS Working Group WRB (2015). *World Reference Base for Soil Resources 2014, update 2015*. International soil classification system for naming soils and creating legends for soil maps. World Soil Resources Reports No. 106. Rome: FAO.

Jenerette, G. D., and Wu, J. (2004). Interactions of ecosystem processes with spatial heterogeneity in the puzzle of nitrogen limitation. *OIKOS* 107, 273–282. doi: 10.1111/j.0030-1299.2004.13325.x

Jenkinson, D. S. (1988). "Determination of microbial biomass carbon and nitrogen in soil," in *Advances in Nitrogen Cycling in Agricultural Ecosystems*, ed J. R., Wilson (Wallingford: CAB International), 368–386.

Joergensen, R. G. (1995). The fumigation extraction method to estimate soil microbial biomass: extraction with 0.01 M $CaCl_2$. *Agrobiol. Res.* 48, 319–324.

Joosten, H. (1997). European mires: a preliminary status report. *Int. Mire Conserv. Group Members Newslett.* 3, 10–13.

Joosten, H., and Clarke, D. (2002). *Wise Use of Mires and Peatlands -Background and Principles Including a Framework for Decision-Making*. Saarijärvi: International Mire Conservation Group and International Peat Society.

Joosten, H., Tanneberger, F., and Moen, A. (2017). *Mires and Peatlands of Europe: Status, Distribution and Conservation*. Stuttgart: Schweizerbart Science Publishers.

Kang, H., Kim, S., Fenner, N., and Freeman, C. (2005). Shifts of enzymes activities in wetlands exposed to elevated CO_2. *Sci. Total Environ.* 337, 207–2012. doi: 10.1016/j.scitotenv.2004.06.015

Karki, S., Elsgaard, L., Kandel, T. P., and Lærke, P. E. (2016). Carbon balance of rewetted and drained peat soils used for biomass production: a mesocosm study. *GCB Bioenergy* 8, 969–980. doi: 10.1111/gcbb.12334

Kercher, S. M., and Zedler, J. B. (2004). Multiple disturbances accelerate invasion of reed canary grass (*Phalaris arundianaceae* L.) in a mesocosm study. *Oecologia* 138, 455–464. doi: 10.1007/s00442-003-1453-7

Klironomos, J. N., McCune, J., Hart, M., and Neville, J. (1999). Designing belowground field experiments with the help of semi-variance and power analyses. *Appl. Soil Ecol.* 12, 227–238. doi: 10.1016/S0929-1393(99)00014-1

Kravchenko, A. N., Robertson, G. P., Snap, S. S., and Smucker, A. J. M. (2006). Using information about spatial variability to improve estimates of total soil carbon. *Agron. J.* 98, 823–829. doi: 10.2134/agronj2005.0305

Krohn, J., Lozanovska, I., Kuzyakov, Y., Parvin, S., and Dorodnikov, M. (2017). CH_4 and CO_2 production below two contrasting peatland micro-relief forms: an inhibitor and $\delta^{13}C$ study. *Sci. Total Environ.* 586, 142–151. doi: 10.1016/j.scitotenv.2017.01.192

Krüger, J. P., Leifeld, J., Glatzel, S., Szidat, S., and Alewell, C. (2015). Biogeochemical indicators of peatland degradation – a case study of a temperate bog in northern Germany. *Biogeosciences* 12, 2861–2871. doi: 10.5194/bg-12-2861-2015

Kumar, S. (2015). Estimating spatial distribution of soil organic carbon for the Midwestern United States using historical database. *Chemosphere* 127, 49–57. doi: 10.1016/j.chemosphere.2014.12.027

Kumar, S., Lal, R., and Liu, D. S. (2012). A geographically weighted regression kriging approach for mapping soil organic carbon stock. *Geoderma* 189–190, 627–634. doi: 10.1016/j.geoderma.2012.05.022

Ladd, J. N., and Buttler, H. A. (1972). Short-term assays of soil proteolytic enzyme activities using proteins and dipeptide derivates as substrates. *Soil Biol. Biochem.* 4, 19–30. doi: 10.1016/0038-0717(72)90038-7

Lamers, L. P. M., Vile, M. A., Grootjans, A. P., Acreman, M. C., Diggelen, R., Evans, M. G., et al. (2015). Ecological restoration of rich fens in Europe and North America: from trial and error to an evidence-based approach. *Biol. Rev.* 90, 182–203. doi: 10.1111/brv.12102

Landry, J., and Rochefort, L. (2012). *The Drainage of Peatlands: Impacts and Rewetting Techniques*. Available online at: http://www.gret-perg.ulaval.ca/uploads/tx_centrerecherche/Drainage_guide_Web_03.pdf (assessed on January 16, 2019).

Larkin, D. J. (2016). "Wetland Heterogeneity," in *Wetland Book*, eds C. M. Finlayson, M. Everard, K. Irvine, R. J. McInnes, B. A. Middleton, A. A. van Dam, and N. C. Davidson (Heidelberg: Springer).

Litaor, M. I., Reichmann, O., Belzer, M., Auerswald, K., Nishri, A., and Shenker, M. (2003). Spatial analysis of phosphorus sorption capacity in a semiarid altered wetland. *J. Environ. Qual.* 32, 335–343. doi: 10.2134/jeq2003.0335

Liu, Y., Guo, L., Jiang, Q., Zhang, H., and Chen, Y. (2015). Comparing geospatial techniques to predict SOC stocks. *Soil Tillage Res.* 148, 46–58. doi: 10.1016/j.still.2014.12.002

Marton, J. M., Chowdhury, R. R., and Craft, C. B. (2015). A comparison of the spatial variability of denitrification and related soil properties in restored and natural depression wetlands in Indiana, USA. *Int. J. Biodiv. Sci. Ecosyst. Services Manag.* 11, 36–45. doi: 10.1080/21513732.2014.950981

Mentzer, J. L., Goodman, R., and Balser, T. C. (2006). Microbial seasonal response to hydrologic and fertilization treatments in a simulated wet prairie. *Plant Soil* 284, 85–100. doi: 10.1007/s11104-006-0032-1

Mitchell, R. J., Hester, A. J., Campbell, C. D., Chapman, S. J., Cameron, C. M., Hewison, R. L., et al. (2010). Is vegetation composition or soil chemistry the best predictor of the soil microbial community? *Plant Soil* 333, 417–430. doi: 10.1007/s11104-010-0357-7

Nair, V. D. (2014). Soil phosphorus saturation ratio for risk assessment in land use systems. *Front. Environ. Sci.* 2:6. doi: 10.3389/fenvs.2014.00006

Nair, V. D., and Reddy, K. R. (2013). "Phosphorus sorption and desorption in wetland soils," in *Methods in Biogeochemistry of Wetlands*. SSSA Book Series, no. 10., eds R. D. DeLaune, K. R. Reddy, C. J. Richardson, and J. P. Megonigal (Madison, WI: Soil Science Society of America), 667–681.

Nkheloane, T., Olaleye, A. O., and Mating, R. (2012). Spatial heterogeneity of soil physic-chemical properties in contrasting wetland soils in two agro-ecological zones of Lesotho. *Soil Res.* 50, 579–589. doi: 10.1071/SR12145

Oksanen, J., Blanchet, F. G., Kindt, R., Legendre, P., Minchin, P. R., O'Hara, R. B., et al. (2017). *Vegan (2000): Community Ecology Package*. R package version 2.4-4. Available online at: https://www.scirp.org/-(S(i43dyn45teexjx455qlt3d2q))/reference/ReferencesPapers.aspx?ReferenceID$=$2134091 (accessed March 06, 2019).

Reddy, K. R., and DeLaune, R. D. (2008). *Biogeochemistry of Wetlands:-Science and Applications*. New York, NY: Taylor and Francis Group.

Romanowicz, K. J., Kane, E. S., Potvin, L. R., Daniels, A. L., Kolka, R. K., and Lilleskov, E. A. (2015). Understanding drivers of peatland extracellular enzyme activity in the PEATcosm experiment: mixed evidence for enzymic latch hypothesis. *Soil Plant* 397, 371–386. doi: 10.1007/s11104-015-2746-4

Rossi, R. E., Mulla, D. J., Journel, A. G., and Franz, E. H. (1992). Geostatistical tools for modeling and interpreting ecological spatial dependence. *Ecol. Monogr.* 62, 277–314. doi: 10.2307/2937096

Ruffo, M. L., Bollero, G. A., and Bullock, D. G. (2005). "Spatial variability of the Illinois soil nitrogen test: implications for soil sampling," in *Precision Agriculture 05,* ed J. V. Stafford (Wageningen: Wageningen Academic Publishers), 751–757.

Salazar, S., Sánchez, L. E., Alvare, J., Valverde, A., Galindo, P., Igual, J. M., et al. (2011). Correlation among soil enzyme activities under different forest system management practices. *Ecol. Eng.* 37, 1123–1131. doi: 10.1016/j.ecoleng.2011.02.007

SAS Institute Inc. (2013). *SAS® 9.4 Statements: Reference*. Cary: SAS Institute Inc.

Schlichting, A., Leinweber, P., Meissner, R., and Altermann, M. (2002). Sequentially extracted phosphorus fractions in peat derived soils. *J. Plant Nutr. Soil. Sci.* 165, 290–298. doi: 10.1002/1522-2624(200206)165:3<290::AID-JPLN290>3.0.CO;2-A

Schwertmann, U. (1964). Differenzierung der eisenoxide des bodens durch extraktion mit ammoniumoxalat- Lbsung. *Z. Pflanzenern. Dffng. Bodenk.* 105, 194–202. doi: 10.1002/jpln.3591050303

Soil Survey Staff (1999). *Soil taxonomy: A Basic System of Soil Classification for Making and Interpreting Soil Surveys, 2nd Edn*. Washington, DC: Natural Resources Conservation Service. U.S. Department of Agriculture Handbook.

Stark, C. H. E., Condron, L. M., Stewart, A., Di, H. J., and O'Callaghan, M. (2004). Small-scale spatial variability of selected soil biological properties. *Soil Biol. Biochem.* 36, 601–608. doi: 10.1016/j.soilbio.2003.12.005

Strack (2008). *Peatlands and Climate Change*. Jyväskylä: International Peat Society.

Štursová, M., Bárta, J., Šantručková, H., and Baldrian, P. (2016). Small-scale spatial heterogeneity of ecosystem properties, microbial community composition and microbial activities in a temperate mountain forest soil. *FEMS Microbiol. Ecol.* 92:fiw185. doi: 10.1093/femsec/fiw185

Tabatabai, M. A. (1994). "Soil enzymes," in *Methods of Soil Analysis. Part 2. Microbiological and Biochemical Properties*, eds P. S. Bottomley, J. S. Angle, and R. W. Weaver (Madison, WI: Soil Science Society of America), 778–833.

Tokarz, E., and Urban, D. (2015). Soil redox potential and its impact on microorganisms and plants of wetlands. *J. Ecol. Eng.* 16, 20–30. doi: 10.12911/22998993/2801

Truu, M., Juhanson, J., and Truu, J. (2009). Microbial biomass, activity and community composition in constructed wetlands. *Sci. Total Environ.* 407, 3958–3971. doi: 10.1016/j.scitotenv.2008.11.036

Ulanowski, T. A., and Branfireun, B. A. (2013). Small-scale variability in peatland pore-water biogeochemistry, Hudson Bay Lowland, Canada. *Sci. Total Environ.* 454–455, 211–218. doi: 10.1016/j.scitotenv.2013.02.087

Vance, E. D., Brookes, P. C., and Jenkinson, D. S. (1987). An extraction method for measuring soil microbial biomass C. *Soil Biol. Biochem*. 19, 703–707. doi: 10.1016/0038-0717(87)90052-6

Waddington, J. M., and Roulet, N. T. (1996). Atmosphere-wetland carbon exchange: scale dependency of CO_2 and CH_4 exchange on the developmental topography of a peatland. *Global Biogeochem. Cycles* 10, 233–245. doi: 10.1029/95GB03871

Wang, K., Zhang, C., and Li, W. (2013). Predictive mapping of soil total nitrogen at a regional scale: a comparison between geographically weighted regression and cokriging. *Appl. Geogr*. 42, 73–85. doi: 10.1016/j.apgeog.2013.04.002

Whiting, G. J., and Chanton, J. P. (2001). Greenhouse carbon balance of wetlands: methane emission versus carbon sequestration. *Telus* 53B, 521–542. doi: 10.3402/tellusb.v53i5.16628

Wiedermann, M. M., Kane, E. S., Potvin, L. R., and Lilleskov, E. A. (2017). Interactive plant functional group and water table effects on decomposition and extracellular enzyme activity in *Sphagnum* peatlands. *Soil Biol. Biochem.*108, 1–8. doi: 10.1016/j.soilbio.2017.01.008

Wolinska, A., and Stepniewska, Z. (2012). Dehydrogenase activity in the soil environment. *IntechOpen*. doi: 10.5772/48294

Wuenscher, R., Unterfrauner, H., Peticzka, R., and Zehetner, F. (2015). A comparison of 14 soil phosphorus extraction methods applied to 50 agricultural soils from Central Europe. *Plant Soil Environ.* 61, 86–96. doi: 10.17221/932/2014-PSE

Yang, F., Tiana, J., Fang, H., Gao, Y., Zhang, X., Yu, G., et al. (2018). Spatial heterogeneity of microbial community and enzyme activities in a broad-leaved Korean pine mixed forest. *Eur. J. Soil Biol.* 88, 65–72. doi: 10.1016/j.ejsobi.2018.07.001

Zak, D., Gelbrecht, J., Wagner, C., and Steinberg, C. E. W. (2008). Evaluation of the phosphorus mobilization potential in re-wetted fens by an improved sequential chemical extraction procedure. *Eur. J.Soil Sci.* 59, 1191–1201. doi: 10.1111/j.1365-2389.2008.01081.x

Zerbe, S., Steffenhagen, P., Parakenings, K., Timmermann, T., Frick, A., Gelbrecht, J., et al. (2013). Restoration success regarding ecosystem services after 10 years of rewetting peatlands in NE Germany. *Environ. Manage*. 51, 1194–1209. doi: 10.1007/s00267-013-0048-2

Zhang, C.-B., Wang, J., Liu, W.-L., Zhu, S.-X., Liu, D., Chang, S. X., et al. (2010). Effects of plant diversity on nutrient retention and enzyme activities in a full-scale constructed wetland. *Bioresour. Technol.* 101, 1686–1692. doi: 10.1016/j.biortech.2009.10.001

Conflict of Interest Statement: The authors declare that the research was conducted in the absence of any commercial or financial relationships that could be construed as a potential conflict of interest.

frontiers in Environmental Science

ORIGINAL RESEARCH
published: 04 October 2019
doi: 10.3389/fenvs.2019.00147

Unraveling the Importance of Polyphenols for Microbial Carbon Mineralization in Rewetted Riparian Peatlands

Dominik Zak[1,2,3]*, *Cyril Roth*[1], *Viktoria Unger*[3], *Tobias Goldhammer*[1], *Nathalie Fenner*[4], *Chris Freeman*[4] and *Gerald Jurasinski*[3]

[1] Department of Chemical Analytics and Biogeochemistry, Leibniz-Institute of Freshwater Ecology and Inland Fisheries (IGB), Forschungsverbund Berlin e.V., Berlin, Germany, [2] Department of Bioscience, Aarhus University, Silkeborg, Denmark, [3] Institute of Landscape Ecology and Site Evaluation, University of Rostock, Rostock, Germany, [4] School of Natural Sciences, Bangor University, Bangor, United Kingdom

There have been widespread attempts to rewet peatlands in Europe and elsewhere in the world to restore their unique biodiversity as well as their important function as nutrient and carbon sinks. However, changes in hydrological regime and therefore oxygen availability likely alter the abundance of enzyme-inhibiting polyphenolic compounds, which have been suggested as a "latch" preventing large amounts of carbon from being released into the atmosphere by microbial mineralization. In recent years, a variety of factors have been identified that appear to weaken that latch including not only oxygen, but also pH. In minerotrophic fens, it is unknown if long-term peat mineralization during decades of drainage and intense agricultural use causes an enrichment or a decline of enzyme-inhibiting polyphenols. To address this, we collected peat samples and fresh roots of dominating plants (i.e., the peat parent material) from the upper 20 cm peat layer in 5 rewetted and 6 natural fens and quantified total phenolic content as well as hydrolysable and condensed tannins. Polyphenols from less decomposed peat and living roots served partly as an internal standard for polyphenol analysis and to run enzyme inhibition tests. As hypothesized, we found the polyphenol content in highly decomposed peat to be eight times lower than in less decomposed peat, while condensed tannin content was 50 times lower in highly degraded peat. In addition, plant tissue polyphenol contents differed strongly between peat-forming plant species, with the highest amount found in roots of *Carex appropinquata* at 450 mg g^{-1} dry mass, and lowest in *Sphagnum* spp. at 39 mg g^{-1} dry mass: a 10-fold difference. Despite large and clear differences in peat and porewater chemistry between natural and rewetted sites, enzyme activities determined with Fluorescein diacetate (FDA) hydrolysis and peat degradation were not significantly correlated, indicating no simple linear relationship between polyphenol content and microbial activity. Still, samples with low contents of polyphenols and condensed tannins showed the highest microbial activities as measured with FDA.

Keywords: decomposition, enzyme inhibition, microbial activity, peatland restoration, *Sphagnum*, tannins

OPEN ACCESS

Edited by:
Colin McCarter, University of Toronto Scarborough, Canada

Reviewed by:
James McLaughin, Ontario Ministry of Natural Resources, Canada
Jos Thomas Antonius Verhoeven, Utrecht University, Netherlands

***Correspondence:**
Dominik Zak
doz@bios.au.dk

Specialty section:
This article was submitted to Biogeochemical Dynamics, a section of the journal Frontiers in Environmental Science

Received: *19 May 2019*
Accepted: *17 September 2019*
Published: *04 October 2019*

Citation:
Zak D, Roth C, Unger V, Goldhammer T, Fenner N, Freeman C and Jurasinski G (2019) Unraveling the Importance of Polyphenols for Microbial Carbon Mineralization in Rewetted Riparian Peatlands. Front. Environ. Sci. 7:147. doi: 10.3389/fenvs.2019.00147

INTRODUCTION

Despite covering only 2–3% of the land surface, peatlands store approximately one third of global soil carbon (C; Gorham, 1991; Jenkinson et al., 1991; Yu et al., 2010). Due to the anaerobic conditions in waterlogged peat, the rate of production of organic matter exceeds its decomposition (Pind et al., 1994; Williams and Yavitt, 2003; Freeman et al., 2004). Peatlands also play a significant role in water cycling and nutrient retention in river catchments (Verhoeven et al., 2006) and often support unique biodiversity (Zerbe et al., 2013). However, despite their importance from local to global scales, a significant loss in global peatland area continues (Joosten, 2010; IPCC, 2014) and attempts to restore these important ecosystems are widespread. In NE Germany, more than 30,000 hectares of drained minerotrophic (groundwater-fed) peatlands (i.e., fens) have been rewetted over the last 30 years to restore their ecological functions (Zak et al., 2018). Due to their extended drainage history, a re-establishment of their original state is not expected in a human life time perspective (Zak et al., 2018), but they may eventually return to a carbon neutral state (Joosten et al., 2015). The post-rewetting dynamics of carbon cycling in fens are, however, still poorly constrained.

The peatland carbon imbalance is regulated by the prevalence of polyphenolic compounds that inhibit microbial carbon mineralization and the enzymes that act upon them (Freeman et al., 2001). In ombrotrophic (rain-fed) peatlands (bogs), the enzyme phenol oxidase represents a key regulator for microbial carbon mineralization (Freeman et al., 2001, 2004). Phenol oxidase depends on molecular oxygen (O_2) and is highly active under drained conditions. This increased activity reduces the amount of polyphenolic compounds and limits their inhibiting effect on microbial decomposition. In contrast, when oxygen is depleted under waterlogged conditions, phenol oxidase is inactive, polyphenols accumulate, and microbial carbon mineralization becomes limited. This mechanism is so effective that it has been termed an "enzymic latch" on the peatland carbon store (Freeman et al., 2001). The "enzymic latch" theory is still discussed widely, with some suggesting greater complexity than previously assumed based on research in tropical peats (Hall et al., 2014) and temperate systems (Fenner and Freeman, 2011; Brouns et al., 2016; Bonnett et al., 2017).

Despite its possible central role for organic matter decomposition in bogs, the "enzymic latch" has rarely been investigated in fens (but see Pinsonneault et al., 2016). This mechanism may be particularly relevant in previously drained fens, because prolonged drainage exposes the peat surface to oxygen and allows phenol oxidase to activate, essentially enhancing peat decomposition that may even continue under rewetted conditions, as long as polyphenol content is considerably reduced. In addition, drainage leads to warming of the soil. This may further weaken the "latch" since temperature seems to be an important control on phenol oxidase activity across peatland types (Pinsonneault et al., 2016). A biogeochemical legacy of draining is well-documented in several other aspects of fen carbon and nutrient dynamics. For example, a strong increase in methane emissions is typically measured in rich fens after rewetting (Hahn-Schöfl et al., 2011; Franz et al., 2016). Elevated concentrations of dissolved organic carbon, ammonium, and phosphate at levels of one to three orders higher compared to pristine systems have been measured in porewaters of the upper degraded peat layers of rewetted fens (Zak and Gelbrecht, 2007), indicating potentially increased microbial turnover of organic matter in degraded topsoil of formerly drained fens. Laboratory incubations under stationary conditions have shown that microbially mediated redox processes are more intense in highly decomposed vs. less decomposed peat, partly explained by enhanced availability of nutrients and terminal electron acceptors (Zak and Gelbrecht, 2007; Cabezas et al., 2012). On the contrary, there is evidence that the general availability of organic substrate within the decomposed peat layer is lower because it has already undergone mineralization over decades of drainage, and it is expected to be more recalcitrant due to the enrichment of polyphenols, in particular of lignin and tannin, that can inhibit enzymatic systems important for microbial carbon cycling (Bader et al., 2018).

Polyphenols are a large and diverse group of organic substances in which at least two hydroxyl (OH-) groups are bound to aromatic ring structures. They are typical plant metabolites that are synthesized to support a variety of physiological functions such as morphology and energy metabolism (e.g., pigments), structure (e.g., lignin), and pathogen or predator resistance (e.g., flavonoids and tannins; Bravo, 1998). Tannins are of particular ecological importance, as these high-molecular weight polyphenols (500–3,000 Da; Swain, 1979) possess protein deactivation potential by forming insoluble protein complexes, and therefore affect many microbial processes that are enzyme-mediated (Bravo, 1998). They are the fourth-most abundant class of biochemical compounds in terrestrial biomass after cellulose, hemicelluloses, and lignin, and are found in the bark, wood, leaves, fruits, and roots of a wide variety of vascular plants (Cowan, 1999; Hernes and Hedges, 2000; Mueller-Harvey, 2001). Due to their multiple phenolic hydroxyl groups and high molecular weights, tannins, in contrast to low molecular weight phenolic acids such as gallic, vanillic, or ferulic acids, may limit litter decomposition more effectively in a number of different ways: (1) by complexing or deactivating microbial exoenzymes, (2) by complexing metals essential to enzyme activity, (3) by direct toxicity to microbes, (4) by themselves being resistant to decomposition, (5) by sequestering proteins in tannin-protein complexes that are resistant to decomposition and finally, (6) by coating other compounds, such as cellulose, and protecting them from microbial attack (Kraus et al., 2003). To unravel the importance of these single processes, it seems mandatory to complement bulk polyphenol analysis by further characterizing the biochemical properties of the polyphenol assemblage (Mole and Waterman, 1987; Appel, 1993; Nelson et al., 1997; Hättenschwiler and Vitousek, 2000; Rautio et al., 2007). Analytically, tannins can be divided into two major groups: hydrolysable tannins and condensed tannins (**Figure 1**); the latter also termed proanthocyanidins (PAs). Hydrolysable

tannins are composed of gallic acid or hexahydroxydiphenic acid esterified to a sugar moiety while condensed tannins are polymers of three ring flavan-3-ols joined with C-C bounds.

Due to these unique properties of polyphenols, we expect that their effect on carbon turnover should be similar to the "enzyme latch" described in bogs. We hypothesize that highly degraded peat of rewetted fens contains less enzyme-inhibiting polyphenols compared to less decomposed peat of pristine fens due to break up of polyphenols during the drainage phase. We analyzed fen peat substrates as well as peat-forming plant tissues from rewetted and pristine fens for representative polyphenol fractions—total phenol content, hydrolysable and condensed tannins—and for bulk microbial activity. Further, we tested microbial inhibition with PAs and characterized the peat samples chemically.

METHODS

Study Sites and Sampling

The investigated fens are situated along freshwater sources in the postglacial landscape of northeast Germany and northwest Poland (**Figure 2**). The rewetted fens Hasenfelde, Sauwinkel, Menzlin, Zarnekow, and Jargelin have been subject to long-term drainage and were used mostly as grassland over several decades. At the time of sampling, their upper soil layer therefore consisted of highly decomposed peat until a depth of ∼0.3 m, followed by less decomposed peat until a depth of up to 10 m (Zak and Gelbrecht, 2007). Three to Twelve years after rewetting, all sites were dominated by helophytes such as *Phragmites australis* and *Typha latifolia* in permanent flooded areas, and by *Phalaris arundinacea* in areas experiencing wet-dry cycles (Zak et al., 2015).

The hydrology of the sites Dollgensee, Töpchin, Gützkow, Triebschsee, and Rzecin was not or only slightly disturbed by drainage or similar measures in the past. In all areas the peat at the soil surface was only slightly decomposed, i.e., H1–4 according to the von Post humification scale (Von Post, 1922). All of these near to pristine peatlands can be classified as mesotrophic subneutral fens and are dominated by brown mosses (e.g., *Bryum pseudotriquetum, Campylium stellatum, Plagiomnium elatum*), and low sedges like *Carex hostiana, C. flacca, and C. panacea* (Zak et al., 2010). Furthermore, sparse stands of *Phragmites australis* occur in all the pristine sites, which represents the main peat-forming plant apart from *Carex spp*. and brown mosses. For the rewetted sites, the peat parent material was not recognizable any more due to the amorphous character of the soil, however deeper layers which were unaffected by water table drawdown indicate the same peat-parent material as in the undisturbed sites.

Peat samples were collected in triplicate from the top layers using a knife (ca. 10–20 cm depth) and transported to the lab within 1 day in an insulated cooler with ice, and analyzed for the characterization of total microbial activity immediately or frozen at −18°C for polyphenol analysis. Select data on porewater chemistry and peat characteristics are compiled in **Tables 1**, **2**. A detailed description of conducted bulk peat analyses (total contents of phosphorus, carbon, nitrogen, iron, and organic matter), porewater sampling, and chemical analysis of dissolved matter concentrations (phosphate, ammonium, dissolved organic carbon, sulfate, iron, and calcium) can be found in Zak et al. (2010). Furthermore, plant samples (roots or moss litter) were taken from site Triebschsee (*Carex appropinquata*, brown mosses) and an additional natural poor fen, Kablow-Ziegelei (*Eriophorum angusitfolium, Vaccinium oxycoccos*, *Sphagnum* spp.) and treated analogously to the peat samples.

Polyphenol Analysis

Sample Preparation and Extraction of Phenolic Substances

For the extraction of phenols, we followed the protocol of Hagerman (2002) taking into the account that phenols are not stable at light and higher temperature with slight adaptations. Thus, after removing coarse living plant roots, collected peat samples were freeze-dried, finely ground in an agate ball mill, and stored at 18°C in the dark. Phenolic substances were extracted with 10 mL 70% aqueous acetone (v/v) three times sequentially from 0.2 g of the lyophilized peat material in screw cap plastic tubes. During extraction, tubes were suspended for 20 min in an ultrasonic water bath cooled to temperatures below 20°C. The used sonicator allowed samples to be maintained in the dark during the extraction period. The extracts were decanted after centrifugation at 10,600 g for 5 min (Universal 30F, Hettich, Tuttlingen, Germany) and combined in Erlenmeyer flasks on ice for further analysis. For the acid butanol assay and for purification of PAs from the extracts, 2 mg ascorbic acid L^{-1} were initially added to the 70% aqueous acetone (v/v) to prevent oxidation of the extracted PAs. No ascorbic acid was added when extracts were used for the analysis of total phenolics since ascorbic acid strongly interferes with the color reaction by reducing the Folin-Ciocalteau reagent (Box, 1983; Georgé et al., 2005).

Isolation of Proanthocyanidins

PAs were obtained from peat samples of the five pristine sites following Giner-Chavez et al. (1997), where water-solved PAs are precipitated with trivalent ytterbium acetate, with slight modifications. The extraction procedure for obtaining of PAs was performed as described before with the exception that 1 g instead of 0.2 g of the lyophilized peat were extracted in order to yield higher amounts of tannins. The extraction was performed in six parallel runs to gain sufficient tannin material from each peat soil. After combination the extracts were washed three times with 50 ml n-hexane to remove lipids, and three times with 50 ml ethyl acetate to remove other remaining non-tannin components from the crude peat extract. Rotoevaporation was used in addition to separating funnels to remove acetone and traces of organic solvents yielding approximately 40 mL of an aqueous tannin solution. Ten ml 0.1 M ytterbium acetate ($Yb(C_2H_2O_2)_3 \cdot 4H_2O$) and 2 ml 0.5 M triethanolamine as buffer ($N(CH_2CH_2OH)_3$) were added to this solution and the extracts were stored in the dark for 20 h at 4°C to precipitate solved tannins. After centrifugation, the pellet was washed twice with 20 mL of 70% acetone (v/v) and PAs were recovered from

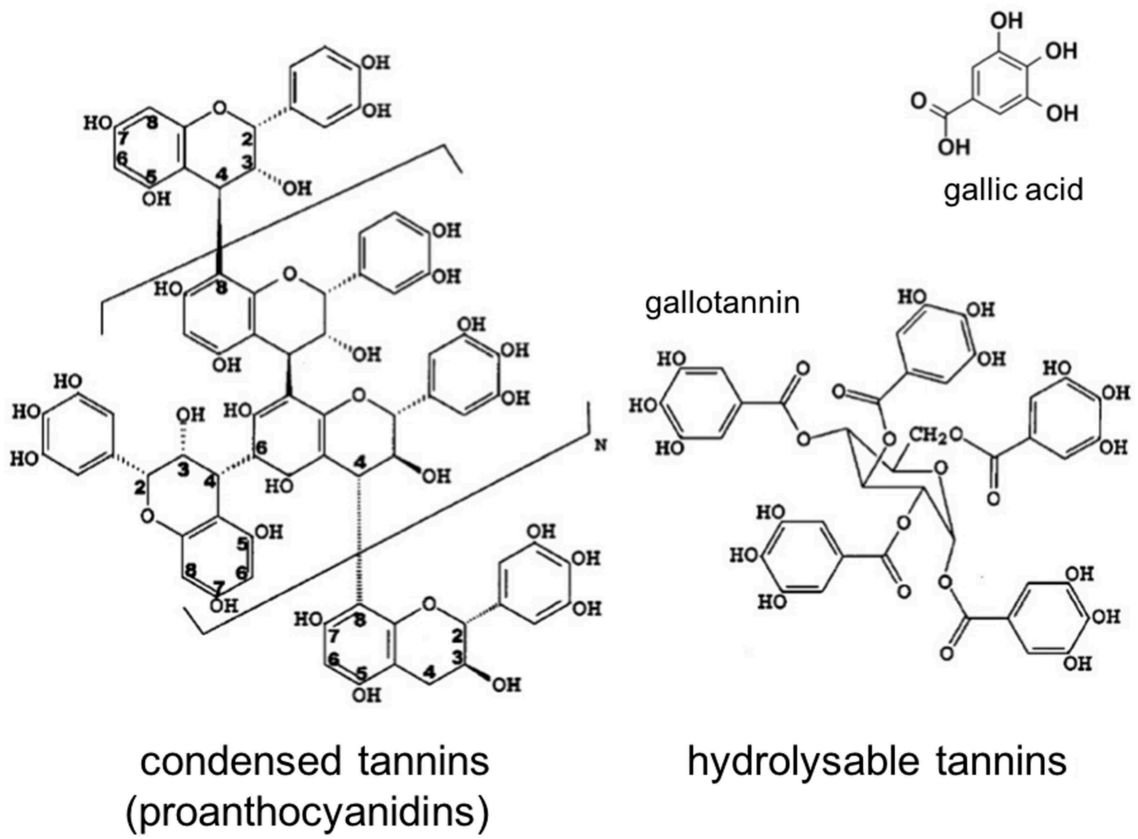

FIGURE 1 | Structure of condensed and hydrolysable tannins (modified after Hernes and Hedges, 2000).

the formed complexes using cation exchange resin (Nyamambi et al., 2000). For this purpose, tannin ytterbium complexes were mixed with 2 g exchange resin (Amberlite IRP-64, Sigma-Aldrich, Schnelldorf, Germany) and with three times 40 mL 70% acetone (v/v) sequentially in screw top glass tubes placed in a cooled sonicator for 20 min. Free PAs left in solution were then separated from the resin by centrifugation and filtration, from acetone by rotoevaporation and freeze dried to yield solid samples.

The PAs were used to determine their inhibitory activity on enzymes originating from peat, and as internal standards for colorimetric analyses. Analysis of UV spectra of the colored anthocyanidins formed during the acid butanol assay were conducted to verify the quality of isolated PAs and their suitability as internal standards (**Figure 3**).

Quantification of Total Phenolics

The simple, non-specific Folin-Ciocalteau assay quantifies total concentrations of phenolic hydroxyl groups in plant extracts (Box, 1983). The method was slightly modified most notably by using only half of the given volumes and reducing reaction times to 30 min (Hilt et al., 2006). 0.3–0.5 mL aliquots of the combined extracts were increased to volumes of 5 ml with deionized water in 10 mL screw cap glass tubes to obtain absorbance below 0.5. After addition of 0.75 ml of sodium carbonate solution (75 g Na_2CO_3 L^{-1}) and 0.25 ml Folin-Ciocalteau reagent (Merck KGaA, Darmstadt, Germany), tubes were vortexed for 5 s. Absorbance was read at 750 nm (Photometer Spekol 221, Iskra Elektronik, Stuttgart, Germany) exactly 30 min after addition of the Folin-Ciocalteau reagent. The assay was calibrated with tannic acid (Fluka/Sigma-Aldrich, Munich, Germany) and tannins isolated from peat material. Analyses for polyphenols were carried out on three technical replicates per field sample. The same holds for all steps regarding the general chemical characterization of the field samples.

Quantification of Hydrolysable Tannins

Hydrolysable tannins were measured after saponisation and extraction after Luthria and Pastor-Corrales (2006) modified or peat soils. Specifically, 0.2 g of the lyophilized and grounded peat was digested by adding 2.5 mL 2 M NaOH containing 10 M EDTA and 1% ascorbic acid in an ultrasonic water bath at 45°C. The extraction was conducted with 4 mL ethyl acetate after acidification with 7.2 mL 2 M HCl. After shaking for 30 min the samples were centrifuged at 10,600 g for 5 min. The extraction was repeated one time and combined supernatants were dried by rotoevaporation under nitrogen atmosphere. Capturing was done with 300 μL 0.1% formic acid. Analyses were conducted using High-Performance Liquid Chromatography (Gynkotek)

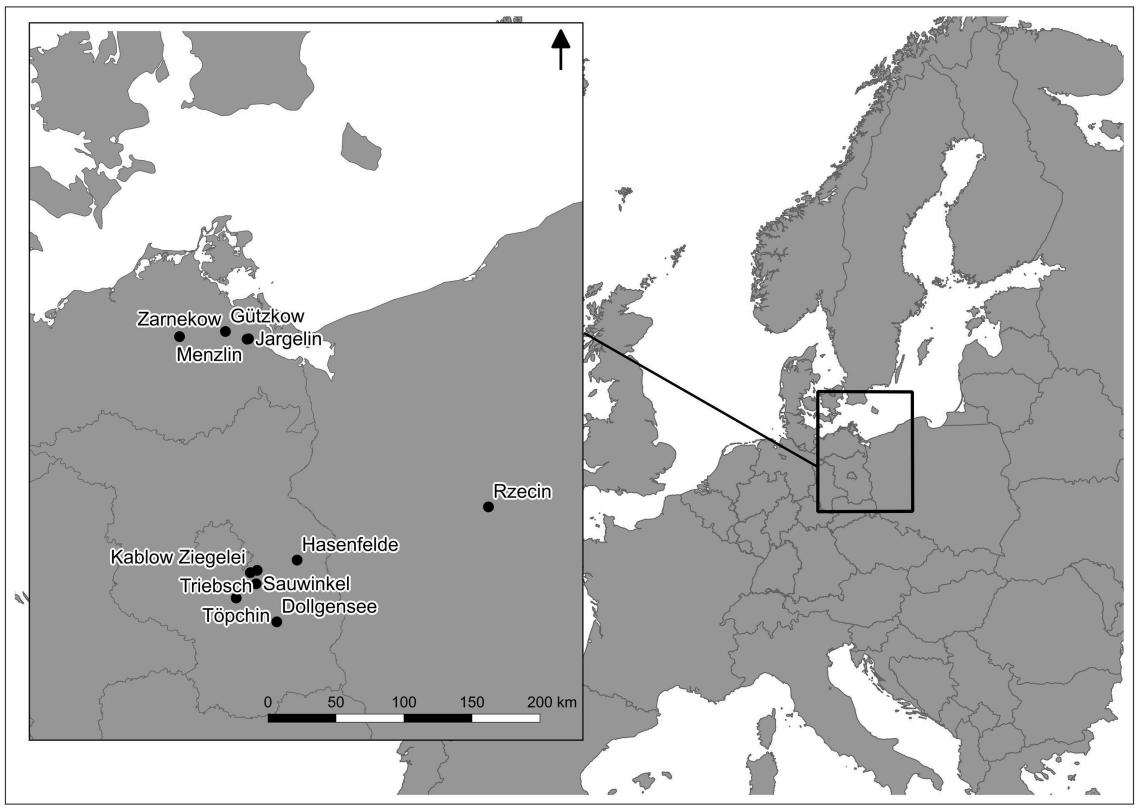

FIGURE 2 | Location of sampled peatlands in NE Germany and NW Poland.

with UV detection at 280 nm. Separation was achieved using the column Phenomex Prodigy PH3 5 µ (250 × 4.6 mm) at constant flow mode and temperature (1.9 mL min^{-1}, 25°C). The mobile phase was a constant mixture of methanol/0.1 % HCOOH (80%/20%, v/v). For calibration, gallic acid was used (Fluka/Sigma-Aldrich, Munich, Germany).

Quantification of Condensed Tannins

Condensed tannins or PAs were, respectively, measured with the acid butanol method (Porter et al., 1986), by adding 6 mL acid butanol reagent (nbutanol/concentrated HCl, 95:5 by volume) and 0.2 mL iron reagent (2% ferric ammonium sulfate dodecahydrate salt, $FeNH_4(SO_2)_4 \cdot 12H_2O$, in 2 M HCl) to 1 ml extract solution. Samples were then vortexed for 5 s and placed for 50 min in a water bath at 95°C. After cooling the samples to room temperature, absorbance was measured at 550 nm (Photometer Spekol 221, Iskra Elektronik, Stuttgart, Germany). Since samples from different peat soils were already colored to different extents before heating, absorbance was also read before the production of colored anthocyanidins and subtracted from the values measured after heating. This approach led to a conservative estimate of tannin concentrations, since some chromophores might have been destroyed upon heating (Hagerman, 2002). Analyses of UV spectra (200–700 nm) were conducted to confirm the subtraction of background color. The acid butanol assay was calibrated with cyanidin chloride (Carl Roth, Karlsruhe, Germany) and the tannins isolated from peat material.

Microbial Activity in Peat Soils

Fluorescein diacetate (FDA) hydrolysis was performed to measure the enzyme activity of microbes according to Schnürer and Rosswall (1982) and optimized for peat analysis. Always, ca. 0.6 g (±0.1 g) fresh peat were directly weighed into screw cap glass tubes out of ca. 15 g fresh bulk peat sample. The samples were mixed with 4 mL potassium phosphate buffer (pH 7.6; 8.7 g K_2HPO_4 and 1.3 g KH_2PO_4 in 1 L distilled water), 1 mL distilled water, and 0.3 mL FDA solution (1 mg FDA in 1 mL acetone). Peat slurries were shaken then for 25 min on a rotary shaker and centrifuged at 4,200 g for 5 min (Heraeus Labfuge 400, DJB Labcare, Buckinghamshire, England). 0.5 mL of the supernatant was diluted with 1.5 mL potassium phosphate buffer solution before measurement at 490 nm on a spectrophotometer (Photometer Spekol 221, Iskra Elektronik, Stuttgart, Germany). Blanks were measured without the addition of FDA to correct for background absorbance and concentrations of released fluorescein were determined by calibration with a fluorescein sodium salt solution ($C_{20}H_{10}Na_2O_5$, Sigma Aldrich, Schnelldorf, Germany). Hydrolysis rates of FDA were expressed as µg fluorescein h^{-1} mg^{-1} oven dry (105°C) peat. Dry matter of aliquots withdrawn from the slurry and of weighed peat soils from pristine sites were measured for each analytical run.

TABLE 1 | Select data on porewater chemistry (EC—electrical conductivity, SRP—soluble reactive phosphorus).

Sites		EC	SRP	NH_4^+	DOC	Sulfate	Fe^{2+}	Ca^{2+}
	n	[μS cm^{-1}]	[mg L^{-1}]					
NATURAL PEATLANDS								
Dollgensee	6	183	0.11	0.4	53	45	5.9	20
Töpchin	3	717	0.56	2.1	28	11	9.0	125
Gützkow	24	930	0.07	0.7	14	108	0.3	155
Triebschsee	8	701	0.06	1.4	14	81	0.1	103
Rzecin	6	180	0.06	0.5	37	0.5	0.2	29
Kablow Ziegelei	6	65	0.04	1.1	66	1.5	2.2	4.5
REWETTED PEATLANDS								
Hasenfelde	3	2,466	1.63	15.5	117	150	45	550
Sauwinkel	4	–	3.82	2.2	57	230	76	150
Menzlin	33	1,051	10.10	10.2	87	2	17	148
Zarnekow	120	2,636	2.10	12.0	184	741	56	730
Jargelin	33	1,606	3.90	3.8	82	8	80	233

Data represent average values from a soil depth of 0–0.6 m (see Zak et al., 2010 for detailed description of porewater sampling and water analysis).

TABLE 2 | Selected peat characteristics of sampling sites: (C_t, N_t, P_t, and Fe_t–total contents of carbon, nitrogen, phosphorus, and iron), dry bulk density (Dbd) calculated from the dry matter according to Scheffer and Blankenburg (1993), the degree of peat decomposition (H) according to von Post-scale (Von Post, 1922) and organic matter (OM) in % of dry matter determined by loss on ignition.

Sampling site	pH	Dbd[a]	H[b]	OM[c]	C_t	N_t	P_t	Fe_t
		[g cm^{-3}]		[%]	[mg g^{-1} dry mass]			
NATURAL PEATLANDS								
Dollgensee	4.5	0.049	2–3	95	400	10	0.53	2.6
Töpchin	6.8	0.088	4	84	402	23	1.1	9.3
Gützkow	6.1	0.074	3	86	426	22	0.68	2.5
Triebschsee	6.9	0.084	1–3	88	433	18	0.54	3.0
Rzecin	5.4	0.11	2	94	423	11	0.42	0.75
REWETTED PEATLANDS								
Hasenfelde	7.2	0.42	10	41	216	17	1.5	19
Sauwinkel	5.3	0.28	10	75	393	29	1.0	5.4
Menzlin	6.4	0.23	10	70	364	32	1.5	10
Zarnekow	6.9	0.27	10	77	394	34	1.2	22
Jargelin	7.0	0.41	10	39	193	18	1.0	19

Inhibition of Microbial Activity With Proanthocyanidins

To evaluate the inhibitory activity of PAs, the FDA hydrolysis assay was performed as described above, adding PAs dissolved in 1 mL distilled water to a 4 mL slurry just before starting the hydrolysis reaction with FDA solution. Absorbance of formed fluorescein at 490 nm was related to a reference sample that did not contain any tannin and results were expressed in percentage inhibition. PAs from the five pristine sites as well as tannic acid (Fluka/Sigma-Aldrich, Munich, Germany) as model substance were added to yield final concentrations of 100 mg L^{-1} in the test tubes. This concentration corresponded to a tannin/peat ratio of ∼1:140. Additionally, PAs from Rzecin and tannic acid were added to yield concentration related inhibition with concentrations between 0–150 mg L^{-1} and 0–400 mg L^{-1}, respectively. All inhibition tests were conducted with highly decomposed peat material from a long-term experiment containing peat from Zarnekow (Zak and Gelbrecht, 2007). Analyses of microbial activities and inhibition of microbial activity was carried out on four to five technical replicates of each field sample.

Statistical Analysis

Statistical tests were performed using SPSS 14.0 for windows (SPSS Inc., 2005) and R (R Core Team, 2018). On the one hand, we simply compared the variables introduced above across two peatland types—degraded and near-natural—treating the samples from the different sites as replicates among peatland types. We analyzed whether there were significant differences between samples from these two peatland types with respect

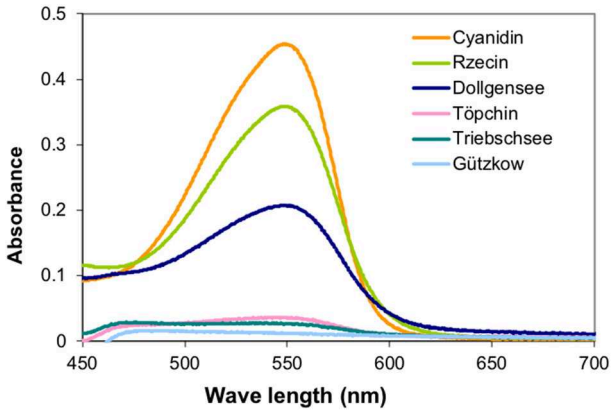

FIGURE 3 | UV spectra of the colored anthocyanidins formed during the acid butanol assay were conducted to verify the quality of separated PAs and their suitability as internal standards for pristine peatlands.

to the inhibitory activity of proanthocyanidins on enzyme-activity in samples, the amounts of phenolics as well as of hydrolysable and condensed tannins, and microbial activity using either one-way ANOVA or alternatively the parameter free Kruskal–Wallis test when conditions for the ANOVA were not satisfied. Significance was tested against an α level of 0.05.

On the other hand, we investigated the relationships between the total concentrations of phenolic hydroxyl groups (A750) and condensed tannins (A550), the estimated total microbial activity according to the FDA analysis (FDA), and the multivariate characteristics of the peat (OM, C:N, C, N, P, Fe:P, P, bulk density, von Post scale) with NMDS (non-metric multi-dimensional scaling) ordination. NMDS allows for the exploration of multivariate data in low dimensional space. The NMDS based on the characteristics of the peat was performed with function metaMDS() of package vegan (Oksanen et al., 2017) for R with default settings. Sub-sequentially we fitted the above stated variables to the ordination result using the function envfit() of package vegan. This approach is closely related to the concept of multiple regression and allows to investigate the possible relationship of a number of predictors on the multivariate configuration of the peat samples defined by all their relevant characterizing variables. The significance of relationships was determined with the build in permutation test of envfit() (999 runs). Variables with $p < 0.05$ were deemed significantly related to the ordination configuration.

To test whether microbial activity was determined by inhibitory compounds (A750, A550) and/or some of the other peat characterizing variables we constructed a multiple linear regression with estimated total microbial activity (FDA) as response and all variables that were identified as significant in the NMDS as drivers. The primary model was then further simplified using the function step() in R that runs an iterative approach of combined forward and backward selection, using the lowest AIC as selection criterion for deciding on the final regression equation.

RESULTS

Proanthocyanidins

Extraction of PAs from the different slightly decomposed peat soils yielded <1% of initial peat material on a dry matter basis. Although precipitation of tannins with trivalent ytterbium was not used for gravimetric quantification, it was a good indicator of tannin concentration in washed extract solutions. Extracts from peat of the pristine sites Rzecin and Dollgensee almost immediately showed precipitation of tannin-ytterbium complexes whereas peat extracts from Gützkow precipitated small amounts only perceptible after centrifugation. Calibrations of the acid butanol and the Folin-Ciocalteau assay with separated tannins are presented in **Figure 4**. Separated tannins from Gützkow, Triebschsee and Töpchin were characterized by particularly low absorbance values (<0.035 at 550 nm) in the acid butanol assay. Analysis of UV spectra showed that, in the case of tannins isolated from Gützkow peat, no absorbance maximum could be detected at 550 nm (**Figure 3**) although tannin concentrations were as high as 0.61 mg mL^{-1} (**Figure 4**). In the cases of Triebschsee and Töpchin, absorbance maxima could be identified but were not significantly different from background absorbance. Therefore, only calibrations for peat from the sites Rzecin and Dollgensee were used as internal standards for the quantification of PAs. All tannins, however, showed relevant concentrations of total phenolics during the Folin-Ciocalteau assay. Comparison of internal standards and the commercially available standards cyanidin chloride and tannic acid illustrates the advantage of internal standards. In any case, quantification with cyanidin or tannic acid would lead to a considerable underestimation (80–97%) of phenolic concentrations in peat soils (**Table 3**). Unfortunately, the purification of internal standards is impractical when peat samples contain only small amounts of tannins. Consequently, as no adequate internal standards could be separated for each peat soil, especially not for highly decomposed peat, further comparisons of concentrations were conducted with values expressed in absorbance units (AU) per dry mass (AU_{750}/AU_{550} g^{-1} DM). However, to enable comparison with other studies, AU values were translated to commonly used tannic acids equivalents and cyanidin equivalents (TAE/CAE g^{-1} DM) as summarized in **Table 3**.

Polyphenol Contents

Absorbance values of extractable total phenolics and PAs ranged between 0.121–3.275 AU_{750} g^{-1} DM and 0.01–1.682 AU_{550} g^{-1} DM, respectively (**Table 3**). Hydrolysable tannins were not detectable in any of the peat samples. Both total phenolics and PAs were significantly higher in peat soils from pristine sites than in peat soils from degraded sites, with a strong correlation between both factors (Spearman's R 0.92). Notably, peat from Gützkow did not show higher values in comparison to the degraded sites and peat from Triebschsee had comparatively high concentration of total phenolics not reflected in high PA concentrations. The two sites Rzecin and Dollgensee stood out by their 139- and 40-fold higher concentrations of extractable PAs compared to degraded sites. Calibration of the acid Butanol

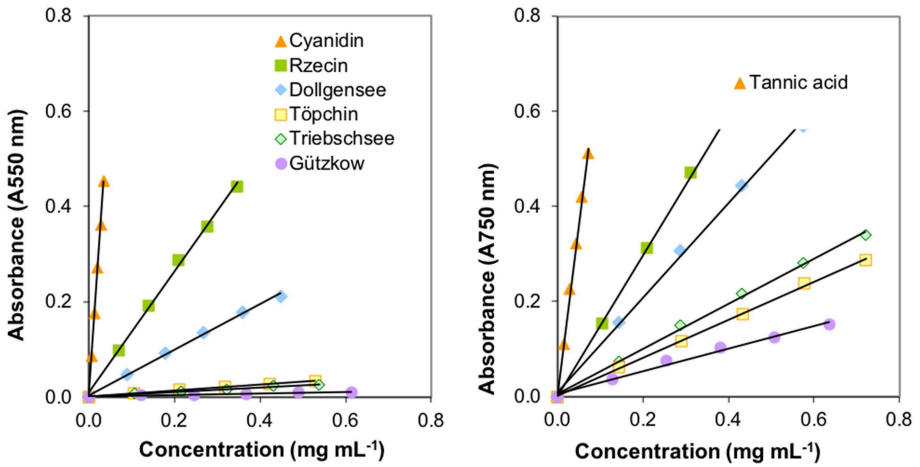

FIGURE 4 | Calibrations of the acid butanol (left image) and the Folin-Ciocalteau assay (right image) with isolated tannins from less decomposed peat of pristine peatlands.

TABLE 3 | Total phenolics and proanthocyanidins in differently decomposed peat soils referring to dry mass.

	Sites	Total phenolics			Proanthocyanidins		
		[AU_{750} g^{-1}]	[mg TAE g^{-1}]	[mg g^{-1}]	[AU_{550} g^{-1}]	[mg CAE g^{-1}]	[mg g^{-1}]
NATURAL PEATLANDS							
Less de-composed peat	Dollgensee	1.557	6.3	45.5	0.490	1.17	29.5
	Töpchin	0.776	3.1	59.1	0.093	0.25	1.2–4.5*
	Gützkow	0.347	1.3	39.8	0.013	0.06	0
	Triebschsee	1.323	5.3	81.7	0.031	0.11	0–0.7*
	Rzecin	3.275	13.5	66.4	1.682	3.92	38.6
REWETTED PEATLANDS							
Highly de-composed peat	Hasenfelde	0.121	0.3	2.3–11.1*	0.013	0.07	0*
	Sauwinkel	0.387	1.4	7.7–44.8*	0.013	0.07	0*
	Menzlin	0.157	0.5	3.0–15.7*	0.010	0.06	0*
	Zarnekow	0.419	1.6	8.3–49*	0.015	0.07	0*
	Jargelin	0.312	1.1	6.1–35.4*	0.010	0.06	0*

Values represent averages (means, n = 3) referring to dry mass and are expressed in three different ways using (i) absorbance units (AU), (ii) tannic acids and cyanidin equivalents (TAE/CAE), and (iii) internal phenolic standard. Internal standards could be only obtained for peat from "Dollgensee" and "Rzecin" so that in all other cases (*) these two standards were used to calculate ranges out of the AU medians (for details see section Proanthocyanidins).

and Folin-Ciocalteau assay with the same internal standard allowed an estimate of the size of the PA fraction in terms of total phenolics for peat from Rzecin and Dollgensee. Here, proanthocyanidins accounted for 58 and 65% of total phenolics, respectively, with total phenolics representing 6% of peat soil organic matter on an average.

Microbial Activity and Inhibition

The microbial activity of studied peat soils measured as hydrolysis rate of FDA ranged between 0.4 and 1.57 μg fluorescein h^{-1} mg^{-1} DM (**Figure 5**). The production of fluorescein was not significantly lower in the slightly decomposed peat soils, although Dollgensee and Triebschsee clearly had the lowest rates of FDA hydrolysis. However, peat from Gützkow showed very high activities for an only slightly decomposed peat soil, with presumably low microbial activities, and had the second highest activity after Menzlin.

All extracted tannins from pristine sites generated a significant inhibition of FDA hydrolysis when added to highly decomposed Zarnekow peat, with the exception of tannins from Gützkow peat (**Figure 6**). Significant inhibitions ranged between 12.3 and 17.9% and were achieved without any preliminary incubation times of tannins mixed with peat material. These values were lower compared to the inhibition produced by the addition of tannic acid as model substance (30.1%). Suppression of FDA hydrolysis with tannins was poorly reproducible between runs, most probably because of the great heterogeneity of the analyzed peat material. We attribute varying inhibition to the fact that

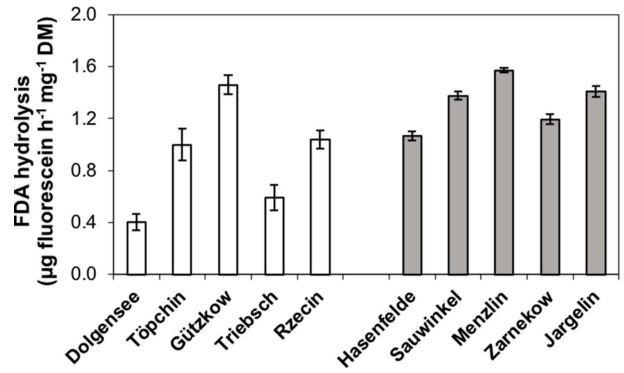

FIGURE 5 | Microbial activity of studied peat soils measured as hydrolysis rate of fluorescein diacetate (FDA) for pristine peatlands with less decomposed peat (white bars) and rewetted peatlands with highly decomposed peat (gray bars).

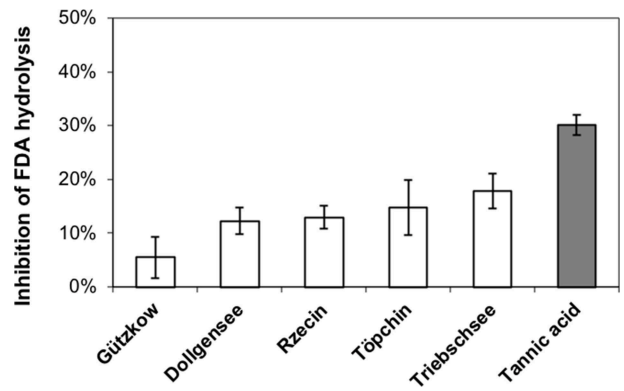

FIGURE 6 | Inhibition of fluorescein diacetate (FDA) hydrolysis in highly decomposed peat from rewetted peatland "Zarnekow" using isolated tannins from less decomposed peat of pristine peatlands (white bars) and commercial tannic acid standard (gray bar).

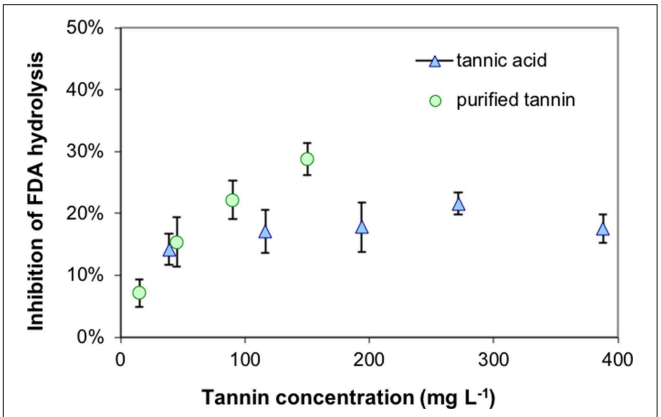

FIGURE 7 | Suppression of fluorescein diacetate (FDA) hydrolysis with increasing concentrations of tannins at the example of highly decomposed peat from rewetted peatland "Zarnekow" using commercial tannic acid and a isolated tannin of less decomposed peat from pristine peatland "Rzecin".

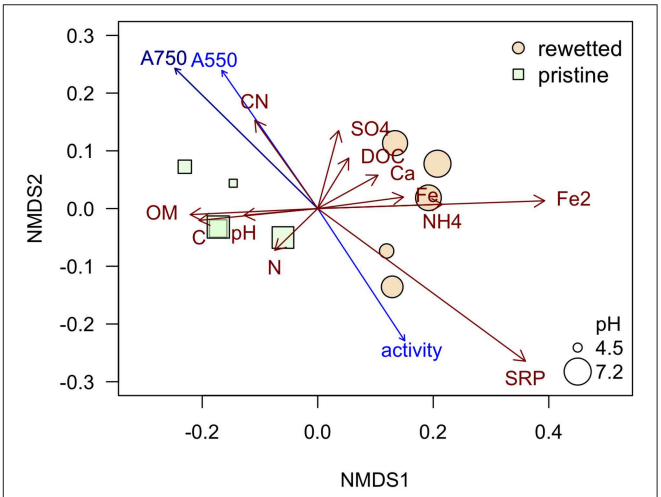

FIGURE 8 | NMDS plot based on the chemical characteristics of the peat and porewater analyses. The NMDS was run with defaults using function metaMDS of package vegan in R. Final stress was 0.059. Red arrows represent the included variables with vector lengths ≥0.1. Blue arrows are the *post-hoc* fitted variables on phenolic compounds and FDA, dark blue represents a variable that is significantly related to the ordination configuration with $p < 0.05$.

inhibition tests with 100 mg tannins L^{-1} were below saturation point (**Figure 7**).

Relationships Between Variables

The peat from the pristine and the altered sites are clearly separated in the NMDS plot (**Figure 8**) while the generalizing characteristic of the pH value (size of bubbles in **Figure 8**) doesn't seem to play an important role. The iron contents in the sites, mainly the Fe^{2+} concentrations in the porewater, have a strong influence on the ordination pattern and are associated with relatively low contents of organic matter (OM) in the peat. A similar negative relationship appears for the microbial activity (as measured with FDA) and the two variables representing total phenolic compounds (A750) and condensed tannins (A550) that were fitted *post-hoc* to the ordination and point at opposite directions (**Figure 8**). Interestingly these variables don't follow the pristine—rewetted gradient but are almost orthogonal to the latter. Only A750 is significantly related to the ordination configuration. While C and N in the peat show a similar direction like the organic matter, the CN ratio increases with the content of polyphenolics. Soluble reactive phosphorus increases in the opposite direction and thus relates well to increased microbial activity (**Figure 8**). We tested all variables for relationships to the microbial activity. Only three showed significant relation according to singular linear models: N content, A550, and A750 after omitting Rzecin which had a much lower Fe content (with high coefficient of variation) and a much higher total phenolic content (A750) than all other samples. Only total polyphenol content (A750) had a strong negative linear relationship with microbial activity ($R^2 = 0.83$, $p << 0.001$; **Figure 9**). This result was confirmed by the multiple regression approach. While N content, A750 and A550 (including a possible interaction between the latter) entered the analysis, the final model contained

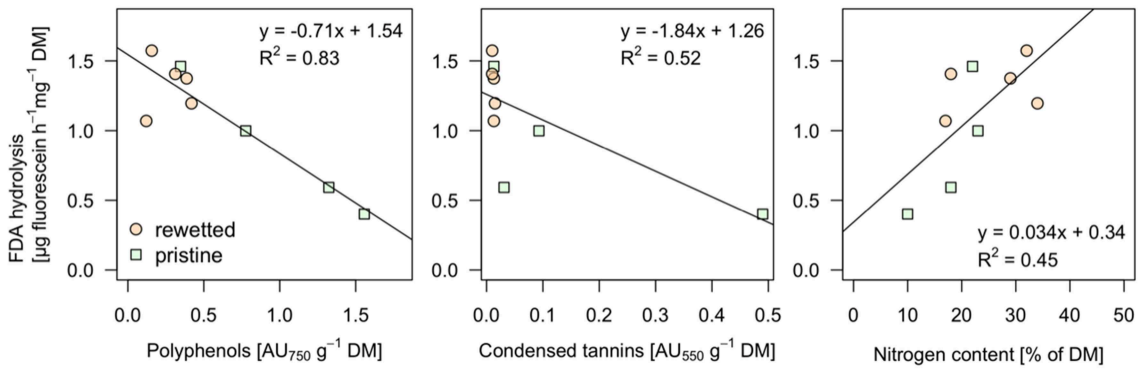

FIGURE 9 | Significant linear relationships between microbial activity and other measured variables. The microbial activity was determined as enzyme activity using fluorescein diacetate (FDA) hydrolysis. Values are given on dry mass (DM) basis. The complete variable set (peat chemistry, pore water chemistry, and potentially inhibiting substances) were tested. Only relationships with linear models significant with $p < 0.05$ are displayed.

only total polyphenol content as a driver and was, thus, essentially the model depicted in **Figure 9**.

DISCUSSION

Supporting our initial hypothesis, we found that highly degraded peat contained eight times lower levels of total polyphenols and 50 times lower levels of condensed tannins than less decomposed peat. Thus, draining and subsequent peat degradation effectively removes major parts of the tannin stock of fens by former mentioned oxidation processes and eliminates their potential function as an "enzymic latch" on the fen carbon store. The total phenolic contents of less decomposed peat from the pristine fens in this study (**Table 3**) corresponded well with concentrations of less decomposed *Sphagnum* peat (ca. 4–8 mg TAE g^{-1} DM) from different European peatlands (Dorrepaal et al., 2005; Bragazza and Freeman, 2007). Since peat-parent material in our study was mostly polyphenol-rich *Carex* spp. (**Table 4**) higher contents could be expected but certain *Carex* species might differ strongly regarding polyphenol contents/composition and some part of polyphenols might be decomposed during peat formation (see below). The concentrations in peat porewater were much higher and ranged up to 100 mg L^{-1}. To put this into perspective, inhibitory effects on hydrolase activity were already recorded under phenolic contents between 2 and 5 mg L^{-1} for a Welsh peatland (Freeman et al., 2004). Soil pore water was not analyzed for polyphenols in this study, however according to the amount of water-extractable polyphenols of 0.7 mg TAE g^{-1} DM and a dry bulk density of 100 g L^{-1}, as determined for peat from Dollgensee (results not shown) inhibition-relevant porewater concentration of about 70 mg TAE L^{-1} can be expected.

Naturally, the complex nature of polyphenols with potentially more than 8,000 individual molecule structures cannot be reflected in the analysis of total phenolics. Nevertheless, this unspecific proxy has shown some good correlation with decomposition patterns in peatland studies (Dorrepaal et al., 2005; Bragazza and Freeman, 2007; Bragazza et al., 2007) and has proven to be a suitable predictor for tannin inhibition of microbial growth of ruminal bacteria (Nelson et al., 1997).

TABLE 4 | Average contents of total phenolics and proanthocyanidins (median, $n = 3$) in roots from selected peat-forming vascular plant and from moss litter (for plant sampling sites see section Study sites and sampling).

Plant species	Total phenolics [mg g^{-1} dry mass]	Proanthocyanidins [mg g^{-1} dry mass]
Carex appropinquata	450	49
Eriophorum angustifolium	120	90
Vaccinium oxycoccos	134	100
Brown mosses	68	23
Sphagnum spp.	39	25

Individual processes such as litter decay, however, may depend much more on the type of polyphenol, rather than just on the total content. Despite their large diversity, their functioning with regards to metabolic processes can be classified as "ineffective," "inhibiting," or "promoting" (e.g. Bonnett et al., 2017). The latter refers *inter alia* to their ability to mediate redox-processes in soils as described for the quinone already in the beginning of the Twentieth century (Erdtman, 1933a,b). Likewise, the inhibitory properties of phenolics are well-known even for more than 100 years for *sphagnum*-derived phenolic acids as earlier reviewed by Verhoeven and Liefveld (1997). The suppression of microbial activity in *Sphagnum* peat was partially attributed to a tanning-like process involving 5-keto-D-mannurionic acid, associated with contributing to the famous preservation property of *Sphagnum* bogs (Vanbreemen, 1995). In vascular plant-dominated minerotrophic peatlands, tannins e.g. derived from *Eriophorum* spp. (Williams et al., 2000), could play an equally important role in the inhibition of microbial activity. Accordingly, it seems advantageous to obtain more detailed characterization of the biochemically diverse tannin fraction than to measure total phenolic contents alone.

The better solubility of hydrolysable tannins in water and their distinct complexing behavior, which depends on prevailing pH and redox conditions (Martin and Martin, 1983; Appel, 1993), promote them as potent enzyme inhibitors. On the other hand, their stability even in the form of tannin-protein-complexes may be too low to persist in the long term (Bravo, 1998; Fierer et al.,

2001). According to the absence of hydrolysable tannins in all tested peat soils, the inhibiting role of tannins must be solely attributed to the group of condensed tannins. Unfortunately, there is no reference for PA concentrations in peat, but some information is available for plant samples. For example, for conifers, the proportion was higher than 50% of total phenolic content, similar to peat samples from the natural sites Dollgensee and Rzecin. While our data analysis shows that isolated PAs from less decomposed peat of natural peatlands inhibited the activity of hydrolases (**Figure 7**), enzyme activities did not differ significantly between different degraded peat samples (**Figure 5**). Still, at least when correcting for an obvious outlier we find a strong linear relationship between total polyphenol content and microbial activity (**Figure 9**), supporting the validity of the "enzymic latch" for fen peat. However, the linear relationship between the content of condensed tannins and microbial activity hinges on one data point only and the data rather suggest a threshold below which microbial activity can go up.

We assume that enzyme activity levels and decomposition of organic matter are not only related to the presence or absence of polyphenols, but are a concert of multiple factors and processes which is also represented in the direction of the dichotomy between microbial activity and the inhibitory compounds in the NMDS plot which does not follow the gradient from pristine to altered sites that is otherwise well-represented along the first NMDS axis. Yet another limiting factor is the availability of resources (C and other nutrients) for decomposing organisms (Yavitt et al., 2005). Litter decomposition thus depends on substrate quality, e.g., C:N ratio, and lignin content. The bulk parameter C:N ratio scales well with the amount of potentially inhibitory substances in the NMDS. Polymers such as cellulose and hemicelluloses are readily degraded by microbial exoenzyme systems into energy-yielding dimers and monomers. Lignin or lignin-like phenolic polymers as found in *Sphagnum* are more recalcitrant in comparison.

Plant litter with high nutrient concentration generally decomposes relatively fast (Couteaux et al., 1995; Laiho, 2006). In *Sphagnum* litter, Bragazza et al. (2007) found the polyphenol/nutrient ratio to be one of the primary parameters controlling decomposition. Unlike in pristine bog peatlands, the decomposition of organic matter in the degraded and rewetted fens is strongly controlled by the biogeochemical regime including the elevated availability of electron acceptors like ferric iron and sulfate, enhanced nutrient availability, and circum-neutral pH (Zak and Gelbrecht, 2007; Brouns et al., 2014). Respiration measurements with different organic substrates from rewetted peatlands suggest that degraded peat without any fresh plant-derived material is relatively inert in terms of decomposition, whereas significant anaerobic CO_2 and CH_4 production in peat only occurs when enough labile organic matter is available (e.g., from remaining roots or root exudates; Hahn-Schöfl et al., 2011). The role of polyphenols for the decomposition of fresh aboveground litter and from wetland plants was tested by anaerobic incubation experiments showing that the availability of nutrients rather than polyphenol contents were significant factors (Zak et al., 2015). The polyphenol concentrations of tested plant litter samples ranged between 14 and 68 mg g^{-1} DM and were, thus, at the lower level of root and moss litter from this study (39–450 mg g^{-1} DM, **Table 3**). Unfortunately, the proportion of tannins was not quantified in this work, however it was interesting to note that in non-peat forming plants (*Phalaris arundinacea, Ceratophyllum demersum, Typha latifolia*) the content of polyphenols was reduced between 50 and 95%, while in the peat forming plants (*Phragmites australis, Carex riparia*) the reduction was much lower (<20% after 150 days).

At time of peat sampling, non-peat forming plants still dominated the studied rewetted sites. After 10 to 20 years of rewetting, however, a distinct succession toward peat-forming reed communities is evident, while the re-colonization with brown mosses and low sedges characterized by higher polyphenol contents seems to be retarded over several decades, depending on the drainage and land use history (Zerbe et al., 2013; Zak et al., 2015) as observed in other rewetting projects (Koch et al., 2017). Also, if peat forming plants are re-established the quality and quantity of polyphenols in plant tissues might differ substantially from their natural counterparts as long as nutrient levels are higher as under pre-drained conditions. Low nutrient levels are known for promoting the production of secondary metabolites *inter alia* to protect the plants against herbivory or pathogens (Verhoeven and Liefveld, 1997). All things considered, it remains uncertain about how long it would take for enzyme-inhibiting polyphenols in soils to reach concentrations that would have a significant impact on microbial metabolism. For such an assessment it might also be considered that phenol oxidases could be activated under oxygen-free conditions in case of elevated concentrations of other electron acceptors, such as sulfate and oxidized but soluble or less crystalline ferric iron (Van Bodegom et al., 2005; Fenner and Freeman, 2011). Thus, elevated sulfate concentrations in soil water of the pristine sites Gützkow and Triebschsee (>80 mg L^{-1}, **Table 1**) might be responsible for the comparatively low polyphenol contents in peat from such sites. Eventually, there might be other anaerobic decomposition pathways depending on certain abiotic factors and/or presence of fungal and bacterial communities (e.g., Fuchs et al., 2011) which needs detailed consideration in order to better understand different patterns of organic matter decomposition in peatlands.

CONCLUSIONS

The drainage of fens and their use as grassland over approximately three decades caused a significant loss of condensed tannins. Accordingly, organic matter decomposition may continue at about the same pace as before the rewetting because of the (almost) absence of the "latch" provided by the phenols. Despite their presumed role as enzyme-inhibiting substances, hydrolysable tannins may play an insignificant role in decomposition processes since they do not accumulate in the peat in contrast to condensed tannins. Their capacity to reduce the microbial enzyme activity was clearly confirmed in assays using tannins from less decomposed peat of pristine fens. However, the substantial differences in polyphenol contents, in particular for condensed tannins, did not correspond with significant

differences in hydrolytic enzyme activities in highly decomposed peat compared to less decomposed peat. Future research must clarify if and how long it may take after rewetting for polyphenol content and composition to return to those of pristine fens, and whether the repression of hydrolase enzymes eventually resumes, as this will be important for the long-term carbon accumulation. According to the high complexity of possible metabolic processes and driving factors both under aerobic and anaerobic conditions the measurement of single parameters like redox-conditions, nutrient availability or pH will be not sufficient to make a reasonable estimate of carbon turnover in rewetted peatlands. However, it can be presumed that the re-establishment of peat-forming *Carex* species or brown mosses characterized by high tannin contents could represent the switch for the "enzymic latch" mechanism. Another important precondition might be a significant reduction of electron acceptor availability and nutrient levels (Brouns et al., 2016). Altogether, there is evidence that polyphenol elimination by fen drainage must be ameliorated before rehabilitation of rewetted peatlands in the context of carbon cycling can be considered a success in decades to come. The removal of the degraded peat layer can be a suitable method to re-establish low-nutrient conditions and facilitate the re-colonization by peat-forming plants within few years only (Zak et al., 2017). However, top soil removal can be a rather expensive measure and, particularly if the objective of the peatland restoration is to target mitigation of climate change, its carbon footprint needs to be carefully assessed (Zak et al., 2018). Alternatively, harvesting of wetland helophytes and their commercial use (Wichmann, 2017) can be another viable option to support the succession toward natural conditions but again longer time periods (>>10 years) must be tolerated (Zak et al., 2014).

DATA AVAILABILITY STATEMENT

The datasets generated and analyzed for this study can be found in an electronic supplement to this article (Data_Supplement-Zak_et_al.xlsx in **Supplementary Material**).

AUTHOR CONTRIBUTIONS

DZ and CR designed the study and CR conducted the experiments. CR and GJ performed data analysis. DZ and CR compiled the manuscript. All authors contributed to the text.

FUNDING

The study was supported by Deutsche Forschungsgemeinschaft (DFG), Grant/Award Number: ZA 742/2-1; Department of Environment of Mecklenburg-Vorpommern, Grant/Award Number: LUNG-230-5325.60-7-34; European Agriculture Guidance and the Guarantee Fund, Grant/Award Number: LUNG-230-5325.60-7-34. Finalization of the study was funded by the European Social Fund (ESF) and the Ministry of Education, Science and Culture of Mecklenburg-Western Pomerania within the scope of the project WETSCAPES (ESF/14-BM-A55-0030/16). VU was financed within the framework of the Research Training Group Baltic TRANSCOAST funded by the DFG under grant number GRK 2000.

ACKNOWLEDGMENTS

Many thanks to all colleagues of the Department of Chemical Analytics and Biogeochemistry of the Leibniz-Institute of Freshwater Ecology and Inland Fisheries supporting the comprehensive chemical analyses and for their technical assistance during fieldwork. In particular we gratefully acknowledge Jörg Gelbrecht for advice and help with peat and plant sampling. Steffen Vogler, Etienne Brunet, and Angela Krüger are acknowledged for conducting microbial activity tests and phenol analysis.

SUPPLEMENTARY MATERIAL

The Supplementary Material for this article can be found online at: https://www.frontiersin.org/articles/10.3389/fenvs.2019.00147/full#supplementary-material

REFERENCES

Appel, H. M. (1993). Phenolics in ecological interactions - the importance of oxidation. *J. Chem. Ecol.* 19, 1521–1552. doi: 10.1007/BF00984895

Bader, C., Müller, M., Schulin, R., and Leifeld, J. (2018). Peat decomposability in managed organic soils in relation to land use, organic matter composition and temperature. *Biogeosciences* 15, 703–719. doi: 10.5194/bg-15-703-2018

Bonnett, S. A. F., Maltby, E., and Freeman, C. (2017). Hydrological legacy determines the type of enzyme inhibition in a peatlands chronosequence. *Scient. Rep.* 7, 1–14. doi: 10.1038/s41598-017-10430-x

Box, J. D. (1983). Investigation of the folin-ciocalteau phenol reagent for the determination of polyphenolic substances in natural-waters. *Water Res.* 17, 511–525. doi: 10.1016/0043-1354(83)90111-2

Bragazza, L., and Freeman, C. (2007). High nitrogen availability reduces polyphenol content in *Sphagnum* peat. *Sci. Total Environ.* 377, 439–443. doi: 10.1016/j.scitotenv.2007.02.016

Bragazza, L., Siffi, C., Iacumin, P., and Gerdol, R. (2007). Mass loss and nutrient release during litter decay in peatland: the role of microbial adaptability to litter chemistry. *Soil Biol. Biochem.* 39, 257–267. doi: 10.1016/j.soilbio.2006.07.014

Bravo, L. (1998). Polyphenolics, dietary sources, metabolism and nutritional significance. *Nutr. Rev.* 56, 257–267. doi: 10.1111/j.1753-4887.1998.tb01670.x

Brouns, K., Keuskamp, J. A., Potkamp, G., Verhoeven, J. T. A., and Hefting, M. M. (2016). Peat origin and land use effects on microbial activity, respiration dynamics and exo-enzyme activities in drained peat soils in the Netherlands. *Soil Biol. Biochem.* 95, 144–155. doi: 10.1016/j.soilbio.2015.11.018

Brouns, K., Verhoeven, J. T. A., and Hefting, M. M. (2014). Short period of oxygenation releases latch on peat decomposition. *Sci. Total Environ.* 481, 61–68. doi: 10.1016/j.scitotenv.2014.02.030

Cabezas, A., Gelbrecht, J., Zwirnmann, E., Barth, M., and Zak, D. (2012). Effects of degree of peat decomposition, loading rate and temperature on dissolved nitrogen turnover in rewetted fens. *Soil Biol. Biochem.* 48, 182–191. doi: 10.1016/j.soilbio.2012.01.027

Couteaux, M. M., Bottner, P., and Berg, B. (1995). Litter decomposition, climate and litter quality. *Trends Ecol. Evol.* 10, 63–66. doi: 10.1016/S0169-5347(00)88978-8

Cowan, M. M. (1999). Plant products as antimicrobial agents. *Clin. Microbiol. Rev.* 12, 564–582. doi: 10.1128/CMR.12.4.564

Dorrepaal, E., Cornelissen, J. H. C., Aerts, R., Wallen, B., and van Logtestijn, R. S. P. (2005). Are growth forms consistent predictors of leaf litter quality and decomposability across peatlands along a latitudinal gradient? *J. Ecol.* 93, 817–828. doi: 10.1111/j.1365-2745.2005.01024.x

Erdtman, H. G. H. (1933a). Studies on the formation of complex oxidation and condensation products of phenols. A contribution to the investigation of the origin and nature of humic acid. 1. Studies of the reactivity of simple monocyclic quinones. *Proc. Roy. Soc. A* 143,177–191. doi: 10.1098/rspa.1933.0212

Erdtman, H. G. H. (1933b). Studies on the formation of complex oxidation and condensation products of phenols. 2. Coupling of simple phenols and quinones to diphenyl derivatives. *Proc. Roy. Soc. A* 143, 191–222. doi: 10.1098/rspa.1933.0213

Fenner, N., and Freeman, C. (2011). Drought-induced carbon loss in peatlands. *Nat. Geosci.* 4, 895–900. doi: 10.1038/ngeo1323

Fierer, N., Schimel, J. P., Cates, R. G., and Zou, J. (2001). Influence of balsam poplar tannin fractions on carbon and nitrogen dynamics in Alaskan taiga floodplain soils. *Soil Biol. Biochem.* 33,1827–1839. doi: 10.1016/S0038-0717(01)00111-0

Franz, D., Koebsch, F., Larmanou, E., Augustin, J., and Sachs, T. (2016). High net CO_2 and CH_4 release at a eutrophic shallow lake on a formerly drained fen. *Biogeosciences* 13, 3051–3070. doi: 10.5194/bg-13-3051-2016

Freeman, C., Ostle, N., and Kang, H. (2001). An enzymic 'latch' on a global carbon store - A shortage of oxygen locks up carbon in peatlands by restraining a single enzyme. *Nature* 409:149. doi: 10.1038/35051650

Freeman, C., Ostle, N. J., Fenner, N., and Kang, H. (2004). A regulatory role for phenol oxidase during decomposition in peatlands. *Soil Biol. Biochem.* 36,1663–1667. doi: 10.1016/j.soilbio.2004.07.012

Fuchs, G., Boll, M., and Heider, J. (2011). Microbial degradation of aromatic compounds – from one strategy to four. *Nat. Rev. Microbiol.* 9, 803–816. doi: 10.1038/nrmicro2652

Georgé, S., Brat, P., Alter, P., and Amiot, M. J. (2005). Rapid determination of polyphenols and vitamin C in plant-derived products. *J. Agric. Food Chem.* 53, 1370–1373. doi: 10.1021/jf048396b

Giner-Chavez, B. I., van Soest, P. J., Robertson, J. B., Lascano, C., Reed, J. D., and Pell, A. N. (1997). A method for isolating condensed tannins from crude plant extracts with trivalent ytterbium. *J. Sci. Food Agric.* 74, 359–368. doi: 10.1002/(SICI)1097-0010(199707)74:3<359::AID-JSFA811>3.0.CO;2-C

Gorham, E. (1991). Northern peatlands role in the carbon cycle and probable responses to climatic warming. *Ecol. Appl.* 1, 182–195. doi: 10.2307/1941811

Hagerman, A. E. (2002). *The Tannin Handbook*. Available online at: https://www.users.miamioh.edu/hagermae/ (accessed September 10, 2019).

Hahn-Schöfl, M., Zak, D., Minke, M., Gelbrecht, J., Augustin, J., and Freibauer, A. (2011). Organic sediment formed during inundation of a degraded fen grassland emits large fluxes of CH_4 and CO_2. *Biogeosciences* 8, 1539–1550. doi: 10.5194/bg-8-1539-2011

Hall, S. J., Treffkorn, J., and Silver, W. L. (2014). Breaking the enzymatic latch: impacts of reducing conditions on hydrolytic enzyme activity in tropical forest soils. *Ecology* 95, 2964–2973. doi: 10.1890/13-2151.1

Hättenschwiler, S., and Vitousek, P. M. (2000). The role of polyphenols in terrestrial ecosystem nutrient cycling. *Trends Ecol. Evol.* 15, 238–243. doi: 10.1016/S0169-5347(00)01861-9

Hernes, P. J., and Hedges, J. I. (2000). Determination of condensed tannin monomers in environmental samples by capillary gas chromatography of acid depolymerization extracts. *Analyt. Chem.* 72, 5115–5124. doi: 10.1021/ac991301y

Hilt, S., Ghobrial, M. G., and Gross, E. M. (2006). *In situ* allelopathic potential of *Myriophyllum verticillatum* (*Halorgagaceae*) against selected phytoplankton species. *J. Phycol.* 42, 1189–1198. doi: 10.1111/j.1529-8817.2006.00286.x

IPCC (2014). *2013 Supplement to the 2006 IPCC Guidelines for National Greenhouse Gas Inventories*. Wetlands: IPCC.

Jenkinson, D. S., Adams, D. E., and Wild, A. (1991). Model estimates of CO_2 emissions from soil in response to global warming. *Nature* 351, 304–306. doi: 10.1038/351304a0

Joosten, H. (2010). *The Global Peatland CO_2 Picture: Peatland Status and Drainage Related Emissions in All Countries of the World*. Netherlands: Wetland International, Ede.

Joosten, H., Brust, K., Couwenberg, J., Gerner, A., Holsten, B., Permien, T., et al. (2015). *MoorFutures® Integration of Additional Ecosystem Services (Including Biodiversity) Into Carbon Credits – Standard, Methodology and Transferability to Other Regions*. Bonn: Bundesamt für Naturschutz (Federal Ministry for the Environment, BfN).

Koch, M., Koebsch, F., Hahn, J., and Jurasinski, G. (2017). From meadow to shallow lake: monitoring secondary succession in a coastal fen after rewetting by flooding based on aerial imagery and plot data. *Mires Peat* 19, 1–17. doi: 10.19189/MaP.2015.OMB.188

Kraus, T. E. C., Dahlgren, R. A., and Zasoski, R. J. (2003). Tannins in nutrient dynamics of forest ecosystems - a review. *Plant Soil* 256, 41–66. doi: 10.1023/A:102620651

Laiho, R. (2006). Decomposition in peatlands: reconciling seemingly contrasting results on the impacts of lowered water levels. *Soil Biol. Biochem.* 38, 2011–2024. doi: 10.1016/j.soilbio.2006.02.017

Luthria, D. L., and Pastor-Corrales, M. A. (2006). Phenolic acids content of fifteen dry edible bean (*Phaseolus vulgaris* L.) varieties. *J. Food Comp. Anal.* 19, 205–2011. doi: 10.1016/j.jfca.2005.09.003

Martin, J. S., and Martin, M. M. (1983). Tannin assays in ecological-studies - precipitation of ribulose-1,5-bisphosphate carboxylase oxygenase by tannic-acid, quebracho, and oak foliage extracts. *J. Chem. Ecol.* 9, 285–294. doi: 10.1007/BF00988046

Mole, S., and Waterman, P. G. (1987). A critical analysis of techniques for measuring tannins in ecological-studies II. *Tech. Biochem. Def. Tann. Oecol.* 72, 148–156. doi: 10.1007/BF00385059

Mueller-Harvey, I. (2001). Analysis of hydrolysable tannins. *Anim. Feed Sci. Technol.* 91, 3–20. doi: 10.1016/S0377-8401(01)00227-9

Nelson, K. E., Pell, A. N., Doane, P. H., GinerChavez, B. I., and Schofield, P. (1997). Chemical and biological assays to evaluate bacterial inhibition by tannins. *J. Chem. Ecol.* 23, 1175–1194. doi: 10.1023/B:JOEC.0000

Nyamambi, B., Ndlovu, L. R., Read, J. S., and Reed, J. D. (2000). The effects of sorghum proanthocyanidins on digestive enzyme activity *in vitro* and in the digestive tract of chicken. *J. Sci. Food Agric.* 80, 2223–2231. doi: 10.1002/1097-0010(200012)80:15<2223::AID-JSFA768>3.0.CO;2-I

Oksanen, J., Blanchet, F. G., Friendly, M., Kindt, R., Legendre, P., McGlinn, D., et al. (2017). *Vegan: Community Ecology Package, R package version 2.4-5*. Available online at: https://CRAN.R-project.org/package=vegan (accessed September 10, 2019).

Pind, A., Freeman, C., and Lock, M. A. (1994). Enzymatic degradation of phenolic materials in peatlands - measurement of phenol oxidase activity. *Plant Soil* 159, 227–231. doi: 10.1007/BF00009285

Pinsonneault, A. J., Moore, T. R., and Roulet, N. T. (2016). Temperature the dominant control on the enzyme-latch across a range of temperate peatland types. *Soil Biol. Biochem.* 97, 121–130. doi: 10.1016/j.soilbio.2016.03.006

Porter, L. J., Hrstich, L. N., and Chan, B. G. (1986). The conversion of procyanidins and prodelphinidins to cyanidin and delphinidin. *Phytochemistry* 25, 223–230. doi: 10.1016/S.0031-9422(00)94533-3

R Core Team (2018). *R: A Language and Environment for Statistical Computing*. Vienna: R Foundation for Statistical Computing. Available online at: https://www.R-project.org/ (accessed September 10, 2019).

Rautio, P., Bergvall, U. A., Karonen, M., and Salminen, J. P. (2007). Bitter problems in ecological feeding experiments: commercial tannin preparations and common methods for tannin quantifications. *Biochem. System. Ecol.* 35, 257–262. doi: 10.1016/j.bse.2006.10.016

Scheffer, B., and Blankenburg, J. (1993). The determination of the bulk-density of peat soils. *Agribiol. Res. Zeitschr. Agrarbiol. Agrik. Okol.* 46, 46–53.

Schnürer, J., and Rosswall, T. (1982). Fluorescein diacetate hydrolysis as a measure of total microbial activity in soil and litter. *Appl. Environ. Microbiol.* 43, 1256–1261.

SPSS Inc. (2005). *SPSS Conjoint 14.0 [Software]*. Chicago, IL: SPSS, Inc.

Swain, T. (1979). "Tannins and lignins," in *Herbivores: Their Interaction With Secondary Plant Metabolites,* eds G. Rosenthal and D. H. Janzen (New York, NY: Academic Press), 657–682.

Van Bodegom, P. M., Broekman, R., Van Dijk, J., Bakker, C., and Aerts, R. (2005). Ferrous iron stimulates phenol oxidase activity and organic matter decomposition in waterlogged Wetlands. *Biogeochemistry* 76, 69–83. doi: 10.1007/s10533-005-2053-x

Vanbreemen, N. (1995). How *Sphagnum* bogs down other plants. *Trends Ecol. Evol.* 10, 270–275. doi: 10.1016/0169-5347(95)90007-1

Verhoeven, J. T., and Liefveld, W. M. (1997). The ecological significance of organochemical compounds in *Sphagnum*. *Acta Bot. Neerl.* 46, 117–130. doi: 10.1111/plb.1997.46.2.117

Verhoeven, J. T. A., Arheimer, B., Yin, C. Q., and Hefting, M. M. (2006). Regional and global concerns over wetlands and water quality. *Trends Ecol. Evol.* 21, 96–103. doi: 10.1016/j.tree.2005.11.015

Von Post, L. (1922). Sveriges geologiska undersöknings torvinventering och några av dess hittills vunna resultat. *Sven. Mosskulturfören. Tidskr* 1, 1–27.

Wichmann, S. (2017). Commercial viability of paludiculture: a comparison of harvesting reeds for biogas production, direct combustion, and thatching. *Ecol. Eng.* 103, 497–505. doi: 10.1016/j.ecoleng.2016.03.018

Williams, C. J., Shingara, E. A., and Yavitt, J. B. (2000). Phenol oxidase activity in peatlands in New York state: response to summer drought and peat type. *Wetlands* 20, 416–421. doi: 10.1672/0277-5212(2000)020[0416:POAIPI]2.0.CO;2

Williams, C. J., and Yavitt, J. B. (2003). Botanical composition of peat and degree of peat decomposition in three temperate peatlands. *Ecoscience* 10, 85–95. doi: 10.1080/11956860.2003.11682755

Yavitt, J. B., Williams, C. J., and Wieder, R. K. (2005). Soil chemistry versus environmental controls on production of CH_4 and CO_2 in northern peatlands. *Eur. J. Soil Sci.* 56, 169–178. doi: 10.1111/j.1365-2389.2004.00657.x

Yu, Z., Loisel, J., Brosseau, D. P., Beilman, D. W., and Hunt, S. J. (2010). Global peatland dynamics since the last glacial maximum. *Geophys. Res. Lett.* 37:L13402. doi: 10.1029/2010GL043584

Zak, D., and Gelbrecht, J. (2007). The mobilisation of phosphorus, organic carbon and ammonium in the initial stage of fen rewetting (a case study from NE Germany). *Biogeochemistry* 85, 141–151. doi: 10.1007/s10533-007-9122-2

Zak, D., Gelbrecht, J., Zerbe, S., Shatwell, T., Barth, M., Cabezas, A., et al. (2014). How helophytes influence the phosphorus cycle in degraded inundated peat soils – implications for fen restoration. *Ecol. Eng.* 66, 82–90. doi: 10.1016/j.ecoleng.2013.10.003

Zak, D., Goldhammer, T., Cabezas, A., Gelbrecht, J., Gurke, R., Wagner, C., et al. (2018). Top soil removal reduces water pollution from phosphorus and dissolved organic matter and lowers methane emissions from rewetted peatlands. *J. Appl. Ecol.* 55, 311–320. doi: 10.1111/1365-2664.12931.

Zak, D., Meyer, N., Cabezas, A., Gelbrecht, J., Mauersberger, R., Tiemeyer, B., et al. (2017). Topsoil removal to minimize internal eutrophication in rewetted peatlands and to protect downstream systems against phosphorus pollution: a case study from NE Germany. *Ecol. Eng.* 103, 488–496. doi: 10.1016/j.ecoleng.2015.12.030.

Zak, D., Reuter, H., Augustin, J., Shatwell, T., Barth, M., Gelbrecht, J., et al. (2015). Changes of the CO_2 and CH_4 production potential of rewetted fens in the perspective of temporal vegetation shifts. *Biogeosciences* 12, 2455–2468. doi: 10.5194/bg-12-2455-2015

Zak, D., Wagner, C., Payer, B., Augustin, J., and Gelbrecht, J. (2010). Phosphorus mobilization in rewetted fens: the effect of altered peat properties and implications for their restoration. *Ecol. Appl.* 20, 1336–1349. doi: 10.1890/08-2053.1

Zerbe, S., Steffenhagen, P., Parakenings, K., Timmermann, T., Frick, A., Gelbrecht, J., et al. (2013). Restoration success regarding ecosystem services after 10 years of rewetting peatlands in NE Germany. *Environ. Manage.* 51, 1194–1209. doi: 10.1007/s00267-013-0048-2

Conflict of Interest: The authors declare that the research was conducted in the absence of any commercial or financial relationships that could be construed as a potential conflict of interest.

frontiers in Environmental Science

ORIGINAL RESEARCH
published: 09 October 2019
doi: 10.3389/fenvs.2019.00137

Shallow Salt Marsh Tidal Ponds–An Environment With Extreme Oxygen Dynamics

Ketil Koop-Jakobsen[1]* *and Martin S. Gutbrod*[2]

[1] MARUM–Center for Marine Environmental Sciences, University of Bremen, Bremen, Germany, [2] Precision Sensing GmbH, Regensburg, Germany

In marshes, tidal ponds are increasing in number and areal coverage. Getting a better understanding of their unique biogeochemistry is a prerequisite for foreseeing their future role in salt marsh ecosystems. Using *in situ* microprofiling, this study investigated the spatiotemporal dynamics of O_2, pH, and CO_2 in shallow salt marsh tidal ponds in the summer time. High benthic photosynthetic activity, fueled by CO_2 from the sediment, resulted in steep vertical O_2 gradients at the sediment-water interface, increasing from anoxia to extremely supersaturated peak concentrations up to 886 ± 139 μmol L^{-1} (391% atmospheric O_2 saturation) over a short distance of 6 mm. These characteristic peaks developed even at low light conditions down to 150 μmol photons m^{-2} s^{-1} photosynthetically active radiation (PAR). The oxygen gradients were restricted to the layer of benthic microalgae on the sediment surface and did not extend into the water column, which was well-mixed throughout the day showing no vertical variation. The benthic photosynthesis and respiration controlled the oxygen concentration in the water column, creating net supersaturated conditions during the day and hypoxic conditions at night. The tidal ponds were generally well-buffered showing only attenuated pH fluctuations ranging from 6.2 to 7.3, and no persistent gradients built up, despite the high photosynthetic activity at the sediment water interface. CO_2 accumulated in the sediment and was present in the water column during the morning hours, but depleted in the afternoon due to the high photosynthetic uptake. Tidal ponds also experienced event-driven changes in their biogeochemistry. Sea foam developed on the water surface during the day and accumulated on one side of the pond blocking light penetration and lowering oxygen concentrations under the foam. Inundation at high tide caused a short-lived temporal variation in O_2 and pH, which was restricted to the time of the flood. As the flooding water receded, the preceding O_2 and pH conditions were immediately restored. Altogether shallow tidal ponds comprise a marsh habitat with distinctive spatiotemporal oxygen dynamics driven by benthic photosynthesis and respiration, which differ from the surrounding vegetated marsh, and could drive changes in salt marsh biogeochemistry in response to increased pond coverage.

Keywords: O_2, CO_2, pH, optode, salt marsh, microprofiling, benthic microalgae (BMA), Plum Island Estuary

OPEN ACCESS

Edited by:
Fereidoun Rezanezhad, University of Waterloo, Canada

Reviewed by:
Amanda C. Spivak, University of Georgia, United States
Hollie Emery, Harvard University, United States

***Correspondence:**
Ketil Koop-Jakobsen
kjakobsen@marum.de

Specialty section:
This article was submitted to Biogeochemical Dynamics, a section of the journal Frontiers in Environmental Science

Received: *16 May 2019*
Accepted: *04 September 2019*
Published: *09 October 2019*

Citation:
Koop-Jakobsen K and Gutbrod MS (2019) Shallow Salt Marsh Tidal Ponds–An Environment With Extreme Oxygen Dynamics. Front. Environ. Sci. 7:137. doi: 10.3389/fenvs.2019.00137

INTRODUCTION

Tidal ponds, also referred to as tide pools or potholes, are naturally occurring in salt marshes, creating a mosaic of permanently inundated ponds with bare sediment on the otherwise vegetated salt marsh platform (Harshberger, 1916; Adamowicz and Roman, 2005). Tidal ponds are widespread on the marsh platform occupying typically around 5–15% of the total marsh area (Adamowicz and Roman, 2005; Millette et al., 2010; Wilson et al., 2014), but areal coverages up to 60% has been observed (Schepers et al., 2017). The ponds have an important ecological function as shelter, feeding ground, and spawning area for a large variety of fish, shellfish, and crustaceans (Smith and Able, 1994, 2003; Raposa and Roman, 2001; Allen et al., 2017), and play a significant role supporting fish production in the coastal area (Mackenzie and Dionne, 2008).

Salt marsh tidal ponds constitute a unique habitat characterized by rapid fluctuations in O_2, temperature and salinity, which can reach extreme levels over a day-night cycle (Smith and Able, 2003). The ponds can be very shallow, down to 3–5 cm. The surrounding marsh vegetation provides little shading from direct exposure to sunlight, which causes the water temperature to increase significantly during hot summer days and salinity to increase in response to high evaporation (Lillebø et al., 2010). A diverse and highly specialized microbial community inhabits the sediment surface (Kearns et al., 2017), and benthic microbial mats dominated by cyanobacteria can form in the summer time (Harshberger, 1916; Ruber et al., 1981). Consequently, there is high benthic photosynthetic O_2 production during the day, and a high sediment O_2 demand caused by microbial respiration and reoxidation of reduced compounds, which leads to marked daily O_2 fluctuations (Ruber et al., 1981).

Under warm and sunny summer conditions, the water column in tidal ponds becomes supersaturated with O_2 during the day, and high respiratory activity results in a depletion of O_2 at night, where the water column can reach hypoxic conditions (Smith and Able, 2003; Lillebø et al., 2010; Baumann et al., 2015; Spivak et al., 2017). This makes harsh living conditions for the organisms that inhabit or get trapped in the tidal ponds after the receding tide. In contrast, the tidal pond water is well-buffered, and pH does not reach extreme values, but fluctuates daily in a range from 7 to 8.5 in the summer months (Lillebø et al., 2010; Baumann et al., 2015; Kearns et al., 2017). Previous studies of daily variations of O_2, pH, and temperature were primarily conducted as point-measurement in the water column, following the temporal variation over the course of the day. However, *in-situ* data about the gradients, which may build up within this shallow ecosystem, and their spatial and temporal dynamics are lacking, and the causes of these extreme oxygen dynamics are not fully understood.

Therefore, we investigated both the daily temporal and spatial dynamics of O_2, pH, and CO_2 in shallow salt marsh tidal ponds, highlighting the development of gradients across the sediment-water interface. Using an automated profiling system with needle optodes, high resolution vertical profiles of O_2, pH, and CO_2 were measured from the air-water interface, through the water column and into the sediment, exploring the daily variation in vertical gradients and their dependence on light exposure. The investigations were conducted *in situ* and under controlled light conditions in the laboratory.

METHODS AND MATERIALS

Study Site

The investigation of shallow salt marsh tidal ponds was conducted in the high marsh of the Plum Island Estuary, MA, USA (42°44′19″N,70○50′48″W; **Figure 1A**). Three closely located soft-bottomed tidal ponds were investigated (**Figure 1B**). The bottom of the tidal ponds was characterized by a thick layer of photosynthesizing benthic microalgae (**Figure 1C**). The ponds, which are located on the marsh platform, have an area between ∼30 and 100 m^2, and a shallow water-depth (<10 cm) (**Figures 1D–F**).

Experimental Design

The overall scope was to elucidate the daily spatiotemporal variations of O_2, pH, and CO_2 in shallow salt marsh tidal ponds and to resolve the role of light as a controlling factor. A series of five investigations were designed (**Table 1**). To investigate the spatial variation, vertical profiles were measured with high spatial resolution using an automated needle optode microprofiling device. To account for the daily variation in the profiles, these measurements were conducted in the morning, afternoon, and at night. The impact of light on the spatial variation was investigated on cores from the field in a laboratory-study under controlled light regimes. To further evaluate the temporal variation, a 24 h time-series measurement was conducted in the same pond at a fixed position in the water column with high temporal resolution. Spatial variations within a pond and the influence of sea foam was studied in detail in a forth experiment, and in order to account for differences among different tidal ponds, profiling was conducted consecutively in three independent but closely located ponds within a short timeframe.

All *in situ* measurements were conducted in July 2018 on days with clear skies, where the tidal ponds were directly exposed to sunlight. All laboratory measurements were conducted in July 2017. The investigations focussed primarily on oxygen, which was measured in all investigations, whereas pH and CO_2 were only measured in selected studies (**Table 1**).

Experimental Set-Up

The experimental set-up is shown in **Figure 2**. O_2, pH, and CO_2 profiling was conducted using a novel optode microprofiling device from PreSens GmbH (Germany, www.presens.de) with an Automated Micromanipulator (AM), needle-type optodes for measurements of oxygen (PM-PSt7), pH (PM-HP5), and CO_2 (PM-CDM1 prototypes), respectively. The sensors were pre-calibrated by the manufacturer, rendering *in situ* calibrations superfluous, which was an advantage, especially in the dark. Prior to the *in situ* and laboratory investigations, the sensors were tested against a known standard. Corrections were not necessary. For *in situ* profiling, an aluminum stand (6 × 6 cm) holding the Automated Micromanipulator and sensors, was mounted on 1 m

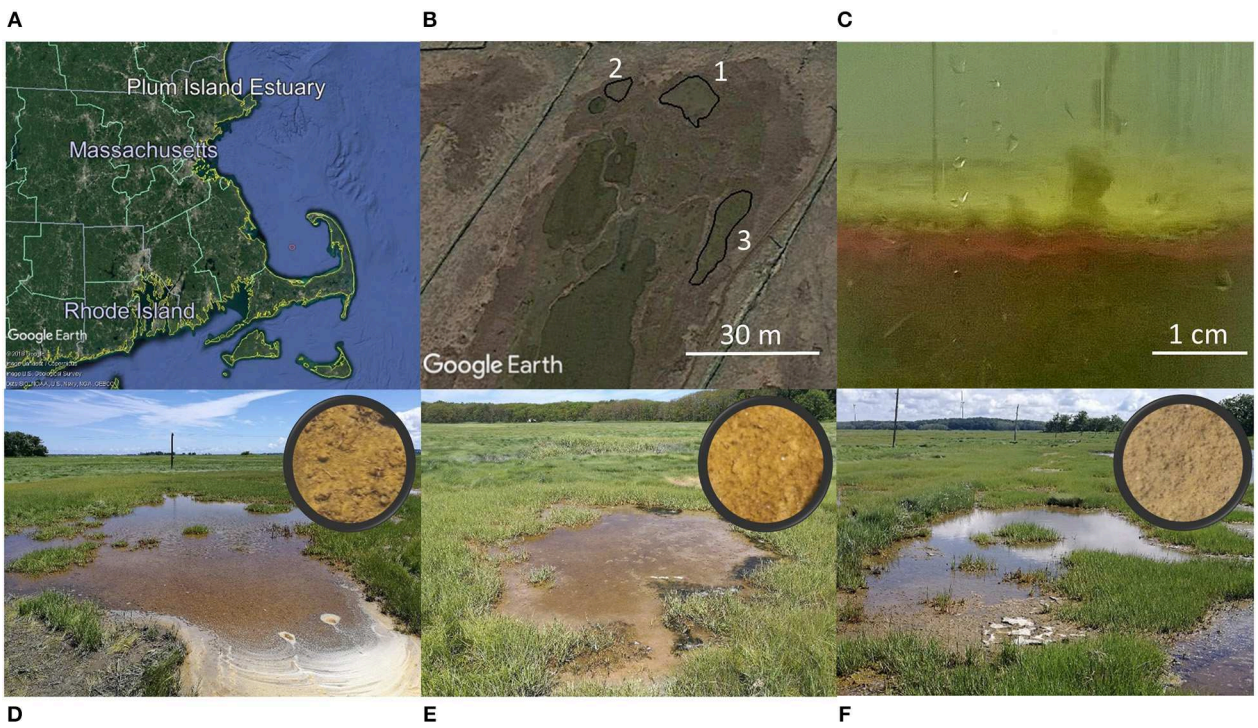

FIGURE 1 | Study site. (Top panel) Plum Island Estuary in Massachusetts, USA (Image: ©2018 Google. Image Landsat/Copernicus. Image U.S. Geological Survey. Data SIO, NOAA, U.S.Navy, NGA, GEBCO) **(A)**. Investigations were conducted in three closely located tidal ponds (image from Google Earth) **(B)**. A thick layer of photosynthesizing benthic microalgae covered the bottom of the tidal ponds **(C)**. (Bottom panel) The three ponds investigated are located on the marsh platform. Circles show close-up images of the sediment surface **(D–F)**.

TABLE 1 | Overview of *in situ* and laboratory investigations conducted to determine the spatiotemporal variation of O_2, pH, and CO_2 in shallow salt marsh tidal ponds and the role of light as a controlling factor.

	Scope	Conditions	Parameters	Spatiotemporal observations
1	Investigation of spatiotemporal variation over the course of day	*In situ*	O_2, pH, CO_2	Vertical profiles from water surface to anoxic sediment. Measured in the morning, afternoon and night with a resolution of 300–1000 μm.
2	Investigation of light control of spatial variation	Lab.	O_2, pH	Vertical profiles across the sediment-water interface with a resolution of 150–250 μm. Measured under different light regimes: 0, 25, 150, 350 μmol photons $m^{-2}sec^{-1}$ PAR.
3	Investigation of temporal variation during a day	*In situ*	O_2, pH	Point measurements in the water column. Time-series - 24 hour. Resolution:1 min^{-1}
4	Investigation of internal spatial variation of O_2 within a pond	*In situ*	O_2	Vertical profiles from water surface to anoxic sediment. Measured around noon with a resolution of 300–1000 μm under various thickness of sea foam.
5	Investigation of spatial variation among different tidal ponds	*In situ*	O_2	Vertical profiles from water surface to anoxic sediment. Measured with a resolution of 300–1000 μm within one afternoon.

long spikes and pushed into the soft sediment of the tidal ponds securely fastening the microprofiling device in a stable position. For laboratory profiling, the aluminum stand was mounted on a heavy base plate.

For *in situ* profiling, the needle optode sensors were fastened in a custom-made extended sensor holder allowing the sensor-tips to reach the sediment, while the micromanipulator and its electronics were kept at a safe distance from the water. All other electronic components were packed inside a cooler for protection from sun, rain, wind and sea-spray, and placed on a table out of tidal range. A cardboard box inside the cooler functioned as a shelf, and as a humidity buffer preventing condensation directly on the equipment during the morning hours.

The system was operated from a laptop and powered by a car-battery with a DC–AC power invertor (12–110 V).

Light and temperature in the water-column was measured with a HOBO Pendant© Temperature/Light Datalogger. Furthermore, light data of the photosynthetically active radiation

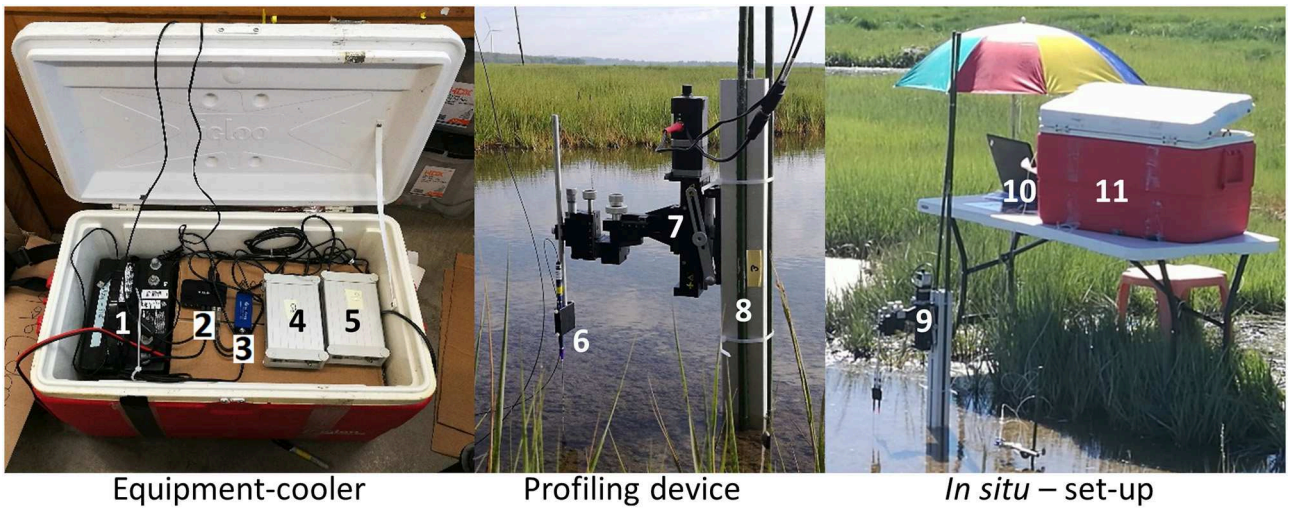

FIGURE 2 | Experimental set-up for *in situ* microprofiling of O_2, pH, and CO_2. Equipment cooler: (1) Car-battery, (2) USB-hub, (3) O_2-meter, (4) CO_2-meter, (5) pH-meter. Power inverter, 6-way socket, and individual power supplies are located under the cardboard box. Profiling device: (6) Sensor holder with sensor, (7) Automated Micromanipulator, (8) Aluminum stand with spikes. *In situ* set-up: (9) profiling device, (10) laptop, (11) equipment cooler.

(PAR) was received from a nearby weather station (PIE LTER *Marshview Farm* weather station). Salinity measurements were performed using a refractometer.

Profiling

In situ vertical profiles were measured from the water-air interface, through the water column, and into the sediment until stable anoxic conditions were reached (**Figure 3**). The resolution was adjusted to the O_2 variability, measuring with 1,000 µm-steps through the water column, and 300 µm per step through the sediment-water interface, where the O_2 gradients became steep. Each steady-state profile was conducted within 10–20 min depending on water depth.

In the laboratory, profiling was conducted in sediment cores (Ø: 7 cm) and vertical profiles were measured from ∼1 cm above to ∼1 cm below the sediment-water interface. The spatial resolution was 500 µm per step through the water column and 150 µm per step through the sediment-water interface. During profiling, the water column was kept in motion by gently letting air stream over the water surface.

Due to a thick layer of fluffy benthic microalgae on top of the sediment (**Figures 1C**, **3**), the transition from water column to sediment was not sharp, and therefore difficult to detect visually. Consequently, the sediment-water interface was defined as the top of the benthic microalgal layer and represents depth "zero," which was determined visually by lowering the white-colored tip of the needle optode through the water until it reached the top of the algal layer. The actual sediment surface below the microalgae was not visible. In the profile, positive values represent the water column, and negative values represent the sediment including the benthic microalgae layer. This caused the oxygen peaks generated by the benthic microalgae to be located below depth "0" and replicate profiles to differ slightly in height of the water column (**Figure 3**). Average water column

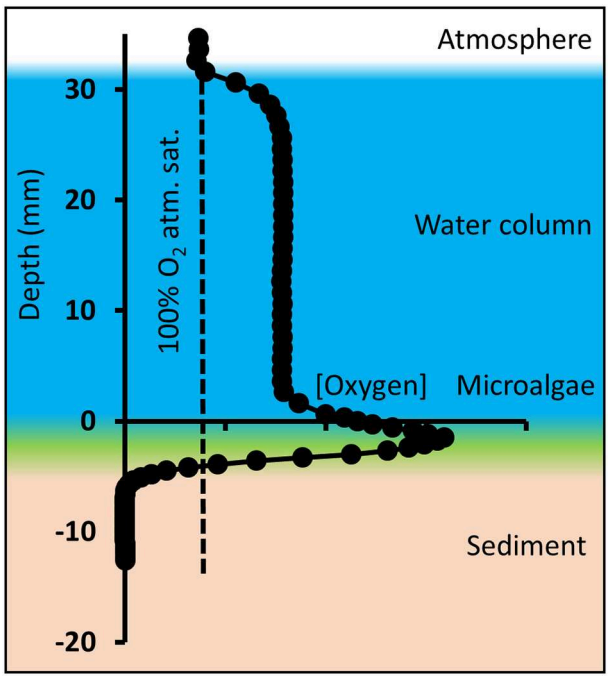

FIGURE 3 | Schematic overview of oxygen microprofiles in shallow tidal ponds, here exemplified with an oxygen profile measured in the afternoon. Microprofiling was conducted from the atmosphere through the water column and layer of benthic microalgae into the sediment. Depth "zero" is defined as the top of the microalgal layer.

concentrations, average benthic peak concentrations and oxygen penetration depth was calculated from the profiles. The average concentrations and average pH for the tidal ponds, which are shown in tables in the results section, were calculated from the

average of the profile-values at depth from 1 to 2 cm. Benthic peak O_2 concentrations were calculated as an average of the maximum concentrations measured at the sediment-water interface, and O_2 penetration depth was measured as the distance from the top of the sediment-water interface ("depth 0") to the depth, where the sediment became anoxic. Conversion between % atmospheric O_2 saturation and molar concentrations (μmol L^{-1}) was conducted compensating for temperature and salinity using conversion equations from Weiss (1970). Oxygen fluxes across the diffusive boundary layer (DBL) between the overlaying pond water and the sediments were calculated from the linear DBL gradients of the oxygen profiles according to Fick's first law of diffusion:

$$J = D_0 \times \frac{dC}{dx}$$

Diffusion coefficients (D_0) of seawater were derived from Broecker and Peng (1974) and compensated for temperature and salinity according to the Stokes-Einstein relation (Yuan-Hui and Gregory, 1974). The fluxes therefore represent the diffusive oxygen fluxes between the water column and the underlying microalgae layer.

Investigations

1) *In situ* Investigation of Spatiotemporal Variations of O_2, pH, and CO_2. Replicate O_2 ($n = 3$) and pH ($n = 2$) profiles were measured at different positions within a 30 cm radius in the morning (07:30–09:30), afternoon (14:00–16:00) and at night (00:30–02:30). CO_2 sensors are sensitive to sulfide, which is present in the sediment pore water, hence CO_2 profiles were only measured a short distance into the sediment and as single profiles.

2) Laboratory Investigation of Light Control of the Spatial Variations of O_2 and pH. For investigation of the light dependency of benthic O_2 and pH dynamics, profiling was conducted in sediment cores under different light regimes. Light exposures were set to 0, 25, 150, and 350 μmol photons m^{-2} s^{-1} photosynthetically active radiation (PAR), respectively, and temperature was fixed at 20°C and salinity at 35‰. To assure equilibrium conditions, the cores were exposed to each light setting for 6 h prior to profiling. Light conditions were measured at the sediment surface with a handheld light meter (LiCor LI-250). Sediment cores from the study site were collected by hand using Plexiglas cylinders (ϕ = 7cm). The cores were kept in a growth chamber for 2 days prior to profiling investigation at 20°C with a 12/12 h dark light cycle. The water columns were maintained with water from the pond and aerated with an aquarium pump. There were three independent replicate cores per light treatment ($n = 3$).

3) *In situ* Investigation of Daily Temporal Variations of O_2 and pH. For investigation of temporal variation, needle optodes for O_2 and pH were placed in a fixed position at a distance of 2 cm above the sediment-water interface. O_2 and pH were monitored for 24 h at 1-min intervals. The measurements included one tidal inundation.

4) Internal Spatial Variation of O_2 Within Shallow Tidal Ponds–The Role of Sea Foam. In the late morning, sea foam developed on the water surface and accumulated on one side of the pond depending on the wind direction, providing natural light and wind shading of the water column and sediment surface. For investigation of its impact on the spatial internal variation in oxygen distribution, profiles were measured in three locations in the pond with variable foam thickness. A light logger was placed under the foam in order to determine light penetrability to the sediment surface.

5) Investigation of Spatial Variations Among Independent Tidal Ponds. In order to investigate the variation between different tidal ponds, replicate O_2 profiles ($n = 3$) were measured in three closely located tidal ponds (**Figures 1B,D–F**). The ponds were investigated consecutively in the afternoon within the shortest possible time-frame (11:10–14:40) to assure comparable environmental conditions.

Statistical Analysis

Statistical analysis of differences among time of day (1), light exposure (2), and different ponds (3), respectively, were analyzed statistically using a one-way ANOVA with Tukey's HSD ($\alpha = 0.05$) *post hoc* tests. The analyses were generated using the Real Statistics Resource Pack software (Release 6.2, www.real-statistics.com). Statistical analyses are limited to the experiments where $n \geq 3$.

RESULTS

1) *In situ* Investigation of Spatiotemporal Variations of O_2, pH, and CO_2. The tidal ponds had high O_2 dynamics ranging from anoxic conditions inside the sediment to extreme supersaturation. The largest concentration was 1,016 μmol L^{-1} (460% atmospheric O_2 saturation) measured at the sediment water interface during the morning hours (**Figure 4**).

A thick layer of benthic microalgae was present on the sediment surface (**Figure 1C**) resulting in a marked peak in O_2 and steep O_2 gradients during daylight. The top of the algal layer was defined as "depth zero" in the profiles, and consequently the O_2 peaks were located between 0 and −10 mm depth. The sediments were completely anoxic greater −10 mm depth. The gradients were restricted to the layer of benthic microalgae and their DBL and did not extend into the water column. The benthic O_2 peaks were already established in the morning (07:50) with a concentration of 886 ± 139 μmol L^{-1}, and peaks remained in the afternoon, where the oxygen was slightly lower 593 ± 177 μmol L^{-1}. At night the peak disappeared as the concentration dropped to 45.9 ± 3.6 μmol L^{-1}, at the sediment-water interface. The O_2 penetration depth, measured from the top of the microalgal layer, varied over the course of the day from 10 and 7.6 mm in the morning and afternoon, respectively, to only 1.8 mm at night (**Figure 4**).

The shallow water column showed little vertical variation in O_2, pH, and CO_2. The average water-column O_2 varied over the course of the day. In the morning, the O_2 concentration was close to the atmospheric equilibrium 293 ± 47 μmol L^{-1}, but increased rapidly, which was demonstrated in the profiles, where the concentration in the water column increased from ∼240 to ∼350 μmol L^{-1} in the consecutively measured

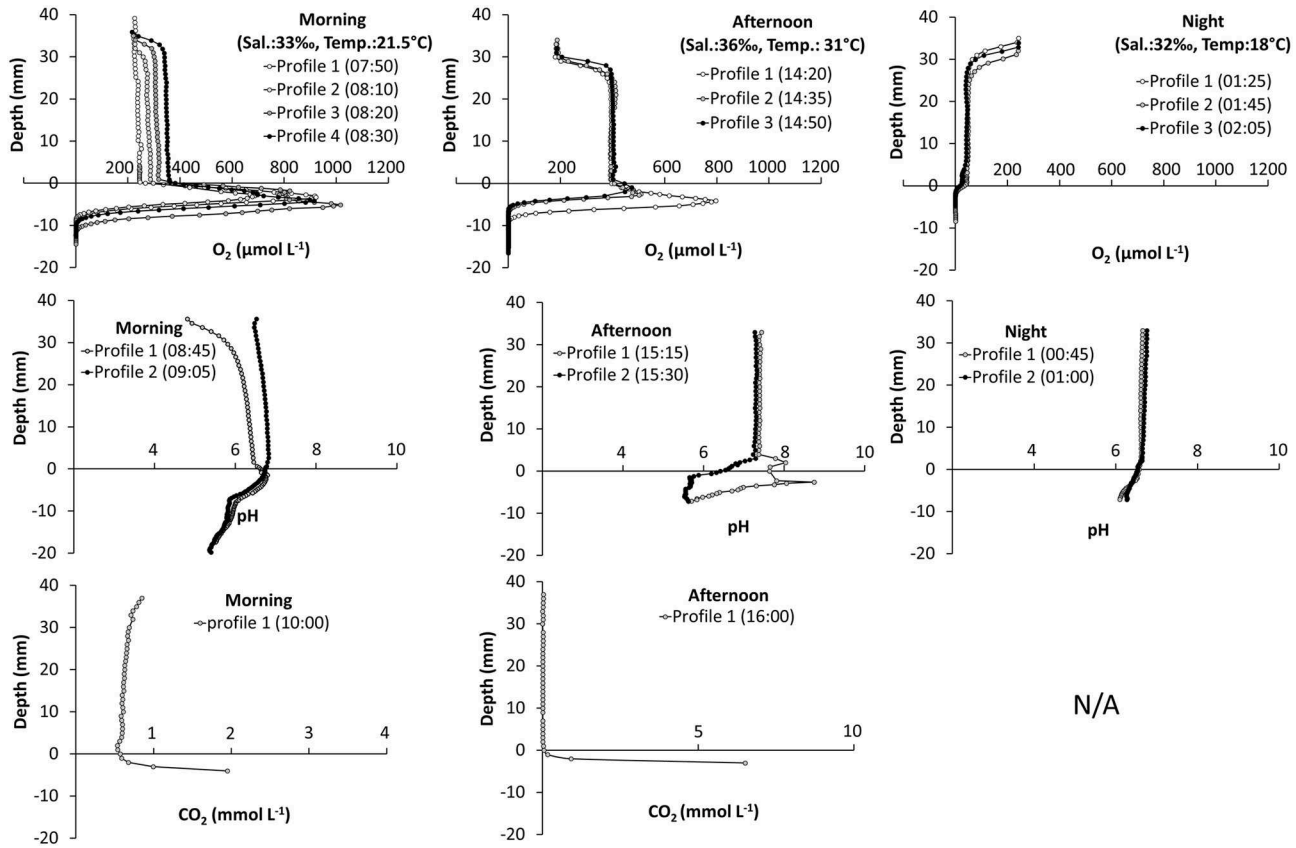

	Morning	Afternoon	Night
O_2 water column (µmol L^{-1}) (n=3-4)	293±47 (129%)	404±14 (212%)	45.7±2.0 (19%)
O_2 benthic peak (µmol L^{-1})(n=3)	886±139 (391%)	593±177 (312%)	45.9±3.6 (19%)
O_2 penetration depth (mm) (n=3)	10.0±1.3	7.6±1.4	1.8±0.5
O_2 fluxes (mmol m^{-2} h^{-1}) (n=3)	1.48±0.38	0.77±0.51	-0.11±0.03
pH water column (n=2)	6.5±0.4	7.3±0.1	6.7±0.1
CO_2 water column (mmol L^{-1}) (n=1)	0.6	0.01	N/A

FIGURE 4 | Spatiotemporal variations of O_2, pH, and CO_2 in a salt marsh tidal pond. *In situ* investigation. (Top panels) Vertical profiles of O_2, pH, and CO_2 measured from the air-water interface through the water-column and into the sediment. Profiles were measured in the morning, afternoon and at night. (Table inlet) Table showing average O_2, pH, and CO_2 conditions at different times of the day. Percent (%) refers to % O_2 atmospheric saturation. CO_2 measurements were not possible at night.

profiles. In the afternoon, the oxygen in the water-column reached a supersaturated level at 404 ± 14 µmol L^{-1}, which also resulted in an O_2 gradient building up at the water-air interface. At night, O_2 was depleted in the water column to hypoxic conditions at an average of 45.7 ± 2.0 µmol L^{-1}. O_2 fluxes between the sediment and the water column varied accordingly with net average O_2 fluxes of 1.48 ± 0.38, 0.77 ± 0.51, and −0.11 ± 0.03 mmol m^{-2} h^{-1} in the morning, afternoon and night, respectively. Oxygen fluxes changed by an order of magnitude between day and night, underpinning the strong benthic control on the O_2 content of the shallow water column (**Figure 4**).

For O_2, a one-way ANOVA showed significant differences between morning, afternoon and nighttime for water column concentration ($F = 104.8$, $p = 0.00001$), O_2 penetration depth ($F = 41.4$, $p = 0.0001$), and benthic peak concentration ($F = 35.3$, $p = 0.0002$). *Post hoc* tests (Tukey's HSD $\alpha = 0.05$) showed that water column concentrations in morning, afternoon, and night were all significantly different ($p \leq 0.007$). This was also the case for benthic O_2 peak concentration ($p \leq 0.05$). For O_2 penetration depth night conditions were significantly different from both morning and afternoon ($p \leq 0.001$).

The tidal ponds had a pH environment within the normal range for marine sediments ranging from 5.8 to 8.7 over the course of a day. In the water column, pH was highest in the afternoon (7.3 ± 0.1), and was slightly lower in the morning (6.5 ± 0.4), and at night (6.7 ± 0.1). In the morning, pH varied

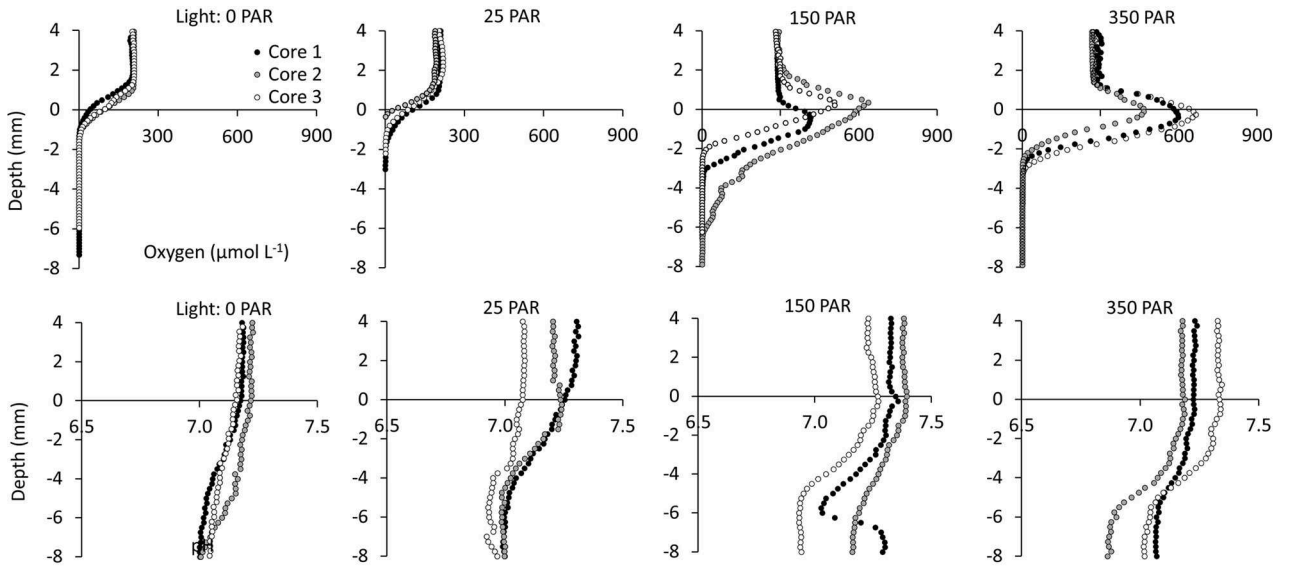

	0 PAR	25 PAR	150 PAR	350 PAR
O_2 water column (µmol L^{-1}) (n=3)	209±1 (91%)	205±12 (89%)	288±5 (125%)	266±8 (115%)
O_2 benthic peak (µmol L^{-1}) (n=3)	80±32 (35%)	79±27 (34%)	562±67 (244%)	576±101 (250%)
O_2 penetration depth (mm) (n=3)	1.3±0.2	1.2±0.8	4.4±2.0	3.4±0.4
pH water column (n=3)	7.2±0.01	7.2±0.2	7.3±0.1	7.3±0.1

FIGURE 5 | Spatiotemporal variation of O_2 and pH in salt marsh ponds under different light regimes. Laboratory investigation. (Top panels) Vertical profiles of O_2 and pH at light intensities of 0, 25, 150, 350 µmol photons m^{-2} s^{-1} photosynthetically active radiation (PAR). (Table inlet) Table of average O_2 and pH conditions at different light intensities. Percent (%) refers to % O_2 atmospheric saturation.

between profiles in the water column, but in the afternoon and at night the profiles were similar. Despite the high benthic microalgal activity, there was no characteristic pattern for pH at the sediment-water interface. In the afternoon, the profiles varied markedly at the sediment surface showing both a peak and decrease in pH. However, in the morning, when the algal activity was highest, there was no corresponding variation in pH. In the water column, the CO_2 profile was vertically stable at a concentration of ∼0.6 mmol L^{-1} in the morning, but by the afternoon CO_2 was completely depleted. CO_2 accumulated in the sediment showing steep gradients toward the sediment surface. The nighttime CO_2 profile was omitted, due to sensor malfunction. No statistic analyses are available for pH and CO_2, due to low sample size (**Figure 4**).

2) Laboratory Investigation of Light Control of the Spatial Variations of O_2 and pH. In light (150 and 350 µmol m^{-2} s^{-1} PAR), oxygen accumulated at the sediment-water interface reaching concentrations of 562 ± 67 and 576 ± 101 µmol L^{-1}, respectively. In darkness and at very low light (0 and 25 µmol m^{-2} s^{-1} PAR), there was no benthic O_2 accumulation, and O_2 concentrations declined across the sediment-water interface and became anoxic within the first millimeters of the sediment. Light had a marked impact on the O_2 penetration depth, which increased from ∼1.3 mm in darkness and at very low light (0 and 25 µmol m^{-2} s^{-1} PAR) to 4.4 and 3.4 mm at 150 and 350 µmol m^{-2} s^{-1} PAR, respectively (**Figure 5**). For O_2, a one-way ANOVA showed significant differences between light exposure treatments for water column concentration ($F = 78.7$, $p = 0.000003$), benthic peak ($F = 58.2$, $p = 0.00001$) and O_2 penetration depth ($F = 5.8$, $p = 0.02$). *Post hoc* tests (Tukey's HSD $\alpha = 0.05$) showed that water column and benthic peak O_2 concentrations in 0 and 25 µmol m^{-2} s^{-1} PAR were significantly different from 150 to 350 µmol m^{-2} s^{-1} PAR ($p \leq 0.0001$). For the O_2 penetration depth, 0 and 25 µmol m^{-2} s^{-1} PAR were only significantly different from 150 µmol m^{-2} sec^{-1} PAR ($p \leq 0.04$).

pH in the water column varied between 7.2 and 7.4. From the sediment surface to a depth of 6–8 mm, pH slowly declined by ∼0.2 pH units. Although the O_2 profiles showed a marked photosynthetic activity during light exposure, this activity did not affect pH at the sediment-water interface, and no spatial differences in the pH profiles were observed among different light treatments (**Figure 5**). For pH no significant differences were found between light treatments ($F = 0.84$, $p = 0.5$).

3) *In situ* Investigation of Daily Temporal Variation. From mid-afternoon (∼15:00), O_2 in the water column decreased from an oversaturated level at 436 µmol L^{-1} (241% O_2 atm. sat.) to 33 µmol L^{-1} (14 % O_2 atm. sat.) at ∼23:00, only interrupted by fluctuations during tidal inundations at ∼16:45. The nighttime O_2 concentration remained at this level

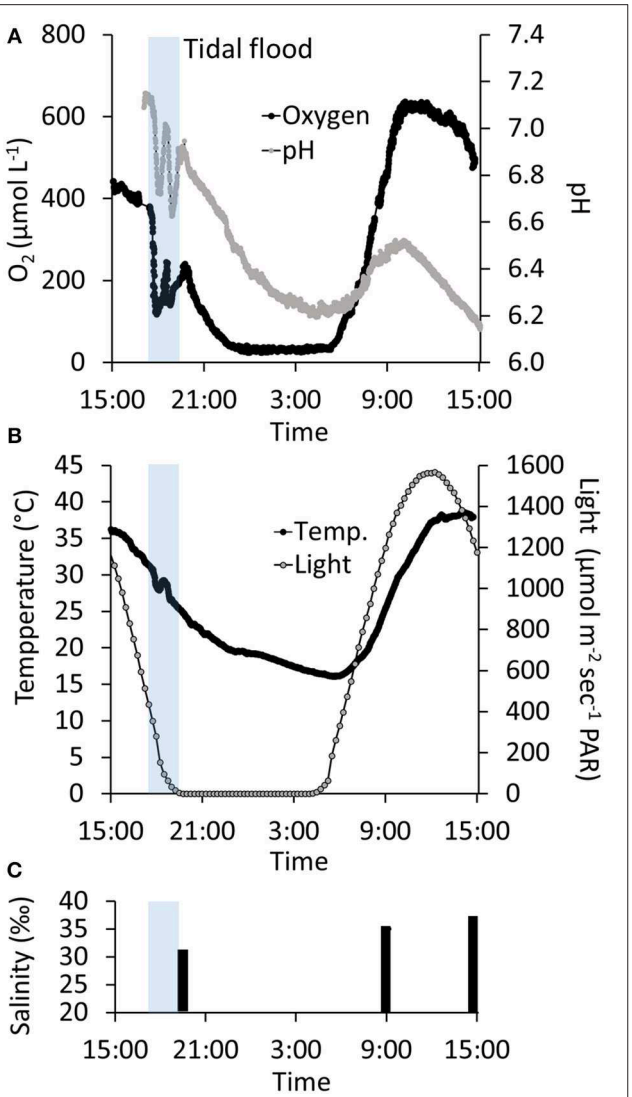

FIGURE 6 | Twenty-four hour time-series of the temporal variation in water column oxygen, pH, temperature, light exposure, and salinity in a salt marsh tidal pond. Transparent blue bar indicates the time-frame where the marsh was flooded at high tide **(A)** Twenty-four h monitoring of oxygen and pH in the water column 2 cm above the sediment surface. **(B)** Twenty-four hour monitoring of temperature and light. **(C)** Water column salinity.

throughout the night, and the water column never became anoxic. The O_2 concentration began to increase drastically in the early morning hours starting at 05:20, about 45 min after the break of dawn (04:30). The O_2 concentration increased to reach a maximum of 638 µmol L^{-1} (346% O_2 atm. sat.) at ∼10:00, about 3 h before the highest light intensity. The O_2 concentration remained at this level for 1.5 h and subsequently decreased to 495 µmol L^{-1} at 15:00, reaching a level very close to the O_2 concentration at which the measurements began 24 h earlier (**Figure 6A**).

From mid-afternoon (∼15:00), pH in the water column decreased from 7.1 to 6.2 in the middle of the night (∼04:00), only interrupted by fluctuations during a tidal inundation. Subsequently, pH increased to 6.5, which was reached at ∼10:00, after which it began to decrease again and steadily decreased to 6.1 at 15:00 at the end of the time-series measurements (**Figure 6A**). Temperature showed marked daily fluctuations, ranging from 18 to 38°C measured at night (03:30) and in the afternoon (14:00), respectively (**Figure 6B**). Salinity was 32‰ right after the tidal inundation at 19:00. Subsequently, the salinity increased to 35‰ at 09:00 the following morning and reached 37‰ at 15:00 in the afternoon (**Figure 6C**). During the 24 h monitoring period, there was one inundation at high tide in the late afternoon (∼16:45). The subsequent high tide 12 h later was too low to reach the marsh platform and the tidal ponds.

O_2 and pH were markedly affected by the tidal inundation. On the incoming tide, tidal water was mixed with the pond water column, lowering the oxygen concentration and pH. During the short period at the peak of the tide, where the water movement ceased, the oxygen and pH returned to the conditions before the flood. This pattern was repeated on the outgoing tide leaving a characteristic "W"-pattern in the oxygen and pH time-series (**Figure 6**). In contrast, the impact of flooding on temperature was negligible (**Figure 6**).

4) Internal Spatial Variation of O_2 Within Shallow Tidal Ponds–The Role of Sea Foam. Oxygen profiles were measured *in situ*; under a thick sea foam layer, under a thin sea foam layer, and in an area with no sea foam, respectively (**Figure 7**). Water column oxygen was lower under the thick sea foam layer compared to thin sea foam layers and no seafoam (**Figure 7**). A light logger placed under the foam showed no light penetrability through the thickest layers of seafoam, and a marked reduction of light penetrability under the thin sea foam layer.

5) Investigation of Spatial Variations Among Independent Tidal Ponds. All three tidal ponds had similar O_2 concentrations in the water column around 400 µmol L^{-1}, and there were no significant differences between tidal ponds ($F = 0.12$, $p = 0.88$; **Figure 8**). All tidal ponds showed a peak in O_2 concentration at the sediment water interface. However, the peak concentration differed among tidal ponds ($F = 10.46$, $p = 0.01$), where pond 1 showed significantly larger peaks than pond 2 and 3 (Tukey's HSD–$\alpha = 0.05$, $p \leq 0.01$).

DISCUSSION

Salt marsh tidal ponds are a unique environment characterized by its distinct light, temperature, salinity and oxygen dynamics during the summer-time (**Figures 4**, **6–8**). In this study conducted in July, oxygen varied daily from hypoxic conditions at nighttime to highly supersaturated concentrations during the daytime (**Figures 4**, **6**) with peak concentrations at the sediment-water interface reaching a maximum of 886 ± 139 µmol L^{-1}

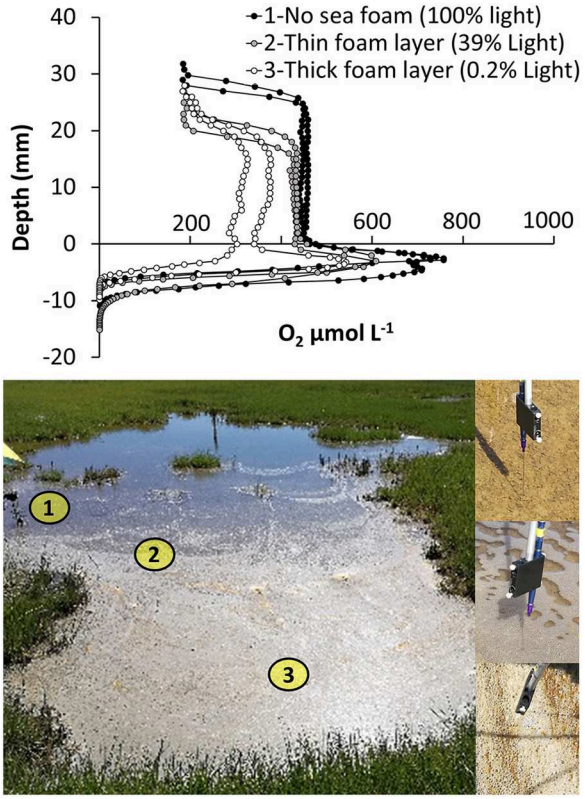

FIGURE 7 | Spatial variations in oxygen distribution within a salt marsh tidal pond. Oxygen profiles were measured at three locations with increasing thickness of sea foam and variable light penetrability: (1) no sea foam (65,000 ± 1,000 lux−100% light penetration) (2) a thin seafoam layer (26,000 ± 9,000 lux−39% light penetration), and (3) a thick seafoam layer (150 ± 75 lux−0.2% light penetration).

(391% O_2 atm. sat.) during the morning hours (**Figure 4**). The temperature swings in the water spanned from 16°C in the nighttime to 38°C in the middle of the day (**Figure 6**). Due to high evaporation, salinity also increased over the course of the day, especially in the shallowest ponds, where salinities up to 42‰ were observed (**Figure 8**). Despite these harsh living conditions, tidal ponds provide an important ecological function as a low-tide refuge for endemic salt marsh species (Raposa, 2008; Allen et al., 2017), and various fishes and shrimps were observed in the ponds between tides during these experiments. This study specifically targets shallow marsh tidal ponds with a depth below 10 cm, high light penetrability and domination of benthic microalgae on the sediment surface. In this way, these ponds may share some of the characteristics of salt pannes. However, in contrast to pannes, the water generally remains between tides in these shallow tidal ponds, and thereby they also share characteristics with the deeper ponds in the area.

Benthic Oxygen Dynamics

A thick layer of benthic microalgae covered the sediment surface and controlled oxygen dynamics in the tidal ponds. The spatial distribution of the microalgae was uneven and occasional wads stretched into the water column (**Figure 1C**). The benthic algae caused a high net oxygen production and fluxes into the water column in light, and created a thick diffusion limited layer on top of the sediment, where oxygen rapidly accumulated resulting in characteristic peaks at the sediment-water interface during light hours (**Figures 4**, **5**, **7**, **8**). The opposite situation was present in the nighttime, where the oxygen flux was reversed and oxygen was taken up across the sediment-water interface resulting in a hypoxic water column (**Figure 4**).

Both the *in situ* profiling (**Figure 4**) and the light dependency measurements in the laboratory (**Figure 5**) showed that light

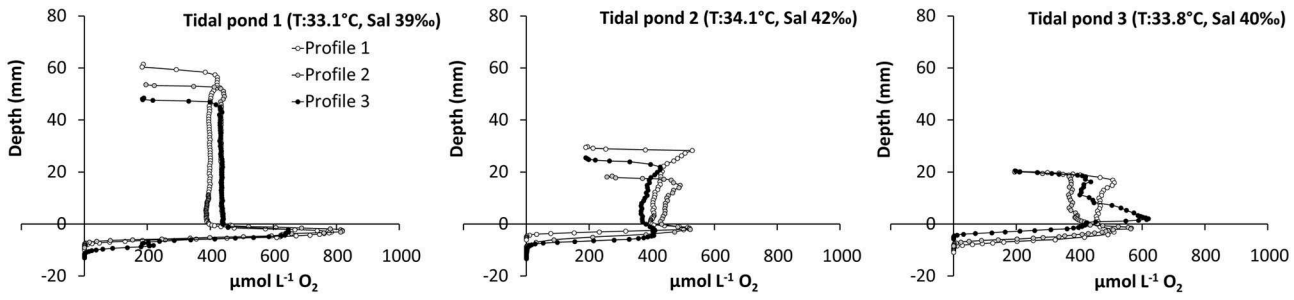

	Pond 1	Pond 2	Pond 3
O_2 water column (µmol L^{-1}) (n=3)	421±26 (232%)	415±41 (236%)	431±53 (241%)
O_2 benthic peak (µmol L^{-1})(n=3)	750±90 (414%)	487±68 (277%)	565±55 (317%)
O_2 penetration depth (mm) (n=3)	9.0±1.9	7.9±2.8	7.2±2.2
O_2 fluxes (mmol m^{-2} h^{-1}) (n=3)	2.55±0.58	0.68±0.60	0.95±0.79

FIGURE 8 | Spatiotemporal variation of O_2 in three independent, but closely located salt marsh ponds. Vertical profiles of O_2 measured from the air-water interface through the water-column and into the sediment. Profiles were measured consecutively within a 2.5 h period; (Top panel) pond 1 (Time: 11:10–12:30), pond 2 (Time: 12:45–13:45), and pond 3 (14:00–14:45). (Table inlet) Table of the average O_2 and pH conditions. Percent (%) refers to the % O_2 atmospheric saturation.

controlled the oxygen penetration depth that varied from a few millimeters at night and up to 10 mm in the morning, where the oxygen production was highest. As depth "zero" was the top of the microalgae layer, the oxygen penetration depth represents oxygen penetration through the microalgae layer as well as the sediment. The diminishing gradients at the sediment-water interface were steep, and in the morning, oxygen went from peak concentrations of 886 ± 139 to 0 μmol L^{-1} over a distance of only ∼6 mm indicating that the sediment has a high oxygen demand (**Figure 4**).

High photosynthetic benthic oxygen production was present even at low light intensities, and the development of benthic oxygen peaks occurred at light intensities as low as 150 μmol m^{-2} s^{-1} PAR and did not increase at higher light intensities (**Figure 5**). This indicates that the benthic microalgae reach their maximum photosynthetic capacity at very low light levels. *In situ*, this light level was reached at ∼06:00 in the morning, which also coincided with the time where the water column oxygen concentration began to increase rapidly after being low during the nighttime (**Figure 6**).

The benthic peak oxygen concentration was highest in the morning. In the afternoon, the average oxygen peak was slightly lower (**Figure 4**). Previous studies have demonstrated photoinhibition of benthic microalgae in salt marshes in full sunlight (Whitney and Darley, 1983), and it is likely to have played a role lowering the afternoon benthic oxygen production. Furthermore, the temperature increased about 10°C from the morning to the afternoon, which likely increased the microbial oxygen demand, and contributed to the lower peak concentrations. This also markedly lowered the oxygen flux from the sediment surface to the water column.

Water Column Oxygen Dynamics

Photosynthesis and respiration of benthic microalgae and sediment determined the oxygen saturation state of the bulk water column, creating net supersaturated conditions during the day and hypoxic water column conditions during the nighttime (**Figures 4**, **6**).

In situ, the water column was characterized by a vertically stable oxygen concentration without gradients (**Figures 4**, **7**, **8**). Gradients were spatially restricted to the benthic microalgae layer and the water-atmosphere interface, and did not extend into the water column. The lack of gradients building up from the bottom indicates that the water column is well-mixed. This was likely facilitated by a combination of wind-driven mixing and turbulence from actively swimming fauna in the ponds.

The water column oxygen concentration varied over the course of the day, spanning more than an order of magnitude. However, even though the oxygen dynamics was proven to be tightly coupled to light availability in the laboratory experiments (**Figure 5**), *in situ*, the daily temporal oxygen variation was skewed compared to the daily variation in light availability (**Figure 6**), indicating that other factors also influenced the oxygen variation in the ponds. In the morning, oxygen increased rapidly from 33 to 638 μmol L^{-1} within a short 5-h period, but reached the maximum oxygen concentration at 10:00 at a light intensity of ∼1,000 μmol m^{-2} s^{-1} PAR, approximately 3 h before the light intensity reached its maximum (**Figure 6**). This rapid increase was also reflected in the morning oxygen profiles, where the water column oxygen increased continuously in four consecutively measured profiles (**Figure 4**). Subsequently, the oxygen concentration decreased slowly for more than 12 h over the afternoon and evening (**Figure 6**). This discrepancy between the oxygen dynamics and light availability can be caused by multiple factors. The oxygen flux from the sediment surface was markedly lower in the afternoon showing a more than 50% reduction in the oxygen export from the microalgae layer to the water column compared to the morning (**Figure 4**). This was likely due to a combination of factors including photoinhibition and increased respiratory demands at higher temperatures. Furthermore, a recent study has shown that gas exchange via gas bubbles (ebullition) also influences oxygen dynamics in salt marsh tidal ponds (Howard et al., 2018), facilitating a route of oxygen exchange between the sediment surface and the atmosphere that bypasses transport of dissolved oxygen through water column. In the present study, gas bubbles were also observed developing at the sediment water interface. Hence, ebullition, driven by high biological oxygen production and a marked increase in temperature, lowering saturation state of dissolved gases, is expected to have played a role in oxygen exchange lowering both oxygen concentrations in the water column and the peak concentration at the sediment-water interface in the afternoon (**Figures 4**, **6**).

The development of seafoam on the water-surface generated a horizontal variation in the vertical oxygen profiles within the ponds. The seafoam had a marked impact on light penetration to the sediment surface. However, only under the thickest layer of seafoam, where light penetration was almost completely blocked, were the oxygen profiles affected, showing a lower concentration in the water column (**Figure 7**). This supports the findings of the light dependency study, showing that the benthic microalgae community is able to maintain high oxygen production even under reduced light conditions (**Figure 5**). The development of seafoam also has an impact on pond ecology. Studies have shown that meiobenthic swimmers in intertidal zones change their behavior in response to the formation of sea foam, accumulating under the foam using it for shading and hiding (Armonies, 1989, 1991). It is possible that the shaded sea foam areas, in addition to providing shade, may also function as a refuge from the highly supersaturated oxygen conditions, which can be toxic to aquatic animals stimulating the generation of free radicals (Sebert et al., 1984; Lushchak and Bagnyukova, 2006).

The characteristic oxygen profiles in light; with highly supersaturated water columns and benthic peaks restricted to microalgae layer at the sediment water interface, were reproducible across ponds (**Figure 8**). There was some variation in the benthic peak concentrations, penetration depth, and oxygen fluxes, possibly caused by the time lag between measurements, but the water column oxygen concentrations were very similar across ponds (**Figure 8**). Based on these similar patterns in spatial oxygen distribution across different ponds, the *in situ* profiles described in this study (**Figures 4**, **5**, **7**, **8**) were found to be generally representative for shallow salt marsh ponds in the area.

pH and CO_2

The water column was well-buffered, and despite the intense photosynthetic and respiratory activity changing over the course of day, the pH showed attenuated fluctuations and did not reach extreme values, ranging from 6.2 to 7.1 in the time-series study (**Figure 6**) and 6.5–7.3 in the *in situ* profiles (**Figure 4**). pH in the water column followed a similar trend as O_2, decreasing in the afternoon and increasing in the morning (**Figure 6**). Increased photosynthetic activity at the sediment-water interface had no direct effect on pH, neither in the *in situ* profiles (**Figure 4**) nor in response to increasing light conditions (**Figure 5**). The afternoon *in situ* profiles showed some unusual pH activity at the sediment surface, but the two profiles show opposite trends and no conclusions can be drawn on these observations.

Carbon dioxide (CO_2) accumulated in the sediment resulting in steep gradients at the sediment-water interface spatially aligned with the benthic O_2 peak. The sediment therefore fulfills an important function in the tidal ponds as a CO_2 reservoir for the benthic primary production as the water column was almost devoid of CO_2 in the afternoon (**Figure 4**). This supports previous observations from deeper tidal ponds in the same marshes, where Spivak et al. (2018) found a significant DIC efflux from the sediment to the water.

The Impact of Tidal Flooding on O_2, pH, and Temperature

Tidal inundation had a high, but short-lived, impact on oxygen and pH (**Figure 6**), which was restricted to the period of the flooding, which lasted 3 h (16:45–19:45). It is noteworthy that after the flood and even during the peak of the flood, where the water is stagnant, the pond O_2 and pH immediately returned to the previous conditions, showing that the driving factors internally in the pond exert a strong control on the pond biogeochemistry. The impact of flood tides is likely to change at different times of the day, as the difference in oxygen, pH, and temperature between tidal water and pond water may be different.

Differences Between *in situ* and Laboratory Profiles

In the field, the benthic oxygen peaks were restricted to the layer of benthic microalgae. In the laboratory investigations, the benthic oxygen peak extended slightly higher into the water column (**Figures 4**, **5**, note the different y-axis scales). This was likely caused by the less excessive artificial stirring of the water column in the laboratory, increasing the DBL thickness, and partly by differences in the visual determination of the sediment-water interface. In the laboratory, the sediment surface could be determined visually close-up from the side of the core. In the field, the visual determination occurred from above and at a distance. This may have resulted in differences in the perception of the location of the sediment-water interface ("depth 0") between the *in situ* and laboratory investigations.

Comparison to Other Studies of Oxygen and pH in Salt Marsh Tidal Ponds

Only a few other studies have investigated oxygen dynamics in salt marsh tidal ponds. In the Plum Island Estuary, where the present study was also conducted, Spivak et al. (2017), investigated the biogeochemistry of the deeper ponds in the area (depth: 25–40 cm) and found the largest oxygen variation in July ranging from supersaturated concentrations of 625 μmol L^{-1} at noon to 0 μmol L^{-1} in the night time, while the daily variation was lower in the fall. This indicates that the daily oxygen variation also has a seasonal variation and that the oxygen dynamics presented in the current study was measured at the time of the year with the highest oxygen variation. It is noteworthy that Spivak et al. (2017), found the deeper ponds to become anoxic at night, whereas the shallower ponds investigated in the current study reached hypoxic conditions, but did not become anoxic. It is likely that the shallow depth combined with high wind exposure causes mixing that prevents anoxia in the water column. Similar oxygen dynamics were observed in shallower ponds of the Ria de Aveiro salt marshes in Portugal, where Lillebø et al. (2010) found oxygen concentrations to reach a maximum of 250 μmol L^{-1} in June, and also here did the oxygen decrease at night, but it did not reach anoxic conditions. In other areas, Salman et al. (2015) measured O_2 profiles in the laboratory on cores from ponds in Sippewissett marsh, Massachusetts, USA, and found marked differences between light and dark conditions. Smith and Able (2003) observed similar diurnal oxygen variation in tidal ponds of New Jersey marshes, with peak concentration in the water column occurring in the late afternoon. These observations are consistent with the findings in the current study.

pH generally shows very attenuated fluctuations in tidal marsh ponds. Lillebø et al. (2010) found small variations around a pH of 7.5 in the Ria de Aveiro salt marshes. Catallo (1999) investigated pH directly at the sediment surface and found very little pH variation at the sediment surface in a Louisiana marsh tidal pond, despite marked changes in water redox potential. These observations of O_2 and pH are consistent with the finding of the present study showing a dynamic oxygen environment with marked swings between day and night, but with well-buffered pH conditions showing only minor pH fluctuations.

In other ponds of the Plum Island Estuary marshes with a depth of ∼20 cm, Kearns et al. (2017) demonstrated that short-term changes of environmental conditions can alter the structure of active microbial communities in the water column, whereas the sediment showed low variation of the abiotic environmental conditions and a stable active microbial community. Similar impact on the microbial community is expected to occur in the ponds investigated in the current study. Our detailed profiling of the vertical oxygen distribution revealed a 1 cm layer right around the sediment surface, with the most drastic variation in oxygen. Within this layer, the extreme oxygen variation could have a unique impact on the microbial community, which should be emphasized in future studies.

In situ data on oxygen fluxes for salt marsh tidal ponds are lacking in the literature, but the oxygen fluxes measured in

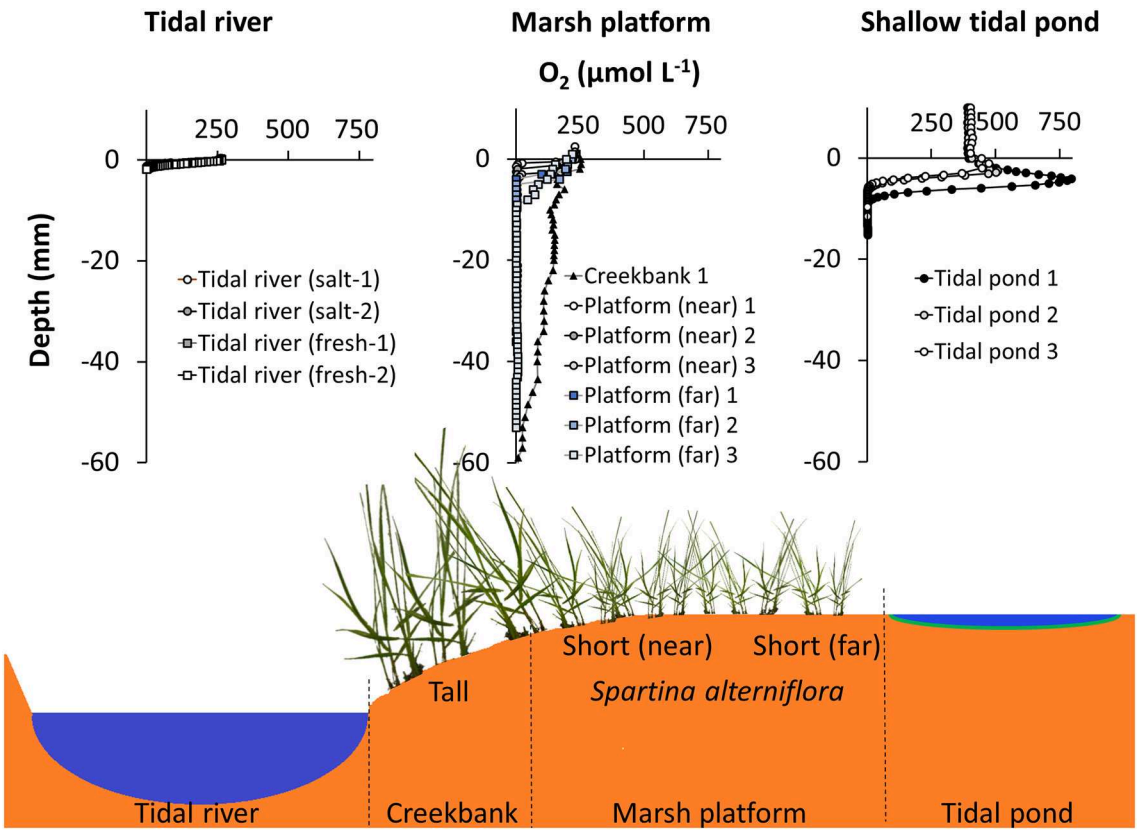

FIGURE 9 | Comparison of oxygen profiles in the sediment from different marsh habitats during daylight conditions. (Top panel, Left) Oxygen profiles from the Parker River in the Plum Island Estuary, MA, USA from a freshwater and saltwater-dominated area, respectively (Laboratory core profiling, July 2015). (Mid) Oxygen profiles from three locations on vegetated marsh platform; creekbank and two locations in the low marsh, near, and far from the creekbank. Great Sippewissett Marsh, MA, USA (*in situ* profiling July 2016). (Right) Oxygen profiles in shallow tidal ponds (this study, afternoon profiles) (Bottom panel): Cross section of salt marsh ecosystem, schematically depicting the different habitats, where oxygen was profiled; tidal river, marsh platform, and tidal ponds.

this study were on the same order of magnitude as reported from other marsh habitats. Low marsh sediments showed a net oxygen uptake also during the day time with a net flux of 0.58 mmol m^{-2} h^{-1} in Nova Scotia marshes (Schwinghamer et al., 1991) and 0.9 mmol m^{-2} h^{-1} in Australian marshes (Brodersen et al., 2019). In tidal marsh creeks, oxygen uptake rates were found ranging from 0 to 3.2 mmol O_2 m^{-2} h^{-1} (Macpherson et al., 2007). In comparison, the oxygen fluxes of shallow tidal ponds are markedly more dynamic and driven by photosynthetic activity of the benthic microalgae, which resulted in oxygen fluxes out of the sediment in the daytime and oxygen uptake at night. In this way, the oxygen dynamics in shallow tidal ponds more resembles the oxygen dynamics found on intertidal flats (Magalhães et al., 2002; Denis and Desreumaux, 2009; Jansen et al., 2009).

The tidal pond oxygen profiles differed markedly from other marsh habitats (**Figure 9**). In preceding studies also conducted with needle optode profiling under daylight conditions in July of 2015 and 2016, we measured oxygen profiles *in situ* on the vegetated marsh platform of Great Sippewissett Marsh (MA, USA), and in sediment cores from the Parker river in the Plum Island Estuary (MA, USA). On the marsh platform, oxygen penetration was high on creek banks, where drainage is high, going down to ∼60 mm, but decreased further up on the platform to <10 mm, where the sediment is more permanently waterlogged. The sediment surface was air-exposed and the top sediment was always near atmospheric O_2 concentrations (**Figure 9**). This is consistent with other studies demonstrating that the typical oxygen profile in the top sediment of the vegetated marsh platform follows a steady decrease from atmospheric saturation at the surface to anoxia within the first 1 cm (Holmer et al., 2002; Brodersen et al., 2019). Below the top 1 cm, the sediment was anoxic on the marsh platform (**Figure 9**). This is also consistent with previous studies demonstrating that even though the *Spartina*-plants on marsh platform are capable of translocating oxygen and generating oxic root zones (Maricle and Lee, 2002; Koop-Jakobsen et al., 2018), it has limited impact on the bulk rhizosphere sediment that remain anoxic in the summertime (Koop-Jakobsen et al., 2017). In the permanently inundated sediment of the tidal river, the oxygen penetration was very shallow reaching <2 mm into the sediment, and there was no increased oxygen production at the sediment-water interface. Hence, with the highly supersaturated conditions of the bulk seawater and distinct oxygen peak at the sediment-water interface during the day, the tidal ponds have a markedly different spatial distribution of oxygen compared to other marsh

habitats, and its impact on the microbial community and benthic biogeochemistry needs further attention.

Perspective

In many North American marshes, tidal ponds are increasing in numbers and areal coverage in response to increased disturbance of the vegetation. A wide range of natural and anthropogenic impacts, including sea-level rise, diching, and dredging; are contributing to this process (Kirwan et al., 2008; Millette et al., 2010; Wilson et al., 2014; Schepers et al., 2017). Hence, salt marsh tidal ponds may play a more prominent role in salt marsh ecosystems in the future. Consequently, getting a better comprehension of the biogeochemistry in this unique environment is essential for understanding the impact it may have on key ecosystem services; such as nutrient retention and carbon sequestration. Our study demonstrates that tidal ponds comprise a marsh habitat with distinctive spatiotemporal oxygen dynamics driven by benthic respiration and photosynthesis, which is primarily controlled by the light exposure of the sediment surface. These conditions differ from the surrounding vegetated marsh, where the sediment surface is shaded by a vascular plant canopy and directly exposed to the atmosphere. Consequently, an increased coverage of tidal ponds on the vegetated marsh platform is likely to alter the overall salt marsh biogeochemistry; to a system with more dynamic oxygen conditions, switching from high oxygen production at the sediment surface during the day to high oxygen demand at night.

DATA AVAILABILITY STATEMENT

The datasets generated for this study are available on request to the corresponding author.

AUTHOR CONTRIBUTIONS

KK-J conceived this research idea, designed the experiment, conducted the research, analyzed the data, and wrote the manuscript. MG conducted the flux analysis and contributed to method development, data analysis, and manuscript writing. Both authors have approved the manuscript.

FUNDING

For KK-J, this research was supported by MARUM–Center for Marine Environmental Sciences, University of Bremen, Germany. MG was funded by the PreSens GmbH.

ACKNOWLEDGMENTS

We thank the Plum Island Ecosystems LTER (NSF-OCE 1637630) and the Ecosystems Center at the Marine Biological Laboratory in Woods Hole, MA, USA, for hosting this study, and we thank the researchers at the *Marshview* and *Rowley-house* field stations for helping out with the logistics of the fieldwork.

REFERENCES

Adamowicz, S. C., and Roman, C. T. (2005). New England salt marsh pools: a quantitative analysis of geomorphic and geographic features. *Wetlands* 25, 279–288. doi: 10.1672/4

Allen, D. M., Ogburn-Matthews, V., and Kenny, P. D. (2017). Nekton use of flooded salt marsh and an assessment of intertidal creek pools as low-tide refuges. *Estuar. Coasts* 40, 1450–1463. doi: 10.1007/s12237-017-0231-4

Armonies, W. (1989). Occurrence of meiofauna in *Phaeocystis seafoam*. *Mar. Ecol. Progr. Series* 53, 305–309. doi: 10.3354/meps053305

Armonies, W. (1991). "Transport of benthos with tidal waters: another source of indetermination," in *Report From the Workshop–Modelling the Benthos*, eds P. M. J. Herman, C.H.R. Heip (Yerseke: Delta Institute for Hydrological Research–Royal Netherlands Academy of Arts and Sciences), 11–28.

Baumann, H., Wallace, R. B., Tagliaferri, T., and Gobler, C. J. (2015). Large natural pH, CO_2 and O_2 Fluctuations in a temperate tidal salt marsh on diel, seasonal, and interannual time scales. *Estuar. Coasts* 38, 220–231. doi: 10.1007/s12237-014-9800-y

Brodersen, K. E., Trevathan-Tackett, S. M., Nielsen, D. A., Connolly, R. M., Lovelock, C. E., Atwood, T. B., et al. (2019). Oxygen consumption and sulfate reduction in vegetated coastal habitats: effects of physical disturbance. *Front. Mar. Sci.* 6:14. doi: 10.3389/fmars.2019.00014

Broecker, W. S., and Peng, T. H. (1974). Gas exchange rates between air and sea. *Tellus* 26, 21–35. doi: 10.3402/tellusa.v26i1-2.9733

Catallo, W. J. (1999). *Hourly and Daily Variation of Sediment Redox Potential in Tidal Wetland Sediments*. Biological Division Science Report USGS/BRD/BSR-1999–0001. U.S. Geological survey.

Denis, L., and Desreumaux, P.-E. (2009). Short-term variability of intertidal microphytobenthic production using an oxygen microprofiling system. *Mar. Freshw. Res.* 60, 712–726. doi: 10.1071/MF08070

Harshberger, J. W. (1916). The origin and vegetation of salt marsh pools. *Proc. Am. Philos. Soc.* 55, 481–484.

Holmer, M., Gribsholt, B., and Kristensen, E. (2002). Effects of sea level rise on growth of *Spartina anglica* and oxygen dynamics in rhizosphere and salt marsh sediments. *Mar. Ecol. Progr. Series* 225, 197–204. doi: 10.3354/meps225197

Howard, E. M., Forbrich, I., Giblin, A. E., Lott Iii, D. E., Cahill, K. L., and Stanley, R. H. R. (2018). Using noble gases to compare parameterizations of air-water gas exchange and to constrain oxygen losses by ebullition in a shallow aquatic environment. *J. Geophys. Res.* 123, 2711–2726. doi: 10.1029/2018JG004441

Jansen, S., Walpersdorf, E., Werner, U., Billerbeck, M., Böttcher, M. E., and De Beer, D. (2009). Functioning of intertidal flats inferred from temporal and spatial dynamics of O_2, H_2S and pH in their surface sediment. *Ocean Dynam.* 59, 317–332. doi: 10.1007/s10236-009-0179-4

Kearns, P. J., Holloway, D., Angell, J. H., Feinman, S. G., and Bowen, J. L. (2017). Effect of short-term, diel changes in environmental conditions on active microbial communities in a salt marsh pond. *Aquat. Microb. Ecol.* 80, 29–41. doi: 10.3354/ame01837

Kirwan, M. L., Murray, A. B., and Boyd, W. S. (2008). Temporary vegetation disturbance as an explanation for permanent loss of tidal wetlands. *Geophys. Res. Lett.* 35:L05403. doi: 10.1029/2007GL032681

Koop-Jakobsen, K., Fischer, J., and Wenzhöfer, F. (2017). Survey of sediment oxygenation in rhizospheres of the saltmarsh grass - *Spartina anglica*. *Sci. Total Environ.* 589, 191–199. doi: 10.1016/j.scitotenv.2017.02.147

Koop-Jakobsen, K., Mueller, P., Meier, R. J., Liebsch, G., and Jensen, K. (2018). Plant-sediment interactions in salt marshes–an optode imaging study of O_2, pH, and CO_2 gradients in the rhizosphere. *Front. Plant Sci.* 9:541. doi: 10.3389/fpls.2018.00541

Lillebø, A. I., Válega, M., Otero, M., Pardal, M. A., Pereira, E., and Duarte, A. C. (2010). Daily and inter-tidal variations of Fe, Mn and Hg in the water column of a contaminated salt marsh: Halophytes effect. *Estuar. Coast. Shelf Sci.* 88, 91–98. doi: 10.1016/j.ecss.2010.03.014

Lushchak, V. I., and Bagnyukova, T. V. (2006). Effects of different environmental oxygen levels on free radical processes in fish. *Compar. Biochem. Physiol. B* 144, 283–289. doi: 10.1016/j.cbpb.2006.02.014

Mackenzie, R. A., and Dionne, M. (2008). Habitat heterogeneity: importance of salt marsh pools and high marsh surfaces to fish production in two Gulf of Maine salt marshes. *Mar. Ecol. Progr. Series* 368, 217–230. doi: 10.3354/meps07560

Macpherson, T. A., Cahoon, L. B., and Mallin, M. A. (2007). Water column oxygen demand and sediment oxygen flux: patterns of oxygen depletion in tidal creeks. *Hydrobiologia* 586, 235–248. doi: 10.1007/s10750-007-0643-4

Magalhães, C. M., Bordalo, A. A., and Wiebe, W. J. (2002). Temporal and spatial patterns of intertidal sediment-water nutrient and oxygen fluxes in the Douro River estuary, Portugal. *Mar. Ecol. Progr. Series* 233, 55–71. doi: 10.3354/meps233055

Maricle, B. R., and Lee, R. W. (2002). Aerenchyma development and oxygen transport in the estuarine cordgrasses *Spartina alterniflora* and *Spartina anglica*. *Aquat. Botany* 74, 109–120. doi: 10.1016/S0304-3770(02)00051-7

Millette, T. L., Argow, B. A., Marcano, E., Hayward, C., Hopkinson, C. S., and Valentine, V. (2010). Salt marsh geomorphological analyses via integration of multitemporal multispectral remote sensing with LIDAR and GIS. *J. Coast. Res.* 26, 809–816. doi: 10.2112/JCOASTRES-D-09-00101.1

Raposa, K. B. (2008). Early ecological responses to hydrologic restoration of a tidal pond and salt marsh complex in Narragansett Bay, Rhode Island. *J. Coast. Res.* 180–192. doi: 10.2112/SI55-015

Raposa, K. B., and Roman, C. T. (2001). Seasonal habitat-use patterns of nekton in a tide-restrickted and unrestricted New England salt marsh. *Wetlands* 21, 451–461. doi: 10.1672/0277-5212(2001)021<0451:SHUPON>2.0.CO;2

Ruber, E., Gillis, G., and Montagna, P. A. (1981). Production of dominant emergent vegetation and of pool algae on a Northern Massachusetts Salt Marsh. *Bull. Torrey Bot. Club* 108, 180–188. doi: 10.2307/2484897

Salman, V., Yang, T., Berben, T., Klein, F., Angert, E., and Teske, A. (2015). Calcite-accumulating large sulfur bacteria of the genus Achromatium in Sippewissett Salt Marsh. *Isme J.* 9:2503. doi: 10.1038/ismej.2015.62

Schepers, L., Kirwan, M., Guntenspergen, G., and Temmerman, S. (2017). Spatio-temporal development of vegetation die-off in a submerging coastal marsh. *Limnol. Oceanogr.* 62, 137–150. doi: 10.1002/lno.10381

Schwinghamer, P., Kepkay, P. E., and Foda, A. (1991). Oxygen flux and community biomass structure associated with benthic photosynthesis and detritus decomposition. *J. Exp. Mar. Biol. Ecol.* 147, 9–35. doi: 10.1016/0022-0981(91)90034-T

Sebert, P., Barthelemy, L., and Peyraud, C. (1984). Oxygen toxicity in trout at two seasons. *Comp. Biochem. Physiol. A* 78, 719–722. doi: 10.1016/0300-9629(84)90622-4

Smith, K. J., and Able, K. W. (1994). Salt-marsh tide pools as winter refuges for the mummichog, *Fundulus heteroclitus*, in New Jersey. *Estuaries* 17, 226–234. doi: 10.2307/1352572

Smith, K. J., and Able, K. W. (2003). Dissolved oxygen dynamics in salt marsh pools and its potential impacts on fish assemblages. *Mar. Ecol. Progr. Series* 258, 223–232. doi: 10.3354/meps258223

Spivak, A. C., Gosselin, K., Howard, E., Mariotti, G., Forbrich, I., Stanley, R., et al. (2017). Shallow ponds are heterogeneous habitats within a temperate salt marsh ecosystem. *J. Geophys. Res.* 122, 1371–1384. doi: 10.1002/2017JG003780

Spivak, A. C., Gosselin, K. M., and Sylva, S. P. (2018). Shallow ponds are biogeochemically distinct habitats in salt marsh ecosystems. *Limnol. Oceanogr.* 63, 1622–1642. doi: 10.1002/lno.10797

Weiss, R. F. (1970). The solubility of nitrogen, oxygen and argon in water and seawater. *Deep Sea Res. Oceanogr. Abstr.* 17, 721–735. doi: 10.1016/0011-7471(70)90037-9

Whitney, D. E., and Darley, W. M. (1983). Effect of light intensity upon salt marsh benthic microalgal photosynthesis. *Mar. Biol.* 75, 249–252. doi: 10.1007/BF00406009

Wilson, C. A., Hughes, Z. J., Fitzgerald, D. M., Hopkinson, C. S., Valentine, V., and Kolker, A. S. (2014). Saltmarsh pool and tidal creek morphodynamics: Dynamic equilibrium of northern latitude saltmarshes? *Geomorphology* 213, 99–115. doi: 10.1016/j.geomorph.2014.01.002

Yuan-Hui, L., and Gregory, S. (1974). Diffusion of ions in sea water and in deep-sea sediments. *Geochim. Cosmochim. Acta* 38, 703–714. doi: 10.1016/0016-7037(74)90145-8

Conflict of Interest: The sensor company, PreSens Precision Sensing GmbH, Regensburg, Germany, provided the needle optode profiling equipment for this study. PreSens GmbH had no restrictive rights in regards to this publication beyond those entitled by their Co-Authorship. All final decisions on the content of this manuscript was solely the responsibility of KK-J.

The remaining author declares that the research was conducted in the absence of any commercial or financial relationships that could be construed as a potential conflict of interest.

frontiers in Environmental Science

ORIGINAL RESEARCH
published: 13 November 2019
doi: 10.3389/fenvs.2019.00179

Wind Sheltering Impacts on Land-Atmosphere Fluxes Over Fens

Jessica Turner[1]*, *Ankur R. Desai*[2], *Jonathan Thom*[3], *Kimberly P. Wickland*[4] and *Brent Olson*[5]

[1] Nelson Institute for Environmental Studies, University of Wisconsin-Madison, Madison, WI, United States, [2] Department of Atmospheric and Oceanic Sciences, University of Wisconsin-Madison, Madison, WI, United States, [3] Space Science and Engineering Center, University of Wisconsin-Madison, Madison, WI, United States, [4] United States Geological Survey, Water Mission Area, Boulder, CO, United States, [5] United States Geological Survey, Upper Midwest Water Science Center, Rhinelander, WI, United States

Wetlands and their ability to mitigate climate change motivates restorative and protective action; however, scientific understanding of land-atmosphere interactions is restricted by our limited continuous observations of gaseous fluxes. Many wetlands are small in spatial scale and embedded in forested landscapes. Yet, little is known about how the relative sheltering of forests affects net carbon (C) and energy balance. Here, we analyze coterminous USGS and Ameriflux eddy covariance flux tower observations over 3 years in two shrub fens in Northern Wisconsin, one more sheltered (US-ALQ) than the other (US-Los). Unsurprisingly, the open site showed higher overall wind speeds. This should have implications for atmospheric fluxes in wetlands as wind-forced processes are essential in promoting gas exchange over water. While both sites had similar half-hourly net ecosystem exchange of CO_2 (NEE) during daytime, there were significant differences in nighttime NEE, as well as in net radiation partitioning in early spring and late summer. Sensible heat (H) fluxes were smaller at the sheltered fen except for the months of July–September. In contrast, latent heat (LE) fluxes were higher in every month except July. Additionally, sheltered fen ecosystem respiration had a weaker linear correlation with air temperature (R: 0.08 vs. 0.57 for the open fen). Our work suggests that canopy sheltering does not cause significant differences in half-hourly NEE during the day, but rather the largest differences such as lower CO_2 emissions occur at nighttime due to higher variance at very low wind speeds. Sheltering also influenced direction of air flow, mean wind speeds in day vs. night, energy balance, and sensible and latent heat fluxes. We discuss implications of these findings for wetland restoration.

Keywords: fens, fluxes, carbon, wind, wetlands

KEY POINTS

- Because wetlands are often small and embedded in forested landscapes, wind sheltering may influence land-atmosphere fluxes uniquely in wetlands.
- Eddy covariance estimates show similarities in half-hourly NEE from 7:30 am to 4:30 pm between sites, but higher NEE at an open fen (US-Los) than sheltered fen (US-ALQ) at night.
- Lower sensible heat (H) and higher latent heat (LE) during most of the growing season suggests sheltered fens offer more surface cooling than open fens.

OPEN ACCESS

Edited by:
Bernd Lennartz,
University of Rostock, Germany

Reviewed by:
James McLaughin,
Ontario Ministry of Natural Resources, Canada
Baoli Wang,
Tianjin University, China

***Correspondence:**
Jessica Turner
jlturner4@wisc.edu

Specialty section:
This article was submitted to Biogeochemical Dynamics, a section of the journal Frontiers in Environmental Science

Received: *20 June 2019*
Accepted: *25 October 2019*
Published: *13 November 2019*

Citation:
Turner J, Desai AR, Thom J, Wickland KP and Olson B (2019) Wind Sheltering Impacts on Land-Atmosphere Fluxes Over Fens. Front. Environ. Sci. 7:179. doi: 10.3389/fenvs.2019.00179

INTRODUCTION

Wetland comparison studies often seek to understand gaseous fluxes according to wetland classification type, i.e., marsh, forested wetland, shrub etc. (Bernal and Mitsch, 2012; Turetsky et al., 2014; Coffer and Hestir, 2019). Others aim to resolve errors in upscaling due to heterogeneous land cover (Desai et al., 2007; Xiao et al., 2011; Aurela et al., 2015). Studies that focus solely on the effects of sheltering of wetlands through forests are limited. Yet, sheltering is important in many wetlands which are small in size and surrounded by forest.

Co-located flux towers in a sheltered and open fen with overlapping observations would allow us to test the role that sheltering has on carbon (C) uptake and energy balance as indicated by Bowen ratio [sensible heat flux (H)/latent heat flux (LE)]. Two eddy covariance flux tower sites, Lost Creek (US-Los) and Allequash Creek (US-ALQ), are used here to yield comparisons of gas exchange over wetlands in Northern Wisconsin and provide an opportunity for a more in-depth look than laboratory studies or large-scale syntheses.

One laboratory-based study on gas exchange in marshes with emergent vegetation concluded that thermal convection is a more important driver than wind for CO_2 (carbon dioxide) exchange over surface water (Poindexter and Variano, 2013). Although gas transfer velocities in the model wetland did not depend on in-canopy wind speed, gas transfer velocities were positively correlated with wind speed and were greater than gas velocities predicted by thermal convection alone when mean in-canopy wind speed surpassed field-observed values (4.1 ms^{-1} mean wind speed above canopy, with in-canopy gusts up to 1.7 ms^{-1}). Another study on wind sheltering of a lake by a tree canopy or bluff found that the inhibition of shear stress as a result of sheltering could be measured at a distance of 50 times the canopy height downwind from the canopy (Markfort et al., 2010). Results were the same for both wind tunnel and field experiments. Downstream wind velocity profiles took longer to recover from the sheltering effect of the canopy and were affected by the shape of canopy elements and canopy porosity.

Shade provided by canopies has been shown to alter the energy balance. In a 2009 study on agroforesty in coffee plantations, plants with no shade experienced higher temperatures and less relative humidity than plants at sites with low, medium or high shade (Lin, 2010). Average yearly potential transpiration for plants at a low shade site was also significantly higher than for those at medium and high shade sites. Plants at the low shade site lost significantly more water than those at the medium and high shade sites due to plant evaporative demand and soil evaporative demand rates. Plant transpiration demand had a close relationship with seasonality and shade, and further varied with changes in microclimate. Following these outcomes, lower LE would be expected at the open fen as a consequence of less shade.

Wetlands emit small amounts of C in winter, but accumulate C in the summer months as a result of vascular plant activity and the gradual accumulation of peat created by submerged and anaerobic water conditions. Previous wetland studies have synthesized global flux data to quantify wetland carbon accumulation (Gorham, 1991; Bridgham et al., 2006) and have outlined CO_2 flux responses to water table level and air temperature (Sulman et al., 2010; Pugh et al., 2017). Since high winds promote evaporation from surface water and can decrease humidity, one might expect differences in energy balance between sheltered and open fens.

Comparative studies of LE and daily total evapotranspiration (ET) in wetlands tend to attribute differences between open and closed canopy sites to vegetation type and growth phase of dominant vegetation (Brown et al., 2010) as well as incoming solar radiation and albedo (Lafleur and Rouse, 1988), but also surface wetness or soil moisture (Lafleur, 1990b). The study by Lafleur (1990b) suggested that the impact of canopy sheltering is not fully offset by transpiration from aquatic vegetation, resulting in lower ET at shaded sites compared to sites with open water. On the contrary, a study by Drexler et al. (2004) determined that transpiration contribution from plants can exceed evaporation over an open water surface in wetlands in some cases. Evidently, literature does not show a consensus regarding whether evaporation or transpiration is more influential. Results are site-specific (Mohamed et al., 2012).

Regardless of whether transpiration or evaporation contributes more, LE dominates surface heat balance in wetlands, leading to a Bowen ratio less than one. Dense vegetation, large leaf surface area, high soil moisture, and surface roughness are also conducive to high LE. However, there are other factors that influence transpiration including canopy size, plant species, climate, measurement method, and plant density (Crundwell, 1986).

A number of environmental factors not previously mentioned that have been shown to control net ecosystem exchange (NEE) of CO_2 in various types of ecosystems include substrate quality, light quality, and incoming solar radiation (Rg). Low water table level and stream flow can also alter emissions in fens (Chimner and Cooper, 2003; Drewer et al., 2010; Sonnentag et al., 2010). For example, vascular plants can emit more CO_2 when water levels are low but can also have specific water levels where CO_2 uptake is optimized. Streams will alter eddy covariance estimates of NEE by discharging CO_2 that would have otherwise been sequestered in peat (Billett et al., 2010; D'Acunha et al., 2019). In this study, we considered how nighttime air temperature influences NEE at each site. Site-specific responses of CO_2 uptake to air temperature have clear implications in a changing climate.

Here, we compared wind variability, CO_2 flux, Bowen ratio, and nighttime NEE-air temperature sensitivities of two co-located eddy covariance flux towers to understand how sheltering might alter the energy balance and carbon cycling of wetlands. We then test the hypothesis that increased surface roughness from nearby trees leads to lower wind speeds in sheltered wetlands. Lower wind speeds would then promote weaker net CO_2 uptake and ET at sheltered wetlands. Shading should further contribute to lower ET and CO_2 flux at sheltered sites. Despite differences in sheltering, ecosystem properties such as air temperature sensitivity of NEE should be similar.

Through our analyses, we attempt to answer the following questions:

(1) What is the role of landscape sheltering on wetland ecosystem characteristics and energy balance?
(2) What is the effect of sheltering on channelized flow, mean wind speeds (day vs. night), mean latent heat flux, and daily CO_2 cycle?
(3) What do the wetland-atmosphere interactions observed in this study imply for wetland restoration and climate adaptation?

METHODS

Site Descriptions

The most common wetlands in Wisconsin are freshwater marshes, sedge meadows, aquatic beds, forested, and scrub/shrub wetlands (Wisconsin Department of Natural Resources., 2017b). Categorization of wetland type is according to soil type, vegetation, and degree of saturation. The two wetlands referred to in this study are mosaics of sedge meadow, forested, and scrub/shrub wetland. They are located ∼29 km apart.

To assess the amount of open area at each wetland, we measured the area of conjoined pieces of land that were not visibly forested and did not contain dense shrub vegetation within a specific radius. Aerial imagery was taken by United States Department of Agriculture Farm Service Agency and accessed via Google Earth Pro (Google earth V 7.3.2.5776, 2016a,b). The radius was equal to 100 times the tower height, representing a maximum likely flux footprint or influence area for each site (Schmid, 2002). Small, isolated patches of open land were not included in the calculation. At the sheltered fen, open area was located along the stream (**Figure 1A**). At the open fen, open area followed the stream and extended outwards (**Figure 1B**). We also considered land cover classifications within the radius. Land cover classifications that accounted for less than one percent of the area within the circle were not included in the pie charts (**Figure 2**). Soil at both sites was categorized as wet palustrine soil unless otherwise stated. Specific land cover classifications were determined using the Wisconsin Wetland Inventory maps in the Surface Water Data Viewer web mapping application (Wisconsin Department of Natural Resources., 2017a). Wisconsin DNR completed the statewide map in 1984. The classification system is explained in the Wisconsin Wetland Inventory Classification Guide (Wisconsin Department of Natural Resources., 1992).

A detailed description of the sheltered fen (US-ALQ) can be found in Anderson and Lowry (2007). The 32 ha fen is situated in Trout Lake Basin in northern WI (46.030759, −89.606730). It is part of the National Science Foundation's North Temperate Lakes Long-Term Ecological Research (NTL-LTER) as well as the US Geological Survey's Water, Energy and Biogeochemical Budgets Program (WEBB) Trout Lake site. The soil comprises outwash sand and gravel atop crystalline bedrock. Due to the glacial outwash, the soil is highly conductive and promotes groundwater discharge to the nearby creek. A headwater stream, Allequash Creek, flows from the southeast to the northwest through the fen. The eddy covariance flux tower is located along the stream which is surrounded by tree stands to the northeast and southwest that create a "valley" and cause channelized flow in the direction of the stream (**Figure 1A**).

The valley of the sheltered fen is ∼140 m wide adjacent to the tower. Land cover in the valley is classified as a mix of broad-leaved evergreen scrub/shrub wetland and narrow-leaved persistent (cattail, grass, or sedge) emergent/wet meadow (**Figure 2A**). The mix of sedge and shrubs lining Allequash Creek comprises ∼17% of the area under consideration at this site. The rest of the sheltered fen is comprised of broad-leaved scrub/shrub wetland (30%) and coniferous forested wetland (16%). Land cover not classified as wetland appears to be forested with some shrubs at the outskirts of the study region. Approximately 29% of the study area is open.

A detailed description of the more open-in-scale fen (US-Los) can be found in Sulman et al. (2009) and Pugh et al. (2017). The tower is positioned adjacent to Lost Creek in North Central Wisconsin, USA (46.082777, −89.978611). As stated in Sulman et al., this wetland is representative of many minerotrophic wetlands in the Great Lakes region because of its long and narrow shape and proximity to a stream or river (2009). Long, narrow wetlands such as these have higher ET than more dispersed wetlands as a product of ventilation though a small, isolated plant canopy (Drexler et al., 2004).

Vegetation cover at the open fen is predominantly classified as broad-leaved deciduous scrub/shrub wetland (20%), with 15% located in a floodplain complex and the rest in wet palustrine soil (**Figure 2B**). The open fen also consists of dispersed portions of needle-leaved forested wetland (10%) among fragments of broad-leaved deciduous scrub/shrub wetland and narrow-leaved persistent (cattail, sedge, or grass) emergent/wet meadow (9%). Approximately 45% of the study area is completely open (**Figure 1B**).

Flux Instrumentation

Instrumentation at the sheltered fen included a sonic anemometer (Campbell Scientific, Inc., Logan, UT, CSAT-3), open path infrared gas analyser (LiCor, Inc., Lincoln, NE, LI-7500A), and air temperature and humidity measurements (Campbell Scientific, Inc., Logan, UT, Vaisala HMP45C platinum-resistance thermometer). Solar radiation (Rg) was not measured at this location during the time of study. Rg was replaced with data from the open fen. Air temperature and vapor pressure deficit (VPD) were gap-filled with data from the open fen. The tripod eddy covariance tower at the sheltered fen is ∼2.4 m tall.

Instrumentation at the open fen included a sonic anemometer (Campbell Scientific, Inc., Logan, UT, CSAT-3), open path infrared gas analyser (LiCor, Inc., Lincoln, NE, LI-7500A), temperature/relative humidity sensor (Campbell Scientific, Inc., Logan, UT, CS215), radiation sensor (Kipp & Zonen North America, Sterling, USA, Kipp-Zonen CNR4), and quantum sensor which measures photon flux (LiCor, Inc., Lincoln, NE, LI-190). The tripod eddy covariance tower at the open fen is ∼10 m tall. Both towers collected data at a frequency of 10 Hz, which was then averaged every half hour after processing.

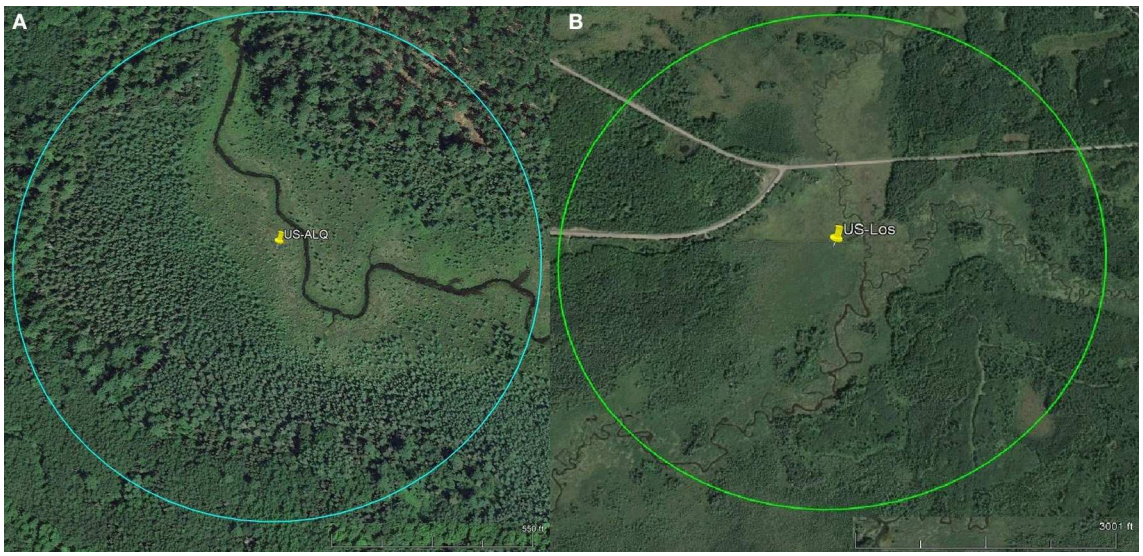

FIGURE 1 | Pins represent tower location. Scales for each site are located at the bottom right of each aerial photo. Circles indicate flux footprints. **(A)** Aerial imagery of sheltered fen US-ALQ (Google earth V 7.3.2.5776, 2016a). Radius: 238 m. **(B)** Aerial imagery of open fen US-Los (Google earth V 7.3.2.5776, 2016b). Radius: 1,033 m.

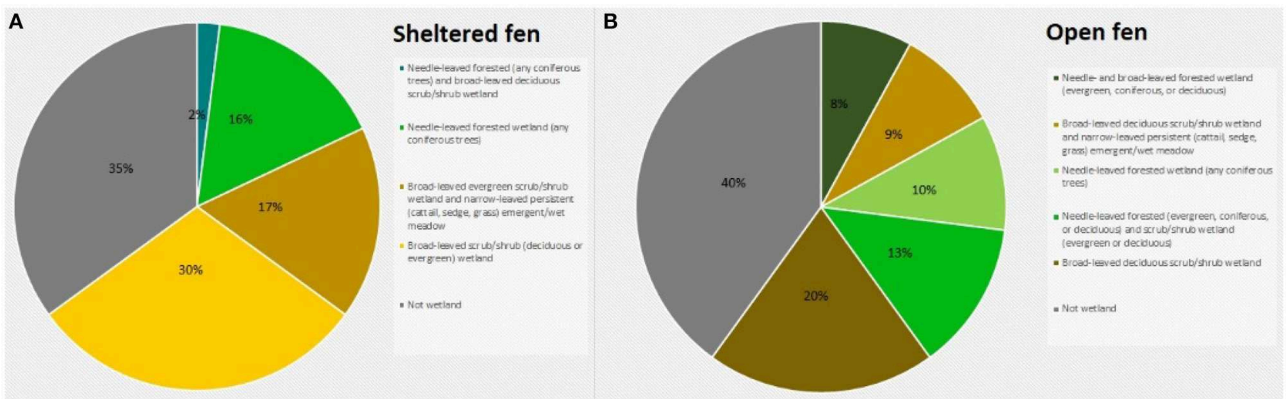

FIGURE 2 | (A) Land cover classification at the sheltered fen (US-ALQ). **(B)** Land cover classification at the open fen (US-Los). Blue, needle-leaved forested (any coniferous trees) and broad-leaved deciduous scrub/shrub wetland; bright green, needle-leaved forested wetland (any coniferous trees); light brown, broad-leaved evergreen scrub/shrub wetland and narrow-leaved persistent (cattail, sedge, grass) emergent/wet meadow; yellow, broad-leaved scrub/shrub (deciduous or evergreen) wetland; gray, not wetland; dark green, needle- and broad-leaved forested wetland (evergreen, coniferous, or deciduous), light green, needle-leaved forested wetland (and coniferous trees); dark brown, broad-leaved deciduous scrub/shrub wetland.

Quality Control

The datasets analyzed in this study both begin on April 11th, 2015 and end on April 25th, 2017.

Eddy covariance flux data for the sheltered fen were calculated using EddyPro software (Olson, 2018). Eddypro calculates quality flags for sensible and latent heat, momentum, and gas fluxes using the steady state test and the developed turbulent conditions test (Foken and Wichura, 1996; Foken et al., 2004; Göckede et al., 2008). For more information on the specific tests, see cited literature.

Outliers were removed after processing with EddyPro. NEE outliers were values over 20 or under -50 μmol m^{-2} s^{-1}. Outliers of LE were values >600 or <-100 W m^{-2}. Outliers of H were values >600 or <-300 W m^{-2}. Low-quality NEE, LE, and H data (quality control flag = 2) were also removed.

Missing and screened flux data from both sites were gap-filled using the Marginal Distribution Sampling technique, which was selected as the standard method of FluxNet. Marginal Distribution Sampling involves estimating missing flux values using a moving look-up table, based on Rg, Tair or Tsoil, VPD, and NEE from surrounding days. More information on the specific technique is outlined in Reichstein et al. (2005) and Wutzler et al. (2018). U-star filtering and daytime-based flux

partitioning (Lasslop et al., 2010) was performed on REddyProc using the moving point test and continuous seasoning from December of the previous year to January and February.

Only considering the data that we used during the study, the sheltered fen (US-ALQ) originally had 50.52% missing NEE (44.75% of daytime, 58.19% of nighttime). After gap-filling, this number was reduced to 24.79% (23.16% of daytime, 26.96% of nighttime). The amount of data that was gap-filled totalled 25.72%.

Half-hourly flux data for the open fen were downloaded from Ameriflux (Desai, 2017). The open fen (US-Los) originally had 33.41% missing NEE (25.29% of daytime, 44.38% of nighttime). After gap-filling, this number was reduced to 0% for both daytime and nighttime. The amount of gap-filled data at the open fen was 33.41%.

All statistical analysis was performed using growing season data from both sites because it had the most reliable, continuous flux data. "Growing season" in this study refers to a rough estimate of carbon uptake period, from April 1st to October 31st. This estimate is similar to carbon uptake periods used in other C flux studies in North America (Frank and Dugas, 2001; Raczka et al., 2013). NEE calculations were also performed for spring, summer, and fall. Spring was defined as April 1st to June 15th. Summer was June 16th to August 31st. Fall was September 1st to October 31st. The year with the least amount of missing data during both day and nighttime for the sheltered fen was 2016. As a result, data from 2016 were selected for full-year comparisons.

Analysis

Eddy covariance half-hourly turbulent flux measurements are temporally auto-correlated, have a double-exponential error distribution, and heteroskedastic error (Richardson et al., 2006). However, averaged NEE over the daily scale, or analysis of large sample sizes tends to converge to Gaussian behavior. While methods exist to account for these factors, including degree of freedom reduction and uncertainty propagation (Desai, 2014), our approach here was a first-cut test of difference.

A Q_{10} function for NEE-air temperature sensitivity was calculated using nighttime NEE and air temperature when air temperature was above zero. Q_{10} was calculated using the formula:

$$Q_{10} = \left(\frac{R_2}{R_1}\right)^{\frac{10^\circ c}{(T_2 - T_1)}}$$

The parameters T_2 and R_2 represent mean air temperature and mean half-hourly NEE at each site, respectively. Incorporating the means of air temperature and half-hourly NEE into the equation helped to eliminate bias from large fluctuations in NEE. The difference of T_2 and T_1 was plotted vs. ratio of R_2 to R_1, and Q_{10} was estimated to be the y-value at $(T_2\text{-}T_1) = 10$, or 10° above the mean air temperature at each site. Pearson correlation coefficients were also calculated between the data displayed on the x and y axes in order to estimate the strength of the linear relationship between nighttime NEE and air temperature. A second-order polynomial was fit to the Q_{10} function of each fen. The polynomial was then back-solved for y at $x = 10$.

Variance analysis and significance testing was performed to understand temporal similarities in NEE between sites. This was done using Morlet wavelet coherence of half-hourly NEE from each site and a histogram of daily mean NEE from each site. Morlet wavelet coherence was calculated using half-hourly NEE values when wind speeds at each site were within $\pm$ 0.2 m s^{-1} of each other. Wind speeds not within this range were removed along with corresponding NEE values and were replaced with a random scalar drawn from the standard normal distribution.

Standard error of the mean was calculated for half-hourly NEE averaged over the entire growing season for each site (**Figure 8**) and for monthly average daytime Bowen ratios (**Table 3**). Standard error of the mean was calculated using standard deviation (σ) and number of data points (n). The formula is shown below:

$$\sigma_x = \frac{\sigma}{\sqrt{n}}$$

Two-sample *t*-testing was used to determine significant differences between sites regarding daily average Bowen ratios and half-hourly NEE. Testing performed on Bowen ratios compared daily average Bowen ratios for each month separately. Half-hourly NEE values were also compared separately by splitting data according to time of day and calculating the results of 48 different *t*-tests, one for each half-hour. All *t*-testing was performed at the 99% confidence level. The null hypothesis was that data in each set came from normally distributed, independent random samples with equal means and equal but unknown variances. Although Bowen ratios did not meet the initial assumption that data is normally distributed, a cumulative distribution function showed that the data were very close to standard normal distribution, but slightly skewed to the right because growing season Bowen ratios tend to be positive. We believe the results of these tests are accurate based on the Central Limit Theorem, which states that as sample size grows toward infinity the distribution of sample means approaches normal. Bowen ratios >10 or <-10, and nighttime values, were not included in statistical tests of the Bowen ratio.

Pearson correlation coefficients (R) and correlation significance were calculated in order to understand the strength of the linear relationship of NEE between sites, as well as the relationship between nighttime NEE and air temperature at each site. Pearson correlation was estimated for daily mean NEE during the entire growing season, and for spring, summer, and fall individually. Correlation significance was determined using the Pearson correlation coefficient (R) and number of samples (n). The null hypothesis of the correlation significance test was that the true correlation of X and Y is zero. The *p*-value was calculated from the *t*-value, whose equation is shown below:

$$t = \frac{r}{\sqrt{\frac{1-r^2}{n-2}}}$$

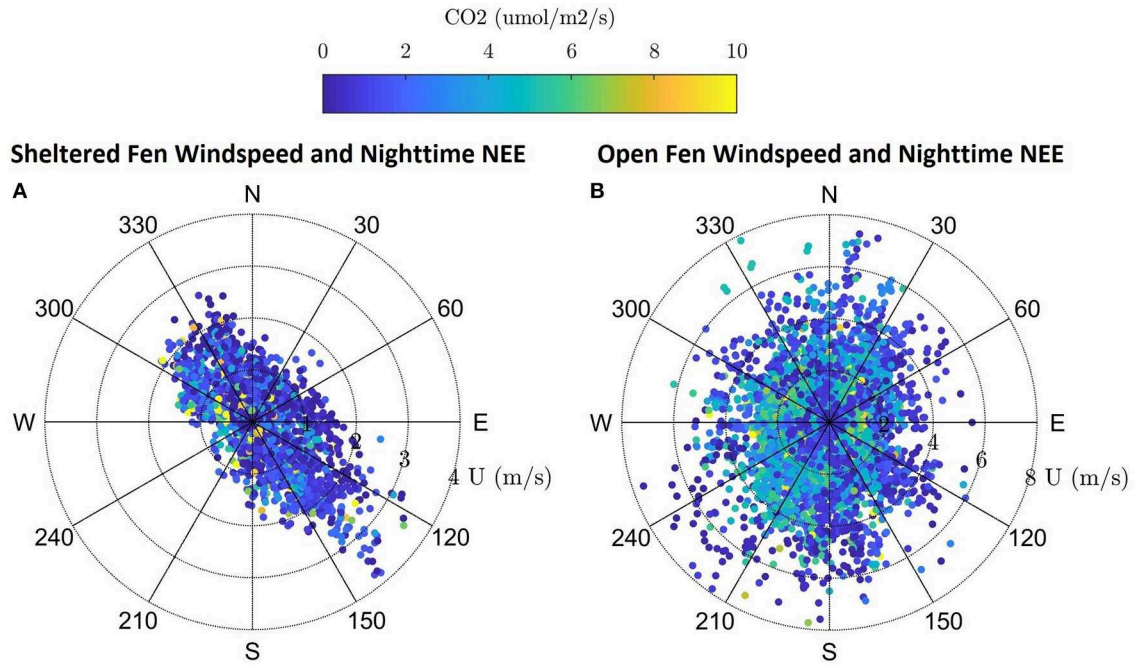

FIGURE 3 | (A,B) Windrose for the sheltered fen US-ALQ with nighttime NEE, wind speed and direction during growing season 2015–2017. Windrose for the open fen US-Los with nighttime NEE, wind speed and direction during growing season 2015–2017.

RESULTS

Wind Speeds and Variability

Dominant flow at the sheltered fen was northwest and southeast following the stream (**Figure 3A**). Mean wind speed at the sheltered fen was 1.09 $ms^{-1} \pm 0.66$ and 0.56 $ms^{-1} \pm 0.62$ for day and nighttime, respectively, from 2015 to 2017. In contrast, the open fen did not display a dominant wind direction (**Figure 3B**). Mean wind speed at the open fen was 2.90 $ms^{-1} \pm 1.50$ and 2.07 $ms^{-1} \pm 1.37$ for day and nighttime, respectively, from 2015 to 2017.

Directional flow at the sheltered fen was likely due to dense (at least 300 m thick) tree formations located just 95 m to the northeast and 42 m to the southwest of the eddy covariance tower. Although the valley consists of low-lying sedge and provides an open area for high wind flow to develop, it is not wide enough for the wind to overcome the sheltering effect.

Vegetation also appears to follow the path of the stream in the eastern portion of the open fen. However, the "valley" created by vegetation surrounding the stream at the open fen is much wider than the valley at the sheltered fen (330 m as compared to 140 m). Land cover at the open fen also contains many random patches of trees in scrub/shrub wetland or emergent/wet meadow (**Figure 1B**). The nearest patch of trees more than 150 m thick is 230 m to the northeast of the tower at the open fen. Open space dominates to the north and southwest of the open fen.

Nighttime wind speeds at each site were lower than overall mean wind speed (36% lower for sheltered, 19% for open). However, mean nighttime wind speed at the open fen was more than three times the mean nighttime wind speed at the sheltered fen (**Figures 4B**, **5B**). Daytime wind speed at the open fen was also higher (1.81 ms^{-1} more than the sheltered fen) (**Figures 4A**, **5A**).

Variance in nighttime NEE spikes up to ∼180 when WS is $<$ ∼0.1 ms^{-1}, but there does not appear to be a strong linear relationship with variance of NEE as WS increases at nighttime either (**Figure 4C**). Mean variance of NEE at nighttime (45.71) is higher than at daytime. Variance of daytime NEE has an initially high peak but declines strongly as WS increases from 0 to 1 ms^{-1} at the sheltered fen (**Figure 4D**). This peak in variance at very low WS causes the mean variance of daytime NEE (35.81) to be higher overall, despite low variances from 1 to 4 ms^{-1}. There does not appear to be any relationship between WS and variance of NEE at daytime for WS over 1 ms^{-1}.

There are some spikes in variance of nighttime NEE between 0 and 2.2 ms^{-1} at the open fen, but there is not a clear linear relationship between WS and variance of nighttime NEE (**Figure 5C**). Mean variance of daytime NEE is similar to the open fen (32.73, compared to 35.81), but mean variance of nighttime NEE is much lower than the open fen (6.35, compared to 45.71). Variance of daytime NEE increases from 0 to 1 ms^{-1} at the open fen (**Figure 5D**). Variance does not appear to be influenced by WS until ∼5 ms^{-1}, when variance of daytime NEE decreases with increasing WS.

Evapotranspiration

Monthly average Bowen ratio at the start of the 2016 growing season was 0.95 at the sheltered fen (**Table 1**). Bowen ratios then began to decrease as latent heat fluxes dominated net radiation partitioning due to ET from new vegetation. The lowest Bowen ratio of 0.21 was reached in July. Monthly average Bowen ratio

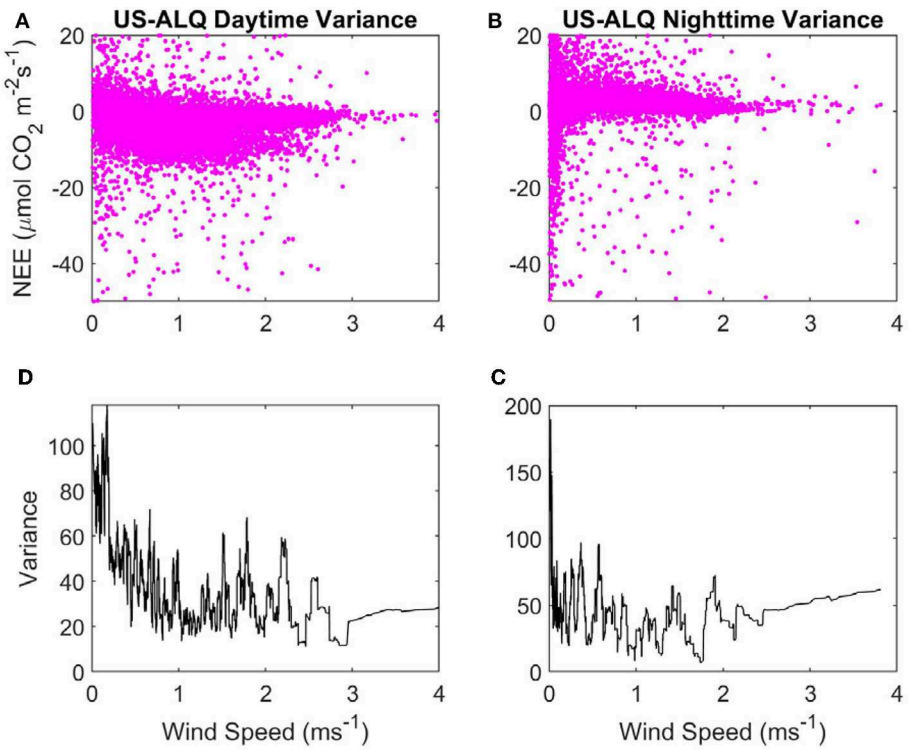

FIGURE 4 | Variance of NEE with WS at the sheltered fen US-ALQ: **(A)** Daytime NEE vs. WS. **(B)** Nighttime NEE vs. WS. **(C)** Variance of nighttime NEE vs. WS. **(D)** Variance of daytime NEE vs. WS. Pink, half-hourly NEE; black, variance of NEE.

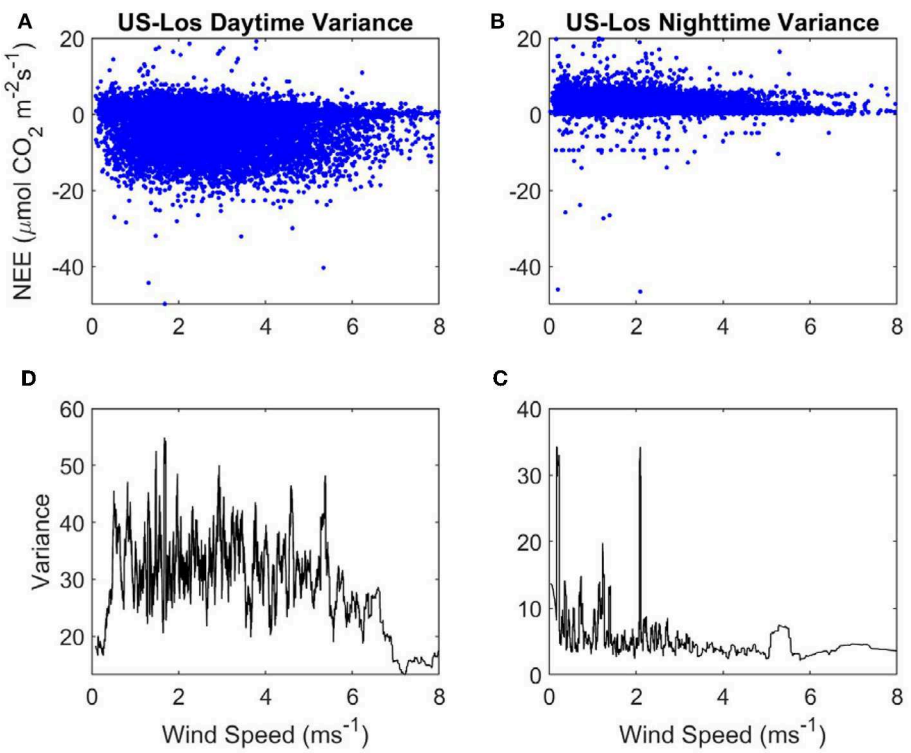

FIGURE 5 | Variance of NEE with WS at the open fen US-Los: **(A)** Daytime NEE vs. WS. **(B)** Nighttime NEE vs . WS. **(C)** Variance of nighttime NEE vs. WS. **(D)** Variance of daytime NEE vs. WS. Blue, half-hourly NEE; black, variance of NEE.

TABLE 1 | Energy balance at the sheltered fen.

	April	May	June	July	August	September	October
Bowen ratio	0.86 ± 0.03 (−0.42, 1.87)	0.72 ± 0.02 (−0.01, 1.42)	0.35 ± 0.02 (−0.35, 0.75)	0.21 ± 0.02 (−0.28, 0.52)	0.33 ± 0.02 (−0.06, 0.84)	0.22 ± 0.03 (−0.37, 0.96)	0.73 ± 0.04 (−0.81, 2.01)
H (Wm^{-2})	34.67	48.24	40.32	34.80	31.66	18.55	14.95
LE (Wm^{-2})	42.14	63.19	90.71	97.93	85.77	61.89	29.40

Range in parentheses. Bowen ratio includes standard error of the mean for each monthly average.

TABLE 2 | Energy balance at the open fen.

	April	May	June	July	August	September	October
Bowen ratio	1.46 ± 0.04 (−0.90, 3.11)	1.03 ± 0.04 (−0.45, 2.73)	0.34 ± 0.02 (−0.43, 0.98)	0.15 ± 0.03 (−1.14, 0.66)	0.19 ± 0.03 (−0.52, 0.82)	0.20 ± 0.03 (−2.20, 1.18)	0.90 ± 0.06 (−2.81, 3.53)
H (Wm^{-2})	48.89	57.12	42.02	35.75	23.51	20.46	19.71
LE (Wm^{-2})	29.90	46.52	81.18	100	77.33	57.91	22.96

Range in parentheses. Bowen ratio includes standard error of the mean for each monthly average.

FIGURE 6 | Half-hourly characteristics of selected fluxes in April 2016: **(A)** solar radiation **(B)** sensible heat **(C)** latent heat **(D)** Bowen ratio. Pink, sheltered fen (US-ALQ); blue, open fen (US-Los); green, Rg for both sites.

maintained a low value during August and September. The Bowen ratio then increased to 0.73 in October.

Unlike the sheltered fen where latent heat flux dominated in early spring, sensible heat dominated at the open fen at the beginning of the 2016 growing season with a monthly average Bowen ratio of 1.55. Bowen ratios then decreased going into summer (**Table 2**). The lowest Bowen ratio occurred in July, and values stayed low until October. The open fen had noticeably

higher H in April and May compared to the sheltered fen, but noticeably lower H in August. Additionally, mean monthly LE was markedly lower at the open fen during every month of the growing season except July and September, when the difference in LE was within 4 Wm^{-2}.

Peak Bowen ratios co-occurred with peak incoming solar radiation at both sites (**Figures 6A,D**). This indicates a strong daily cycle during the entire growing season at both sites. When considering the entire dataset, daily average Bowen ratios had significant differences in mean in April, May, and August ($p < 0.01$) but no difference in other months. Monthly average Bowen ratio was higher at the open fen in April and May, but lower in August.

In 25 out of 28 recorded days in April 2016, daily average Bowen ratio was higher at the sheltered fen than the open fen (**Figure 6D**). The pattern occurred due to higher H (**Figure 6B**) and lower LE (**Figure 6C**) at the sheltered fen, and continued into May. Starting in June, daily average Bowen ratios became more variable and one site was not consistently higher than the other. Monthly average Bowen ratios for both sites were lowest in July and stayed low until October. This pattern indicates a prominent seasonal trend in net radiation partitioning (**Tables 1**, **2**). Bowen ratio appears to be influenced by vegetation growth and senescence in the spring and fall, but microclimate likely became a determining factor during growing season, causing variability on a daily scale between the two sites.

Monthly average air temperatures were lower at the sheltered fen (US-ALQ) than the open fen (US-Los), with the strongest differences occurring in the first half of the growing season (**Table 3**). Higher VPD at the open fen during most of the growing season also indicates drier conditions in the air.

TABLE 3 | Average monthly air temperature and VPD at both sites.

	Sheltered fen Tair (US-ALQ)	Open fen Tair (US-Los)	Difference in Tair	Sheltered fen VPD (US-ALQ)	Open fen VPD (US-Los)
April	4.71	5.58	0.87	2.57	4.02
May	11.69	12.39	0.70	3.96	5.51
June	15.74	16.67	0.93	3.83	5.46
July	18.70	19.54	0.84	4.87	6.47
August	18.14	18.37	0.23	3.99	4.47
September	15.88	15.89	0.01	3.66	3.66
October	7.52	7.95	0.43	2.12	2.55

Air temperature in °C. VPD in hPa.

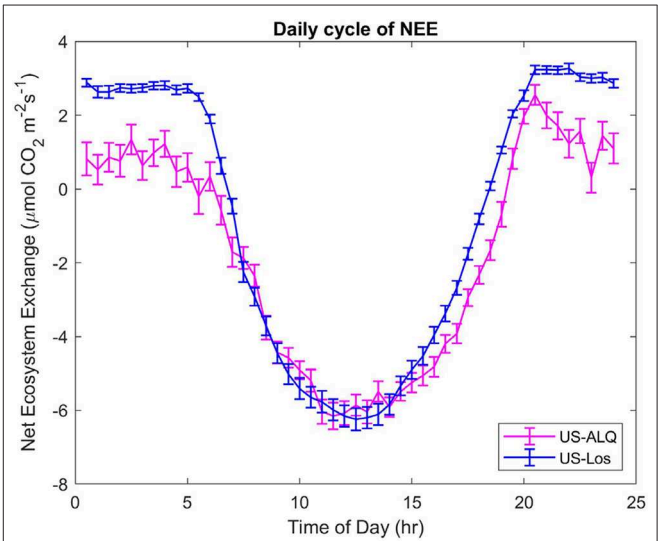

FIGURE 7 | Daily cycles of NEE for both sites. Half-hourly fluxes were averaged over the entire growing season. Error bars represent standard error of the mean. Pink, sheltered fen (US-ALQ); blue, open fen (US-Los).

Carbon Dioxide Fluxes

Average daily NEE during spring at the sheltered fen was −1.91 $\mu mol\ m^{-2}\ s^{-1} \pm 1.88$ (standard deviation). The CO_2 sink grew going into the summer season with an average daily NEE of $-3.05\ \mu mol\ m^{-2}\ s^{-1} \pm 2.01$. The site became a weak CO_2 sink in fall with an average daily NEE of $-0.27\ \mu mol\ m^{-2}\ s^{-1} \pm 1.53$.

Average daily NEE during spring at the open fen was less than half that of the sheltered fen, at $-0.88\ \mu mol\ m^{-2}\ s^{-1} \pm 1.88$. The CO_2 sink was largest in summer when average daily NEE became $-2.09\ \mu mol\ m^{-2}\ s^{-1} \pm 1.63$, but remained smaller than the sheltered fen. The open fen then became a C source in the fall with a daily average NEE of $0.45 \pm 1.03\ \mu mol\ m^{-2}\ s^{-1}$.

The daily CO_2 cycle displays half-hourly NEE averaged over the entire growing season, at each half-hour of the day (**Figure 7**). A significant difference ($p < 0.01$) of the means and variances of half-hourly NEE between the two fens can be seen at the start and end of the daily cycle, which represents differences that occur at nighttime (**Figure 7**). Fluxes of CO_2 at the sheltered fen are lower than fluxes at the sheltered fen in the early morning and afternoon, but there is no significant difference in half-hourly NEE from 7:30 a.m. to 4:30 p.m. It is interesting to note that both sites achieve the same uptake of NEE ($\sim 6\ \mu molm^{-2}s^{-1}$) around 1 pm on average throughout the growing season.

The wavelet coherence displays intermittent high coherence of NEE between sites on daily, weekly, and monthly scales throughout the 2016 growing season (**Figure 8**). There was some correlation on timescales under a day in the middle of the growing season, but little to no correlation between 16 and 30 days. However, there did appear to be a correlation on the scale of the summer overall or at a period of ∼70–128 days.

Daily mean NEE at the sheltered fen during the year of 2016 has a mean of $-1.81\ \mu mol\ m^{-2}\ s^{-1}$ and standard deviation of 2.2 (**Figure 9**). Daily mean NEE at the open fen peaks around 0.5 and $-2.5\ \mu mol\ m^{-2}\ s^{-1}$, and an average of $-0.92\ \mu mol\ m^{-2}\ s^{-1}$ with a standard deviation of 1.94. The distribution of daily mean NEE at the open fen indicates a confounding or external factor impacting the dataset. There was significant ($p < 0.001$) linear correlation of daily mean NEE between the two fens in 2016 ($R = 0.72$). Spring NEE showed almost the same linear correlation between the two sites ($p < 0.001$, $R = 0.71$) as summer ($p < 0.001$, $R = 0.69$). There was also significant correlation of daily mean NEE between sites during fall, but the correlation coefficient

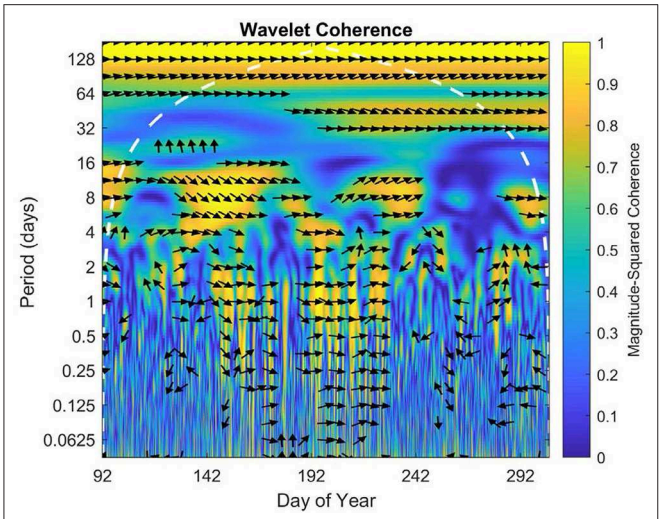

FIGURE 8 | Wavelet coherence for growing season 2016. The x axis represents time, while y axis represents frequency. The direction of each arrow represents phase lag of half-hourly NEE of the open fen with respect to the sheltered fen on a unit circle. Phase arrows pointing right mean data is in-phase. Left is anti-phase. Down means the open fen leads by 90°. Up means the sheltered fen leads by 90°. The white dashed line is the cone of influence, which eliminates data potentially impacted by edge-effect artifacts. Yellow indicates high coherence of data, while blue indicates low coherence.

showed a less linear relationship than the other seasons ($p < 0.001$, $R = 0.44$).

Environmental Controls of Carbon Dioxide Flux

The sheltered fen (US-ALQ) had a Q_{10} of 1.98 (**Figure 10A**). The open fen (US-Los) had a similar Q_{10} of 2.04 (**Figure 10B**). Despite similarities in Q_{10} between sites, air temperature had a stronger linear correlation with nighttime NEE at the open fen ($R = 0.57$) than the sheltered fen ($R = 0.08$). Quantum yield of GPP was also higher at the open fen, by $\sim 4\ \mu molm^{-2}s^{-1}$.

Although Q_{10} is essentially the same at both sites, higher variance of NEE during nighttime at the sheltered fen results in a much less linear relationship with air temperature. In other words, the result of increasing nighttime air temperature at the sheltered fen is less predictable than at the open fen.

Risk of Analysis Biases

Location of the tower at Allequash Creek (US-ALQ) within a clearing of trees brings into question whether the tower measurements reflect large eddies that would have otherwise been broken up by trees and other surface heterogeneities, given that there is some directional flow of CO_2 (**Figures 3A,B**). Because we did not see any "hot spots" of high fluxes of CO_2 in the wind roses, we continued our analysis on the assumption that the valley did not skew flux data at the sheltered fen.

A further cause for concern was outdated land cover classifications. Wisconsin Wetland Inventory maps used to determine vegetation cover were completed in 1984 (**Figures 2A,B**). Comparisons of land cover were based on the assumption that ecological succession was negligible from 1984 to 2017. This is an appropriate assumption for most wetlands, which do not undergo traditional succession because of flooded conditions (Wilcox, 2004 and Kratz et al., 1998). Additionally, aerial imagery from Google Earth from 2015 and 2016 over the flux tower locations appeared to match classifications in the Surface Water Data Viewer (**Figures 1A,B**).

DISCUSSION

Effect of Sheltering on Energy Balance and NEE

In this study, we sought to find out the role of landscape sheltering on wetland ecosystem characteristics and energy balance. We also aimed to understand how sheltering might impact other micrometeorological conditions such as channelized flow, mean wind speeds, and daily CO_2 cycle. These questions were answered by comparing the daily CO_2 cycle, daily mean Bowen ratios for each month of the growing season, variances of NEE on varying time scales, and coherence of NEE from two fens. Results showed that landscape sheltering can cause channelized flow and lower mean wind speeds during both day and nighttime (**Figures 3A,B**, **4A,B**). Sheltering can also alter the energy balance in spring by lowering H and raising LE, and in late summer by partitioning more net radiation into H relative to LE compared to an open fen (**Figure 6**, **Tables 1**, **2**). Daily NEE also has a weaker linear correlation between sheltered and open fens in the fall. However, sheltering does not appear to impact other factors; these include energy balance during early summer and fall, half-hourly NEE during the daytime (**Figure 7**), and Q_{10} respiration function although the linear correlation of nighttime NEE and air temperature is weaker (**Figures 10A,B**). Wavelet coherence of NEE between sites acted as a way to confirm earlier results (**Figure 8**).

One study that also examined wetland ET found seasonal variation was predominantly controlled by net radiation and air temperature (Zhou and Zhou, 2009). Another study, which used data from 2001-2007 at the open fen, positively linked ET and water table level (Sulman et al., 2009). Water table level was not included in the analysis because it was not recorded at the sheltered fen (US-ALQ).

A comparative analysis of CO_2 exchange across northern peatland and tundra sites determined a significant relationship between NEE and leaf area index, and pH on an annual scale (Lund et al., 2010). Our results agree that net radiation has an impact on energy balance (**Figure 6**), and there is a clear seasonal trend of Bowen ratio at both sites (**Tables 1**, **2**). However, there were significant differences in Bowen ratio that could not be explained solely by climate. More extensive information on vegetation types at each fen could allow for analysis of differences due to leaf area index. Leaf area index was not calculated in this study.

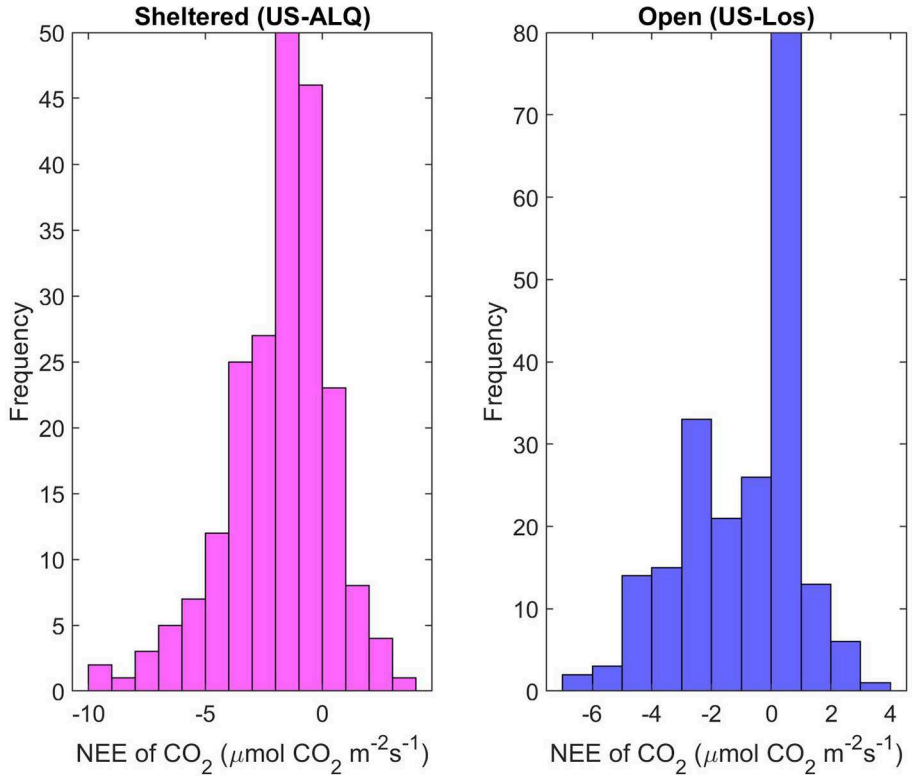

FIGURE 9 | Histograms of daily mean NEE for each site for growing season 2016. Pink, sheltered fen (US-ALQ); blue, open fen (US-Los).

Growing season Bowen ratios calculated in this study had similarities to wetland values calculated in the central US, Poland, and Canada (Lafleur et al., 1997; Lenters et al., 2011; Siedlecki et al., 2016). Bowen ratios at the sheltered and open fen were similar to those listed in Siedlecki et al. (2016) and Lafleur et al. (1997) except for in July, when the monthly average Bowen ratio at the open fen dropped as low as 0.09 ± 0.03. However, the low Bowen ratio at the open fen in July was consistent with the monthly average Bowen ratio for July from Lenters et al. (2011), which represented a wetland in Nebraska dominated by common reed.

Differences in Vegetation Type

Differences in vegetation type between the sheltered and open fen should be considered for their impact on energy balance. Ratio of transpiring to non-transpiring vegetation, and surface litter are some factors that influence ET rate (Drexler et al., 2004). Evidently, vegetation can have an impact on wetland characteristics and micrometeorology.

Stomatal conductance—the rate of CO_2 or water vapor entering or exiting a leaf—of wetland vegetation is another potential source of dissimilarity when performing flux comparisons. It has been noted as a control over wetland ET particularly in vascular plants (Lafleur, 1990a; Drexler et al., 2004). In wetland tundra, stomatal resistance in sedges was the cause of higher ET during hot, dry weather as opposed to cool, wet conditions which one might expect to have been more favorable (Rouse et al., 1992).

Although we focused on growing season data in this study, the insulation capability of dry lichen hummocks in winter should be considered (Drexler et al., 2004). Insulation is important because colder soils will produce smaller CO_2 emissions after thawing, which could potentially be attributed to CO_2 build up and release from the ground, or intensified microbial activity due to freeze-thaw dynamics. Although one would expect similar snow fall at both sites in winter, a higher presence of sedge hummocks at one site compared to the other may lead to differences in H in the early spring and late fall. This insulating factor could provide an explanation for lower H at the sheltered fen throughout most of the growing season.

The hypothesis presented in this study is complicated by the presence of sedge vs. shrub. Shrubs have a high fraction of leaf to vascular tissue area, minimal vertical shading, and high adaptability. Studies have shown shrubs will extend roots to maintain transpiration rates in the case of lowering water table level (Reynolds et al., 1999). According to a study on deciduous shrubs and *Artemisia* subshrubs, shrubs can handle a wider range of moisture stress in soil and air than other plants (Gao et al., 2013) including grass (Kemp et al., 1997; Reynolds et al., 2006). Stomatal conductance of shrubs from a global model had a maximum of 0.83 mol H_2O m^{-2} s^{-1} when soil water potential was set to field capacity ($\psi = -0.033$ MPa). Only

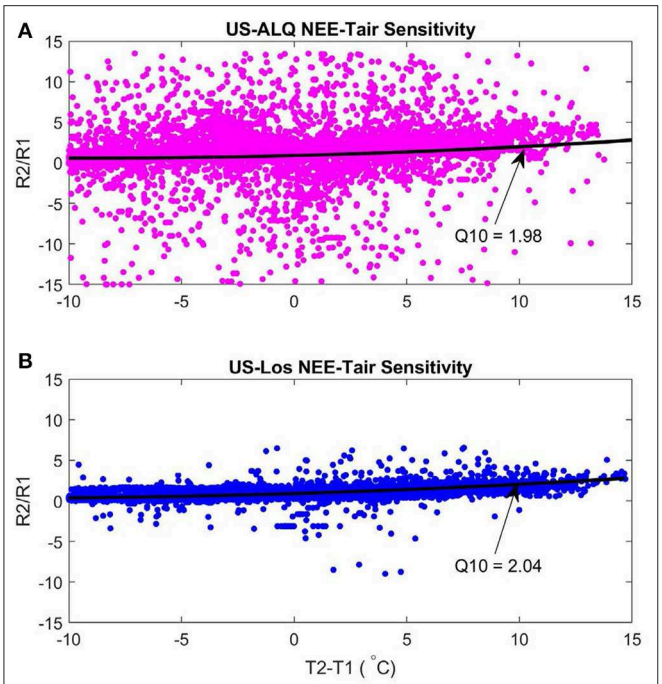

FIGURE 10 | Q_{10} functions of nighttime NEE-air temperature sensitivity 2015–2017. Black line is the second-degree polynomial fit line. **(A)** Sheltered fen Q_{10}. Root Mean Square Error: 5.17. **(B)** Open fen Q_{10}. Root Mean Square Error: 5.13. Pink, sheltered fen (US-ALQ); blue, open fen (US-Los); black, second-degree polynomial.

when soil moisture is abundant do grasses have higher stomatal conductance than shrubs. One type of wetland sedge, *Carex paleacea*, has a small stomatal conductance compared to other wetland species and is lowest during high evaporative demand (Lafleur, 1990b).

Higher LE at the sheltered fen during most of the growing season does not support the idea that sedges in the valley had lower stomatal conductance than shrubs at the open fen. Yet, the prominence of shrubs at the open fen suits the higher evaporative demand at that location. Average growing season VPD was higher at the open fen (4.54) than the sheltered fen (3.20), meaning that there was less humidity in the air and more evaporative demand on vegetation.

Sources of Uncertainty

Some environmental effects make it difficult to attribute notable differences in fluxes to specific conditions at the sheltered fen vs. open fen. Non-normal distribution of daily mean NEE at the open fen implies there is a confounding or external factor influencing fluxes (**Figure 9**). Stream flow and water table level are two such conditions. Recent studies have analyzed how net ecosystem C balance of wetlands may change due to lateral export via streams or open water (D'Acunha et al., 2019). During growing season, dissolved organic C flux represented 5% of the eddy covariance-based estimate of C uptake (4.6 ± 1.5 g C m^{-2} per season) at Burns bog in Canada. Dissolved organic C flux was more important in November and March as a result of lower rainfall and higher ET. The amount of C leaving the sheltered vs. open fen may change according to stream flow rates and percent open water, impacted by the water table level, throughout the year. Stream CO_2 concentration was not recorded at either location during the time of study and thus was not included in the analysis.

Differences in NEE between sites bring about the question of differing water table levels. Water table level measurements exist for the open fen (US-Los) but not for the sheltered fen (US-ALQ). A previous study at the open fen proved that higher water table level caused lower ecosystem respiration and lower GPP, resulting in no net changes in NEE. Thus, NEE was not governed by water table level (Sulman et al., 2009). A more recent study at the open fen supported the hypothesis that mean summer net ecosystem production was not correlated with discharge, but ecosystem respiration and gross primary production were significantly correlated with annual maximum monthly-average discharge (Pugh et al., 2017). Given that the largest difference in variance of half-hourly NEE between sites occurred at nighttime (6.35 at open fen, compared to 45.71 at sheltered), the discrepancy was more likely a result of very low WS (**Figures 5C,D**) rather than fluctuations in water table level.

One study that took place in boreal peatlands found that natural open mires had more consistent summertime Bowen ratios than tree-covered and agricultural peatlands (Alekseychik et al., 2018). The results of our study did not display this trend, as variance of daily average Bowen ratio from June to August was actually larger at the open fen (0.10) than the sheltered fen (0.03). Additionally, Bowen ratio at one of the tree-covered peatlands in Alekseychik et al. (2018) appeared to have a stronger correlation with precipitation pattern than with water table. As mentioned previously, water table level was not recorded at both fens and so was not included in data analysis.

A short-term study on evaporation from sedge-dominated wetland surfaces in Canada looked at one fen on a dry, low ridge with ample soil moisture and another in a depression where soil was covered with standing water. Dead vegetation covered the surface of the dry site and hindered evaporation prior to leaf-out in June (Lafleur, 1990b). LE was only dominant shortly after rain events, after which dead vegetation would dry out and LE and H would equilibrate again. Differences in ET rates between the two sites became less evident after vegetation was established. The results of our study were comparable to these, as daily average Bowen ratios showed no significant differences between sites starting in June, with an exception in August.

Another source of uncertainty was the use of open fen Rg to gap-fill sheltered fen fluxes. While it is likely a good assumption most of the day, differences due to sheltering may magnify at sunrise and sunset due to direct beam Rg in proportion to diffuse Rg. Radiation regimes may also vary internally within sites due to canopy height and resulting albedo, and potentially longwave radiation balance (Goodin et al., 1996).

Implications for Wetland Restoration

Wetland restoration has been suggested as an ecosystem management tool to enhance the terrestrial C sink for climate change mitigation (Bridgham et al., 2006). Not only do vascular

plants assimilate CO_2 via photosynthesis, but also they help sequester C in wetland peat. Our work shows forested wetlands have stronger C sinks throughout the entire growing season due to lower nighttime NEE. Forested wetlands also produce lower H and higher LE that would make them ideal for lowering surface temperatures and promoting ET. Monthly average air temperatures were also lower at the sheltered fen (**Table 3**).

One implication of similar daytime half-hourly NEE between fens is that while areally-averaged C uptake rates in shrub wetlands in our study region can primarily be predicted by vegetation type and age, wind-sheltering driven changes in energy balance may influence the over-all water balance depending on controls on local water table. Depending on restoration goals, this effect may also need to be considered for C and water management.

Removal of natural vegetation can cause large reductions in evaporative source for surrounding areas. This was the case in a study that modeled the effects of land cover change in the world's productive agricultural regions (Bagley et al., 2012). Terrestrial evaporation from land cover to the south of growing regions in the Midwestern US was found to provide moisture for maize. Other studies had similar findings contributing moisture in the US to the Great Plains low-level jet (Schuber and Helfand, 1999). Altering land surface cover in the southern US would prevent surface absorption and re-transpiration of moisture transported by fast-moving winds. Especially during dry years, there is an increased reliance on regional moisture sources for precipitation as opposed to other sources such as onshore moisture flow from the ocean (Bagley et al., 2014). These studies show that ecosystem services offered by wetlands such as ET, lower surface temperatures, and moisture can be transferred throughout a region by fast-moving winds and are not strictly limited to nearby areas.

Several studies have been motivated by the issue of upscaling of land cover with high heterogeneity (Desai et al., 2007; Xiao et al., 2011; Aurela et al., 2015). Despite variations in land cover classification, there were similarities in half-hourly NEE during daytime between fens (**Figure 7**) as well as some coherence on the weekly scale and the summer overall (**Figure 8**). Thus, our study supports that upscaling NEE in order to understand fluxes from wetlands can involve simpler calculations that may not require detailed information about wetland vegetation specific species type.

A recent study on net radiation partitioning in wetlands revealed that wetlands with tall, emergent canopy structures had values of canopy aerodynamic conductance to heat exchange that were nearly twice that of a drained peatland used for growing alfalfa, all located in the Sacramento-San Joaquin Delta of California (Hemes et al., 2018). The short, smooth canopy of alfafa caused lower canopy aerodynamic conductance to heat exchange and consequently, a lower amount of turbulent fluxes that would otherwise transfer LE and H into the atmosphere. Water availability was also listed as an important factor in the relative partitioning of heat. Wetlands with open water and rough surfaces store more energy in the daytime, experience lower H during the day and more LE at night because of stronger aerodynamic and surface conductance. Younger wetlands are also able to store much more excess radiation during the daytime than older wetlands or agricultural plots inside their water column. Regardless of wetland age, all wetlands in the study cooled the surface more than the plot of alfalfa during peak growing season.

Bulk surface resistance is a composite variable that represents leaf water potential, temperature, VPD, and solar irradiance that can also impact net radiation partitioning. Wetlands can be prevented from reaching the potential rate of ET when increased atmospheric demand (VPD) favors net radiation partitioning into LE in the presence of increased bulk surface resistance (Liljedahl et al., 2011). The differences in net radiation partitioning were likely due to lower aerodynamic conductance for heat transfer and canopy boundary layer conductance for CO_2 transfer at the sheltered fen (0.024 and 0.038 ms^{-1}, vs. 0.028 and 0.052 for open fen).

One might expect that H was lower at the sheltered fen (US-ALQ) as a result of lower momentum transport. Although there was lower momentum transport at the sheltered fen, noticeably lower air temperatures throughout most of the growing season indicated that a lack of higher wind speeds was not the only cause of low H (**Table 3**). The sheltered fen also showed lower VPD during the growing season, except for in August when VPD was the same at both sites. This information lends to the idea that the presence of trees impacts wetland atmospheric fluxes in more than one way.

CONCLUSION

Comparing eddy covariance flux tower data from two co-located fens in northern WI revealed that landscape sheltering can impact mean wind speed, wind direction, energy balance, and nighttime NEE, but does not significantly affect daytime NEE. A sheltered fen had lower H in spring and late fall (**Tables 1**, **2**), as well as higher LE in every month of the growing season except July compared to an open fen located only 29 km away. There were significant differences in net radiation partitioning between sites in April, May, and August according to daily average Bowen ratio. Mean nighttime wind speed was also three times less than that of the open fen (0.56 vs. 2.07 ms^{-1}). There were clear differences in wind direction due to the canopy at the sheltered fen (**Figure 3A**), but no significant difference in half-hourly NEE during daytime or Q_{10} air temperature sensitivity of NEE (**Figures 7**, **10**). However, the sheltered fen showed a much weaker linear correlation between nighttime NEE and air temperature than the open fen (*R*: 0.08 vs. 0.57), due to higher variance of nighttime NEE.

Consistent, high quality flux measurements from the sheltered fen during the non-growing season and less gaps in growing season data would allow a comparison of yearly C accumulation between the two sites. Stream CO_2 data, knowledge about the aquatic chemistry of Allequash Creek and Lost Creek, and a record of percent open water at each site throughout the year could contribute to an analysis of lateral fluxes out of the fens. Stomatal conductance measurements could also determine vegetation responses to landscape sheltering. High precision measurements of water table level and precipitation could also build a more complete picture of factors that impact energy balance.

The results of this study, in combination with prior studies on the cooling effect of vegetation (Armson et al., 2012; Hemes et al., 2018), imply that sheltered fens are of high importance for protection and restoration due to their ecosystem services of lower CO_2 source at nighttime and in the fall, stronger growing season CO_2 sink, and higher surface cooling. Shorter spring and fall seasons may also lead to higher H and LE during growing season as the effects of sheltering during spring and late summer disappear. We recognize that some similarities, such as coherence on the scale of summer overall (**Figure 8**), are undoubtedly caused by the proximity of the fens in our study, and the general nature of fens compared to other wetland types. There is a need for further research on wetland canopy sheltering in other regions before these results can be interpreted more broadly.

DATA AVAILABILITY STATEMENT

The datasets analyzed for this study can be found on the Ameriflux website. Data for US-ALQ here: [http://dx.doi.org/10.17190/AMF/1480323]. Data for US-Los here: [http://dx.doi.org/10.17190/AMF/1246071].

DISCLOSURE

Any use of trade, firm, or product names is for descriptive purposes only and does not imply endorsement by the U.S. Government.

AUTHOR CONTRIBUTIONS

JTu (lead author) performed data analysis and quality control and wrote the manuscript draft. JTh (co-author) and BO aided in data collection and analysis. KW and AD provided review, editing, and final approving on the manuscript.

FUNDING

Funding for instrumentation at US-ALQ was supplied by United States Geological Survey Water, Energy, and Biogeochemical Budgets Program. Funding for instrumentation at US-Los was sponsored by the U.S. Department of Energy Office of Biological and Environmental Research through National Institute for Climatic Change Research, Midwestern Region Subagreement 050516Z19.

ACKNOWLEDGMENTS

We acknowledge support from the NSF North Temperate Lakes LTER program (NSF DEB-1440297, NTL LTER), United States Geological Survey (Water, Energy, and Biogeochemical Budgets Program; LandCarbon Program; Water Mission Area), and the Department of Energy Ameriflux Network Management Program. We would also like to thank our reviewers for their valuable feedback on our study.

REFERENCES

Alekseychik, P., Mammarella, I., Lindroth, A., Lohila, A., Aurela, M., Laurila, T., et al. (2018). Surface energy exchange in pristine and managed boreal peatlands. *Mires Peat* 21, 1–26. doi: 10.19189/MaP.2018.OMB.333

Anderson, M., and Lowry, C. (2007). *Transient Functioning of a Groundwater Wetland Complex, Allequash Basin, Wisconsin*. Available online at: www.wri.wisc.edu/wp-content/uploads/FinalWR05R007.pdf

Armson, D., Stringer, P., and Ennos, A. R. (2012). The effect of tree shade and grass on surface and globe temperatures in an urban area. *Urban Forest. Urban Green.* 11, 245–255. doi: 10.1016/j.ufug.2012.05.002

Aurela, M., Lohila, A., Tuovinen, J.-P., Hatakka, J., Penttilä, T., and Laurila, T. (2015). Carbon dioxide and energy flux measurements in four northern-boreal ecosystems at Pallas. *Boreal Environ. Res.* 20, 455–473. Available online at: http://www.borenv.net/

Bagley, J. E., Desai, A. R., Dirmeyer, P. A., and Foley, J. A. (2012). Effects of land cover change on moisture availability and potential crop yield in the world's breadbaskets. *Environ. Res. Lett.* 7:014009. doi: 10.1088/1748-9326/7/1/014009

Bagley, J. E., Desai, A. R., Harding, K. J., Snyder, P. K., and Foley, J. A. (2014). Drought and deforestation: has land cover change influenced recent precipitation extremes in the Amazon? *J. Climate* 27, 345–361. doi: 10.1175/JCLI-D-12-00369.1

Bernal, B., and Mitsch, W. J. (2012). Comparing carbon sequestration in temperate freshwater wetland communities. *Glob Change Biol.* 18, 1636–1647. doi: 10.1111/j.1365-2486.2011.02619.x

Billett, M. F., Charman, D. J., Clark, J. M., Evans, C. D., Evans, M. G., John Ostle, N., et al. (2010). Carbon balance of UK peatlands: current state of knowledge and future research challenges. *Clim. Res.* 45:13–29. doi: 10.3354/cr00903

Bridgham, S. D., Megonigal, J. P., Keller, J. K., Bliss, N. B., and Trettin, C. (2006). The carbon balance of North American wetlands. *Wetlands* 26, 889–916. doi: 10.1672/0277-5212(2006)26[889:TCBONA]2.0.CO;2

Brown, S. M., Petrone, R. M., Mendoza, C. and Devito, K. J. (2010). Surface vegetation controls on evapotranspiration from a sub-humid Western Boreal Plain wetland. *Hydrol. Process.* 24, 1072–1085. doi: 10.1002/hyp.7569

Chimner, R. A., and Cooper, D. J. (2003). Influence of water table levels on CO2 emissions in a Colorado subalpine fen: an in situ microcosm study. *Soil Biol. Biochem.* 35, 345–351. doi: 10.1016/S0038-0717(02)00284-5

Coffer, M. M., and Hestir, E. L. (2019). Variability in trends and indicators of CO2 exchange across arctic wetlands. *J. Geophys. Res. Biogeosci.* 124, 1248–1264. doi: 10.1029/2018JG004775

Crundwell, M. E. (1986). A review of hydrophyte evapotranspiration. *Rev. Hydrobiol. Trop.* 19, 215–232.

D'Acunha, B., Morillas, L., Black, A. T., Christen, A., and Johnson, M. S. (2019). Net ecosystem carbon balance of a peat bog undergoing restoration: integrating CO_2 and CH_4 fluxes from eddy covariance and aquatic evasion with DOC drainage fluxes. *J. Geophys. Res. Biogeosci.* 124, 884–901. doi: 10.1029/2019JG005123

Desai, A. R. (2014). Influence and predictive capacity of climate anomalies on daily to decadal extremes in canopy photosynthesis. *Photosynth. Res.* 119, 31–47. doi: 10.1007/s11120-013-9925-z

Desai, A. R., Moorcroft, P. R., Bolstad, P. V., and Davis, K. J. (2007). Regional carbon fluxes from an observationally constrained dynamic ecosystem model: impacts of disturbance, CO2 fertilization, and heterogeneous land cover. *J. Geophys. Res.* 112:G01017. doi: 10.1029/2006JG000264

Desai, A. R. *Data From US-Los Lost Creek*. AmeriFlux. (2017). doi: 10.17190/AMF/1246071

Drewer, J., Lohila, A., Aurela, M., Laurila, T., Minkkinen, K., Penttilä, T., et al. (2010). Comparison of greenhouse gas fluxes and nitrogen budgets from an ombotrophic bog in Scotland and a minerotrophic sedge fen in Finland. *Eur. J. Soil Sci.* 61: 640–650. doi: 10.1111/j.1365-2389.2010.01267.x

Drexler, J. Z., Snyder, R. L., Spano, D., and Paw U, K. T. (2004). A review of models and micrometeorological methods used to estimate wetland evapotranspiration. *Hydrol. Process.* 18, 2071–2101. doi: 10.1002/hyp.1462

Foken, T., Gockede, M., Mauder, M., Mahrt, L., Amiro, B. D., and Munger, J. W. (2004). "Post-field quality control," in *Handbook of Micrometeorology: A Guide for Surface Flux Measurements*, eds X. Lee, W. Massman, and B. Law (Dordrecht: Kluwer Academic), 81–108.

Foken, T., and Wichura, B. (1996). Tools for quality assessment of surface-based flux measurements. *Agric. Forest Meteorol.* 78, 83–105. doi: 10.1016/0168-1923(95)02248-1

Frank, A. B., and Dugas, W. A. (2001). Carbon dioxide fluxes over a northern, semiarid, mixed-grass prairie. *Agric. Forest Meteorol.* 108, 317–326. doi: 10.1016/S0168-1923(01)00238-6

Gao, Q., Yu, M., and Zhou, C. (2013). Detecting the differences in responses of stomatal conductance to moisture stresses between deciduous shrubs and artemisia subshrubs. *PLoS ONE* 8:e84200. doi: 10.1371/journal.pone.0084200

Göckede, M., Foken, T., Aubinet, M., Aurela, M., Banza, J., Bernhofer, C., et al. (2008). Quality control of CarboEurope flux data - part 1: coupling footprint analyses with flux data quality assessment to evaluate sites in forest ecosystems. *Biogeosciences* 5, 433–450. doi: 10.5194/bg-5-433-2008

Goodin, D. G., Peake, J. S., and Barmann, J. A. (1996). Analysis and modeling of the radiation budget and net radiation of a Sandhills wetland. *Wetlands* 16, 66–74. doi: 10.1007/BF03160646

Google earth V 7.3.2.5776 (2016a). *US-ALQ, Wisconsin. 46° 1′50.73″N, 89° 36′24.23″W, Eye alt 3000 Feet*. Maxar Technologies, USDA Farm Service Agency 2019. Available online at: https://www.google.com/earth/ (accessed August 18, 2019).

Google earth V 7.3.2.5776 (2016b). *US-Los, Wisconsin. 46° 4′57.85″N, 89° 58′42.83″W, Eye alt 14000 Feet*. Maxar Technologies, USDA Farm Service Agency 2019. Available online at: https://www.google.com/earth/ (accessed August 18, 2019).

Gorham, E. (1991). Northern Peatlands: role in the carbon cycle and probable responses to climatic warming. *Ecol. Appl.* 1, 182–195. doi: 10.2307/1941811

Hemes, K. S., Eichelmann, E., Chamberlain, S. D., Knox, S. H., Oikawa, P. Y., Sturtevant, C. S., et al. (2018). A unique combination of aerodynamic and surface properties contribute to surface cooling in restored wetlands of the Sacramento-San Joaquin Delta, California. *J. Geophys. Res. Biogeosci.* 123, 2072–2090. doi: 10.1029/2018JG004494

Kemp, P. R., Reynolds, J. F., Pachepsky, Y., and Chen, J-L. (1997). A comparative modelling study of soil water dynamics in a desert ecosystem. *Water Resour. Res.* 33, 73–90. doi: 10.1029/96WR03015

Kratz, T. K., Soranno, P. A., Baines, S. B., Benson, B. J., Magnuson, J. J., et al. (1998). Interannual synchronous dynamics in north temperate lakes in Wisconsin, USA. *Manage. Lakes Reserv. During Glob. Clim. Change* 42, 273–287. doi: 10.1007/978-94-011-4966-2_19

Lafleur, P. (1990a). Evaporation from wetlands. *Can. Geographer Géographe Can.* 3, 79–82. doi: 10.1111/j.1541-0064.1990.tb01072.x

Lafleur, P. M. (1990b). Evapotranspiration from sedge-dominated wetland surfaces. *Aquatic Bot.* 27, 341–353. doi: 10.1016/0304-3770(90)90020-L

Lafleur, P. M., McCaughey, J. H., Joiner, D. W., Bartlett, P. A., and Jelinski, D. E. (1997). Seasonal trends in energy, water, and carbon dioxide fluxes at a northern boreal wetland. *J. Geophys. Res.* 102, 29009–29020. doi: 10.1029/96JD03326

Lafleur, P. M., and Rouse, W. R. (1988). The influence of surface cover and climate on energy partitioning and evaporation in a subarctic wetland. *Bound. Layer Meteorol.* 44, 327–347. doi: 10.1007/BF00123020

Lasslop, G., Reichstein, M., Papale, D., Richardson, A., Arneth, A., Barr, A., et al. (2010). Separation of net ecosystem exchange into assimilation and respiration using a light response curve approach: critical issues and global evaluation. *Glob. Change Biol.* 16, 187–208. doi: 10.1111/j.1365-2486.2009.02041.x

Lenters, J. D., Cutrell, G. J., Irmak, A., Eisenhauer, D. E., Instanbulluoglu, E., Scott, D., et al. (2011). Seasonal energy and water balance of a Phragmites australis-dominated wetland in the Republican River basin of south-central Nebraska. *J. Hydrol.* 408, 19–43. doi: 10.1016/j.jhydrol.2011.07.010

Liljedahl, A. K., Hinzman, L. D., Harazono, Y., Zona, D., Tweedie, C. E., Hollister, R., et al. (2011). Nonlinear controls on evapotranspiration in arctic coastal wetlands. *Biogeosciences* 8, 3375–3389. doi: 10.5194/bg-8-3375-2011

Lin, B. B. (2010). The role of agroforestry in reducing water loss through soil evaporation and crop transpiration in coffee agroecosystems. *Agric. Forest Meteorol.* 150, 510–518. doi: 10.1016/j.agrformet.2009.11.010

Lund, M., Lafleur, P. M., Roulet, N., Lindroth, A., Christensen, T. R., Aurela, M., et al. (2010). Variability in exchange of CO_2 across 12 northern peatland and tundra sites. *Glob. Change Biol.* 16, 2436–2448. doi: 10.1111/j.1365-2486.2009.02104.x

Markfort, C. D., Perez, A. L. S., Thill, J. W., Jaster, D. A., Porté-Agel, F., and Stefan, H. G. (2010). Wind sheltering of a lake by a tree canopy or bluff topography. *Water Resour. Res.* 46:W03530. doi: 10.1029/2009WR007759

Mohamed, Y. A., Bastiaanssen, W. G. M., Savenije, H. H. G, Van den Hurk, B. J. J. M, and Finlayson, C. M. (2012). Wetland versus open water evaporation: an analysis and literature review. *Phys. Chem. Earth* 47–48, 144–121. doi: 10.1016/j.pce.2011.08.005

Olson, B. *Data From: US-ALQ Allequash Creek Site*. AmeriFlux. (2018).

Poindexter, C. M., and Variano, E. A. (2013). Gas exchange in wetlands with emergent vegetation: The effects of wind and thermal convection at the air-water interface. *J. Geophys. Res. Biogeosci.* 118, 1297–1306. doi: 10.1002/jgrg.20099

Pugh, C. A., Reed, D. E., Desai, A. R., and Sulman, B. N. (2017). Wetland flux controls: how does interacting water table levels and temperature influence carbon dioxide and methane fluxes in northern Wisconsin? *Biogeochemistry* 137, 15–25. doi: 10.1007/s10533-017-0414-x

Raczka, B. M., Davis, K. J., Huntzinger, D., Neilson, R. P., Poulter, B., Richardson, A. D., et al. (2013). Evaluation of continental carbon cycle simulations with North American flux tower observations. *Ecol. Monogr.* 83, 531–556. doi: 10.1890/12-0893.1

Reichstein, M., Falge, E., Baldocchi, D., Papale, D., Aubinet, M., Berbigier, P., et al. (2005). On the separation of net ecosystem exchange into assimilation and ecosystem respiration: review and improved algorithm. *Glob. Change Biol.* 11, 1424–1439. doi: 10.1111/j.1365-2486.2005.001002.x

Reynolds, J. F., Kemp, P. R., Ogle, K., Fernandez, R. J., Gao, O., and Wu, J. (2006). "Modeling the unique attributes of arid ecosystems: Potentials and limitations based on lessons from the Jornada Basin," in *Structure and Function of Chihuahuan Desert Ecosystem, The Jornada Basin Long-Term Ecological Research Site*, eds K. Havstad, L. F. Huenneke, and W. H. Schlesinger (New York, NY: Oxford University Press), 321–353.

Reynolds, J. F., Virginia, R. A., Kemp, P. R., de Soyza, A. G., and Tremmel, D. C. (1999). Impact of drought on desert shrubs: effects of seasonality and degree of resource island development. *Ecol. Monogr.* 69, 69–106. doi: 10.1890/0012-9615(1999)069[0069:IODODS]2.0.CO;2

Richardson, A. D., Hollinger, D. Y., Burba, G. G., Davis, K. J., Flanagan, L. B., Katul, G. G., et al. (2006). A multi-site analysis of random error in tower-based measurements of carbon and energy fluxes. *Agric. Forest Meteorol.* 136, 1–18. doi: 10.1016/j.agrformet.2006.01.007

Rouse, W. R., Carlson, D. W., and Weick, E. J. (1992). Impacts of summer warming on the energy and water balance of wetland tundra. *Clim. Change* 22, 305–326. doi: 10.1007/BF00142431

Schmid, H. P. (2002). Footprint modeling for vegetation atmosphere exchange studies: a review and perspective. *Agric. Forest Meteorol.* 113, 159–183. doi: 10.1016/S0168-1923(02)00107-7

Schuber, M., and Helfand, S. (1999). Climatology of the simulated great plains low-level jet and its contribution to the continental moisture budget of the United States. *J. Clim.* 8:784. doi: 10.1175/1520-0442(1995)008<0784:COTSGP>2.0.CO;2

Siedlecki, M., Pawlak, W., Fortuniak, K., and Zielinski, M. (2016). Wetland evapotranspiration: Eddy covariance measurement in the Biebrza Valley, Poland. *Wetlands* 36, 1055–1067. doi: 10.1007/s13157-016-0821-0

Sonnentag, O., Van Der Kamp, G., Barr, A. G., and Chen, J. M. (2010). On the relationship between water table depth and water vapor and carbon dioxide fluxes in a minerotrophic fen. *Glob. Change Biol.* 16, 1762–1776. doi: 10.1111/j.1365-2486.2009.02032.x

Sulman, B. N., Desai, A., Cook, B. D., Saliendra, N. Z., and Mackay, D. S. (2009). Contrasting carbon dioxide fluxes between a drying shrub wetland in northern Wisconsin, USA, and nearby forests. *Biogeosciences* 6, 1115–1126. doi: 10.5194/bg-6-1115-2009

Sulman, B. N., Desai, A. R., Saliendra, N. Z., Lafleur, P. M., Flanagan, L. B., Sonnentag, O., et al. (2010). CO_2 fluxes at northern fens and bogs have opposite responses to inter-annual fluctuations in water table. *Geophys. Res. Lett.* 37:L19702. doi: 10.1029/2010GL044018

Turetsky, M. R., Kotowska, A., Bubier, J., Dise, N. B., Crill, P., Hornibrook, E., et al. (2014). A synthesis of methane emissions from 71 northern, temperate, and subtropical wetlands. *Glob. Change Biol.* 20, 2183–2197. doi: 10.1111/gcb.12580

Wilcox, D. A. (2004). Implications of hydrologic variability on the succession of plants in Great Lakes wetlands. *Aquatic Ecosyst. Health Manage.* 7, 223–231. doi: 10.1080/14634980490461579

Wisconsin Department of Natural Resources. (1992). *Wisconsin Wetland Inventory Classification Guide*. Retrieved from https://dnr.wi.gov/topic/wetlands/documents/WWI_Classification.pdf

Wisconsin Department of Natural Resources. (2017a). *Surface Water Data Viewer*. Available online at: https://dnr.wi.gov/topic/surfacewater/swdv/ (accessed June 7, 2019).

Wisconsin Department of Natural Resources. (2017b). *Wetland Types*. Available online at: https://dnr.wi.gov/topic/wetlands/types.html (accessed June 7, 2019).

Wutzler, T., Lucas-Moffat, A., Migliavacca, M., Knauer, J., Sickel, K., Šigut, L., et al. (2018). Basic and extensible post-processing of eddy covariance flux data with REddyProc. *Biogeosciences* 15, 5015–5030. doi: 10.5194/bg-15-5015-2018

Xiao, J., Davis, K. J., Urban, N. M., Keller, K., and Saliendra, N. Z. (2011). Upscaling carbon fluxes from towers to the regional scale: Influence of parameter variability and land cover representation on regional flux estimates. *J. Geophys. Res.* 116:G00J06. doi: 10.1029/2010JG001568

Zhou, L., and Zhou, G. (2009). Measurement and modelling of evapotranspiration over a reed (*Phragmites australis*) marsh in Northeast China. *J. Hydrol.* 372, 41–47. doi: 10.1016/j.jhydrol.2009.03.033

Conflict of Interest: The authors declare that the research was conducted in the absence of any commercial or financial relationships that could be construed as a potential conflict of interest.

frontiers in Environmental Science

ORIGINAL RESEARCH
published: 19 November 2019
doi: 10.3389/fenvs.2019.00182

Inferring Methane Production by Decomposing Tree, Shrub, and Grass Leaf Litter in Bog and Rich Fen Peatlands

Joseph B. Yavitt, Anna K. Kryczka, Molly E. Huber, Gwendolyn T. Pipes and Alex M. Rodriguez*

Department of Natural Resources, Cornell University, Ithaca, NY, United States

Plant litter provides a fresh source of energy and nutrients to fuel microbial activity in soil, and in northern peatlands this can be leaf litter from mosses, graminoids, shrubs, and/or trees. Because *Sphagnum* and other mosses decompose slowly, vascular plant litter assumes a principal role, but its role in microbial methane production is unclear. Therefore, we examined decomposition of leaf litter from nine species, including trees, shrubs, and graminoids, using litterbags positioned for up to 2.5 years in two raised bogs and in two rich fens. Across species leaf litter quality varied for concentrations of nitrogen, soluble organic matter, and cell wall composition. After 2.5 years of decay the amount of leaf litter mass remaining ranged from 43 to 63% in the bogs vs. 17 to 71% in the rich fens. Thus, site conditions interacted with litter quality to determine decay rates but with species-specific patterns. Leaf mass remaining after 0.5, 1.5, and 2.5 years of decay was incubated *in vitro*, without soil, to assess its ability to support methane production and concomitant anaerobic carbon dioxide respiration. Residue from all nine species supported methane production, with the greatest rates (up to 5,000 nmol g^{-1} day^{-1}) in tissue with high concentrations of pectin. Rates were 2- to 700-times greater for the leaf material that decomposed in the rich fens than in the bogs. Production rates were more variable for methane than for anaerobic respiration. As seen for mass loss, differences in litter quality predicted variation in gas production rates but differently in the bogs than in the rich fens. The results underscore the importance of vascular plant litter in the biogeochemistry of carbon and methane in peatlands and why vegetation, plant species composition, and peatland type must be described to put peatland ecosystems into global budgets of carbon and methane.

Keywords: anaerobic respiration, leaf litter decomposition, leaf litter quality, New York State, soil methane production

OPEN ACCESS

Edited by:
Colin McCarter, University of Toronto Scarborough, Canada

Reviewed by:
Bin Yang, Beibu Gulf University, China
Maria Strack, University of Waterloo, Canada

****Correspondence:***
Joseph B. Yavitt
jby1@cornell.edu

Specialty section:
This article was submitted to Biogeochemical Dynamics, a section of the journal Frontiers in Environmental Science

Received: *19 June 2019*
Accepted: *31 October 2019*
Published: *19 November 2019*

Citation:
Yavitt JB, Kryczka AK, Huber ME, Pipes GT and Rodriguez AM (2019) Inferring Methane Production by Decomposing Tree, Shrub, and Grass Leaf Litter in Bog and Rich Fen Peatlands. Front. Environ. Sci. 7:182. doi: 10.3389/fenvs.2019.00182

INTRODUCTION

Plant litter provides a fresh source of energy and nutrients for microorganisms in soil, and in northern peatland ecosystems, microorganisms can choose among a diversity of plant growth forms, including mosses, graminoids, shrubs, and trees. Because most *Sphagnum* and other mosses decompose at a slower rate than vascular plant leaves (Lang et al., 2009), partially decayed moss

tissue is a major component of peat soil (Van Breemen, 1995), and studies show that decaying vascular plant tissue assumes a principal role in energy flow and soil microbial activity (Straková et al., 2011; Del Giudice and Lindo, 2017). This is especially important for anaerobic methane (CH_4) production (methanogenesis) in peat soil (Kotsyurbenko et al., 2019).

Not all vascular plant leaves decompose at the same rate, and many studies show that species-specific leaf traits extend to decomposability. This is summarized in the concept of litter quality, which has three aspects. One is structural traits, such as specific leaf area (SLA) and leaf dry matter content (LDMC), that influence microbial colonization of the tissue. Second are nutrients, primarily nitrogen (N) and phosphorous, that support growth of microbial decomposers. Third are the organic polymers that provide energy for microbial decomposers. These three aspects of litter are especially important in northern peatlands, because the diversity of plant growth forms display a wide range of litter types and decay rates (Belyea, 1996; Dorrepaal et al., 2005; Bragazza et al., 2007; Moore et al., 2007; Ward et al., 2015).

Soil properties also influence litter decay rates. Again, this is especially important for northern peatlands, which range from nutrient-rich fens that have a hydrologic connection with groundwater to nutrient-poor fens and bogs that become increasingly isolated from groundwater inputs (Siegel and Glaser, 1987). As a result, peat soil from poor fens and bogs can rise above the persistent water table level, be drier and more acidic (McLaughlin and Webster, 2010; Webster and McLaughlin, 2010), and have slower rates of microbial activity than in richer fens (Moore et al., 2007). However, the better-aerated conditions in bogs might enhance aerobic decomposition of plant litter to the detriment of anaerobic microorganisms that predominate in the water-saturated portion of the peat soil.

It is well-known that peatland systems support microbial methanogenesis, but there is still uncertainty about the depth at which it occurs in the peat soil. Most of the debate is whether methanogens occur at the top of the persistent water table to take advantage of freshly decaying litter coming from above (Franchini et al., 2015) vs. deeper in the fully anoxic peat soil to avoid aeration (Sundh et al., 1994; Glaser et al., 2016). On the other hand, studies have shown that bacteria and decomposer fungi do colonize decaying litter at the peat soil surface (Andersen et al., 2013), but whether this includes anaerobic methanogens is less well-known. Furthermore, there is the question whether anaerobes colonize the decaying litter at the onset of the process vs. latter as the residue sinks into the surface peat (Corteselli et al., 2017). Showing that anaerobic methanogens can colonize and produce CH_4 in leaf litter that sits well above the water table would add a new dimension to the spatial patterns of methanogenesis in peatland ecosystems.

Therefore, the aims of this study were to examine: (1) the relative importance of plant growth form and peatland type for leaf litter decomposition, (2) how variation in leaf litter quality helps to explain variation in decay rates, and (3) the ability of decaying leaves to support microbial activity, in particular, methanogenesis. The main findings of the study were: (1) leaf litter from broad-leaf trees and graminoids decayed faster in rich fens than in bogs, whereas leaf litter from shrubs and needle-leaf trees had faster decay rates in bogs, (2) several aspects of litter quality helped to explain variation in litter decay rates in rich fens, but the same aspects were less effective predictors in bogs, and (3) the decaying residue supported methanogenesis, especially, in the rich fens.

MATERIALS AND METHODS

Study Sites and Experimental Design

We examined leaf litter decomposition in peatlands located near Ithaca, NY. Mean annual temperature in the region is 8.9°C, with monthly mean temperatures ranging from −4.8°C in January to 20.4°C in July. Mean annual precipitation is 890 m.

Dryden Bog (42°26′51.5″N 76°15′33.3″W) is a small ombrotrophic bog ∼150 m across (1.75 ha area). The maximum peat depth is 8 m. The surface consists of well-developed hummocks, dominated by the shrub *Chamaedaphne calyculata* (leatherleaf) and *Sphagnum* mosses (*S. capillifolium, S. fuscum*). Hollows occur between hummocks and have a mixture of the graminoid *Eriophorum vaginatum* (cotton grass), *Vaccinium macrocarpon* (cranberry), and *Sphagnum* mosses (*S. magellanicum*, *S. angustifolium*, and *S. fallax)*. The water table is close to the surface of hollows following spring snowmelt and it drops about 15 cm below the surface of the hollows by mid-summer.

McLean Bog (42°32′55.4″N 76°15′58.2″W) is an ombrotrophic kettle hole bog ∼70 m across (0.4 ha area). Maximum peat depth is 8 m. The bog surface has a lawn-type microtopography. Evergreen shrubs include leatherleaf, *Rhododendron groenlandicum* (Labrador tea), and *Kalmia angustifolia* (sheep laurel). Cotton grass and *Dulichium arundinaceum* (three-way sedge) have moderate cover. *Sphagnum* mosses include: *S. capillifolium*, *S. fallax*, *S. magellanicum*, and *S. angustifolium*.

McLean Fen (42°32′39.5″N 76°16′05.8″W) is rich fen ∼75 m across (0.5 ha area). Maximum peat depth is 3 m. The wetland is underlain by glacio-fluvial stratified sand and gravel with a highly calcareous matrix. The fen receives water from three groundwater springs. We used an area dominated by *Carex stricta (*tussock sedge).

Salt Road Fen (42°35′53.5″N 76°19′17.8″W) is a rich fen ∼250 m across (6.25 ha area). Maximum peat depth is 2 m. The site has a mixture of sedges and shrub cover, including *Cornus racemose* (gray dogwood) and *Rhamnus alnifolia* (swamp buckthorn). We used an area with *Typha latifolia* (cattail) and several sedge species: *Carex flava*, *C. prairiea*, and *C. atlantica*.

We selected nine plant species (**Table 1**). Two species were broad-leaf deciduous trees: *Acer rubrum* (red maple) and *Alnus glutinosa* (common alder). Two species were shrubs: *Myrica gale* (bog myrtle) and leatherleaf. Two species were graminoids: cattail and *Carex lacustris* (lake sedge). Two species were needle-leaf evergreen trees: *Pinus strobus* (white pine) and *Pinus rigida* (pitch pine). We also selected a needle-leaf deciduous tree species: *Larix laracina* (larch). We refer to the species by common names in the paper.

TABLE 1 | Plant species, growth form, and traits of green leaves.

Species (common name)	Growth Form
Alnus glutinosa (alder)	Broad-leaf deciduous tree (nitrogen-fixing)
Acer rubrum (red maple)	Broad-leaf deciduous tree
Carex lacustris (sedge)	Graminoid
Typha latifolia (cattail)	Graminoid
Myrica gale (bog myrtle)	Deciduous shrub (nitrogen-fixing)
Chamaedaphne calyculata (leatherleaf)	Evergreen shrub
Pinus strobus (white pine)	Needle-leaf evergreen tree
Pinus rigida (pitch pine)	Needle-leaf evergreen tree
Larix laricina (larch)	Needle-leaf deciduous tree

Common name	LLS (mo)	SLA (cm^{-2} g)	LDMC (g g^{-1})
BROAD-LEAF DECIDUOUS TREE			
Alder	4–6	167	0.32
Red maple	4–6	270	0.33
GRAMINOID			
Sedge	12–15	143	0.35
Cattail	4–6	142	0.27
SHRUB			
Bog myrtle	4–6	120	0.50
Leatherleaf	18–24	85	0.49
NEEDLE-LEAF TREE			
White pine	20–40	50	0.47
Pitch pine	20–40	50	0.58
Larch	4–6	130	0.37
Mean		128	0.41

LLS, Leaf lifespan in months; SLA, Specific leaf area; LDMC, Leaf dry mass content.

Two sets of leaves were collected from mature plants growing in close proximity to each other in the Cornell Botanical Gardens. The close proximity ensured exposure to the same soil and climate. Bog myrtle does not occur in the Cornell Botanical Gardens, and thus leaf material was collected from a nearby wetland (Lake Como, NY, outlet stream). Leatherleaf does not occur in the Cornell Botanical Gardens, and thus leaf material was collected from the Dryden Bog study site.

One set consisted of green leaves collected in August 2015 by-hand from fully sun lit parts of five individual plants per species. The other set consisted of leaf litter collected at the end of the growing season in October 2015 by shaking branches gently or with a light touch indicating a well-formed abscission zone. Fallen leaves were gathered from a sheet of plastic placed beneath the canopy. Portions from both collections were air-dried at 24°C to a constant mass before being ground for chemical analyses.

Decomposition Experiment

The senesced leaf litter was used for the decomposition study. For each species, 10–20 g (dry mass equivalent) of leaf litter was sealed within 1.2 mm mesh fiberglass screen measuring 20 × 20 cm. This mesh size allowed access to microbial decomposers as well as oribatid mites and ants, which are the dominant invertebrates in the food web in peat soils (Barreto and Lindo, 2018). One bag of each species was fixed to a piece of 1.65 mm monofilament trimmer line in a random arrangement, resulting in nine bags on each line. Twenty replicate lines of litterbags were placed in each site in November 2015. All bags were placed at the soil surface, about 2–5 cm below the tops of moss plants if present.

The experimental design consisted of four plant growth forms, two plant species per growth form, plus larch, and two peatland types, each with two replicates, with five replicate sets of litterbags per site to be collected after 0.5, 1.5, and 2.5 years in the field ($N = 540$ litterbags). Although we did collect the five replicates per site after 0.5 year, a frisky bear decided to munch on some of the litterbags in McLean Bog and in McLean Fen after that, destroying several replicates. Thus, we reduced the sample size to two replicates per peatland for the 1.5-years collection. However, the bear was apparently not done, and it ate the remaining bags in McLean Bog. Thus, the 2.5-years collection consisted of five replicates from Dryden Bog, three replicates from Salt Road Fen, and two replicates from McLean Fen.

Weather conditions in the 0.5 year prior to the first collection were warmer (+0.38°C) and drier (−121 mm) than normal. Between the first and second collections, weather was warmer (+1.1°C) and wetter (+76 mm) than normal. Air temperature was cooler (+0.3°C) whereas precipitation was normal between the second and third collections.

Upon collection, the litterbags were cleaned of moss and roots before being opened, and the remaining leaf litter residue in each bag was weighed and divided into three portions. One was used to determined water content as the ratio of wet mass to dry mass, following oven drying to a constant mass. The second portion was placed in a plastic bag and stored for a short time (<3 days) in a cold room before being incubated *in vitro* to measure production rates for CH_4 and CO_2 (see below). The third portion was dried at 60°C until constant mass and used for chemical analyses.

Leaf Traits and Litter Quality

The green leaves were used for measures of specific leaf area (SLA) and leaf dry matter content (LDMC). Specific leaf area was calculated as the ratio between projected leaf area (cm^2) and leaf oven-dried mass (g). The adaxial side of needle leaves from coniferous species was determined using microscopy. Leaf dry matter content was calculated as the ratio of oven-dried mass (g) to water-saturated mass (g). Leaves were considered water saturated after being stored in a plastic bag between wet paper towels at 4°C for 2 days.

The chemical composition of leaf litter was determined on samples collected before decay and on the residue from litterbag collections. Portions were analyzed sequentially for neutral detergent fiber (NDF), acid detergent fiber (ADF), and acid-detergent lignin on an ANKOM fiber analyzer (ANKOM Technology, Macedon, New York, USA). The analyses are used to approximate hemicellulose (NDF–ADF), cellulose (ADF–acid-detergent lignin), and lignin (acid-detergent lignin) (Van Soest, 1994). Protocols are available at: https://www.ankom.com/analytical-methods-support/fiber-analyzer-a2000. Total

nitrogen (N) was determined by dry combustion on a LECO CN analyzer.

We further characterized cell wall composition by a sequential extraction procedure described in McLeod et al. (2007). Briefly, tissue (0.2 g) is extracted sequentially to: remove free sugars and polysaccharides (fraction 1, 10% formic acid); remove loosely bound pectin (fraction 2, phosphate buffer (200 mM NaH_2PO_4, 0.5% w/v chlorobutanol, 10 mM $Na_2S_2O_3$, adjusted to pH 7); remove calcium, which releases pectin from the middle lamella (fraction 3, cyclohexanediamine tetra acetic acid (CDTA at pH 7.5; Chapman et al., 1987); break hydrogen bonds and separate pectin from cellulose, and to remove cell wall proteins (fraction 4, urea; Chapman et al., 1987); unmask pectin in the primary cell wall (fraction 5, sodium carbonate (200 mM Na_2CO_3 at 5°C); liberate hemicellulose (fraction 6, sodium hydroxide (6 M NaOH, 1% w/v $NaBH_4$ at 37°C; Carpita, 1984); and, finally remove all remaining non-structural sugars (fraction 7, 5% formic acid). Each extraction took place in a 50 ml centrifuge tube with 6 ml of solvent added and incubated for 24 h. Each solvent was removed by centrifugation and saved for colorimetric analysis.

Total carbohydrates in the solvents were quantified using an o-phenanthroline colorimetric assay (Dubois et al., 1956). Before the colorimetric assay, the extract was diluted with de-ionized water and de-salted through a 10-mL plastic syringe containing around 1-mL of microfiber glass wool and 9-mL exchange resin (Mixed Bed IONAC NM-60 H^+/OH^- Form, Type I, Beads 16–50 Mesh). De-salting was repeated until the remaining salt concentration was below 50 mS m^{-1}. The colorimetric assay was done by mixing 1 mL solution with 50 uL 0.1 M $K_3Fe(CN)_6$ solution, 100 μL alkaline reagent and 1 mL color reagent (o-phenanthroline solution), and quantified by 505 nm wavelength. Hereafter we refer to these as soluble sugars (fractions 1 + 7), middle lamella pectin (fractions 2 + 3), cell wall pectin (fractions 4 + 5), and hemicellulose (fraction 6).

Methanogenesis and Anaerobic Respiration

Portions of the leaf litter residue per litterbag (ca. 5 g at field moisture levels) were placed into 236-mL glass jars containing 10 mL of distilled water, and the jars were sealed with a lid that had a gas-impermeable rubber septum to facilitate taking a sample of the headspace gas for analysis. Each jar was made anoxic by removing the headspace with a vacuum pump for 1 min and replacing with O_2-free N_2, repeated three times. The jars remained closed during a 40-days period, which is an accepted time-period to examine anaerobic processes in peat soils (Yavitt

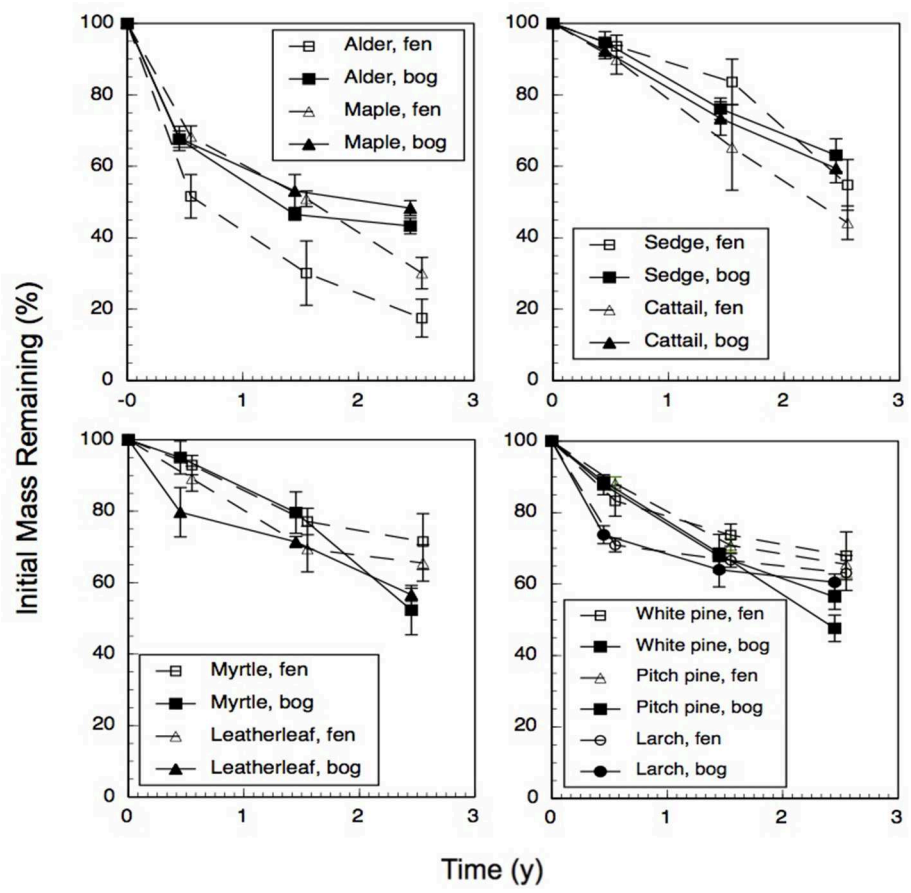

FIGURE 1 | Percentage of initial mass remaining for leaf litter from nine plant species having decayed in bogs or in rich fens for three amounts of time. Values are mean + standard error; $n = 10$ for 0.5 year, $n = 4$ for 1.5 years, $n = 5$ for 2.5 years.

et al., 1997). Periodically, 5-mL gas samples were from the jar headspace, replaced with 5 mL of N_2, and analyzed for CH_4 and CO_2 as described below.

In addition, we examined rates of methanogenesis and anaerobic respiration by peat soils with an addition of leaf

TABLE 2 | Standardized mean effect sizes Cohen's *d* and 95% confidence intervals (CI) of leaf litter decay rate in bogs vs. fens.

	d	95% CI
Broad-leaf deciduous tree	−2.47	[−3.48, −1.20]
Graminoid	−1.00	[−1.92, −0.07]
Shrub	1.11	[0.16, 2.05]
Needle-leaf tree	1.43	[0.45, 2.41]

Faster decay rate in the bogs than in fens has a positive value; faster decay in the fens than in the bogs has a negative value. Strong effect of peatland type is indicated by CI that do not cross zero, i.e., no effect.

TABLE 3 | Cell wall composition of leaf litter.

Common name	N (%)	Soluble (mg g^{-1})	MLP (mg g^{-1})	CWP (mg g^{-1})
BROAD-LEAF DECIDUOUS TREE				
Alder	2.69	277	81	263
Red maple	1.02	309	114	272
GRAMINOID				
Sedge	0.67	76	62	237
Cattail	3.33	28	44	226
SHRUB				
Bog myrtle	1.94	120	60	320
Leatherleaf	1.13	185	112	292
NEEDLE-LEAF TREE				
White pine	0.74	95	56	238
Pitch pine	0.88	130	78	216
Larch	0.95	145	92	259
Mean	1.48	152	78	258

Common name	Hemicell (mg g^{-1})	Cell (mg g^{-1})	Lignin (mg g^{-1})
BROAD-LEAF DECIDUOUS TREE			
Alder	103	163	162
Red maple	75	133	93
GRAMINOID			
Sedge	279	369	58
Cattail	160	370	149
SHRUB			
Bog myrtle	25	141	254
Leatherleaf	38	161	17
NEEDLE-LEAF TREE			
White pine	101	239	161
Pitch pine	198	234	164
Larch	43	191	179
Mean	113	222	155

N, nitrogen; MLP, middle lamella pectin; CWP, cell wall pectin; Hemicell, hemicellulose; Cell, Cellulose; Lignin, Acid-detergent lignin.

TABLE 4 | Fraction remaining (%) of original mass of cell wall components after 2.5 years of decomposition.

	Nitrogen		Soluble	
	Bog	Fen	Bog	Fen
BROAD-LEAF DECIDUOUS TREE				
Alder	57 (12)	28 (9)	9 (8)	2 (2)
Maple	108 (13)	58 (2)	8 (1)	5 (1)
GRAMINOID				
Sedge	113 (15)	111 (17)	55 (15)	30 (10)
Cattail	19 (6)	16 (2)	81 (6)	124 (15)
SHRUB				
Bog myrtle	76 (3)	80 (12)	31 (3)	25 (4)
Leatherleaf	100 (16)	110 (17)	17 (2)	15 (2)
NEEDLE-LEAF TREE				
White pine	84 (5)	99 (10)	32 (13)	53 (11)
Pitch pine	73 (2)	74 (10)	20 (20)	35 (5)
Larch	55 (12)	82 (17)	15 (18)	3 (1)
Mean	76 (30)	73 (34)	30 (24)	32 (38)

	Pectin		Hemicellulose	
	Bog	Fen	Bog	Fen
BROAD-LEAF DECIDUOUS TREE				
Alder	28 (3)	11 (7)	26 (27)	13 (9)
Maple	48 (3)	27 (3)	84 (28)	10 (1)
GRAMINOID				
Sedge	53 (2)	53 (18)	70 (18)	39 (13)
Cattail	59 (28)	42 (5)	115 (26)	44 (5)
SHRUB				
Bog myrtle	47 (18)	42 (6)	78 (31)	14 (2)
Leatherleaf	39 (9)	27 (4)	53(25)	52 (8)
NEEDLE-LEAF TREE				
White pine	51 (7)	66 (13)	67 (24)	28 (6)
Pitch pine	48 (2)	53 (8)	28 (2)	16 (2)
Larch	28 (3)	26 (4)	65 (21)	13 (2)
Mean	44 (11)	38 (17)	65 (27)	25 (16)

	Cellulose		Lignin	
	Bog	Fen	Bog	Fen
BROAD-LEAF DECIDUOUS TREE				
Alder	36 (4)	14 (10)	76 (21)	34 (23)
Maple	36 (18)	29 (3)	108 (2)	58 (6)
GRAMINOID				
Sedge	53 (1)	35 (12)	97 (25)	71 (24)
Cattail	55 (12)	35 (4)	70 (11)	36 (4)
SHRUB				
Bog myrtle	48 (2)	66 (10)	77 (23)	74 (1)
Leatherleaf	60 (5)	69 (11)	98 (4)	109 (17)
NEEDLE-LEAF TREE				
White pine	39 (1)	56 (11)	91 (45)	121 (24)
Pitch pine	45 (9)	54 (7)	90 (1)	113 (15)
Larch	48 (5)	55 (8)	98 (4)	97 (13)
Mean	49 (9)	44 (18)	89 (12)	79 (33)

Values are mean + standard deviation, n = 4.

litter residue from the 0.5- or 1.5-years decay classes. Bulk collection of peat soil from Dryden Bog and McLean Fen was homogenized under constant stream of N_2, and 30 g (fresh mass) portions plus 30 mL of degassed, de-ionized water were placed into 236-mL glass jars, made anoxic as described above. The jars were incubated for 14 days to determine a baseline level of methanogenesis and anaerobic respiration. After this pre-incubation period, the lids were removed and 5 g of air-dried leaf litter residue from individual litterbags was added and pressed down lightly to ensure soil-residue contact. The jars of soil and added litter were resealed, made anoxic, and samples of the jar headspace were collected periodically for 40 days and analyzed for concentrations CH_4 and CO_2.

Methane in the gas samples was analyzed using a Shimadzu GC-14AP Greenhouse Gas Analyzer. This model is equipped with a Flame Ionization Detector (FID) for CH_4. The instrument parameters include a 10-mL sample loop, run time of 5.5-min, ECD temperature of 240°C, column temperature of 60°C, and injection temperature of 65°C. We used 20 mL of each sample to flush and fill the sample loop. Methane peaks are detected by the FID at 1.667-min and compared to known gas standards. Carbon dioxide in the gas samples was analyzed using an open gas exchange system (Li-Cor 6400, Li-Cor Inc., Lincoln, Nebraska, USA) with an in-line septum.

Calculations

Samples of air-dried leaf litter and residue were weighed before and after oven-drying to develop conversion factors to express mass of leaf litter on a dry mass basis. We determined the percentage of leaf litter mass remaining in litterbags at each collection point and fit the data to a single exponential decay equation $y = e^{-kt}$ (Olson, 1963), where y is the percentage of mass remaining, k is the decay rate constant, and t is time in years. We estimated the value for k as the slope of the linear relationship between the natural logarithm of the percentage mass remaining vs. time. We did not include a value for mass prior to placement in the field (100% mass remaining) to account for rapid mass loss due to leaching of soluble compounds.

The analysis of biochemical components in leaf litter, both for the material before decomposition as well as the residue from the litterbags, had to be scaled back due to funding limitations, which precluded analysis of individual samples. Therefore, we

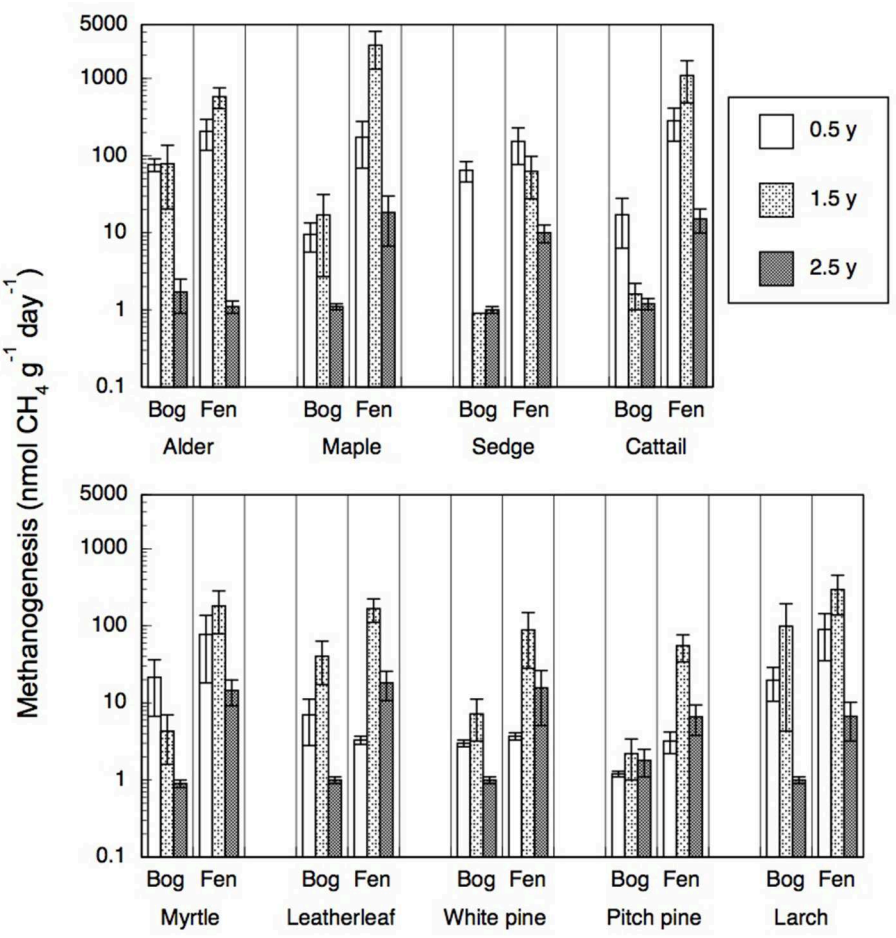

FIGURE 2 | Rates of methanogenesis (nmol CH_4 g^{-1} dry residue d^{-1}) by leaf litter residue from nine species having decayed in bogs or in rich fens for three amounts of time. Values are mean + standard error; $n = 10$ for 0.5 year, $n = 4$ for 1.5 years, $n = 5$ for 2.5 years.

did the analyses on samples pooled by species and site across replicate litterbags. Thus, independent tests of differences in biochemical composition were not possible. The results for biochemical composition should be regarded as suggestive rather than conclusive.

Data Analysis

The low statistical power in the experimental design main effects ($n = 4$ plant growth forms; $n = 2$ species per growth; $n = 2$ peatland types) and interactions constrains our ability to draw real biological inferences with traditional statistics, such as Analysis of Variance (ANOVA). Furthermore, the loss of litterbags from McLean Bog during the decay period and lack of true replication in leaf litter quality makes it difficult to determine if non-significant results were caused by a true lack of differences or simply an artifact of limited sample size.

Therefore, we evaluated the magnitude and direction of treatment effects by calculating the Effect Size, as Cohen's *d* (Nakagawa and Cuthill, 2007). To overcome limitation of small sample size, we compared mass loss and gas production rates in bogs vs. rich fens, with the replicate litterbags used to estimate variability. Rather than claim that differences are statistically significant, we follow the suggestion of Amrhein et al. (2019) and report means, estimates of variation, sample size, and *P*-values.

Relationships among decay rates and rates of methanogenesis and anaerobic respiration with predictors, leaf traits and litter quality, were examined using Pearson Correlation.

TABLE 5 | Standardized mean effect sizes Cohen's *d* and 95% confidence intervals (CI) of leaf litter CH_4 production and CO_2 production in bogs vs. fens.

	d	95% CI
CH_4		
BROAD-LEAF DECIDUOUS TREE		
0.5-year old residue	−0.69	[−1.32, −0.05]
1.5-years old residue	−1.05	[−2.10, 0.01]
2.5-years old residue	−0.60	[−1.50, −0.30]
GRAMINOID		
0.5-year old residue	−0.74	[−1.38, −0.10]
1.5-years old residue	−0.84	[−1.87, 0.19]
2.5-years old residue	−1.78	[−2.84, −0.73]
SHRUB		
0.5-year old residue	−0.27	[−0.89, 0.36]
1.5-years old residue	−1.36	[−2.47, −0.26]
2.5-years old residue	−1.58	[−2.59, −0.56]
NEEDLE-LEAF TREE		
0.5-year old residue	−0.70	[−1.34, −0.06]
1.5-years old residue	−1.11	[−2.17, −0.04]
2.5-years old residue	−0.81	[−1.73, 0.10]
CO_2		
BROAD-LEAF DECIDUOUS TREE		
0.5-year old residue	0.12	[−0.50, 0.74]
1.5-years old residue	2.03	[0.74, 3.26]
2.5-years old residue	−0.21	[−1.09, 0.67]
GRAMINOID		
0.5-year old residue	−0.57	[−1.21, 0.06]
1.5-years old residue	−0.30	[−1.28, 0.69]
2.5-years old residue	−0.01	[−0.98, 0.78]
SHRUB		
0.5-year old residue	−0.57	[−1.20, 0.07]
1.5-years old residue	1.87	[0.67, 3.07]
2.5-years old residue	0.70	[−0.21, 1.60]
NEEDLE-LEAF TREE		
0.5-year old residue	−0.60	[−1.23, 0.04]
1.5-years old residue	1.08	[0.03, 2.14]
2.5-years old residue	0.67	[−0.23, 1.58]

Faster production rates in the bogs than in fens has a positive value; faster decay in the fens than in the bogs has a negative value. Strong effect of peatland type is indicated by CI that do not cross zero, i.e., no effect.

RESULTS

Decomposition

Across the nine species and four sites, an average of 57% of the leaf litter mass remained after 2.5 years of decomposition (**Figure 1**). Fitting a single-exponential decomposition model to the mass remaining, species-specific decomposition rate constants (k) ranged from 0.06 to 0.54 y^{-1}. Decomposition rate constants were fairly similar ($p = 0.7194$) for decay in the bogs ($k = 0.22 \pm 0.075$ y^{-1} [mean ± standard deviation SD], $n = 18$) vs. the rich fens ($k = 0.24 \pm 0.16$ y^{-1}, $n = 18$). Ranking leaf litter decay rates among plant growth forms from fastest to slowest was: broad-leaf deciduous trees, 0.34 y^{-1} > graminoids, 0.26 y^{-1} > shrubs, 0.20 y^{-1} > needle-leaf trees, 0.16 y^{-1}). Peatland type affected decay rates as a function of plant growth form (**Table 2**); leaf litter from the broad-leaf deciduous tree species and the graminoid species decayed faster in the rich fens than in the bogs ($p = 0.0425$), whereas leaf litter from the shrub species and needle-leaf tree species decomposed faster in the bogs than in the rich fens ($p = 0.0688$). Although the two species per plant growth form showed some differences in their temporal patterns of mass loss during the 2.5 years period (**Figure 1**), pairwise comparison of a species effect calculated as Cohen's *d* showed no effect for the four plant growth forms, i.e., 95% C.I. of Cohen's *d* comparing the two species crossed zero.

Leaf Traits and Litter Quality

Traits of green leaves varied among the nine species (**Table 1**): the variation was greater for SLA (Coefficient of Variation, CV = 52% among the nine species) than for LDMC (CV = 25%). In general, green leaves with longer life span (LLS) had smaller values for SLA, whereas LDMC was lower for the broad-leaf deciduous tree species and graminoid species than for the shrub species and needle-leaf tree species.

The cell wall composition of leaf litter (**Table 3**) revealed greater concentrations of pectin and cellulose than concentrations of lignin, hemicellulose, and soluble components. Overall cell wall pectin was the least variable component among the nine species (CV = 13%). Pectin in the middle lamella (CV = 32%), cellulose (CV = 41%), and lignin (CV = 36%) were moderately variable, whereas N (CV = 64%), soluble components (CV = 60%), and hemicellulose (CV = 74%)

were the most variable. There were relative differences among components as a function of plant growth form. For example, the two broad-leaf deciduous tree species were characterized by a relatively large fraction of soluble components; the two graminoid species were characterized by a relatively large fraction of cellulose; and, the shrub species and larch were characterized by a relatively small fraction of hemicellulose but large concentrations of lignin. A large concentration of N was evident in the two species associate with microbial N fixation and in cattail.

We used the fraction of the initial amount of each cell wall component that remained in the residue after 2.5 years of decay to show how components of cell walls changed during decomposition (**Table 4**). For N, leaf litter with a large amount initially, due to N fixation (alder, bog myrtle) or N uptake from the soil (cattail), lost N during decomposition, whereas maple, sedge, and leatherleaf accumulated N during decay period. Ranking mass loss of cell wall components from the most to the least lost was: soluble > pectin = cellulose > hemicellulose > lignin. The broad-leaf deciduous leaf litter was distinguished by large loss of soluble components; the graminoids were distinguished by slower loss of soluble components; the shrubs and needle-leaf litter had average patterns of mass loss for components. Although these patterns were fairly similar between bogs and rich fens, mass loss rates for hemicellulose was much less in the bogs than in the rich fens.

Methanogenesis and Concomitant Anaerobic CO_2 Production

Portions of leaf litter residue incubated *in vitro* without oxygen to assess methanogenesis showed rates that varied by a factor of 5,000, from 1 to 5,172 nmol g^{-1} dry residue d^{-1} (**Figure 2**). Across the nine species and four sites, rates of methanogenesis were greater for the 0.5-year old residue (67 + 84, nmol g^{-1} dry residue d^{-1}, $n = 180$) and the 1.5-years old residue (304 + 658 nmol g^{-1} dry residue d^{-1}, $n = 72$) than for the older 2.5-years old residue (6 + 7, nmol g^{-1} dry residue d^{-1}, $n = 90$). Across the nine species and ages of the residues, rates were greater for leaf litter that decomposed in the rich fens (234 + 545 nmol g^{-1} dry residue d^{-1}, $n = 276$) than in the bogs (18 + 28 nmol g^{-1} dry residue d^{-1}, $n = 276$), with the ranking from greatest to least: broad-leaf deciduous trees > graminoids > shrubs = needle leaf

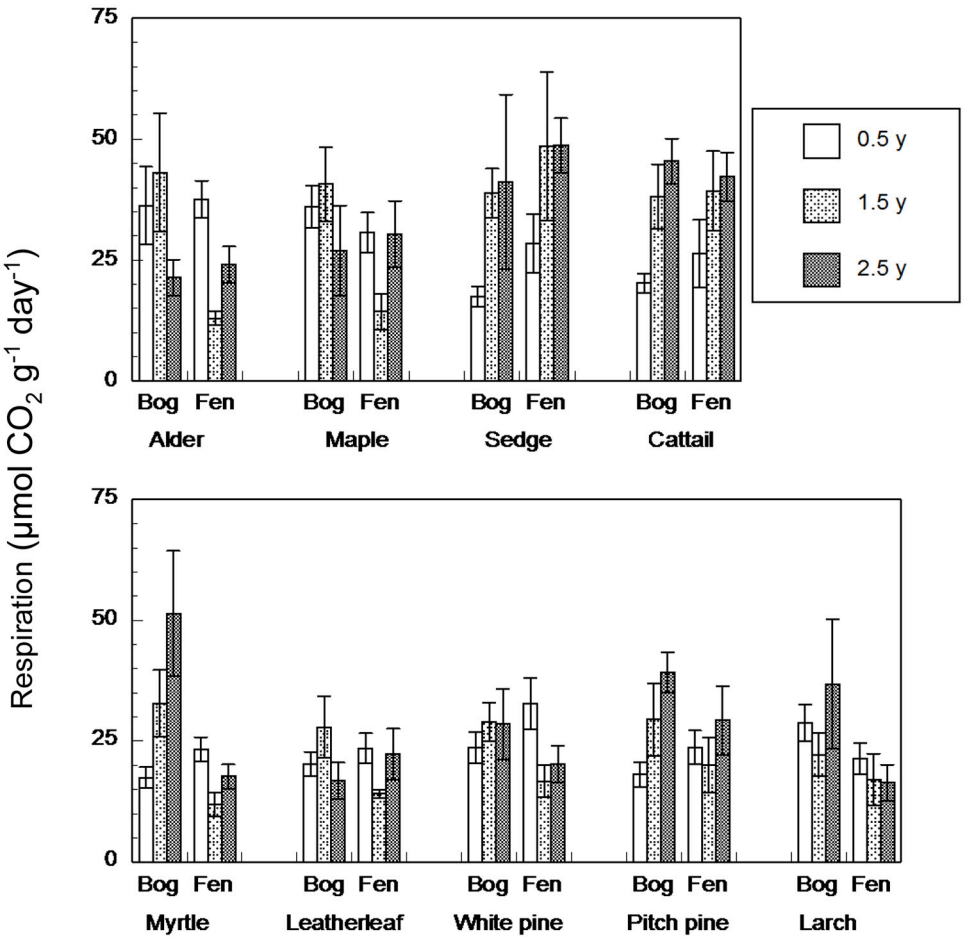

FIGURE 3 | Rates of anaerobic respiration (µmol CO_2 g^{-1} dry residue d^{-1}) by leaf litter residue from nine species having decayed in bogs or in rich fens for three amounts of time. Values are mean + standard error; $n = 10$ for 0.5 year, $n = 4$ for 1.5 years, $n = 5$ for 2.5 years.

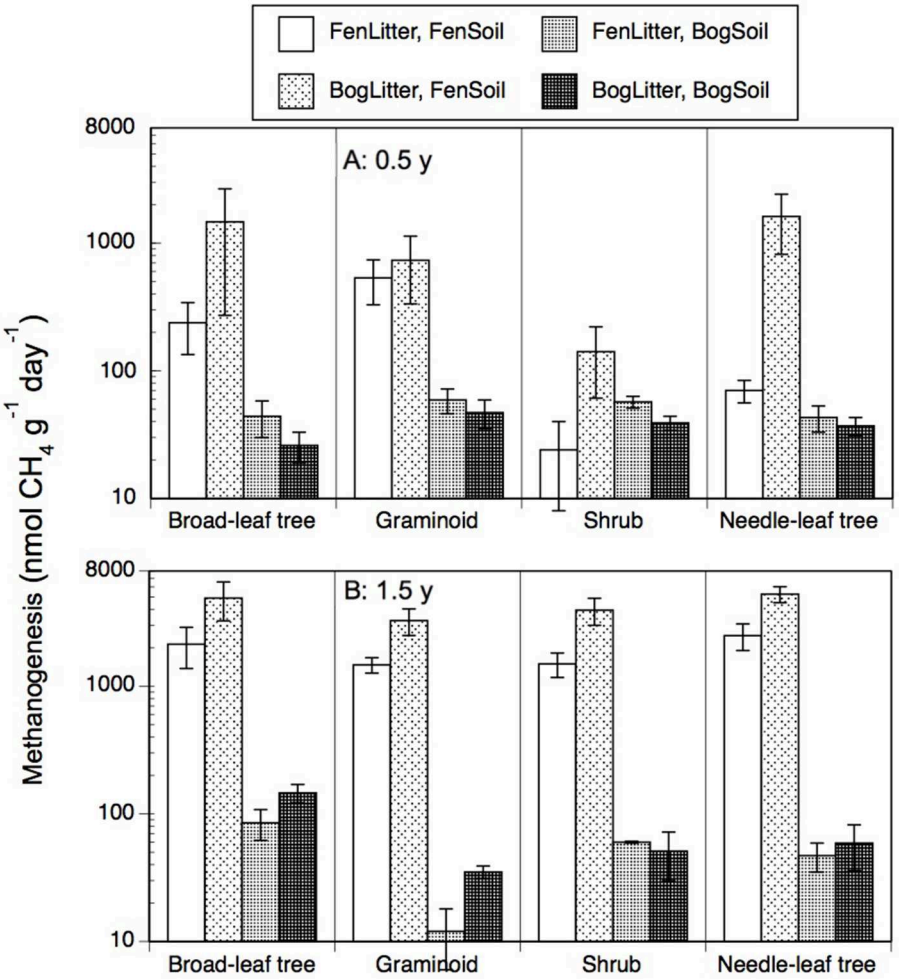

FIGURE 4 | Rates of methanogenesis (nmol CH_4 g^{-1} dry residue d^{-1}) by leaf litter residue from four plant growth forms having decayed in bogs or in rich fens (**A**: 0.5 year, **B**: 1.5 years) mixed with peat soil from a bog or rich fen. Values are mean + standard error; $n = 4$ per plant growth form, 6 for needle-leaf trees.

trees. The effect of peatland type on rates of different plant growth forms (**Table 5**) was stronger for graminoids and shrubs than for the other two growth forms.

In contrast, anaerobic respiration varied by a factor of 25, from 4.2 to 106.7 μmol g^{-1} dry residue d^{-1} (**Figure 3**). Across the nine species and four sites, rates increased with increasing state of decay from the 0.5-years old residue (26 + 7 μmol g^{-1} dry residue d^{-1}, $n = 180$) to the 1.5-years old residue (28 + 12 μmol g^{-1} dry residue d^{-1}, $n = 72$) to the 2.5-years old residue (31 + 11 μmol g^{-1} dry residue d^{-1}, $n = 90$). As a function of growth form, the ranking was: graminoids > broad-leaf deciduous trees > shrubs = needle leaf trees. Although rates were greater for leaf litter that decayed in the bogs (31 + 10 μmol g^{-1} dry residue d^{-1}, $n = 276$) than in the rich fens (26 + 10 μmol g^{-1} dry residue d^{-1}, $n = 276$), the effect of peatland type was evident only for 1.5-years old residue with greater rates for residue from the bogs (**Table 5**).

Portions of leaf litter residue added to soil resulted in rates of methanogenesis that ranged from 6 to 9,312 nmol g^{-1} d^{-1} (**Figure 4**). In contrast, the peat soils without added leaf litter had rates of <20 nmol g^{-1} d^{-1}. Across the nine species and two types of soil, rates were greater with older 1.5-years old residue (1,634 + 2,235 nmol g^{-1} d^{-1}, $n = 72$) than with the less decomposed 0.5-year old residue (337 + 879 nmol g^{-1} d^{-1}, $n = 72$). Also, across the nine species and two types of soil, rates were greater with residue from decay in the bogs (1,405 + 2,272 nmol g^{-1} d^{-1}, $n = 72$) than from decay in the rich fens (566 + 1,049 nmol g^{-1} d^{-1}, n=72). For most of the plant growth forms, the largest rates occurred with residue from decay in the bogs placed on the surface of fen soil.

Rates of anaerobic respiration with leaf litter residue and peat soil ranged from 20 to 232 μmol g^{-1} d^{-1} (**Figure 5**). Across the nine species and two types of soil, rates were 2-times greater with older 1.5-years old residue (99 + 58 mmol g^{-1} d^{-1}, $n = 72$) than with the less decomposed 0.5-year old residue (54 + 22 μmol g^{-1} d^{-1}, $n = 72$). However, across the nine species and two types of soil, rates were similar with residue from decay in the bogs (79 +

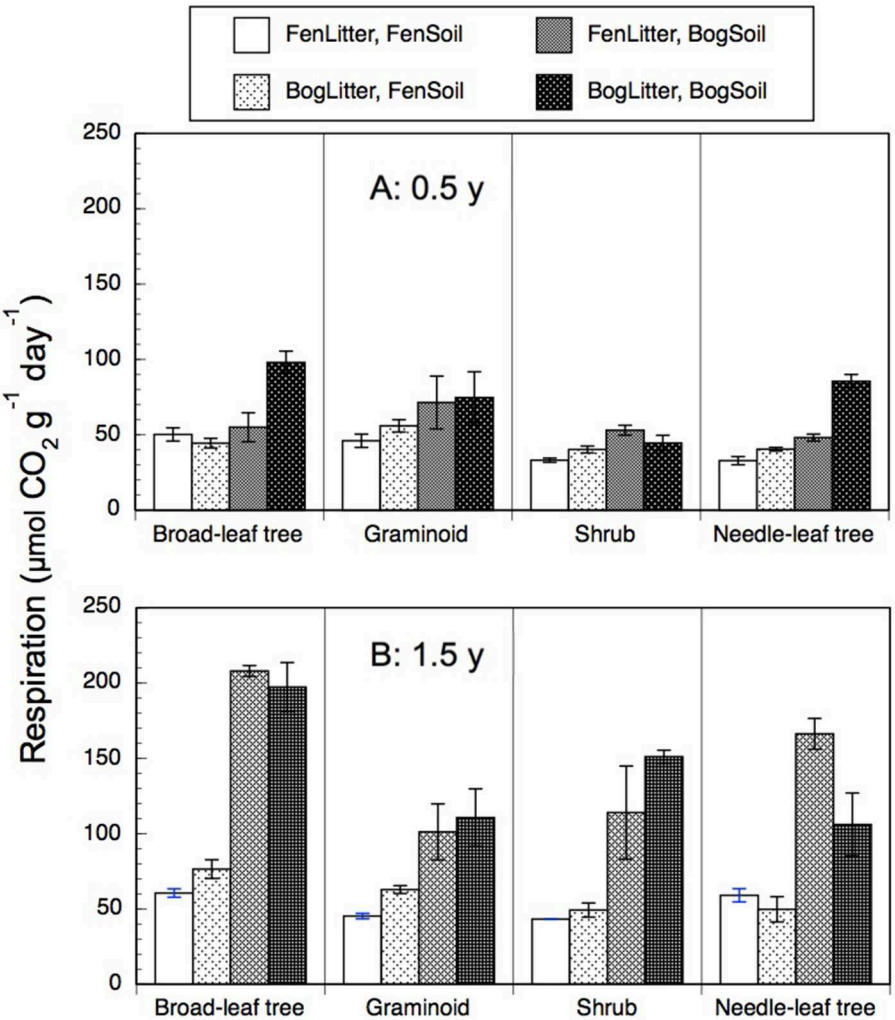

FIGURE 5 | Rates of anaerobic respiration (µmol CO_2 g^{-1} dry residue d^{-1}) by leaf litter residue from four plant growth forms having decayed in bogs or in rich fens (**A**: 0.5 year, **B**: 1.5 years) mixed with peat soil from a bog or rich fen. Values are mean + standard error; $n = 4$ per plant growth form, 6 for needle-leaf trees.

46 µmol g^{-1} d^{-1}, $n = 72$) as with residue from decay rich fens (74 + 52 µmol g^{-1} d^{-1}, $n = 72$). In general, the greatest rates occurred bog soil and 1.5-years old residue regardless where it had decayed.

Leaf litter decay rates showed positive relationships with SLA and the Sum of Cell Wall components (Sum CW) and negative relationships with LDMC and the lignin/N ratio, but only for decay in the rich fens (**Table 6**). None of the aspects of litter provided strong prediction of decay rates in the bogs. For gas production, correlations were calculated between the rate in the residue and the aspect of leaf litter quality measured in the residue at the same time (**Table 6**). Most of the cell wall components predicted rates of CH_4 production by the 2.5-years old residue in the rich fens, with positive relationships for CWP, hemicellulose, and cellulose, whereas the relationship was negative for lignin. The best predictor for CH_4 production in the bogs was for the 0.5-year old residue with a positive relationship for N and a negative relationship for the lignin/N ratio. Hemicellulose was the best predictor of CO_2 production by leaf litter residue from the rich fens.

DISCUSSION

Decomposition

The interaction in leaf litter decay rates between plant growth form and peatland type adds a new dimension to explanations of ecosystem processes in peatlands. Previous studies have shown that leaf litter decay rates vary among plant growth forms (Dorrepaal et al., 2005; Lang et al., 2009) and types of peatlands (Szumigalski and Bayley, 1996; Moore et al., 2007). However, the interaction illustrates why it is necessary to specify vegetation, plant species, and peatland type when putting peatlands into broad cycles of carbon. One hypothesis of a vegetation × site interaction is that leaf litter decays faster in sites in which it came from, the so-called home-field advantage (Gholz et al., 2000). Here for example, sedge and cattail decomposed faster in rich

TABLE 6 | Pearson correlation between aspects of leaf litter quality and mass loss and rates of CH_4 production and CO_2 by decayed residue.

	Mass loss	CH_4			CO_2		
		0.5 year	1.5 years	2.5 years	0.5 year	1.5 years	2.5 years
SLA							
Bog	−0.19	0.26	0.10	0.03	**0.55**	0.40	−0.09
Fen	**0.60**	0.49	**0.79**	0.29	0.22	0.02	0.25
LDMC							
Bog	0.15	−0.42	−0.17	−0.05	−0.42	−0.36	0.03
Fen	**−0.61**	**−0.64**	−0.49	**−0.55**	−0.29	−0.41	−0.46
N							
Bog	0.28	**0.53**	0.27	−0.11	0.42	0.25	−0.39
Fen	0.50	0.18	0.11	−0.15	0.35	−0.41	−0.46
SOLUBLE							
Bog	−0.05	−0.49	−0.36	−0.49	−0.20	0.11	−0.36
Fen	0.41	−0.03	0.10	0.31	−0.38	0.50	0.39
MLP							
Bog	−0.42	−0.10	−0.38	**−0.61**	−0.06	0.07	−0.14
Fen	0.02	−0.05	0.74	0.35	0.24	0.36	0.48
CWP							
Bog	0.10	−0.46	−0.26	−0.25	−0.41	−0.09	−0.43
Fen	−0.10	−0.18	0.41	**0.61**	−0.37	−0.34	**0.61**
HEMICELL							
Bog	−0.05	0.19	−0.33	0.35	−0.13	0.25	0.51
Fen	0.24	0.24	0.03	**0.91**	−0.04	**0.94**	**0.93**
CELL							
Bog	−0.11	0.01	−0.22	0.21	−0.33	0.25	0.37
Fen	0.24	0.28	−0.18	**0.67**	−0.03	0.90	0.70
LIGNIN							
Bog	0.38	−0.12	0.37	−0.10	0.10	0.02	−0.36
Fen	−0.41	−0.10	−0.10	**−0.89**	−0.05	**−0.90**	**−0.90**
SUM CW							
Bog	−0.07	−0.40	−0.26	−0.21	−0.52	−0.09	0.01
Fen	**0.61**	0.02	0.41	**0.59**	−0.02	−0.34	0.59
LIGNIN/N							
Bog	−0.02	**−0.66**	0.19	−0.09	−0.20	−0.45	0.06
Fen	**−0.78**	−0.39	−0.23	**−0.62**	−0.18	−0.27	−0.50

SLA, Specific leaf area; LDMC, Leaf dry matter content; N, nitrogen; MLP, middle lamella pectin; CWP, cell wall pectin: Hemicell, hemicellulose; Cell, Cellulose; Lignin, Acid-detergent lignin.

Bold indicates significance level corrected by Bonferroni for the number of tests; $p < 0.05$.

fens where they occur than in bogs, and leatherleaf decomposed faster in bogs where it occurs than in the rich fens (Schwintzer, 1981). However, home-field advantage did not apply to bog myrtle, which despite its name occurs in fens (Schwintzer, 1984), and to larch, an indicator species for rich fens (Slack et al., 1980), both of which decomposed faster in the bogs. An alternative hypothesis for a vegetation × site interaction is that all litter species decompose at a fast rate in sites dominated by plants with decay-resistant litter, the so-called functional breadth hypothesis (Keiser et al., 2011). The idea is that microbial decomposers can deal with any litter quality when adapted to decay resistant litter, which is *Sphagnum* moss in bogs in this case (Van Breemen, 1995), whereas fastest-decomposing litter shows no preference for site. This applied here to the slowest decaying leaf litter from needle-leaf trees with faster decay rates in the bogs. However, slow-decaying litter from graminoids decayed faster in the rich fens, as opposed to the functional breadth hypothesis. Thus, neither hypothesis for a vegetation × site interaction in litter decay rates applied in toto to the plant species used here in the bog, rich fen contrast.

A key finding of our study is that aspects of litter quality were better predictors of litter decay rates in the rich fens than in the bogs (**Table 6**). For example, SLA and LDMC had strong relationships with litter decay rates but only in the rich fens. One explanation for such relationships is rapid colonization by microbial decomposers (Makita and Fujii, 2015). For example, a large value for SLA presents a large surface area for colonization, resulting in a positive relationship with decay rate. Decomposition in the rich fens also was negatively related to the ratio of acid-detergent lignin to N (**Table 6**). Lignin and N are well-documented predictors of decomposition in terrestrial ecosystems (Melillo et al., 1982; Berg and McClaugherty, 2014) but did not generalize to litter decay rates in the bogs, perhaps because of N mineralization *per se* in the bogs that complicates that relationship. One hypothesis is that N released from decaying tissue is lost quickly from the bog soil, and this seems to slow the decay of vascular plant litter (Reuter et al., 2019).

Pectin in the middle lamella emerged as a stronger predictor of leaf litter decay rates in the bogs (**Table 6**). Pectin is a major component of the middle lamellae (and primary plant cell wall) in vascular plant species and is typically 30–35% of cell wall dry weight (Pelloux et al., 2007), although lower levels of 5–10% are found in some graminoid species (Smith and Harris, 1999). Our finding pectin percentages of 29–42% (mean = 34%) among the nine species here is in line with others for trees, shrubs, and sedges. Because middle lamella pectin plays a functional role gluing cells to each other (Bou Daher and Braybrook, 2015), the negative relationship with litter decay rates suggests that the glue effectively slowed the rate of decay in bogs. Although the functional breadth hypothesis, mentioned above, would predict faster litter decay rates in in the bogs (Keiser et al., 2011; Fanin et al., 2016), and bogs typically harbor microorganisms with pectin-degrading enzymes (Thormann, 2006), these enzymes tend to be deactivated when bound to *Sphagnum* (Børsheim et al., 2001). Therefore, the unique chemistry of *Sphagnum* complicates litter decay in bogs (Van Breemen, 1995).

Our experimental design included two plant species associated with N-fixing microorganisms and cattail that initially had N-rich leaf litter, but these species did not have the most rapid decay rates. This finding is in line with other studies where leaf litter from plants with N-fixers does not decompose faster than leaf litter from non-N-fixing plants (Cornwell et al., 2008; Prescott, 2010). The experimental design also included plant species with a broad range of hemicellulose content. Schädel et al. (2010) examined hemicellulose contents in leaves for a range of plant growth forms and found that the ratio of cellulose + lignin to hemicellulose had a mean value of ca. 1.4 for graminoids, 1.75 for broad-leaf trees, and 2.7 for needle-leaf trees. Values

here are larger, but with the same ranking among plant growth forms, with 2.4 for graminoids, 3.1 for broad-leaf trees, 4.9 for needle-leaf trees, and a notable value of 12.4 for the shrubs. The much larger values here, along with typical values for lignin and cellulose (Preston et al., 2009), point to the importance of pectin rather than hemicellulose in the leaf litter of vascular plant species that occur in peatlands.

After 2.5 years of decay, persistence of lignin in the residue of decaying litter is a well-established phenomenon (Preston et al., 2009). How chemistry of litter residue changes during decomposition has been much debated (cf., Wickings et al., 2012). For example, Soong et al. (2015) argued that lignin and cellulose decompose at similar rates maintaining a constant proportion in the residue over time, but this was not true for all nine of plant species we studied. Likewise, there is a general belief that about 50% of hemicellulose is lost quickly from decaying litter, within the first few months, but what remains does not decompose as easily (Machinet et al., 2011). However, the retention of hemicellulose during litter decay in the bogs vs. 75% of the initial hemicellulose being lost from decaying litter in the rich fens deviated from this conclusion. Overall, pectin is thought to be easily degradable (Jung and Engels, 2002). However, it is well-known that pectin accumulates in peat soils (Waksman and Reuszer, 1932), which is thought to be derived mostly from *Sphagnum* mosses. Thus, our data show that decomposing leaf litter from vascular plants is an additional source of pectin. These findings are important for the link to methanogenesis, as lignin and pectin contain methyl groups that can be fermented to methanol and acetate, which are substrates for methanogenesis (Lever et al., 2010).

Methanogenesis and Anaerobic Respiration

The maximum rates of methanogenesis attained by decaying leaf litter were impressive. Although there is no accepted level that constitutes an active rate vs. a less-active rate, using an arbitrary value of >100 nmol g^{-1} d^{-1} as active, all of the species, except pitch pine, were able to support active CH_4 production. Indeed, upper values achieved by decaying leaf litter are in line with rates observed in peat soils that are known sources of atmospheric CH_4 (Yavitt et al., 2018). This means that leaf litter from species across a broad range of plant growth forms, when decaying on the surface of peat soils, provides a suitable habitat for methanogenic microorganisms and associated anaerobes.

The wide range in rates of methanogenesis by decaying leaf litter, albeit from the nine species of plants, decayed in two types of peatlands, and with three ages of residue is not surprising, given that rates of methanogenesis are notoriously variable in peat soils (Yavitt et al., 1997; Treat et al., 2015; Kotsyurbenko et al., 2019). Many studies have sought the explanation(s) for variation in rates of methanogenesis in peatlands, but the multiple processes acting over a variety of spatial and temporal scales suggest that any one aspect might not be a stronger predictor of the process. For example, much greater rates of methanogenesis by leaf litter residue retrieved from the rich fens than the bogs in this study points to wetter soil conditions year-round in the rich fens that enable the growth and persistence of anaerobic methanogens. However, Godin et al. (2012) found greater diversity in the methanogenic community and active rates of methanogenesis in rich fens across a gradient of fen types, but soil wetness was not a good predictor. Several studies have singled out graminoids in peatlands for their role in methanogenesis (cf., Treat et al., 2015; Strack et al., 2017), given that they assume dominance in rich fens (Schwintzer, 1981).

It is noted that the two species of graminoids examined here were not associated with particularly large rates of methanogenesis. Other studies have attributed the positive effect of graminoids to rapid decay rates (Treat et al., 2015), but that does not apply to the two species here that had relatively slow rates of leaf litter decay. Another hypothesis is that graminoids lack phenolic compounds in litter (Emilson et al., 2018) that are toxic to methanogens. However, leaves from shrubs and needle-leaf trees are notoriously full of phenolics (Dorrepaal et al., 2005), yet decaying leaf litter from shrubs, and from needle-leaf trees here and in other studies (Yavitt and Williams, 2015; Corteselli et al., 2017) supported methanogenesis, which runs counter to the toxicity argument. Moreover, because most phenolics are water soluble (Min et al., 2015), they are likely leached away making the residue a less toxic habitat than expected from initial litter chemistry. Thus, the overwhelming prevalence of methanogenesis associated with litter decay in the rich fens challenges a single explanation.

The mostly negative relationships between aspects of litter quality and rates of methanogenesis for decay in the bogs (**Table 6**) seems to presuppose that leaf litter residue is a poorer substrate for methanogens in bogs. However, we tested this by mixing leaf litter residue retrieved from the bogs with fen soil. Even though it was a short-term *in vitro* study, the large rates of methanogenesis by bog-derived residue indicates no inherent inhibition of CH_4 producers by the residue *per se.* Therefore, low rates of methanogenesis observed by decaying leaf litter in the bogs could be attributed to a relatively depauperate methanogenic community in the bogs vs. that in the rich fens (Dettling et al., 2007; Godin et al., 2012). Likewise, the positive link between pectin and rates of methanogenesis for decaying litter in rich fens but not in the bogs might be related to more active pectin-degrading microorganisms in fens than in bogs (Børsheim et al., 2001). The positive links between hemicellulose and rates of methanogenesis in the rich fens but not in the bogs are notable with further studies needed to pinpoint the mechanistic link.

Also evident in **Table 6** is that the strength a correlation between a particular aspect of leaf litter quality and rates of methanogenesis changed as the residue aged. In some cases, the strength of the relationship weakened with age of the residue, such as with SLA, in other case it strengthened. Explanations for each aspect of litter quality are, of course, complicated by likely changes in the size and activity of different populations of methanogens associated with residue of different age (Sun et al., 2012).

Fairly constant rates of anaerobic respiration as the leaf litter residue aged can be explained by the combination of microbial growth on the residue (Witkamp, 1966) and greater respiration

per unit of mass loss as microbes need to work harder to decompose components that accumulate as the residue ages (Wardle, 1993). This effect of greater CO_2 production associated with decaying litter has been shown in a few studies (McLaren et al., 2017), and the results here extended it to anaerobic respiration. Since our findings include leaf litter that decomposes slowly as well as more quickly, and for decay in bogs and in rich fens, greater microbial respiration on aged litter residue might be a common feature of peatland ecosystems. The implication is that CO_2 produced in peat soil is not always coming from decay of the freshest litter, but rather it is supported by microbial activity on aged litter.

CONCLUSIONS

During 2.5-years of decomposition, we found that decaying leaf litter provided a habitat for anaerobic CH_4-producing microorganisms. This conclusion extended to leaves from trees, shrubs, and graminoids decomposing in bogs and in rich fens. With anaerobic microorganisms invading quickly at the onset of the decomposition process, and persisting in the residue, the results have broadly implications to spatial patterns of methanogenesis within the soil profile of peatland ecosystems. The initial decay rate of leaf litter is relatively slow in these ecosystems, and the decay rate further slows as the litter residue becomes progressively buried in the soil profile (Frolking et al., 2001). Thus, the species-specific responses will help to define whole-ecosystem CH_4 production as the composition of plant species wax and wane over time in peatland ecosystems (Williams and Yavitt, 2003).

DATA AVAILABILITY STATEMENT

The datasets generated for this study are available on request to the corresponding author.

AUTHOR CONTRIBUTIONS

AK and JY designed the experiment. AK, MH, GP, and AR carried out the experiment. JY analyzed the data and wrote the paper with help from all co-authors.

FUNDING

This work was supported by a USDA National Institute of Food and Agriculture, Hatch project (1007286). Any opinions, findings, conclusions, or recommendations expressed in this publication are those of the author(s) and do not necessarily reflect the view of the National Institute of Food and Agriculture (NIFA) or the United States Department of Agriculture (USDA).

ACKNOWLEDGMENTS

We thank Alexis Heinz for indispensable assistance with logics in the laboratory.

REFERENCES

Amrhein, V., Greenland, S., and McShane, B. (2019). Scientists rise up against statistical significance. *Nature* 567, 305–307 doi: 10.1038/d41586-019-00857-9

Andersen, R., Chapman, S. J., and Artz, R. R. (2013). Microbial communities in natural and disturbed peatlands: a review. *Soil Biol. Biochem*. 57, 979–994. doi: 10.1016/j.soilbio.2012.10.003

Barreto, C., and Lindo, Z. (2018). Drivers of decomposition and the detrital invertebrate community differ across a hummock-hollow microtopology in boreal peatlands. *Écoscience* 25, 39–48. doi: 10.1080/11956860.2017.1412282

Belyea, L. R. (1996). Separating the effects of litter quality and microenvironment on decomposition rates in a patterned peatland. *Oikos* 77, 529–539. doi: 10.2307/3545942

Berg, B., and McClaugherty, C. (2014). *Plant Litter: Decomposition, Humus Formation, Carbon Sequestration*. Berlin: Springer Verlag.

Børsheim, K. Y., Christensen, B. E., and Painter, T. J. (2001). Preservation of fish by embedment in *Sphagnum* moss, peat or holocellulose: experimental proof of the oxopolysaccharidic nature of the preservative substance and of its antimicrobial and tanning action. *Innov. Food Sci. Emerg.* 2, 63–74. doi: 10.1016/S1466-8564(00)00029-1

Bou Daher, F., and Braybrook, S. A. (2015). How to let go: pectin and plant cell adhesion. *Front. Plant Sci*. 6:523. doi: 10.3389/fpls.2015.00523

Bragazza, L., Siffi, C., Iacumin, P., and Gerdol, R. (2007). Mass loss and nutrient release during litter decay in peatland: the role of microbial adaptability to litter chemistry. *Soil Biol. Biochem*. 39, 257–267. doi: 10.1016/j.soilbio.2006.07.014

Carpita, N. C. (1984). Fractionation of hemicelluloses from maize cell walls with increasing concentrations of alkali. *Phytochemistry* 23, 1089–1093. doi: 10.1016/S0031-9422(00)82615-1

Chapman,. H. D., Morris, V. J., Selvendran, R. R., and O'Neill, M. A. (1987). Static and dynamic light-scattering studies of pectic polysaccharides from the middle lamellae and primary cell walls of cider apples. *Carbohyd. Res*. 165, 53–68. doi: 10.1016/0008-6215(87)80077-0

Cornwell, W. K., Cornelissen, J. H., Amatangelo, K., Dorrepaal, E., Eviner, V. T., Godoy, O., et al. (2008). Plant species traits are the predominant control on litter decomposition rates within biomes worldwide. *Ecol. Lett*. 11, 1065–1071. doi: 10.1111/j.1461-0248.2008.01219.x

Corteselli, E. M., Burtis, J. C., Heinz, A. K., and Yavitt, J. B. (2017). Leaf litter fuels methanogenesis throughout decomposition in a forested peatland. *Ecosystems* 20, 1217–1232. doi: 10.1007/s10021-016-0105-9

Del Giudice, R., and Lindo, Z. (2017). Short-term leaching dynamics of three peatland plant species reveals how shifts in plant communities may affect decomposition processes. *Geoderma* 285, 110–116. doi: 10.1016/j.geoderma.2016.09.028

Dettling, M. D., Yavitt, J. B., Cadillo-Quiroz, H., Sun, C., and Zinder, S. H. (2007). Soil–methanogen interactions in two peatlands (bog, fen) in Central New York State. *Geomicrobiol. J*. 24, 247–259. doi: 10.1080/01490450701456651

Dorrepaal, E., Cornelissen, J. H., Aerts, R., Wallen, B. O., and Van Logtestijn, R. S. (2005). Are growth forms consistent predictors of leaf litter quality and decomposability across peatlands along a latitudinal gradient? *J. Ecol*. 93, 817–828. doi: 10.1111/j.1365-2745.2005.01024.x

Dubois, M., Gilles, K. A., Hamilton, J. K., Rebers, P. A., and Smith, F. (1956). Colorimetric method for determination of sugars and related substances. *Anal. Chem*. 28, 350–356. doi: 10.1021/ac60111a017

Emilson, E. J., Carson, M. A., Yakimovich, K. M., Osterholz, H., Dittmar, T., Gunn, J. M., et al. (2018). Climate-driven shifts in sediment chemistry enhance methane production in northern lakes. *Nat. Commun*. 9:1801. doi: 10.1038/s41467-018-04236-2

Fanin, N., Fromin, N., and Bertrand, I. (2016). Functional breadth and home-field advantage generate functional differences among soil microbial decomposers. *Ecology* 97, 1023–1037. doi: 10.1890/15-1263

Franchini, A. G., Henneberger, R., Aeppli, M., and Zeyer, J. (2015). Methane dynamics in an alpine fen: a field-based study on methanogenic and methanotrophic microbial communities. *FEMS Microbiol. Ecol.* 91:fiu032. doi: 10.1093/femsec/fiu032

Frolking, S., Roulet, N. T., Moore, T. R., Richard, P. J., Lavoie, M., and Muller, S. D. (2001). Modeling northern peatland decomposition and peat accumulation. *Ecosystems* 4, 479–498. doi: 10.1007/s10021-001-0105-1

Gholz, H. L., Wedin, D. A., Smitherman, S. M., Harmon, M. E., and Parton, W. J. (2000). Long-term dynamics of pine and hardwood litter in contrasting environments: toward a global model of decomposition. *Glob. Change Biol.* 6, 751–765. doi: 10.1046/j.1365-2486.2000.00349.x

Glaser, P. H., Siegel, D. I., Chanton, J. P., Reeve, A. S., Rosenberry, D. O., Corbett, J. E., et al. (2016). Climatic drivers for multidecadal shifts in solute transport and methane production zones within a large peat basin. *Glob. Biogeochem. Cycles* 30, 1578–1598. doi: 10.1002/2016GB005397

Godin, A., McLaughlin, J. W., Webster, K. L., Packalen, M., and Basiliko, N. (2012). Methane and methanogen community dynamics across a boreal peatland nutrient gradient. *Soil Biol. Biochem.* 48, 96–105. doi: 10.1016/j.soilbio.2012.01.018

Jung, H. G., and Engels, F. M. (2002). Alfalfa stem tissues. *Crop Sci.* 42, 524–534. doi: 10.2135/cropsci2002.5240

Keiser, A. D., Strickland, M. S., Fierer, N., and Bradford, M. A. (2011). The effect of resource history on the functioning of soil microbial communities is maintained across time. *Biogeosciences* 8, 1477–1486. doi: 10.5194/bg-8-1477-2011

Kotsyurbenko, O. R., Glagolev, M. V., Merkel, A. Y., Sabrekov, A. F., and Terentieva, I. E. (2019). "Methanogenesis in soils, wetlands, and peat," in *Biogenesis of Hydrocarbons, Handbook of Hydrocarbon and Lipid Microbiology*, eds A. J. M. Stams and D. Z. Sousa (Cham: Springer), 1–18. doi: 10.1007/978-3-319-53114-4_9-1

Lang, S. I., Cornelissen, J. H., Klahn, T., Van Logtestijn, R. S., Broekman, R., Schweikert, W., et al. (2009). An experimental comparison of chemical traits and litter decomposition rates in a diverse range of subarctic bryophyte, lichen and vascular plant species. *J. Ecol.* 97, 886–900. doi: 10.1111/j.1365-2745.2009.01538.x

Lever, M. A., Heuer, V. B., Morono, Y., Masui, N., Schmidt, F., Alperin, M. J., et al. (2010). Acetogenesis in deep subseafloor sediments of the Juan de Fuca Ridge Flank: a synthesis of geochemical, thermodynamic, and gene-based evidence. *Geomicrobiol. J.* 27, 183–211. doi: 10.1080/01490450903456681

Machinet, G. E., Bertrand, I., Barrière, Y., Chabbert, B., and Recous, S. (2011). Impact of plant cell wall network on biodegradation in soil: role of lignin composition and phenolic acids in roots from 16 maize genotypes. *Soil Biol. Biochem.* 43, 1544–1552. doi: 10.1016/j.soilbio.2011.04.002

Makita, N., and Fujii, S. (2015). Tree species effects on microbial respiration from decomposing leaf and fine root litter. *Soil Biol. Biochem.* 88, 39–47. doi: 10.1016/j.soilbio.2015.05.005

McLaren, J. R., Buckeridge, K. M., van de Weg, M. J., Shaver, G. R., Schimel, J. P., and Gough, L. (2017). Shrub encroachment in Arctic tundra: Betula nana effects on above-and belowground litter decomposition. *Ecology* 98, 1361–1376. doi: 10.1002/ecy.1790

McLaughlin, J. W., and Webster, K. L. (2010). Alkalinity and acidity cycling and fluxes in an intermediate fen peatland in northern Ontario. *Biogeochemistry* 99, 143–155. doi: 10.1007/s10533-009-9398-5

McLeod, A. R., Newsham, K. K., and Fry, S. C. (2007). Elevated UV-B radiation modifies the extractability of carbohydrates from leaf litter of *Quercus robur*. *Soil Biol. Biochem.* 39, 116–126. doi: 10.1016/j.soilbio.2006.06.019

Melillo, J. M., Aber, J. D., and Muratore, J. F. (1982). Nitrogen and lignin control of hardwood leaf litter decomposition dynamics. *Ecology* 63, 621–626. doi: 10.2307/1936780

Min, K., Freeman, C., Kang, H., and Choi, S. U. (2015). The regulation by phenolic compounds of soil organic matter dynamics under a changing environment. *Biomed Res. Int.* 2015:825098. doi: 10.1155/2015/825098

Moore, T. R., Bubier, J. L., and Bledzki, L. (2007). Litter decomposition in temperate peatland ecosystems: the effect of substrate and site. *Ecosystems* 1, 949–963. doi: 10.1007/s10021-007-9064-5

Nakagawa, S., and Cuthill, I. C. (2007). Effect size, confidence interval and statistical significance: a practical guide for biologists. *Biol. Rev.* 82, 591–605. doi: 10.1111/j.1469-185X.2007.00027.x

Olson, J. S. (1963). Energy storage and the balance of producers and decomposers in ecological systems. *Ecology* 44, 322–331. doi: 10.2307/1932179

Pelloux, J., Rusterucci, C., and Mellerowicz, E. J. (2007). New insights into pectin methylesterase structure and function. *Trends Plant Sci.* 12, 267–277. doi: 10.1016/j.tplants.2007.04.001

Prescott, C. E. (2010). Litter decomposition: what controls it and how can we alter it to sequester more carbon in forest soils?. *Biogeochemistry* 101, 133–149. doi: 10.1007/s10533-010-9439-0

Preston, C. M., Nault, J. R., Trofymow, J. A., Smyth, C., and CIDET Working Group (2009). Chemical changes during 6 years of decomposition of 11 litters in some Canadian forest sites. Part 1. Elemental composition, tannins, phenolics, and proximate fractions. *Ecosystems* 12, 1053–1077. doi: 10.1007/s10021-009-9266-0

Reuter, H., Gensel, J., Elvert, M., and Zak, D. (2019). Preferential protein depolymerization as a preservation mechanism for vascular plant decomposing in *Sphagnum* peat. *Biogeosciences* 2019, 1–22. doi: 10.5194/bg-2019-176

Schädel, C., Blöchl, A., Richter, A., and Hoch, G. (2010). Quantification and monosaccharide composition of hemicelluloses from different plant functional types. *Plant Physiol. Biochem.* 48, 1–8. doi: 10.1016/j.plaphy.2009.09.008

Schwintzer, C. R. (1981). Vegetation and nutrient status of northern Michigan bogs and conifer swamps with a comparison to fens. *Can. J. Bot.* 59, 842–853. doi: 10.1139/b81-118

Schwintzer, C. R. (1984). Production, decomposition, and nitrogen dynamics of Myrica gale litter. *Plant Soil* 78, 245–258. doi: 10.1007/BF02277855

Siegel, D. I., and Glaser, P. H. (1987). Groundwater flow in a bog-fen complex, Lost River Peatland, northern Minnesota. *J. Ecol.* 75, 743–754. doi: 10.2307/2260203

Slack, N. G., Vitt, D. H., and Horton, D. G. (1980). Vegetation gradients of minerotrophically rich fens in western Alberta. *Can. J. Bot.* 58, 330–350. doi: 10.1139/b80-034

Smith, B. G., and Harris, P. J. (1999). The polysaccharide composition of Poales cell walls: Poaceae cell walls are not unique. *Biochem. Syst. Ecol.* 27, 33–53. doi: 10.1016/S0305-1978(98)00068-4

Soong, J. L., Parton, W. J., Calderon, F., Campbell, E. E., and Cotrufo, M. F. (2015). A new conceptual model on the fate and controls of fresh and pyrolized plant litter decomposition. *Biogeochemistry* 124, 27–44. doi: 10.1007/s10533-015-0079-2

Strack, M., Mwakanyamale, K., Fard, G. H., Bird, M., Bérubé, V., and Rochefort, L. (2017). Effect of plant functional type on methane dynamics in a restored minerotrophic peatland. *Plant Soil* 410, 231–246. doi: 10.1007/s11104-016-2999-6

Straková, P., Niemi, R. M., Freeman, C., Peltoniemi, K., Toberman, H., Heiskanen, I., et al. (2011). Litter type affects the activity of aerobic decomposers in a boreal peatland more than site nutrient and water table regimes. *Biogeosciences* 27, 2741–2755. doi: 10.5194/bg-8-2741-2011

Sun, C. L., Brauer, S. L., Cadillo Quiroz, H., Zinder, S. H., and Yavitt, J. B. (2012). Seasonal changes in methanogenesis and methanogenic community in three peatlands, New York State. *Front. Microbiol.* 3:81. doi: 10.3389/fmicb.2012.00081

Sundh, I., Nilsson, M., Granberg, G., and Svensson, B. H. (1994). Depth distribution of microbial production and oxidation of methane in northern boreal peatlands. *Microb. Ecol.* 27, 253–265. doi: 10.1007/BF00182409

Szumigalski, A. R., and Bayley, S. E. (1996). Decomposition along a bog to rich fen gradient in central Alberta, Canada. *Can. J. Bot.* 74, 573–581. doi: 10.1139/b96-073

Thormann, M. N. (2006). Diversity and function of fungi in peatlands: a carbon cycling perspective. *Can. J. Soil Sci.* 86, 281–293. doi: 10.4141/S05-082

Treat, C. C., Natali, S. M., Ernakovich, J., Iversen, C. M., Lupascu, M., McGuire, A. D., et al. (2015). A pan-Arctic synthesis of CH_4 and CO_2 production from anoxic soil incubations. *Glob. Change Biol.* 21, 2787–2803. doi: 10.1111/gcb.12875

Van Breemen, N. (1995). How *Sphagnum* bogs down other plants. *Trends Ecol. Evol.* 10, 270–275. doi: 10.1016/0169-5347(95)90007-1

Van Soest, P. J. (1994). *Nutritional Ecology of the Ruminant*. Ithaca, NY: Cornell University Press.

Waksman, S. A., and Reuszer, H. W. (1932). On the origin of the uronic acids in the humus of soil, peat, and composts. *Soil Sci.* 33:135. doi: 10.1097/00010694-193202000-00005

Ward, S. E., Orwin, K. H., Ostle, N. J., Briones, M. J., Thomson, B. C., Griffiths, R. I., et al. (2015). Vegetation exerts a greater control on litter decomposition than climate warming in peatlands. *Ecology* 96, 113–123. doi: 10.1890/14-0292.1

Wardle, D. A. (1993). Changes in the microbial biomass and metabolic quotient during leaf litter succession in some New Zealand forest and scrubland ecosystems. *Funct. Ecol.* 7, 346–355. doi: 10.2307/2390215

Webster, K. L., and McLaughlin, J. W. (2010). Importance of the water table in controlling dissolved carbon along a fen nutrient gradient. *Soil Sci. Soc. Am. J.* 74, 2254–2266. doi: 10.2136/sssaj2009.0111

Wickings, K., Grandy, A. S., Reed, S. C., and Cleveland, C. C. (2012). The origin of litter chemical complexity during decomposition. *Ecol. Lett*. 15, 1180–1188. doi: 10.1111/j.1461-0248.2012.01837.x

Williams, C. J., and Yavitt, J. B. (2003). Botanical composition of peat and degree of peat decomposition in three temperate peatlands. *Ecoscience* 10, 85–95. doi: 10.1080/11956860.2003.11682755

Witkamp, M. (1966). Decomposition of leaf litter in relation to environment, microflora, and microbial respiration. *Ecology* 47, 194–201. doi: 10.2307/1933765

Yavitt, J. B., Burtis, J. C., Smemo, K. A., and Welsch, M. (2018). Plot-scale spatial variability of methane, respiration, and net nitrogen mineralization in muck-soil wetlands across a land use gradient. *Geoderma* 315, 11–19. doi: 10.1016/j.geoderma.2017.11.038

Yavitt, J. B., and Williams, C. J. (2015). Conifer litter identity regulates anaerobic microbial activity in wetland soils via variation in leaf litter chemical composition. *Geoderma* 243, 141–148. doi: 10.1016/j.geoderma.2014.12.023

Yavitt, J. B., Williams, C. J., and Wieder, R. K. (1997). Production of methane and carbon dioxide in peatland ecosystems across North America: effects of temperature, aeration, and organic chemistry of peat. *Geomicrobiol. J.* 14, 299–316. doi: 10.1080/01490459709378054

Conflict of Interest: The authors declare that the research was conducted in the absence of any commercial or financial relationships that could be construed as a potential conflict of interest.

frontiers in Environmental Science

ORIGINAL RESEARCH
published: 27 November 2019
doi: 10.3389/fenvs.2019.00189

Sulfate Mobility in Fen Peat and Its Impact on the Release of Solutes

Lennart Gosch[1]*, *Heather Townsend*[2], *Matthias Kreuzburg*[3], *Manon Janssen*[1], *Fereidoun Rezanezhad*[4] and *Bernd Lennartz*[1]

[1] Faculty of Agricultural and Environmental Sciences, University of Rostock, Rostock, Germany, [2] Ecohydrology Research Group, Department of Earth and Environmental Sciences, University of Waterloo, Waterloo, ON, Canada, [3] Leibniz Institute for Baltic Sea Research (LG), Warnemünde, Germany, [4] Ecohydrology Research Group, Water Institute and Department of Earth and Environmental Sciences, University of Waterloo, Waterloo, ON, Canada

Sea-level rise coupled with land subsidence from wetland drainage exposes increasingly large areas of coastal peatlands to seawater intrusion. Seawater contains high concentrations of sulfate (SO_4^{2-}), which can alter the decomposition of organic matter thereby releasing organic and inorganic solutes from peat. In this study, a flow-through reactor system was used in order to examine the transport of SO_4^{2-} through peat as well as its effect on solute release. Moderately-decomposed fen peat samples received input solutions with SO_4^{2-} concentrations of 0, 100, 700, and 2,700 mg L^{-1}; sample effluent was analyzed for a variety of geochemical parameters including dissolved organic carbon (DOC), dissolved inorganic carbon (DIC) and total dissolved nitrogen (TDN) as well as the concentrations of major cations and anions. The input solution remained anoxic throughout the experiment; however, no signs of a pronounced SO_4^{2-} reduction were detected in the effluent. SO_4^{2-} transport in the fen peat resembled non-reactive bromide (Br^-) transport, indicating that in the absence of SO_4^{2-} reduction the anion may be considered a conservative tracer. However, slightly elevated concentrations of DOC and TDN, associated with raised SO_4^{2-} levels, suggest the minor desorption of organic acids through anion exchange. An increased solute release due to stimulated decomposition processes, including SO_4^{2-} reduction, was observed for samples with acetate as an additional marine carbon source included in their input solution. The solute release of peats with different degrees of decomposition differed greatly under SO_4^{2-}-enriched conditions where strongly-decomposed fen peat samples released the highest concentrations of DOC, DIC and TDN.

Keywords: fen peat, sulfate, solute transport, solute release, coastal zone

OPEN ACCESS

Edited by:
Laodong Guo,
University of Wisconsin–Milwaukee, United States

Reviewed by:
Dominik Zak,
Aarhus University, Denmark
John Crusius,
Alaska Science Center (United States Geological Survey), United States

***Correspondence:**
Lennart Gosch
lennart.gosch@uni-rostock.de

Specialty section:
This article was submitted to Biogeochemical Dynamics, a section of the journal Frontiers in Environmental Science

Received: *18 June 2019*
Accepted: *13 November 2019*
Published: *27 November 2019*

Citation:
Gosch L, Townsend H, Kreuzburg M, Janssen M, Rezanezhad F and Lennartz B (2019) Sulfate Mobility in Fen Peat and Its Impact on the Release of Solutes. Front. Environ. Sci. 7:189. doi: 10.3389/fenvs.2019.00189

INTRODUCTION

Over the millennia, large quantities of partly-decomposed organic matter have accumulated in waterlogged peatlands. The hydrological and biogeochemical conditions in a peatland determine whether it may serve as a sink or a source for carbon- and nitrogen-containing compounds. It is well known that the drainage of peatlands for agricultural purposes initiates the aerobic decomposition of organic matter in the top layer, resulting in the enhanced emission of greenhouse gases, including carbon dioxide (CO_2) and nitrous oxide (N_2O) (Kasimir-Klemedtsson et al., 1997) as well as a mobilization of dissolved organic matter (generally measured as dissolved organic carbon, DOC) and other nutrients such as ammonium (NH_4^+) (Zak and Gelbrecht, 2007). Hence, the drainage of

peatlands has ramifications in the exacerbation of global warming, land subsidence and nutrient loads for adjacent aquatic ecosystems.

Under anoxic conditions, the decomposition of organic matter is controlled by the presence of electron acceptors such as sulfate (SO_4^{2-}), an inorganic and highly mobile form of sulfur, which is used in the metabolism of sulfate-reducing bacteria (SRB). While SO_4^{2-} concentrations in terrestrial ecosystems are generally low, marine ecosystems are SO_4^{2-}-enriched as seawater contains approximately 2700 mg L^{-1} (∼29 mM, Algeo et al., 2015). Infiltration of seawater into peatlands can therefore drastically increase SO_4^{2-} concentrations, altering the biogeochemistry of the peat thereby implicating the mineralization of organic matter. Due to climate change and predicted sea level rise, sea water intrusion and the impact on the quality of groundwater resources will be relevant for larger areas of peatlands in the future (Sherif and Singh, 1999; Ardón et al., 2016).

However, when formerly drained peatlands are rewetted (i.e., the water level in the peatland is raised), increased SO_4^{2-} concentrations may aid climate protection by reducing emissions of the greenhouse gas methane (CH_4). The rewetting often results in water levels higher than in the initial state, as the land has subsided, which may result in an emission of a large quantity of CH_4 (Wen et al., 2018). When SO_4^{2-} is present, the SRB, although tending to be low-abundant even under favorable redox conditions, generally outcompete the methanogens in the peat and therefore impede the formation of CH_4 (Hausmann et al., 2016). Coastal peatlands are therefore considered well suited for rewetting projects associated with dyke removal (Koebsch et al., 2019), although under certain circumstances (e.g., abundance of suitable electron donors, Weston et al., 2011) methanogenesis and SO_4^{2-} reduction can occur at the same time (Oremland et al., 1982; Hahn et al., 2015).

While the impact of water salinity and SO_4^{2-} on greenhouse gas emissions in peatlands has aroused scientific interest, there are hardly any studies focusing on the mechanistic understanding of SO_4^{2-} mobility in peat and its impact on the release of solutes from peat. Solute release from peat is known to be affected by a wide range of environmental variables, with water table fluctuations and the associated change of redox conditions being the most prominent one (Borch et al., 2010). In particular, factors prompting the DOC release from peatlands have been studied previously, since DOC concentrations in surface water in Europe have increased in the last decades (Roulet and Moore, 2006), which is for example problematic for drinking water treatment (Ritson et al., 2014). Factors influencing DOC release from peat include ionic strength [and its proxy, electrical conductivity (EC)] and pH of the pore water. When EC increases and pH decreases, amounts of DOC released typically decline as a result of decreased charge density, limiting the solubility of the DOC (Münch et al., 2002; Clark et al., 2011; Ardón et al., 2016; Tiemeyer et al., 2017). Increases in EC have also been observed to impact other geochemical processes in peat, including the desorption of NH_4^+ by salt ions (Ardón et al., 2013), an increase of hydraulic conductivity due to a pore dilation (Ours et al., 1997) and a decrease in plant uptake of nutrients as a result of salt stress (Hanin et al., 2016). The explicit impact of changing SO_4^{2-} concentrations on solute release has been studied mostly for moderately increased concentrations simulating atmospheric deposits (Blodau et al., 2007; up to 10 mg L^{-1}), discharge of river water to a wetland (Lamers et al., 1998; up to 400 mg L^{-1}) or intrusion of highly diluted seawater into a wetland (Ardón et al., 2016; up to 300 mg L^{-1}). In an extensive mesocosm experiment, Lamers et al. (1998) observed an increase in alkalinity due to the consumption of hydrogen ions during SO_4^{2-} reduction, a reduced uptake of nutrients, such as potassium (K^+), due to the toxicity of sulfide (HS^-) and an increased release of NH_4^+ due to the increase of organic matter decomposition. They also observed that increased SO_4^{2-} concentrations can turn peat into a source for phosphate, similar as observed for other aquatic sediments (Caraco et al., 1989). The underlying process is the formation of iron sulfide, which reduces the availability of iron (Fe) as binding partner for P both in the reduced form of vivianite or as oxidized Fe(III)-P binding forms (Zak et al., 2010). However, the sulfur cycle in peatlands is complex as sulfur can occur in various organic and inorganic forms and can be recycled multiple times (i.e., reduced and reoxidized) as stated for bogs (Wieder and Lang, 1988; Blodau et al., 2007), forested wetlands (Mandernack et al., 2000) and salt marshes (Gardner, 1990). To the author's knowledge, there has been no comprehensive study on SO_4^{2-} dynamics and mobility within fen peat with respect to release of solutes from peat induced by SO_4^{2-}-related processes. The main objective of this study was to gain an improved understanding of the processes determining the mobility of SO_4^{2-} of varying concentrations in fen peat samples and their short-term impact on the solute release from the peat.

MATERIALS AND METHODS

Field Sampling and Peat Properties

Fifteen undisturbed core samples of moderately-decomposed reed-sedge fen peat (referred to as "MD-Peat") were collected in May 2018 horizontally at a depth of 50 cm below surface from a drained fen in northwestern Germany ("Pölchow", 54°00′20.3″N, 12°06′58.8″E). The acrylic glass sampling tubes (Ø = 4.2 cm, L = 10 cm, V = 139 cm^3) were incorporated into a sharpened shuttle corer which was pushed manually into the peat. The groundwater level was 75 cm below surface so that the taken peat samples were wet but not completely water-saturated. The peatland has not been affected by Baltic seawater intrusion [SO_4^{2-} concentrations in the groundwater accumulated in the profile pit were low (3.7 mg L^{-1})]. For comparison reasons additional samples ($n = 3$) of two fen peats with a different degree of decomposition were collected: firstly a degraded highly-decomposed peat (referred to as "HD-Peat") taken horizontally from the dried top soil in Pölchow in a depth of 20 cm, secondly a SO_4^{2-}-affected and water-saturated slightly-decomposed peat (referred to as "SD-Peat") taken vertically in a depth of 10 cm in the shallow water of the Baltic Sea adjacent to the coastal fen "Hütelmoor" (54°13′19.38″N, 12°10′7.02″E). The coastline on the latter site has transformed over time to constantly expose parts of the peat layer to seawater (Kreuzburg et al., 2018). Additional disturbed samples of each peat were

TABLE 1 | Basic properties of peat material.

Parameter	SD-Peat	MD-Peat	HD-Peat
Sampling location	Beach of the Baltic Sea in front of the Hütelmoor	Grassland in Pölchow	Grassland in Pölchow
Sampling depth (cm bsf)	10	50	20
Number of samples	3	15	3
Peat type	Sea-exposed, slightly-decomposed reed-sedge fen peat	Moderately-decomposed reed-sedge fen peat	Degraded, highly-decomposed fen peat
Degree of decomposition (von Post)	H4-5	H6	H9
Organic matter content (% dwt)	83.7 ($n = 2$)	83.3 ($n = 2$)	39.8 ($n = 2$)
C_{org} (% dwt)	41.6	39.9	22.0
C_{inorg} (% dwt)	0.05	0.45	0.11
N (% dwt)	1.6	3.1	2.0
S (% dwt)	3.4	0.5	0.3
Fe (mg kg^{-1})	1173	22730	61600
ρ_b (g cm^{-3})	0.17 ($n = 3$)	0.19 ($n = 15$)	0.49 ($n = 3$)
Φ (–)	0.90 ($n = 3$)	0.89 ($n = 15$)	0.78 ($n = 3$)

Bulk density (ρ_b) and porosity (Φ) of the samples were determined for each of the undisturbed peat samples after the experiment, all other parameters were determined on the basis of untreated, disturbed peat material. In case of average values, the number of replicates (n) is indicated in parentheses.

collected to determine the organic matter content as well as the solid-phase total carbon, nitrogen and sulfur (C/N/S) contents. After collection, all peat samples were refrigerated and transported to the Ecohydrology Research Group at the University of Waterloo (Canada) for the laboratory experiments. The basic physicochemical properties of the peat material used in this study are shown in **Table 1**. The C/N/S contents were measured for homogenized and freeze-dried samples on a CHNS Carbo Erba analyzer (method detection limit: 0.1% dwt) without any pre-treatment of the freeze-dried samples. The Fe content was determined by Inductively-Coupled Plasma Optical Emission Spectrometry (ICP-OES) after an aqua regia digestion according to HFA (2014). The bulk density (ρ_b) was determined gravimetrically based on the sample volume and the oven-dried (3 days at 80°C) sample mass. Subsequently, the peat samples were ignited at 550°C to determine the loss on ignition (LOI) as a proxy for the organic matter content (DIN EN 15935, 2012), which was used to calculate the particle density (ρ_s) of the peat samples with standard values for organic (1.4 g cm^{-3}) and mineral (2.65 g cm^{-3}) components [$\rho_s = (1.4 \times LOI + 2.65 \times (100–LOI))/100$]. The total porosity was then calculated from bulk and particle densities ($\Phi = 1 - \rho_b / \rho_s$).

Flow-Through Reactor Experiment

A one-month SO_4^{2-} displacement experiment was carried out using a flow-through reactor (FTR) set-up (**Figure 1**). These reactors are designed to measure biogeochemical reaction rates on undisturbed soils or sediments and yield kinetic parameters and information on reaction pathways that can be extrapolated to natural conditions (Pallud et al., 2007). They have been used to study solute transport in peat (Kleimeier et al., 2017) as well as SO_4^{2-} and nitrate (NO_3^-) reduction in sediments (Pallud and Van Cappellen, 2006; Stam et al., 2010; Laverman et al., 2012). In addition to information on SO_4^{2-} transport, the 1-month monitoring of this experiment also provided insight into the short-term effects of increased SO_4^{2-} concentrations on the release of solutes. The FTRs (21 reactors in total) consisted of the peat core contained within an acrylic glass tube attached to two PVC plate end-caps with an opening for tubing connection. Between each plate end-cap and the soil column an O-ring, a glass fiber filter (pore size 1 µm) and a hydrophilic polypropylene membrane filter (pore size 0.2 µm) were inserted to avoid leakage, uniformize inflow and reduce the filtration effort for the effluent sampling. The bottom end-cap of the FTRs was connected to a peristaltic pump (Gilson MINIPULSE® 3) and served as an inflow channel while the top end-cap connected to the outflow channel allowed the effluent to collect in polyethylene sampling bottles (125 mL). Inflow and outflow channel consisted of viton tubing (ID = 1.59 mm). During the entire experiment duration of 1 month, the pump rate (PR) was set to 4 mL h^{-1} (corresponding to a Darcy flux of 7 cm d^{-1}) with slight differences between the pump channels (range of 3.4 to 4.5 mL h^{-1}).

Triplicates of MD-peat samples were assigned to different SO_4^{2-} treatments corresponding to SO_4^{2-} milieus in terrestrial (0 and 100 mg L^{-1}), brackish (700 mg L^{-1}) and marine (2,700 mg L^{-1}) ecosystems (see **Table 2**). The latter treatment was also applied to the SD-peat and HD-peat samples. Furthermore, another treatment of the MD-peat containing 2,700 mg SO_4^{2-} L^{-1} and 590 mg acetate (CH_3COO^-) L^{-1} (concentration inspired by Schmaljohann, 1996) simulating a potential input of marine dissolved organic matter (DOM) was added to guarantee an excess of electron donors, as the peat consists of rather persistent plant residues. Acetate is generally considered as the most relevant electron donor for anaerobic decomposition of organic matter by SRB in the marine environment (Boschker et al., 2001). In the following, the different treatments are referred to with the labels shown in **Table 2** (e.g., SULF0), the addition of acetate to a treatment is indicated within the label with a "+A."

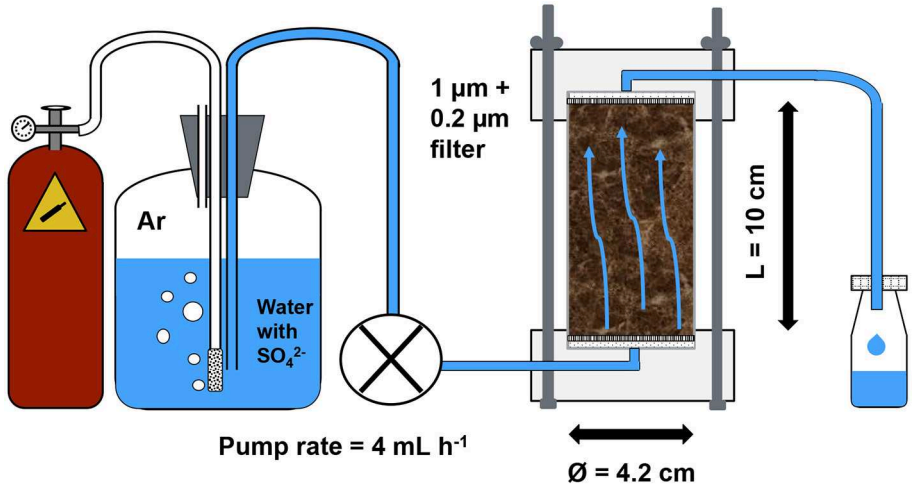

FIGURE 1 | Schematic diagram of the experimental set-up. The reactors were placed in an environmental chamber at constant temperature of 15°C. The sulfate-enriched water was depleted in oxygen via sparging with argon (Ar), flowed with a pump rate of 4 mL h^{-1} through the peat samples and was subsequently collected and sampled.

The artificial brackish input solution was prepared by diluting the quantitatively most important seawater salts according to Kester et al. (1967) (NaCl, KCl, $MgCl_2 \cdot 6H_2O$, $CaCl_2 \cdot 2H_2O$, $NaHCO_3$) in 20-fold dilution in ultra-pure water (Milli-Q) and then adding Na_2SO_4 to adjust the different SO_4^{2-} treatments and $NaCH_3COO$ for the treatment SULF2700+A. The EC of the five different input solutions was between 2.5 and 6.6 mS cm^{-1} (measured with a Horiba LAQUA B-213 Twin EC meter), representing seawater diluted by freshwater in the mixing zone (observed in the Hütelmoor field site, but see also e.g., Jørgensen et al., 2008). To induce the development of anoxic conditions the input solutions to the FTRs were continuously sparged with argon gas reducing oxygen concentrations to levels between 0.2 and 0.9 mg L^{-1} (measured with a Thermo Scientific Orion 5 Star multifunction meter). The continuous sparging with argon also led to an increase in the pH of the input solution (up to 8.8, measured with a Horiba LAQUA B-213 Twin pH meter) due to degassing of carbon dioxide, which was adjusted to values between 7 and 7.5 through addition of minor amount of hydrochlorid acid. However, as the pH of seawater (~8.1) is generally higher than freshwater, variations of pH may also occur under natural field conditions. As the SO_4^{2-} reduction rate is sensitive to the temperature (Stam et al., 2010), the FTR experiment was conducted in an environmental chamber (Percival Scientific CTH-118) at a constant temperature of 15°C representing common summer temperatures in peatland groundwater at the Hütelmoor field site (M. Ibenthal, University of Rostock, personal communication). The placement of the experimental set-up in the chamber also ensured dark conditions to prevent algae growth in the acrylic glass tubes.

Prior to the SO_4^{2-} treatments, a control solution (SULF0) containing 0 mg SO_4^{2-} L^{-1} was pumped (4 mL h^{-1}) into the FTRs for 3 days to purge the cores of gas bubbles that may block water flow as well as to flush out the pre-existing SO_4^{2-} and equilibrate the peat cores with the salt solution. Only for the marine SD-peat a solution with 700 mg SO_4^{2-} L^{-1} was used to maintain the natural SO_4^{2-} milieu in those three samples. The outflow of the first and the last 50 mL of the flushing phase was analyzed to determine the initial and stabilized chemical concentrations. During the SO_4^{2-} treatment phase (1 month), the outflow samples were collected every 24 h for the first 3 days and afterwards every 48 to 72 h. During the first 5 days of the SO_4^{2-} treatment, an additional bromide (Br^-) concentration of 100 mg Br^- L^{-1} was added into the input solutions in form of 149 mg KBr L^{-1} as a step input to obtain a non-reactive tracer breakthrough curve (BTC). During the Br^- injection outflow water samples were collected every 2 h on the first day, every 4 h on the second day, every 8 h on the third day, every 12 h on the fourth day and every 24 h on the fifth day and the samples were analyzed for Br^- concentration with ion chromatography (see below).

Pore Water Geochemistry Analyses

During the SO_4^{2-} treatments, water samples were collected from the outflow of the FTRs and were sub-sampled into separate vials. One milliliter of pore water was refiltered (to protect the measurement device) through a 0.2 µm membrane filter (Thermo Scientific Polysulfone filter) for analysis of major anions including Cl^-, NO_3^- and SO_4^{2-} using ion chromatography (IC, Dionex ICS-5000 with a capillary IonPac® AS18 column). A volume of 7 ml of pore water sample was acidified with 3 drops of 1M HCl and was analyzed for DOC and total dissolved nitrogen (TDN) using the non-purgeable organic carbon method on a total organic carbon analyzer (Shimadzu TOC-LCPH/CPN). Another volume of 7 mL pore water sample was subsampled for concentrations of dissolved inorganic carbon (DIC) that was measured using the same TOC analyzer. For the SULF2700+A treatment, an additional 1 mL sample was treated with 20 µL of a 500 ppm CrO_4^{2-} solution and analyzed for organic acids

TABLE 2 | Overview of the different applied SO_4^{2-} concentrations and associated number of peat samples.

Label of treatment	Simulated SO_4^{2-} milieu	SO_4^{2-} (mg L^{-1}) and (mmol L^{-1})	CH_3COO^- (mg L^{-1}) and (mmol L^{-1})	EC (mS cm^{-1})	Number of samples of		
					SD-Peat	MD-Peat	HD-Peat
SULF0	Control	0 *0.0*	0 *0.0*	2.5		3	
SULF100	Fresh water	100 *1.0*	0 *0.0*	2.6		3	
SULF700	Brackish water	700 *7.3*	0 *0.0*	3.6		3	
SULF2700	Ocean water	2700 *28.1*	0 *0.0*	6.3	3	3	3
SULF2700+A	Ocean water with marine DOM in form of acetate (A)	2700 *28.1*	590 *10.0*	6.6		3	

The number in the label of the treatments refers to the SO_4^{2-} concentration (mg L^{-1}) and "+A" indicates the additional addition of acetate (CH_3COO^-) in form of sodium acetate.

using IC to assess acetate concentrations (method detection limit: 0.017 mg L^{-1}) and subtract them from the measured DOC concentrations to get the "acetate-free" DOC release, accepting inaccuracies due to a potential acetogenesis in the peat. For one FTR per treatment, 10 mL of the water samples were filtered through a 0.45 µm membrane filter (Thermo Scientific Polysulfone filter) and were acidified with 2% ultrapure HNO_3 for analysis of major cations and trace metals including Fe and manganese (Mn) using Inductively-Coupled Plasma Optical Emission Spectrometry (Thermo iCAP 6200 Duo ICP-OES). Once or twice a week a volume of 1.5 mL was collected into vials containing 50 µL of a 5% zinc acetate solution and the concentration of HS^- was measured colorimetrically according to Cline (1969) and using an UV-Visible spectrophotometer (Thermo Scientific Evolution 260 Bio) measuring the absorbance at 670 nm.

Modeling of Breakthrough Curves

For the evaluation of the BTCs the software "STANMOD" (available for download from www.pc-progress.com) with the incorporated model CTXFIT (Toride et al., 1999) was used to determine solute transport parameters by fitting a modeled BTC to the measured data with a least-square fitting procedure. As previous studies have shown that peat acts as a dual porosity medium (e.g., Rezanezhad et al., 2012, 2016), a physical non-equilibrium model was used. The mobile-immobile model (MIM) solves the convection-dispersion equation for a mobile pore region, which exchanges solutes via diffusion with an immobile pore region. The dispersion coefficient D (cm^2 h^{-1}) and the two dimensionless parameters β (equivalent to the mobile water content for non-sorbing solutes) and ω (mass transfer coefficient) served as calibration parameters. The retardation factor R was set to 1 (meaning no adsorption occurs), as a pronounced anion adsorption to organic compounds is generally only expected under acidic conditions (Ottow, 2011) and high organic matter contents adversely affect SO_4^{2-} adsorption (Johnson and Todd, 1983). The average pore water velocity v (cm h^{-1}) was also set to a fixed calculated value [$v = PR/(\text{sample cross section} \times \Phi)$].

RESULTS AND DISCUSSION

Sulfate Transport

The SO_4^{2-} BTCs for the different treatments showed slightly different shapes and reached a similar relative concentration (C/C_0) after approximately three pore volumes, as shown in **Figure 2A**. However, the differences in their shape are not due to differences in the SO_4^{2-} input concentration, they are instead a result of differences in the soil pore distribution for the individual peat samples. This effect is verified by non-reactive Br^- BTCs (which were always performed for the same Br^- concentration) which show a very similar shape to the SO_4^{2-} BTCs, as exemplified in **Figure 2B** for a breakthrough of 100 mg Br^- L^{-1} and 100 mg SO_4^{2-} L^{-1}. These results suggest that no SO_4^{2-} reduction occurred and SO_4^{2-} behaved as a conservative anion (such as Br^-) during solute transport in the studied fen peat samples. The Br^- and SO_4^{2-} BTCs for all tested peats (**Figure 2C**) showed an early breakthrough characterized by a $C/C_0 > 0.5$ at one pore volume (Rezanezhad et al., 2016). This is indicative of non-equilibrium flow, meaning that the MIM serves as an appropriate simulation model in this scenario. The obtained solute transport parameters for the different peats contrasted for Br^- and SO_4^{2-} (**Table 3**) are similar and in the same range as in comparable studies on fen peat (Kleimeier et al., 2017; Liu et al., 2017; McCarter et al., 2018). Generally, the parameters D, β and ω are considered soil sample-specific and should not depend on the applied solute, which also was supported in this study with Wilcoxon signed-rank tests ($\alpha = 0.05$), that did not reveal any significant differences between Br^- and SO_4^{2-} parameters. Yet, the variations between the parameters of the different peats were also minor suggesting that the effect of degree of decomposition and organic matter content on the shape of the BTC is less pronounced than what has been shown in previous studies (Liu et al., 2017).

SO_4^{2-} and sodium (Na^+) concentrations in the outflow of the peat samples reached the input concentration after 5 days for SO_4^{2-} and 10 days for Na^+ and remained stable throughout the experiment. Only during the final phase of the experiment a slight difference in SO_4^{2-} concentration was observed between the

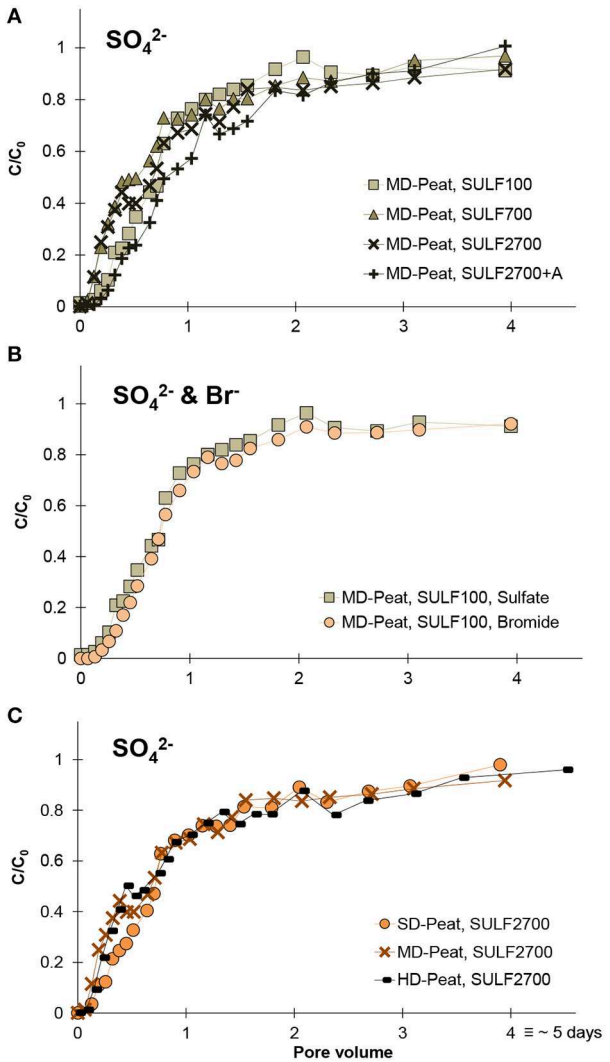

FIGURE 2 | Average ($n = 3$) breakthrough curves for **(A)** all applied SO_4^{2-} concentrations for the moderately-decomposed peat, **(B)** SO_4^{2-} and Br^- for the treatment SULF100 for the moderately-decomposed peat and **(C)** SO_4^{2-} for the treatment SULF2700 for slightly, moderately, and highly-decomposed peat.

TABLE 3 | Average solute transport parameters (± standard deviation) (v = average pore water velocity, D = dispersion coefficient, β = mobile water content, ω = exchange coefficient between mobile and immobile regions) determined with CTXFIT for the slightly, moderately and highly-decomposed peat for SO_4^{2-} and Br^- breakthrough.

	Parameter	SD-Peat	MD-Peat	HD-Peat
Br^-	v (cm h^{-1}) (fixed)	0.32	0.32	0.37
	D (cm^2 h^{-1})	1.17 ± 1.72	0.66 ± 0.43	1.32 ± 0.46
	λ (cm)	3.66 ± 5.36	2.06 ± 1.35	3.56 ± 1.25
	β (–)	0.65 ± 0.14	0.57 ± 0.22	0.62 ± 0.22
	Θ_{mobile} (cm^3 cm^{-3})	0.58 ± 0.12	0.51 ± 0.20	0.49 ± 0.17
	ω (–)	0.99 ± 0.61	1.41 ± 2.22	0.38 ± 0.45
	α (d^{-1})	0.69 ± 0.42	0.98 ± 1.54	0.26 ± 0.31
SO_4^{2-}	v (cm h^{-1}) (fixed)	0.32	0.32	0.37
	D (cm^2 h^{-1})	0.99 ± 1.32	0.93 ± 0.70	0.91 ± 1.01
	λ (cm)	3.10 ± 4.13	2.90 ± 2.20	2.45 ± 2.73
	β (–)	0.60 ± 0.10	0.54 ± 0.22	0.35 ± 0.09
	Θ_{mobile} (cm^3 cm^{-3})	0.54 ± 0.09	0.48 ± 0.19	0.27 ± 0.07
	ω (–)	0.70 ± 0.36	1.06 ± 1.09	0.89 ± 0.45
	α (d^{-1})	0.49 ± 0.25	0.74 ± 0.75	0.62 ± 0.31

For a better comparability with other studies the parameters λ = dispersivity, θ_{mobile} = mobile water content and α = exchange rate coefficient were calculated from the fitted parameters [$\lambda = D / v$; $\theta_{mobile} = \beta \times \Phi$; $\alpha = \omega \times q / L$ with q as the Darcy flux (cm h^{-1})].

input and output concentrations of the SULF2700+A treatment implying that SO_4^{2-} reduction occurred only in the latter case. This is consistent with the results of the measurement of HS^-, which was only detected in higher concentrations (up to 2.4 mg L^{-1}, other treatments of MD-peat: 0.03 to 0.13 mg L^{-1}) for the SULF2700+A treatment in the later phase of the experiment—although a non-detection of HS^- can also be related to reactions of HS^- with other compounds such as ferrous iron (Fe^{2+}) (see effect of acetate). The SD- and HD-peat samples produced HS^- concentrations between 0.06 and 0.2 mg L^{-1} with only a slight increase in effluent concentration occurring over time, indicating a very weak background SO_4^{2-} reduction. Results from all treatments imply that more SO_4^{2-} reduction could have been detected if the experiment was run for a longer duration. For the Fe-rich peat samples, MD-peat and HD-peat, the delayed stimulation of SO_4^{2-} reduction can be attributed to an initial period of Fe(III) reduction. The predominance of Fe(III) reduction over SO_4^{2-} reduction has been observed by Küsel et al. (2008), who found that in an upper peat horizon in a lowland fen with a similar Fe content (33 g kg^{-1}), the Fe(III) reduction made up 72% of the anaerobic organic carbon mineralization. Conversely, for the SO_4^{2-}-affected SD-peat with lower Fe content, it can be postulated that the microbially available carbon pool was depleted due to previous pronounced SO_4^{2-} reduction occurring under field conditions.

Solute Release

Initial Flushing

Containing 40% organic carbon and 3% nitrogen (**Table 1**), the MD-peat represents a potential source for nutrients. During the equilibration period with SO_4^{2-}-free water (3 days = 2.3 PV), the substances which had accumulated in the pore water in the peat were flushed and the concentrations of DOC, DIC and TDN decreased, on average, from 9 to 4 mg DOC L^{-1}, from 16 to 3 mg DIC L^{-1} and from 0.7 to 0.4 mg TDN L^{-1}. The initial values measured for DOC are lower than in previous studies using flow-through experiments with peat [32 mg DOC L^{-1} in Gosch et al. (2018), 11 mg DOC L^{-1} in Tiemeyer et al. (2017)], which can be explained by a larger sample volume of 50 mL in this study causing a dilution of the peak concentration as well as a sample filtration using 0.2 µm filters rather than the commonly used 0.45 µm filters. However, in the cases of this experiment as well as the aforementioned previous studies, the DOC concentrations stabilized in a range of 30 to 40% of the initial concentration. Field concentrations of DOC and TDN

from the sampling site were measured to be 16 mg DOC L^{-1} and 3.6 mg TDN L^{-1}. The apparent discrepancy between the field values and laboratory column experiments has already been observed in other studies (Stutter et al., 2007; Tiemeyer et al., 2017), and is generally explained by longer residence times and limited dilution in the field. The initial values for the HD-peat were higher than for the MD-peat with a decrease from 13 to 6 mg DOC L^{-1}, 17 to 6 DIC mg L^{-1} and 6.6 to 0.5 mg TDN L^{-1}. Formerly drained and degraded peat is known to release more solutes than less decomposed peat, due to the formation of more mobile compounds through aerobic mineralization (Zak et al., 2010). Therefore for rewetting purposes the degraded top soil of formerly drained peatlands is sometimes removed to reduce the leaching of nutrients and emission of greenhouse gases (Zak et al., 2018). In this study, the initial release of 22 mg NO_3^- L^{-1} from the HD-peat was 440 times higher than that of 0.05 mg NO_3^- L^{-1} release occurring from the underlying MD-peat. For the marine SD-peat, which was initially flushed with a 700 mg L^{-1} SO_4^{2-} solution, the concentrations changed from 28 to 25 mg DOC L^{-1}, 12 to 1 mg DIC L^{-1} and 3 to 1 mg TDN L^{-1}, and no NO_3^- was detected in the effluent. The relatively lower decrease in DOC concentrations observed for the MD-peat sample group might be related to the effects of changes in EC wherein the antecedent EC from the marine field conditions was closer to the artificial seawater than in the terrestrial peat.

Effect of Sulfate Concentration

During the SO_4^{2-} application in the FTRs, the solute release evolved differently for the various SO_4^{2-} treatments of the MD-peat (**Figures 3A–C**). For most of the samples DOC and TDN concentrations decreased continuously. However, the higher the SO_4^{2-} concentration in the input solution the lower the average slope of the linear trend for DOC and the higher the average DOC concentration at which the values seemed to stabilize (for SULF0 and SULF100 ∼ 2 mg L^{-1}, for SULF700 ∼3 mg L^{-1} and for SULF2700 ∼5 mg L^{-1}). These results imply a positive correlation between EC and DOC and do not confirm observations by previous studies on DOC fluctuations, who observed a negative correlation between EC and DOC release (Münch et al., 2002; Clark et al., 2011; Tiemeyer et al., 2017). For example, in Tiemeyer et al. (2017) an increase in EC from ∼100 to 1,000 μS cm^{-1} caused a decrease of DOC from ∼10 to 1 mg DOC L^{-1}. However, the results in this study are consistent with a previous study by Gosch et al. (2018), who observed a positive relation between EC and DOC for peat material from the same field site from which samples were collected for this study. The non-validity of the negative correlation between EC and DOC relation for the MD-peat might be attributed to the peat (pore water) chemistry (see effect of peat decomposition degree). The existence of interfering impact factors is also indicated by contradicting effects comparing laboratory and field data (Tiemeyer et al., 2017) or surface water and pore water geochemistry (Knorr, 2013).

This result also does not confirm previous findings by Ardón et al. (2016), who observed a decreasing DOC release with higher SO_4^{2-} concentrations (range of 100 to 300 mg SO_4^{2-} L^{-1}). Ardón et al. (2016) concluded that the consumption of DOC via SO_4^{2-} reduction was responsible for this decline. However, peat samples undergoing the SULF0, SULF100, SULF700, and SULF2700 treatment exhibited no pronounced SO_4^{2-} reduction, hence Ardón et al. (2016) conclusion cannot be considered as the cause for the observed differences in DOC/DIC/TDN between the treatments. Instead, minor differences observed in DOC release from the different SO_4^{2-} treatments may be attributed to anion exchange of DOM anions by SO_4^{2-} (Brouns et al., 2014). An increased dispersion of organic matter caused by a replacement of calcium (Ca^{2+}) by Na^+ (e.g., Edelstein et al., 2010) is considered unlikely as increased Ca^{2+} concentrations were observed in effluent immediately after the start of the SO_4^{2-} treatments (see segment about cation-related processes below). In contrast, DOC release in the different treatments differed more toward the end of the experiment.

The release of TDN over time resembled the release of DOC, which is reflected by a correlation coefficient calculated between 0.5 and 0.9, indicating a strong relationship between these two parameters. This result suggests that the majority of the nitrogen released derived from DOM rather than from NH_4^+. This is consistent with observations made in a shrub-dominated peatland by Wang et al. (2016) who found that 68% of nitrogen compounds released from peat monoliths were dissolved organic nitrogen (DON), while NH_4^+ and NO_3^-/ NO_2^- made up only 8 and 24%, respectively. In this study, NO_3^- (method detection limit: 0.05 mg L^{-1}) was detected only irregularly and in a low concentration between 0 to 0.13 mg L^{-1} in the effluent of MD-peat samples.

The release of DIC as an indicator for decomposition of organic matter showed less treatment-dependent tendencies than DOC and TDN. The SULF0, SULF100, and SULF700 treatments caused similar releases of DIC. Only peat samples treated with SULF2700 led to slightly higher DIC concentrations. However, DIC concentrations in the effluent of all samples first decreased before stabilizing at values between 0 and 1 mg L^{-1}. This supports the assumption that none of the SO_4^{2-} concentrations led to a pronounced SO_4^{2-} reduction in the time frame of this experiment. As the decrease also occurred for the SULF0 treatment, it can be assumed that the decrease is the continuation of the initial leaching of DIC.

Increased Na^+ concentrations from the input solution resulted in cation exchange leading to variable increases in different cation concentrations throughout the experiment (data not shown). For the MD-peat, the concentrations of Ca^{2+} and K^+ increased shortly after the treatment commenced with the highest Ca^{2+}/K^+ peak occurring in samples treated with the greatest Na^+ concentrations (SULF2700 and SULF2700+A) and subsequently decreased toward the value of the input solution. It stands to reason that Ca^{2+} and K^+ were exchanged by Na^+, although Ca^{2+} is generally bound more strongly to the peat than Na^+ as a result of its bivalence (Succow and Joosten, 2001). Magnesium (Mg^{2+}) concentrations increased very slowly over time and had not reached the input concentration value after 31 days, indicating that the displacement of other cations by Mg^{2+} took longer than the experimental duration. Total dissolved manganese (TDMn) (showing a peak right after the start of the treatment and then stabilizing at a

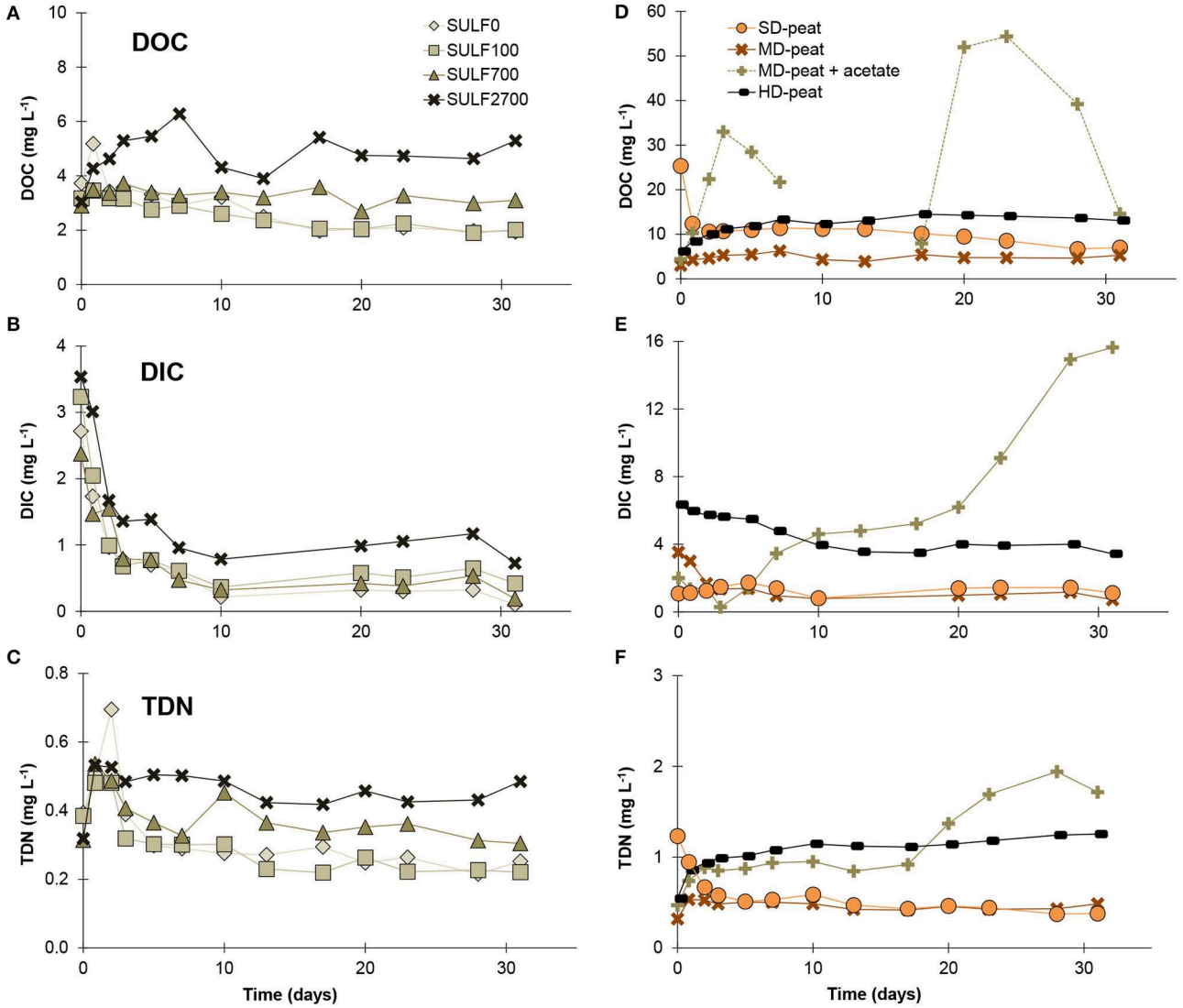

FIGURE 3 | Average concentrations ($n = 3$) for DOC, DIC, and TDN in the effluent of the flow-through reactors during the SO_4^{2-} applications **(A–C)** for the different SO_4^{2-} treatments and **(D–F)** for the different degrees of decomposition for the SULF2700 treatment and for the MD-peat for the SULF2700+A treatment. Note the scaling differences.

value between 0.12 and 0.28 mg L^{-1}) and total dissolved aluminum (TDAl) (stable value, but graduated from SULF0 with 0.01 mg L^{-1} to SULF2700+A with 0.05 mg L^{-1}) concentrations were lowest for the SULF0 treatment and highest for the SULF2700+A treatment suggesting that, for the corresponding ions (Mn^{2+}, Al^{3+}), the Na^{+} concentrations determined the release of these solutes. However, the evaluation is less clear for Fe and Mn as they may potentially be involved in the anaerobic decomposition processes and are present in different oxidation states that ICP measurements cannot distinguish. Increased concentrations of total dissolved iron (TDFe) were observed in all treatments compared to SULF0. Although, the order of magnitude of the measured peaks varied greatly (between 0.8 and 17 mg L^{-1}) and did not correlate with the SO_4^{2-} treatments.

Effect of Acetate

In contrast to the SO_4^{2-}-only treatments, a pronounced increase of DIC release accompanied by an increase in HS^{-} was observed for the acetate-enriched SULF2700+A treatment (**Figure 4**), providing evidence for SO_4^{2-} reduction (with hydrogen carbonate and sulfide as end-products). The duration of the experiment covered only the initial phase of SO_4^{2-} reduction as the concentrations of HS^{-} and DIC were still increasing after 31 days. A pronounced SO_4^{2-} reduction appeared to begin after ∼ 17 days (= ∼ 15 pore volumes). This time period represents a lag time during which redox conditions favorable for SO_4^{2-} reduction established in the samples. The SRB are generally outcompeted by microorganisms active at higher redox potentials that get energy via aerobic respiration, denitrification or Fe(III) and Mn(IV) reduction. As major HS^{-}

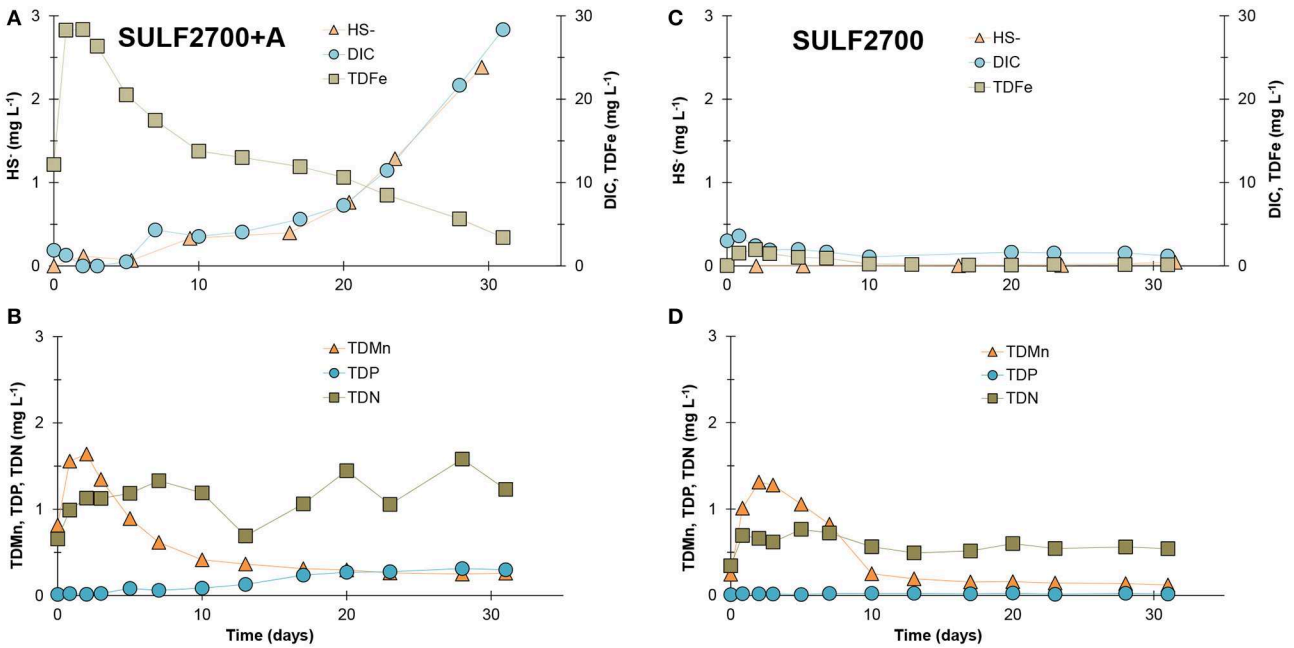

FIGURE 4 | Release of HS^-, DIC, and TDFe as well as TDMn, total dissolved phosphorus (TDP) and TDN measured in the effluent of the flow-through reactor from an individual peat sample during **(A,B)** SULF2700+A and **(C,D)** SULF2700 treatment.

concentrations and DIC increase were only observed in acetate addition treatment (SULF2700+A), it can be assumed that the peat in this study did not represent a suitable carbon source for the SRB under the prevailing laboratory conditions, to which also the non-increase of SO_4^{2-} reduction rate for SO_4^{2-}-treated bog peat has been attributed (Vile et al., 2003). These findings confirm recent results of isotopic measurement of DIC in the pore water of sea-exposed fen peat of the Hütelmoor field site, which indicate that the detected DIC concentrations do not originate from the submerged peat itself, but from easily degradable marine DOM (personal communication with J. Westphal, Leibniz Institute for Baltic Sea Research Warnemünde). The measured HS^- concentrations were considerably lower than the measured DIC concentrations (comparison in molar concentrations see **Figure 5**). This means that either not all HS^- was detected due to its chemical reactivity or other processes than SO_4^{2-} reduction co-drove the DIC production. It is possible that a part of the released HS^- was bound to the DOM (Heitmann and Blodau, 2006) or precipitated as iron sulfide (van der Welle et al., 2007) and was, therefore, not detected with the applied method in this study. Other mineralization processes such as Fe(III) reduction could have driven the DIC production as an increase of DOC and TDN in the SULF2700+A treatment was observed indicating a general stimulation of decomposition processes. Concentrations of TDFe were highly elevated in the SULF2700+A treatment (peak concentration of 28 mg L^{-1}) compared to the acetate-free SULF2700 treatment (peak concentration of 2 mg L^{-1}). These results imply that Fe(III) reduction had occurred, during which Fe^{2+} is released; yet, the time curve of HS^- indicates that DIC production was mainly controlled by SO_4^{2-} reduction

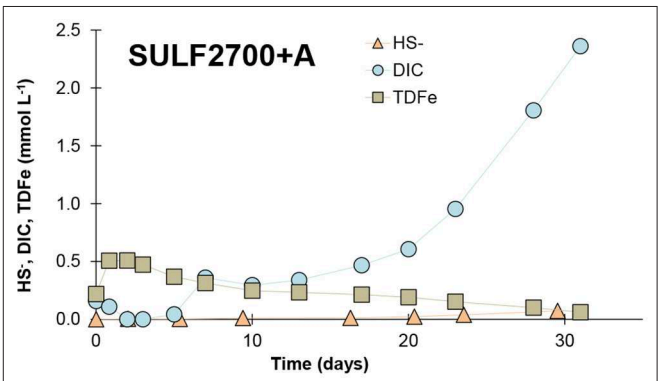

FIGURE 5 | Release of end products of sulfate reduction (HS^-, DIC) and of TDFe as interfering substance in molar concentration measured in the effluent of the flow-through reactor from an individual peat sample during SULF2700+A treatment.

(**Figure 4A**). This also applies to other parameters—overall, the release of DOC, DIC, TDN and total dissolved phosphorus (TDP) was stimulated by SO_4^{2-} reduction. Conversely, the release of TDMn in the SULF2700+A treatment resembled its counterpart (SULF2700) and experienced only a slightly lower peak concentration. This suggests that TDMn-release was mainly affected by cation exchange and not Mn(IV) reduction, which is consistent with the gradations in TDMn-concentrations for the acetate-free treatments following Na^+ input concentrations (see effect of sulfate concentration).

Effect of Peat Decomposition Degree

The observed differences of solute release between the peats of varying degrees of decomposition were more pronounced and clearer than between the different SO_4^{2-} concentrations applied to one peat material (**Figure 3** for DOC/DIC/TDN, **Figure 6** for TDFe). The substance release of the SD-peat matched the expectations that the DOC would decrease abruptly after an EC increase (see effect of sulfate concentration). Following an increase in EC from 3.6 mS cm^{-1} (SULF700) to 6.3 mS cm^{-1} (SULF2700), DOC and TDN concentrations decreased on average by 51 and 22%, respectively. In contrast, DOC and TDN concentrations varied only slightly for the MD-peat and responded immediately with an increase to the SULF2700 treatment for the HD-peat (**Figure 3D**). The observed differences in the time curve of DOC and TDN between the three peats could be related to the large differences in Fe content (**Table 1**), where the HD-peat contains 50 times more Fe than the SD-peat. As previously discussed (see initial flushing), the long-term drained and degraded peat generally has a different composition than less decomposed peat. While the percentage of organic carbon decreases with decomposition, the percentage of phosphorus (P), Fe and Al increases (Zeitz and Velty, 2002; Litaor et al., 2004). Knorr (2013) observed that DOC and TDFe concentrations had a clear positive correlation in pore and surface water while the impact of water salinity was not consistent for the two types of water. Iron salts such as ferric sulfate are well known to induce flocculation of fine organic and inorganic particles from the production of cationic hydrolysis products and are generally used to clean drinking water from DOM (Sharp et al., 2006). However, during Fe(III) reduction Fe^{2+} is released thereby co-mobilizing the previously flocculated DOM with other formerly bound solutes like phosphate. The correlation coefficient R^2 between TDFe and DOC concentrations in the effluent of this study ranged between 0.36 (SULF2700) and 0.95 (SULF100) for the pure SO_4^{2-} treatments of the MD-peat. The Fe-rich HD-peat samples have a calculated R^2 value of 0.58, demonstrating Fe-related interference is an important impact factor for DOC.

The observed differences between the SD-, MD-, and HD-peat in solute release could also be related to their pore-related parameters, such as porosity and proportion of the immobile pore regions detected via BTC analysis. Immobile zones provide an opposing effect on DOC concentrations where stagnant pore water zones may serve as hot spots for DOM production, as they represent the preferred habitat for microorganisms (Nunes et al., 2015; Rezanezhad et al., 2016). Immobile pore regions also increase the average pore water velocity and preferential flow thereby reducing the residence time of the water in the mobile pore regions and the potential for solute exchange between liquid and solid phase (Tiemeyer et al., 2017). However, as the release of DOC/TDN from SD-peat and MD-peat reached comparable values during the experiment, physical differences—whose effect should be long-lasting—may only be relevant to the HD-peat. Generally, the greater the degree of decomposition in peat the more pronounced the preferential flow occurs (Liu et al., 2017) and the immobile pore region fraction increases. In case of the HD-peat the greater proportion of immobile pore water might have contributed to the higher constant release of DOC/TDN.

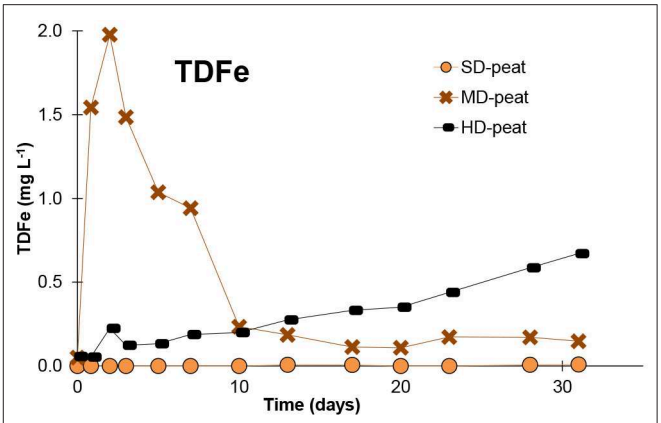

FIGURE 6 | Release of TDFe from SD-, MD-, and HD-peat measured in the effluent of the flow-through reactors.

CONCLUSIONS

In this flow-through experiment peat samples treated with sulfate (SO_4^{2-})-enriched water did not produce pronounced SO_4^{2-} reduction within 1 month's time. SO_4^{2-} and bromide (Br^-) breakthrough curves were similar indicating that SO_4^{2-} behaved as a conservative tracer within the experiment and that the SO_4^{2-} penetration was dependent on the physical properties of the peat samples. The addition of acetate, a major electron donor in marine sediments, initiated SO_4^{2-} reduction after ~17 days and led to a strong increase of release of solutes such as dissolved organic carbon (DOC) and inorganic carbon (DIC). This suggests that under these experimental conditions the composition and decomposability of the organic matter was more important to enabling decomposing processes than the presence of terminal electron acceptors. This was also demonstrated by the increased solute concentrations for peat with a higher degree of decomposition. However, increased SO_4^{2-} concentrations did result in slightly elevated levels of DOC and total dissolved nitrogen (TDN). These results are attributed to the potential desorption of negatively charged organic molecules via anion exchange with SO_4^{2-}. For the different tested peats, the short-term release of DOC was presumably affected not only by the ionic strength of the inflowing water but also by the iron (Fe) content of the peat, as DOC bound to Fe compounds can get mobilized during Fe(III) reduction. Overall, the main short-term effects of SO_4^{2-}-rich seawater inflow in peatlands seem to be desorption processes, whose characteristics are controlled by the ionic composition and strength of the seawater, and peat chemistry, particularly Fe content and degree of decomposition.

Decomposition-related solute release may develop in the long-term, when anoxic, stagnant conditions prevail. This may be accelerated if marine, easily degradable organic matter is flushed in the peatland during seawater flooding even though concentrations of bioavailable DOC might be lower than the applied acetate concentrations in this study. The onset of SO_4^{2-} reduction may reduce the gaseous emissions of carbon-containing methane (CH_4) from the peatland, but may also increase the load of dissolved carbon compounds in the peatland's outflow.

DATA AVAILABILITY STATEMENT

The datasets generated for this study are available on request to the corresponding author.

AUTHOR CONTRIBUTIONS

LG: design of experiment, data acquisition, data analysis, data interpretation, and drafting of manuscript. HT: data acquisition and revision of draft. MK: data interpretation and revision of draft. MJ: design of experiment, data interpretation, and revision of draft. FR: design of experiment, data analysis, data interpretation, and revision of draft. BL: design of experiment and revision of draft.

FUNDING

This study was conducted within the framework of the Research Training Group Baltic TRANSCOAST funded by the DFG (Deutsche Forschungsgemeinschaft) under grant number GRK 2000 (www.baltic-transcoast.uni-rostock.de). This is Baltic TRANSCOAST publication no. GRK2000/0026.

We acknowledge financial support by the DFG and the University of Rostock within the funding programme Open Access Publishing.

ACKNOWLEDGMENTS

We also would like to acknowledge the lab facilities provided by the Canada Excellence Research Chair program in Ecohydrology. We thank Marianne Vandergriendt (Ecohydrology Research Group, University of Waterloo, Canada) for water sample analysis and all members from the Ecohydrology Research Group who helped with the experiment and analysis.

REFERENCES

Algeo, T. J., Luo, G. M., Song, H. Y., Lyons, T. W., and Canfield, D. E. (2015). Reconstruction of secular variation in seawater sulfate concentrations. *Biogeosciences* 12, 2131–2151. doi: 10.5194/bg-12-2131-2015

Ardón, M., Helton, A. M., and Bernhardt, E. S. (2016). Drought and saltwater incursion synergistically reduce dissolved organic carbon export from coastal freshwater wetlands. *Biogeochemistry* 127, 411–426. doi: 10.1007/s10533-016-0189-5

Ardón, M., Morse, J. L., Colman, B. P., and Bernhardt, E. S. (2013). Drought-induced saltwater incursion leads to increased wetland nitrogen export. *Glob. Chang. Biol.* 19, 2976–2985. doi: 10.1111/gcb.12287

Blodau, C., Mayer, B., Peiffer, S., and Moore, T. R. (2007). Support for an anaerobic sulfur cycle in two Canadian peatland soils. *J. Geophys. Res. Biogeosciences* 112, 1–10. doi: 10.1029/2006JG000364

Borch, T., Kretzschmar, R., and Kappler, A. (2010). Biogeochemical redox processes and their impact on contaminant dynamics - environmental science & technology (ACS Publications). *Environ. Sci. Technol.* 44, 15–23. doi: 10.1021/es9026248

Boschker, H. T., De Graaf, W., Köster, M., Meyer-Reil, L. A., and Cappenberg, T. E. (2001). Bacterial populations and processes involved in acetate and propionate consumption in anoxic brackish sediment. *FEMS Microbiol. Ecol.* 35, 97–103. doi: 10.1111/j.1574-6941.2001.tb00792.x

Brouns, K., Verhoeven, J. T. A., and Hefting, M. M. (2014). The effects of salinization on aerobic and anaerobic decomposition and mineralization in peat meadows: the roles of peat type and land use. *J. Environ. Manage.* 143, 44–53. doi: 10.1016/j.jenvman.2014.04.009

Caraco, N. F., Cole, J. J., and Likens, G. E. (1989). Evidence for sulphate-controlled phosphorus release from sediments of aquatic systems. *Nature* 341, 316–318. doi: 10.1038/341316a0

Clark, J. M., Van Der Heijden, G. M. F., Palmer, S. M., Chapman, P. J., and Bottrell, S. H. (2011). Variation in the sensitivity of DOC release between different organic soils following H2SO4 and sea-salt additions. *Eur. J. Soil Sci.* 62, 267–284. doi: 10.1111/j.1365-2389.2010.01344.x

Cline, J. D. (1969). Spectrophotometric determination of hydrogen sulfide in natural waters. *Limnol. Oceanogr.* 14, 454–458. doi: 10.4319/lo.1969.14.3.0454

DIN EN 15935 (2012). (Deutsches Institut für Normung e.V.) *Sludge, Treated Biowaste, Soil and Waste - Determination of Loss on Ignition*. Berlin: Beuth Verlag.

Edelstein, M., Ben-Hur, M., and Plaut, Z. (2010). Water salinity and sodicity effects on soil structure and hydraulic properties. *Adv. Hortic. Sci.* 24, 154–160.

Gardner, L. R. (1990). Simulation of the diagenesis of carbon, sulfur, and dissolved oxygen in salt marsh sediments. *Ecol. Monogr.* 60, 91–111. doi: 10.2307/1943027

Gosch, L., Janssen, M., and Lennartz, B. (2018). Impact of the water salinity on the hydraulic conductivity of fen peat. *Hydrol. Process.* 32, 1214–1222. doi: 10.1002/hyp.11478

Hahn, J., Köhler, S., Glatzel, S., and Jurasinski, G. (2015). Methane exchange in a coastal fen in the first year after flooding - A systems shift. *PLoS ONE* 10:e140657. doi: 10.1371/journal.pone.0140657

Hanin, M., Ebel, C., Ngom, M., Laplaze, L., and Masmoudi, K. (2016). New insights on plant salt tolerance mechanisms and their potential use for breeding. *Front. Plant Sci.* 7:1787. doi: 10.3389/fpls.2016.01787

Hausmann, B., Knorr, K., Schreck, K., Tringe, S. G., Glavina, T., Loy, A., et al. (2016). Consortia of low-abundance bacteria drive sulfate reduction-dependent degradation of fermentation products in peat soil microcosms. *ISME J.* 10, 2365–2375. doi: 10.1038/ismej.2016.42

Heitmann, T., and Blodau, C. (2006). Oxidation and incorporation of hydrogen sulfide by dissolved organic matter. *Chem. Geol.* 235, 12–20. doi: 10.1016/j.chemgeo.2006.05.011

HFA (2014). *(Gutachterausschuss Forstliche Analytik) Handbuch Forstliche Analytik (HFA): Eine Loseblatt-Sammlung der Analysemethoden im Forstbereich. Bundesministerium für Ernährung und Landwirtschaft (BMEL)*, 5th ed. Bonn.

Johnson, D. W., and Todd, D. E. (1983). Relationships among iron, aluminum, carbon, and sulfate in a variety of forest soils. *Soil Sci. Soc. Am. J.* 47:792–800. doi: 10.2136/sssaj1983.03615995004700040035x

Jørgensen, N. O., Andersen, M. S., and Engesgaard, P. (2008). Investigation of a dynamic seawater intrusion event using strontium isotopes (87Sr/86Sr). *J. Hydrol.* 348, 257–269. doi: 10.1016/j.jhydrol.2007.10.001

Kasimir-Klemedtsson, Å., Klemedtsson, L., Berglund, K., Martikainen, P., Silvola, J., and Oenema, O. (1997). Greenhouse gas emissions from farmed organic soils: a review. *Soil Use Manag.* 13, 245–250. doi: 10.1111/j.1475-2743.1997.tb00595.x

Kester, D. R., Duedall, I. W., Connors, D. N., and Pytkowicz, R. M. (1967). Preparation of artificial seawater. *Limnol. Oceanogr.* 12, 176–179. doi: 10.4319/lo.1967.12.1.0176

Kleimeier, C., Rezanezhad, F., Cappellen, P., and Van, L.ennartz, B. (2017). Influence of pore structure on solute transport in degraded and undegraded fen peat soils. *Mires Peat* 19, 1–9. doi: 10.19189/MaP.2017.OMB.282

Knorr, K. H. (2013). DOC-dynamics in a small headwater catchment as driven by redox fluctuations and hydrological flow paths - are DOC exports mediated by iron reduction/oxidation cycles? *Biogeosciences* 10, 891–904. doi: 10.5194/bg-10-891-2013

Koebsch, F., Winkel, M., Liebner, S., Liu, B., Westphal, J., Spitzy, A., et al. (2019). Sulfate deprivation triggers high methane production in a disturbed and rewetted coastal peatland. *Biogeosciences* 16, 1937–1953. doi: 10.5194/bg-16-1937-2019

Kreuzburg, M., Ibenthal, M., Janssen, M., Rehder, G., Voss, M., Naumann, M., et al. (2018). Sub-marine continuation of peat deposits from a coastal peatland in the southern baltic sea and its holocene development. *Front. Earth Sci.* 6:103. doi: 10.3389/feart.2018.00103

Küsel, K., Blöthe, M., Schulz, D., Reiche, M., and Drake, H. L. (2008). Microbial reduction of iron and porewater biogeochemistry in acidic peatlands. *Biogeosciences* 5, 1537–1549. doi: 10.5194/bg-5-1537-2008

Lamers, L. P. M., Tomassen, H. B. M., and Roelofs, J. G. M. (1998). Sulfate-induced eutrophication and phytotoxicity in freshwater wetlands. *Environ. Sci. Technol.* 32, 199–205. doi: 10.1021/es970362f

Laverman, A. M., Pallud, C., Abell, J., and Cappellen, P., Van (2012). Comparative survey of potential nitrate and sulfate reduction rates in aquatic sediments. *Geochim. Cosmochim. Acta* 77, 474–488. doi: 10.1016/j.gca.2011.10.033

Litaor, M. I., Reichmann, O., Auerswald, K., Haim, A., and Shenker, M. (2004). The geochemistry of phosphorus in peat soils of a semiarid altered wetland. *Soil Sci. Soc. Am. J.* 68, 2078–2085. doi: 10.2136/sssaj2004.2078

Liu, H., Forsmann, D. M., Kjærgaard, C., Saki, H., and Lennartz, B. (2017). Solute transport properties of fen peat differing in organic matter content. *J. Environ. Qual.* 46, 1106–1113. doi: 10.2134/jeq2017.01.0031

Mandernack, K. W., Lynch, L., Krouse, H. R., and Morgan, M. D. (2000). Sulfur cycling in wetland peat of the New Jersey Pinelands and its effect on stream water chemistry. *Geochim. Cosmochim. Acta* 64, 3949–3964. doi: 10.1016/S0016-7037(00)00491-9

McCarter, C. P. R., Weber, T. K. D., and Price, J. S. (2018). Competitive transport processes of chloride, sodium, potassium, and ammonium in fen peat. *J. Contam. Hydrol.* 217, 17–31. doi: 10.1016/j.jconhyd.2018.08.004

Münch, J. M., Totsche, K. U., and Kaiser, K. (2002). Physicochemical factors controlling the release of dissolved organic carbon from columns of forest subsoils. *Eur. J. Soil Sci.* 53, 311–320. doi: 10.1046/j.1365-2389.2002.00439.x

Nunes, F. L. D., Aquilina, L., de Ridder, J., Francez, A.-J., Quaiser, A., Caudal, J.-P., et al. (2015). Time-scales of hydrological forcing on the geochemistry and bacterial community structure of temperate peat soils. *Sci. Rep.* 5:14612. doi: 10.1038/srep14612

Oremland, R. S., Marsh, L. M., and Polcin, S. (1982). Methane production and simultaneous sulphate reduction in anoxic, salt marsh sediments. *Nature* 296, 143–145. doi: 10.1038/296143a0

Ottow, J. C. G. (2011). *Mikrobiologie von Böden - Biodiversität, Ökophysiologie und Metagenomik*. Heidelberg: Springer-Verlag. doi: 10.1007/978-3-642-00824-5

Ours, D. P., Siegel, D. I., and Glaser, P. H. (1997). Chemical dilation and the dual porosity of humified bog peat. *J. Hydrol.* 196, 348–360. doi: 10.1016/S0022-1694(96)03247-7

Pallud, C., Meile, C., Laverman, A. M., Abell, J., and Cappellen, P., Van (2007). The use of flow-through sediment reactors in biogeochemical kinetics: methodology and examples of applications. *Mar. Chem.* 106, 256–271. doi: 10.1016/j.marchem.2006.12.011

Pallud, C., and Van Cappellen, P. (2006). Kinetics of microbial sulfate reduction in estuarine sediments. *Geochim. Cosmochim. Acta* 70, 1148–1162. doi: 10.1016/j.gca.2005.11.002

Rezanezhad, F., Price, J. S., and Craig, J. R. (2012). The effects of dual porosity on transport and retardation in peat: a laboratory experiment. *Can. J. Soil Sci.* 92, 723–732. doi: 10.4141/cjss2011-050

Rezanezhad, F., Price, J. S., Quinton, W. L., Lennartz, B., Milojevic, T., and Van Cappellen, P. (2016). Structure of peat soils and implications for water storage, flow and solute transport: a review update for geochemists. *Chem. Geol.* 429, 75–84. doi: 10.1016/j.chemgeo.2016.03.010

Ritson, J. P., Bell, M., Graham, N. J. D., Templeton, M. R., Brazier, R. E., Verhoef, A., et al. (2014). Simulated climate change impact on summer dissolved organic carbon release from peat and surface vegetation: Implications for drinking water treatment. *Water Res.* 67, 66–76. doi: 10.1016/j.watres.2014.09.015

Roulet, N., and Moore, T. R. (2006). Browning the waters. *Nature* 444, 283–284. doi: 10.1038/444283a

Schmaljohann, R. (1996). Methane dynamics in the sediment and water column of Kiel Harbour (Baltic Sea). *Mar. Ecol. Prog. Ser.* 131, 263–273. doi: 10.3354/meps131263

Sharp, E. L., Parsons, S. A., and Jefferson, B. (2006). The impact of seasonal variations in DOC arising from a moorland peat catchment on coagulation with iron and aluminium salts. *Environ. Pollut.* 140, 436–443. doi: 10.1016/j.envpol.2005.08.001

Sherif, M. M., and Singh, V. P. (1999). Effect of climate change on sea water intrusion in coastal aquifers. *Hydrol. Process.* 13, 1277–1287.

Stam, M. C., Mason, P. R. D., Pallud, C., and Van Cappellen, P. (2010). Sulfate reducing activity and sulfur isotope fractionation by natural microbial communities in sediments of a hypersaline soda lake (Mono Lake, California). *Chem. Geol.* 278, 23–30. doi: 10.1016/j.chemgeo.2010.08.006

Stutter, M. I., Lumsdon, D. G., and Cooper, R. J. (2007). Temperature and soil moisture effects on dissolved organic matter release from a moorland Podzol O horizon under field and controlled laboratory conditions. *Eur. J. Soil Sci.* 58, 1007–1016. doi: 10.1111/j.1365-2389.2006.00880.x

Succow, M., and Joosten, H. (2001). *Landschaftsökologische Moorkunde, 2nd ed.* Stuttgart: E. Schweizerbart'sche Verlagsbuchhandlung.

Tiemeyer, B., Pfaffner, N., Frank, S., Kaiser, K., and Fiedler, S. (2017). Pore water velocity and ionic strength effects on DOC release from peat-sand mixtures: results from laboratory and field experiments. *Geoderma* 296, 86–97. doi: 10.1016/j.geoderma.2017.02.024

Toride, N., Leij, F. J., and van Genuchten, M. T. (1999). The CXTFIT *Code for Estimating Transport Parameters from Laboratory or Field Tracer Experiments*. Version 2.1. Riverside, CA: Research Report 137, US Salinity Laboratory, Agricultural Research Service, US Department of Agriculture.

van der Welle, M. E. W., Smolders, A. J. P., Op Den Camp, H. J. M., Roelofs, J. G. M., and Lamers, L. P. M. (2007). Biogeochemical interactions between iron and sulphate in freshwater wetlands and their implications for interspecific competition between aquatic macrophytes. *Freshw. Biol.* 52, 434–447. doi: 10.1111/j.1365-2427.2006.01683.x

Vile, M. A., Bridgham, S. D., and Wieder, R. K. (2003). Response of anaerobic carbon mineralization rates to sulfate amendments in a boreal peatland. *Ecol. Appl.* 13, 720–734. doi: 10.1890/1051-0761(2003)013[0720:ROACMR]2.0.CO;2

Wang, H., Richardson, C. J., Ho, M., and Flanagan, N. (2016). Drained coastal peatlands: A potential nitrogen source to marine ecosystems under prolonged drought and heavy storm events—A microcosm experiment. *Sci. Total Environ.* 566–567, 621–626. doi: 10.1016/j.scitotenv.2016.04.211

Wen, X., Unger, V., Jurasinski, G., Koebsch, F., Horn, F., Rehder, G., et al. (2018). Predominance of methanogens over methanotrophs contributes to high methane emissions in rewetted fens. *Biogeosci. Discuss.* 15, 6519–6536. doi: 10.5194/bg-15-6519-2018

Weston, N. B., Vile, M. A., Neubauer, S. C., and Velinsky, D. J. (2011). Accelerated microbial organic matter mineralization following salt-water intrusion into tidal freshwater marsh soils. *Biogeochemistry* 102, 135–151. doi: 10.1007/s10533-010-9427-4

Wieder, R. K., and Lang, G. E. (1988). Cycling of inorganic and organic sulfur in peat from Big Run Bog, West Virginia. *Biogeochemistry* 5, 221–242. doi: 10.1007/BF02180229

Zak, D., and Gelbrecht, J. (2007). The mobilisation of phosphorus, organic carbon and ammonium in the initial stage of fen rewetting (a case study from NE Germany). *Biogeochemistry* 85, 141–151. doi: 10.1007/s10533-007-9122-2

Zak, D., Goldhammer, T., Cabezas, A., Gelbrecht, J., Gurke, R., Wagner, C., et al. (2018). Top soil removal reduces water pollution from phosphorus and dissolved organic matter and lowers methane emissions from rewetted peatlands. *J. Appl. Ecol.* 55, 311–320. doi: 10.1111/1365-2664.12931

Zak, D., Wagner, C., Payer, B., Augustin, J., and Gelbrecht, J. (2010). Phosphorus mobilization in rewetted fens: the effect of altered peat properties and implications for their restoration. *Ecol. Appl.* 20, 1336–1349. doi: 10.1890/08-2053.1

Zeitz, J., and Velty, S. (2002). Soil properties of drained and rewetted fen soils. *J. Plant Nutr. Soil Sci.* 165, 618–626. doi: 10.1002/1522-2624(200210)165:5<618::AID-JPLN618>3.0.CO;2-W

Conflict of Interest: The authors declare that the research was conducted in the absence of any commercial or financial relationships that could be construed as a potential conflict of interest.

frontiers in Environmental Science

ORIGINAL RESEARCH
published: 07 February 2020
doi: 10.3389/fenvs.2020.00008

Reducing Emissions From Degraded Floodplain Wetlands

Katy E. Limpert, Paul E. Carnell, Stacey M. Trevathan-Tackett and Peter I. Macreadie*

School of Life and Environmental Sciences, Centre for Integrative Ecology, Deakin University, Burwood, VIC, Australia

Globally, freshwater wetlands are significant carbon sinks; however, altering a wetland's hydrology can reduce its ability to sequester carbon and may lead to the release of previously stored soil carbon. Rehabilitating a wetland's water table has the potential to restore the natural process of wetland soil carbon sequestration and storage. Further, little is known about the role of microbial communities that mediate carbon cycling during wetland rehabilitation practices. Here, we examined the carbon emissions and microbial community diversity during a wetland rehabilitation process known as "environmental watering" (rewetting) in an Australian, semi-arid freshwater floodplain wetland. By monitoring carbon dioxide (CO_2) and methane (CH_4) emissions during dry and wet phases of an environmental watering event, we determined that adding water to a degraded semi-arid floodplain wetland reduces carbon emissions by 28–84%. The watering event increased anoxic levels and plant growth in the aquatic zone of the wetland, which may correlate with lower carbon emissions during and after environmental watering due to lower anaerobic microbial decomposition processes and higher CO_2 sequestration by vegetation. During the watering event, areas with higher inundation had lower CO_2 emissions (5.15 ± 2.50 g CO_2 m^{-2} day^{-1}) compared to fringe areas surrounding the wetland (11.89 ± 4.25 g CO_2 m^{-2} day^{-1}). CH_4 flux was inversely correlated with CO_2 emissions during inundation periods, showing a 38% (0.013 ± 0.061 g CO_2-e m^{-2} day^{-1}) increase when water was present in the wetland. During the dry phases of environmental watering, there was CH_4 uptake within the fringe and aquatic zones (-0.013 ± 0.063 g CO_2-e m^{-2} day^{-1}). A clear succession of soil microbial community was observed during the dry-wet phases of the environmental watering process. This suggests that wetland hydrology plays a large role in the microbial community structure of these wetland ecosystems, and is consequently linked to CO_2 and CH_4 emissions. Overall, the total carbon emissions ($CO_2 + CH_4$) were reduced within the wetland during and after the environmental watering event, due to increasing vegetative growth and subsequent CO_2 sequestration. We, therefore, recommend environmental watering practices in this degraded arid wetland ecosystem to improve conditions for wetland carbon sequestration and storage. Further use of this management practice may improve wetland carbon storage across other arid freshwater wetland ecosystems with similar hydrologic regimes.

Keywords: 16S diversity, carbon sequestration, environmental watering, floodplains, greenhouse gas emissions, microbial communities, soil organic carbon

OPEN ACCESS

Edited by:
Bernd Lennartz,
University of Rostock, Germany

Reviewed by:
Britt Dianne Hall,
University of Regina, Canada
Fereidoun Rezanezhad,
University of Waterloo, Canada
Bijendra Man Bajracharya,
University of Waterloo, Canada

****Correspondence:***
Katy E. Limpert
klimpert@deakin.edu.au;
Kelimpert@gmail.com

Specialty section:
This article was submitted to Biogeochemical Dynamics, a section of the journal Frontiers in Environmental Science

Received: *17 May 2019*
Accepted: *13 January 2020*
Published: *07 February 2020*

Citation:
Limpert KE, Carnell PE, Trevathan-Tackett SM and Macreadie PI (2020) Reducing Emissions From Degraded Floodplain Wetlands. Front. Environ. Sci. 8:8. doi: 10.3389/fenvs.2020.00008

INTRODUCTION

Freshwater wetlands are highly productive environments that supply a number of ecosystem services (Strayer and Dudgeon, 2010) such as: nutrient cycling, improving water quality, regulating floods, providing wildlife habitat, and improving plant and animal biodiversity (Mitra et al., 2005; Bernal and Mitsch, 2012). Freshwater wetlands play an essential role in mitigating climate change by sequestering carbon through wetland plant photosynthesis and storing carbon by accumulating organic matter in plant biomass, sediments, and soil (Cole et al., 2007; Lal, 2009; Kayranli et al., 2010). Despite their small terrestrial global surface area of 6–9%, freshwater wetlands contain up to 33% of the world's soil carbon, capturing 1.9–2.2 Gt C $year^{-1}$ (Cole et al., 2007; Limpens et al., 2008; Nahlik and Fennessy, 2016).

In the past few decades, rising temperatures, resulting from anthropogenic carbon emissions, have increased government and industry interest in the ability of freshwater wetlands to sequester and store organic carbon (Bernal and Mitsch, 2012). Quantifying freshwater wetland carbon dynamics is a complex process, with different conditions allowing for variation in carbon storage and release. In general, wetland ecosystems show accelerated plant growth and slower decomposition rates compared to terrestrial ecosystems, both of which facilitate carbon storage (Sun and Liu, 2007). However, anaerobic wetland conditions have the potential to increase methane (CH_4) emissions, a potent greenhouse gas that has a radiative forcing 87 times higher than carbon dioxide (CO_2) over a 20 year time-scale (Neubauer and Megonigal, 2015). Despite this, many freshwater wetlands are typically net annual carbon sinks (Kayranli et al., 2010). The balance between wetland carbon sinks and sources can be attributed to several processes and pathways (**Figure 1**). Wetland soil carbon cycling is influenced by (1) inundated soils that limit oxygen (O_2) diffusion into sediment, (2) anaerobic conditions caused by higher water levels reducing decomposition rates compared to aerobic soils, and (3) the relative reduction in remineralization, providing wetlands with the potential to store large amounts of soil organic carbon (Kayranli et al., 2010; **Figure 1**).

Variable inundation conditions resulting from changing water levels can create aerobic and anaerobic zones that allow for soil carbon to be remineralized by various microbial processes that determine carbon storage and release (Olefeldt et al., 2017). For instance, microbial and vegetative respiration, as well as CH_4 oxidation, occur within aerobic zones, while methanogenesis and fermentation occur under anaerobic conditions (Nahlik and Mitsch, 2011; **Figure 1**). Aerobic soil conditions are more predominant during dry or lower water level periods. A lower water table favors aerobic respiration while creating conditions that increase the availability of fresh, and often labile, organic matter (Yarwood, 2018). The result of these conditions is the promotion of rapid microbial decomposition of plant litter (Rasilo et al., 2017; Yarwood, 2018). During periods of inundation and predominantly anaerobic soil conditions, methanogenesis is a key biogeochemical pathway for carbon remineralization and therefore a source of CH_4 production in many freshwater wetlands (Kayranli et al., 2010).

Hydrological changes, particularly alterations in water table level in freshwater wetlands, influence carbon emissions by altering oxidation and reduction processes. The availability of alternative electron acceptors, such as nitrate, manganese, iron, and sulfate, causes competition between methanogens and other microbes (i.e., denitrifying and sulfate reducing bacteria) for organic substrates within wetland ecosystems (Boon et al., 1997; Ettwig et al., 2010; Zhu et al., 2012). The production of CO_2 and CH_4 is therefore affected by redox reactions driven by water level. For instance, anaerobic oxidation of CH_4 (which is often coupled to SO_4 and NO_3 reduction) within inundated wetlands has been documented to consume potential CH_4 emissions by over 50% (Segarra et al., 2015).

The frequency of fluctuating moisture content within soils has been documented to cause a significant increase of microbial respiration (i.e., the "Birch Effect"; McComb and Qiu, 1998; Wilson and Baldwin, 2008). The mechanisms that alter microbial activity during wetting and drying cycles involve microbial stress and variation in substrate availability for microbial respiration (Xiang et al., 2008). Within dry soils, specifically during prolonged drought conditions, microbes retain high concentrations of solutes to help store water within the cell as a means to prevent dehydration (Schimel et al., 2007). When water enters the system, stored solutes are released from the cell, leading to rapid metabolism of microbial compounds (Halverson et al., 2000; Schimel, 2007). In addition, the physical process of wetland rewetting leads to the redistribution of organic matter (that was previously unavailable) to increase microbial breakdown within the wetland soil profile (Denef et al., 2001; Miller et al., 2005; Cosentino et al., 2006).

Understanding the biogeochemical cycling of wetland ecosystems during various stages of inundation is imperative to inform carbon management in wetland ecosystems. The scenario represented in **Figure 1** assumes little to no alteration to wetland ecosystems; however, on a global scale, 50% of wetland ecosystems have been lost since the 1900s due to land-use changes, agricultural impacts, and hydrologic alterations (Davidson, 2014). Human activity and development continue to have detrimental impacts to carbon storage and often revert wetland ecosystems from sinks into carbon sources (Nahlik and Fennessy, 2016; Hemes et al., 2018). Altering wetland soil conditions has the potential to release significant amounts of soil organic carbon that was previously stored within the wetland soil profile (Lal, 2007; Page and Dalal, 2011). Manipulating water levels, such as creating dams and reservoirs, has contributed to 12% of global CH_4 emissions (St. Louis et al., 2000; **Figure 1**).

The increasing demand for global carbon markets has the Australian government, industry, and research groups considering the incentive potential of rehabilitating freshwater ecosystems for carbon sequestration, storage, and emission reduction. While wetland carbon stocks and sequestration rates are relatively well understood in semi-arid regions of Victoria, Australia (Carnell et al., 2018; Pearse et al., 2018), there is no data on carbon fluxes and the corresponding microbial communities that are responsible for carbon release during rehabilitation practices. To maintain environmental benefits such as increased carbon storage and reduced carbon

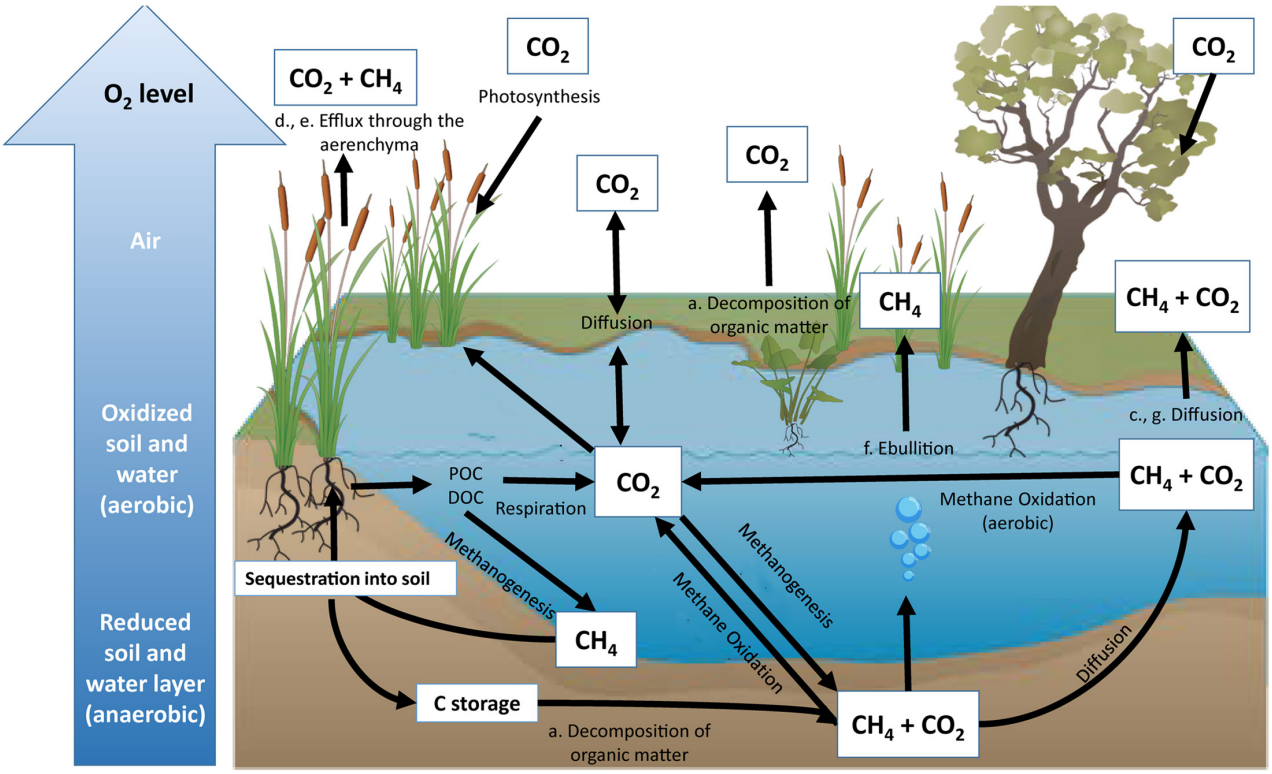

FIGURE 1 | Representation of the inland wetland carbon cycle. Major pathways of carbon sequestration include photosynthesis and organic carbon accumulation through particulate organic carbon (POC) and dissolved organic carbon (DOC). Major pathways of CO_2 emissions include respiration during decomposition of organic matter (a), oxidation of CH_4 (b), diffusion (c), and release of greenhouse gases through plant aerenchyma (d). Major pathways of CH_4 emissions include methanogenesis via efflux through plant aerenchyma (e), ebullition (f), and diffusion (g). All sequestered carbon has the potential to be stored within the soil profile for centuries (Bernal and Mitsch, 2012) unless the wetland is altered.

emissions, further research is required to understand how rehabilitation through environmental watering alters floodplain carbon dynamics. Allocating water in an effort to recreate the natural inundation regime of wetland ecosystems for improving biodiversity and wetland functionality is expensive. According to the National Water Commission (2008), the Australian government allocated $50 million in purchasing 35 GL of water access entitlements at $1131 per ML. Under the Australian emission reduction fund, the average price per ton of carbon is $11.90 (Clarke et al., 2014). Due to the high costs of water rights, determining whether environmental watering can reduce carbon emissions, and by doing so, help pay for the cost of rewetting, would be beneficial to the parties involved in environmental watering management practice. The aim of this study was to determine (1) the magnitude of CO_2 and CH_4 diffusive fluxes from an environmental watering management event and (2) the microbial communities that are potentially responsible for carbon fluxes within a degraded floodplain wetland. The microbial community succession was measured during the watering event to better understand shifts in bacterial and archaeal community diversity and structure while simultaneously measuring CO_2 and CH_4 fluxes. We hypothesized that adding water to this wetland would increase anaerobic microbial respiration and subsequent CH_4 emissions during inundation, while reducing aerobic bacterial communities and CO_2 emissions. The outcomes of this research will provide additional guidance as to whether rehabilitation through environmental watering can maximize carbon offset opportunities, or whether this process promotes carbon emissions in semi-arid floodplain ecosystems.

MATERIALS AND METHODS

Climate

Semi-arid and arid bioregions encompass 70% of the Australian landscape (Byrne, 2008; **Figure 2**), with our study site, Duck Creek North, located in the semi-arid bioregion (**Figure 2A**). The climate of the study area is typical of semi-arid environments, with hot dry summers, cold arid winters, and decreased precipitation over summer (Bsk-Köppen Climate Classification; Peel et al., 2007). The long-term mean annual precipitation in the area is approximately 364.5 mm and the mean annual temperature is 22.9°C (measured at the nearby town, Kerang: 35.72°S, 143.91°E, Bureau of Meteorology [BOM], 2017). Precipitation is higher in the winter and spring months from May to October (32.1 mm month^{-1}, Bureau of Meteorology [BOM], 2017) compared to summer and

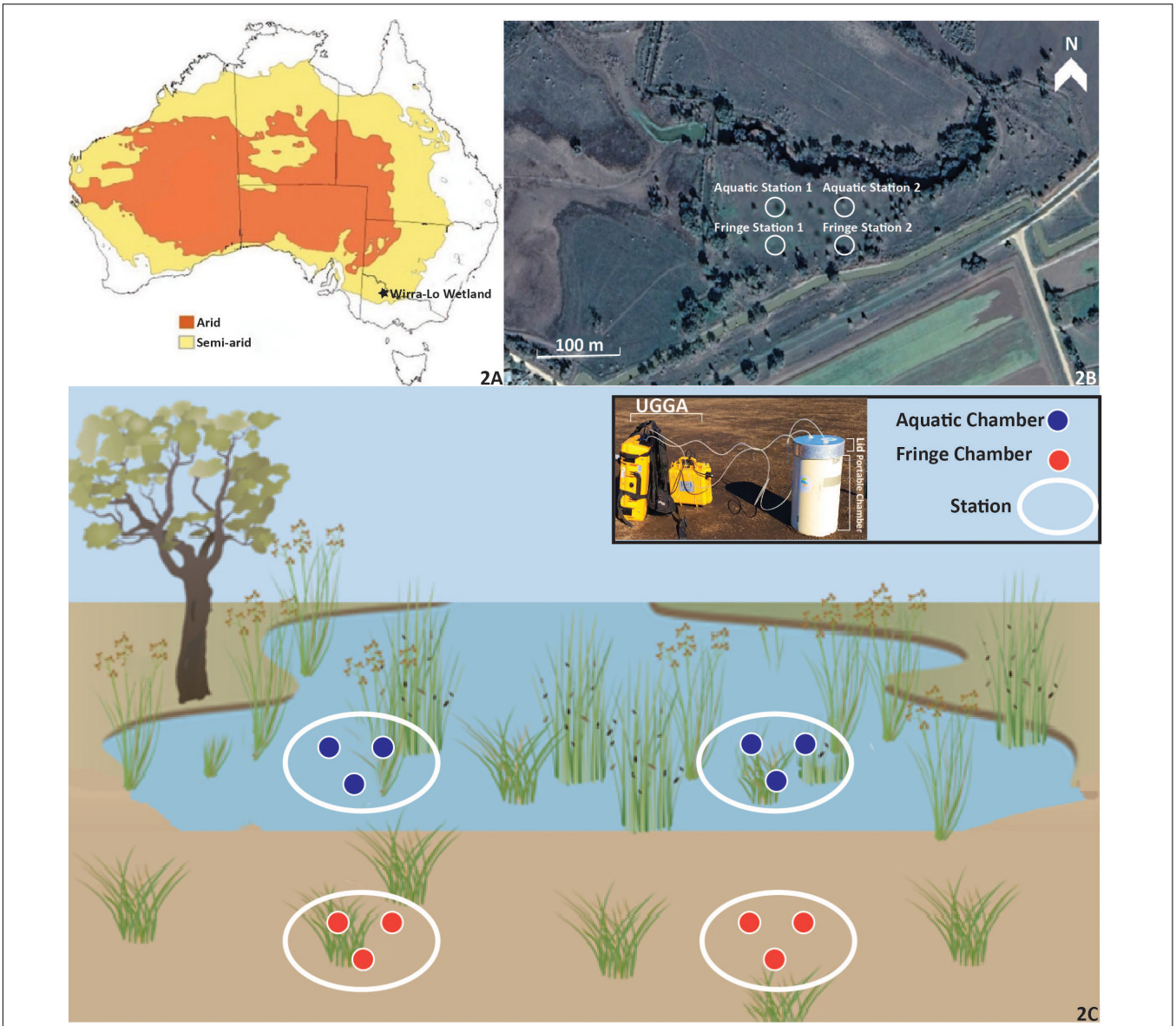

FIGURE 2 | The Wirra-lo wetland complex located in the semi-arid climate of North Central Victoria, Australia (−35.503353, 143.873565). Arid and semi-arid regions of Australia **(A)** are low in annual precipitation (100–500 mm year^{-1}) and experience high evaporation. Duck Creek North **(B)**, a semi-arid floodplain wetland, was measured for carbon emissions within this complex for an entire watering event. The Fringe Zone (samples taken in this zone are shown as orange circles on the edge of the wetland) and Aquatic Zone (samples taken in this zone are shown as blue circles in the inundated portion of the wetland) were identified using wetland delineation techniques (elevation and vegetation type; **C**). Two stations were placed within each zone for further carbon dynamic measurements. Within each of the stations that were nested within each zone, three portable closed-chambers **(C)** were used to measure carbon emissions at Pre, During, Post, and 1 Month phases of environmental watering. The design of each chamber, lid and UGGA used for carbon emission measurements can be seen in the legend of **C**. The water used for the environmental watering event was released from the surrounding irrigation channel. The location of the three chambers within each station can be seen in **B** and **C**. Aquatic Station 1 and 2 and their corresponding chambers were filled with water during the experiment, whereas station and chambers within Fringe Station 1 and 2 remained dry.

autumn months from November to April (17.5 mm month^{-1}, Bureau of Meteorology [BOM], 2017).

Duck Creek North

The wetland investigated in this study is the 3.0 ha semi-arid floodplain wetland Duck Creek North, located at the Wirra-Lo wetland complex (**Figure 2**; −35.503353, 143.873565). The geomorphology of this region is described as the Northern Riverine Plains (Conacher, 2002). The soil in Duck Creek North is composed of a gray silty clay called the Yando Clay, which extends from the soil surface to a depth of 60 m (North Central CMA Report, 2015). Antecedent soil conditions within Duck Creek North were documented to be low in nutrient availability and high in clay content. Total percent phosphorus

was 0.008% and nitrogen levels within sub and topsoil were 0.088% (McKenzie et al., 2000; **Supplementary Table S1**). Soils were primarily clay content (62%) with lower silt and sand content (16 and 22%; **Supplementary Table S1**). Bulk density was 1.5 g cm^{-3} within the subsoil and 1.3 g cm^{-3} in the topsoil. pH levels were slightly basic in the subsoil (7.7) whereas topsoils were slightly acidic (6.6; McKenzie et al., 2000). Encompassing the Wirra-Lo wetland complex are levees intended for crop irrigation and maintaining flood control. During environmental watering events, these levees are opened to allow water into the Wirra-Lo wetland complex. The water for these levees is sourced from the Loddon River.

Prior to European settlement, Duck Creek North would have been regularly inundated due to the close proximity of this wetland to three major waterways (Barr Creek, Loddon River, and Murray River floodplain; Camp Scott Furphy Pty Ltd, 1985; SKM, 2005). In an assessment by the Rakali Ecological Consulting group in 2014, the water regime of the site would have varied between being intermittent and seasonal (Cook, 2014).

Duck Creek North and the surrounding area has been significantly modified since European settlement. The catchment was altered for irrigation; levee banks and roads have disturbed natural flow paths throughout the catchment area (North Central CMA Report, 2015). Artificial levee banks along the major waterways have completely disconnected the complex from flood sources, thus leaving Duck Creek North to only receive flood water in very large (one in 20–50 years) flooding events (North Central CMA Report, 2015). As such, the wetland complex is now largely reliant on the provision of water through the local irrigation system infrastructure (North Central CMA Report, 2015). Duck Creek North received irrigation water and winter precipitation runoff from irrigated pastures within the property as well as from surrounding farms (North Central CMA Report, 2015). By 2006–07, water allocations were significantly reduced and the wetland complex did not receive water until extensive flooding that occurred in January 2011 (North Central CMA Report, 2015). In 2015, a partial watering event (amount of water added was not specified) was implemented in autumn to provide water for stressed river redgum (*Eucalyptus camaldulensis*) trees and aquatic vegetation (North Central CMA Report, 2015). In 2017, from 28 to 30 September, a spring environmental watering event (this study) occurred within Duck Creek North to increase habitat for the growling grass frog (*Litoria raniformis*). Due to the alteration of Duck Creek North's topology by the construction of the surrounding levees, the system is now lotic and has been documented to drain water into the adjacent creek bed within weeks to a couple of months (North Central CMA Report, 2015; observations in the field).

Environmental Watering Measurements

Environmental water from these levees was added to Duck Creek North over 4 days at 10 ML day^{-1}. All measurements occurred during four phases of environmental watering: 2 days of Pre environmental watering, 4 days During environmental watering, 2 days after watering ceased (Post environmental watering), and 2 days after a month from the initial watering date (1 Month). The "Pre" environmental watering (dry) phase measurements were taken before water was released into the wetland. The "During" environmental watering (wetting) phase was identified by the measurements taken while the levee was releasing water into the wetland and water levels were rising in the Aquatic Zone. The "Post" environmental watering (wet) phase was described as the time in which the levee was closed and water levels lowered in Duck Creek North. Finally, the "1 Month" (dry) phase measurements were taken a month after water had left Duck Creek North. During the watering event, dissolved oxygen (DO) measurements were taken using a Hach LDO101 Field Luminescent/Optical DO sensor.

Soil Carbon Analysis

Soil organic carbon content was collected from Duck Creek North before environmental watering and analyzed to determine how much soil organic carbon is currently stored within the wetland, how much soil carbon could potentially be released if further wetland degradation continued, and how this soil could be responsible for variation in fluxes and microbial communities between stations. At each of the four stations, two 4.5 cm (inner-diameter) metal soil cores were hammered into the soil using a petrol-powered corer until a depth of 1 m was reached.

In the laboratory, all soil cores were extruded and sectioned into 5 cm increments from 0 to 20 cm for soil carbon stock calculations. These depths were chosen as an accurate assessment for the amount of soil organic carbon stock and potential carbon flux from the wetland. Soil core samples were then dried at 50°C, measured for dry weight, and used to calculate soil bulk density. Each 5 cm section was then ground to ensure homogeneity of the soil sample using an RM200 Electric Mortar Grinder equipped with a stainless steel mortar and pestle. To determine total organic carbon content for the soil samples, elemental carbon analysis was performed using a EuroVector MicroElemental CN Analyzer. The CN analyzer was equipped with Callidus v.5.1 software. Carbon density (g cm^{-3}) in the top 20 cm of soil was calculated by multiplying the proportion of organic carbon by the dry bulk density value.

CO_2 and CH_4 Flux Measurements

Measurements of CO_2 and CH_4 flux (release and uptake) were taken *in situ* using a Los Gatos ultra-portable greenhouse gas analyzer (UGGA) with a closed-collar dark chamber method (**Figure 2**; Van Huissteden et al., 2011; Musarika et al., 2017). The UGGA reports measurements of CO_2 and CH_4 using cavity enhanced absorption techniques (Baer et al., 2002; Gerardo-Nieto et al., 2019). Each chamber collar (30 cm diameter, 55 cm height, 35 L volume) was made of PVC coupled with a PVC lid. Each chamber was placed over an area with both wetland soil and vegetation to capture total wetland carbon fluxes (Oertel et al., 2016; Ma et al., 2018). Chambers were hammered into the ground (∼1–2 cm) to ensure a complete seal. To avoid altering environmental conditions (i.e., soil and vegetation disturbance) related to inserting the PVC chamber collar into the ground, chambers were installed by inserting them into the wetland soil several hours prior to the initial measurement and remaining in place for the duration of the experiment (Rochette et al., 2011). A small fan powered by a 12 V battery was placed inside the

chamber lid for even air circulation. The PVC lid was connected to the UGGA by two transparent tubes; one taking air to the UGGA and the other delivering it back to the chamber, creating a closed loop. Concentrations of CH_4 and CO_2 were logged by the UGGA every 5 s during 5–10 min intervals on each chamber. The lid was removed when measurements were completed to allow for light and gas exchange to occur within the chamber similar, returning them to ambient environmental conditions (Rochette et al., 2011).

Flux measurements were taken in two zones: the Fringe and the Aquatic Zone (**Figure 2**). The Fringe Zone refers to the edge of the wetland, as identified by higher elevation gradients and a mix of terrestrial and aquatic vegetation. The Aquatic Zone refers to the area located in the lower elevation gradient of the wetland, dominated by aquatic vegetation such as rushes and sedges. Both the fringe and aquatic zones were dominated by graminoid species. A higher abundance of common wallaby grass (*Austrodanthonia caespitosa*) and Spiny Rush (*Juncus acutus*) were found in the aquatic zone whereas pasture grasses and Buckbush (*Salsola tragus*) were abundant in the fringe zone (identified by the Rakali Ecological Consulting group).These zones were chosen due to their influence on the amount and frequency of water received and proximity to terrestrial inputs, both of which may alter wetland carbon fluxes (Altor and Mitsch, 2008; Jimenez et al., 2012).

Two randomly selected stations were nested within each zone to test for spatial variability in response within the wetland. The Aquatic Zone included Aquatic Station 1 and Aquatic Station 2, and the Fringe Zone included Fringe Station 1 and Fringe Station 2. Each station consisted of three 35 L replicate chambers ($n = 12$; **Figure 2**). All measurements occurred during four phases of environmental watering: 2 days of Pre environmental watering, 4 days During environmental watering, 2 days after watering ceased (Post environmental watering), and a month from the Post environmental watering measurements (1 Month). Each day of CO_2 and CH_4 measurements comprised of two sampling times at each collar: once during the day (1–4 pm) and once during the night (3–6 am), to account for any gas flux variation due to light levels (Justine et al., 2015). At each chamber, CH_4 and CO_2 measurements were taken for 5–10 min each.

The regression lines representing carbon fluxes over time were accepted as carbon flux rates from the wetland when the r^2 value was > 0.70 (Repo et al., 2007). Measurements exhibiting negative CO_2 and CH_4 fluxes represent a net uptake (or sequestration) of atmospheric carbon. To prevent a bias toward rapid flux rate measurements, slower flux rates from −0.001 to 0.001 g CH_4 m^{-2} d^{-1} and −0.1 to 0.1 g CO_2 m^{-2} d^{-1} were included in the dataset regardless of their r^2 values. Within this range, r^2 values were limited by the accuracy of the UGGA system and did not necessarily reflect the quality of the measurement (Repo et al., 2007).

CO_2 and CH_4 vary in radiative forcing, which can be represented in measurements of global warming potential (GWP). GWP is a conversion of CH_4 emissions into CO_2 equivalents (CO_2-e) over a projected 20-year period (87 times CO_2), 100-year period (32 times CO_2), or a 500-year period (11 times CO_2). GWP was recently used to calculate the gas pulse decay for global freshwater wetlands over 20 years, to determine whether these systems are net carbon sources or sinks (Neubauer and Megonigal, 2015). To allow for comparison, we also calculated CH_4 flux using the radiative forcing of CO_2-e over a 20-year period (multiplying CH4 emissions by 87).

Microbial DNA Extraction and Bioinformatics

A 60 mL syringe modified with surface (0–1 cm) and subsurface (3–4 cm) sampling ports was used to extract depth-specific soil microbial samples from each aquatic station during each phase, during both the day and night sampling periods (**Figure 2**). The two sampled soil depths (0–1 cm depth and 3–4 cm depth) were homogenized before microbial analysis. Soil microbes were sampled in close proximity (1–2 cm) to the flux collars, to ensure that the microbes accurately corresponded with the carbon emissions for that time period, but so that taking microbial samples themselves would not disturb the soil within the fixed collars. Two cores per aquatic station (two samples per core during the day and night sampling periods) were collected during each environmental watering phase [Pre (22/09/2017), During (28–29/09/2017), Post (01/10/2017), 1 Month (08/11/2017); $n = 4$ per phase]. Pre and 1 Month phases (Pre 1–4 and Mon 1–4) had no water in the wetland whereas During and Post phases (Dur 1–6 and Pos 1–3) were inundated. More samples were taken in the During phase ($n = 6$) as the presence of CH_4 was detected after the initial During phase sampling period. Therefore, extra sampling ensured that bacteria producing CH_4 were captured during this experiment. Samples were placed in vials, stabilized using 1 mL RNA later (Poulos, 2015), and kept cool until the vials could be stored at the laboratory at −80°C.

Due to cost and time constraints, one Aquatic Zone sample per phase of environmental watering was sequenced for identifying soil microbial community composition. A sample in the Post phase was unable to be sequenced ($n = 3$). Genomic DNA was extracted using the Qiagen DNasey PowerSoil kit. The extracted DNA was normalized to 5 ng μL^{-1} prior to performing triplicate PCRs (Caporaso et al., 2012). To ensure DNA extraction and PCR efficiency from each microbial sample, a Qubit fluorometer was used to determine the concentration of nucleic acids after performing each of these steps (**Supplementary Table S2**). Amplification of the 16S rRNA gene was preformed using the 515f–806r primers (Caporaso et al., 2012), with the modified forward primer (Parada et al., 2016). The PCR product was pooled then cleaned with the ZYMO DNA Clean and Concentrator Kit, with modified elution using 10 mM Tris buffer, prior to sequencing on the Illumina MiSeq at Deakin University, Burwood. 16S rRNA amplicon data processing techniques and diversity estimates were performed using the QIIME2 software (Bolyen et al., 2018), while using Divise Amplicon Denoising Algorithm (DADA2) for the bioinformatic analyses (Callahan et al., 2016). In QIIME 2, raw sequence reads went through the process of demultiplexing, sequence quality control, and merging paired-end reads. DADA2 was used to produce amplicon sequence variants (ASVs; Callahan et al., 2016). This algorithm was further used to perform quality control with chimera

detection and elimination, remove sequence errors, singleton exclusion, as well as trimming sequences based on the per-base-pair sequence quality graphs (sequences 25-260 forward, 25-220 reverse). The sequences were then classified against the Greengenes database.

Statistical Analyses

Soil Carbon Stock and Emissions

The flux data from individual collars were analyzed using a repeated measures analysis of variance (ANOVA; IBM SPSS Inc, 2017). The effect of environmental watering on each day's carbon emissions (CO_2 and CH_4) was analyzed by zone, station, and light (day/night) for interactions. To achieve homogeneity of variance among all categorical variables, soil carbon emissions underwent a log transformation prior to statistical analyses. Significance was evaluated at the 0.05 level, and the Bonferroni test was used for comparisons of means between variables. Relationships between each gas flux and environmental parameters, such as air temperature, DO, and water depth, were evaluated using Pearson correlation analyses (IBM SPSS Inc, 2017). A paired sample *t*-test was used to compare soil carbon stock between the Fringe and Aquatic Zones of the wetland ecosystem. When comparing means, a *t*-test adjusted for unequal variance was used when the assumption of equal variances was not satisfied, and the Mann–Whitney *U*-test was used when data were not normally distributed.

Microbial Communities

QIIME2 was used to calculate the alpha diversity indices (ASV richness, Shannon diversity, Faith's phylogenetic diversity, and Pielou's evenness) within each sample across each watering phase and between day/night measurements. A one-way ANOVA was used to compare each diversity indices for each soil sample within the aquatic zones. Varying microbial community structures were analyzed with the weighted UNIFRAC resemblance matrix using q2-diversity beta-group-significance across each phases, station, and between day/night cycles using a two-way (fixed factor) non-parametric permutational multivariate ANOVA (PERMANOVA; **Supplementary Table S3**). Unifrac data were also visualized with a non-metric multi-dimensional scaling (nMDS) plot. A Monte Carlo correction was used for any comparisons with low permutations (<200). SIMPER analyses were performed on the operational taxonomic units (OTUs, 62%) for any significant comparisons, to identify which OTUs were driving the significant differences.

RESULTS AND DISCUSSION

Soil Carbon Density

Soil carbon density prior to watering showed no significant difference between the Aquatic Zone and the Fringe Zone (0.039 ± 0.020 g cm^{-3} $p = 0.475$, 0.038 ± 0.032 g cm^{-3}; $p = 0.259$; **Supplementary Table S4**). This suggests that any potential differences in CO_2 and CH_4 fluxes were not due to the availability of organic carbon in the soil. These soil carbon density values are relatively low, but are in a similar range to those reported for comparable wetland types in semi-arid regions of south-eastern Australia (Carnell et al., 2018). To detect any impacts of environmental watering on soil carbon, we would expect it would take multiple years and multiple watering events, due to the low rates of soil accumulation in wetlands of the region (Carnell et al., 2018). Past studies suggest that further soil analysis [i.e., lead-210 (^{210}Pb) dating to examine sediment accumulation rates) after multiple years of re-wetting may result in significantly higher soil carbon stock within aquatic areas of wetlands. For instance, soil carbon storage in experimental wetlands in Ohio, United States, increased by an average of 14% per year and doubled within the first 10 years, which correlated with increased hydrology and wetland vegetation growth (Bernal and Mitsch, 2013; Waletzko and Mitsch, 2013).

Environmental Watering Succession: Carbon Emissions and Microbial Communities

The impact of wetland drying-rewetting cycles on soil microbial activity, organic matter decomposition, and subsequent carbon emissions (CO_2 and CH_4) have been comprehensively examined (Cosentino et al., 2006; Batson et al., 2015; Nedrich and Burton, 2017). However, research pertaining to the environmental watering management plan in regard of improving degraded freshwater wetland ecosystems has had less attention. Various studies have found that water level fluctuation increases microbial activity and thus carbon emissions through microbial respiration (Fromin et al., 2010; Foulquier et al., 2013). Enhanced soil respiration caused by drying-rewetting cycles potentially releases soil aggregates that were previously unable to be accessed and decomposed by microbes (Moyano et al., 2013; Morillas et al., 2015). As a result, dry and rewetting cycles in freshwater wetlands have been noted to release carbon emissions, SO_4 (sulfide oxidation), and PO_4 (dissolution of iron phosphates) through organic matter decomposition (Venterink et al., 2002; Mikha et al., 2005; Muhr et al., 2010; Baldwin et al., 2013). In this study, we found that drying-rewetting cycles through an entire environmental watering event significantly altered microbial diversity, CO_2 flux, and CH_4 flux (**Supplementary Tables S5, S6**).

Pre Environmental Watering

The degraded wetland conditions of Duck Creek North during the Pre environmental watering phase proved to have the highest release of CO_2 emissions and small levels of CH_4 uptake. CO_2 emissions fluctuated between 6.0 and 9.0 g CO_2 m^{-2} day^{-1}, while there was uptake of CH_4 emissions ranging from -0.03 to -0.1 g CO_2-e m^{-2} day^{-1} (**Table 1**). Prior to environmental watering, there were significantly higher CO_2 emissions during the daylight hours compared to at night (**Figure 3** and **Supplementary Table S7**). CH_4 emissions were inversely correlated with CO_2 emissions during this phase, showing CH_4 emission uptake during the day and a net zero CH_4 flux during the night, throughout each station and zone (**Figure 3**, **Table 1**, and **Supplementary Table S7**).

The higher levels of CO_2 emissions and net CH_4 uptake detected in the Pre environmental watering phase compared

TABLE 1 | Testing the influence of each main factor [zone, light level (day/night), station (zone)] and their interactions against each carbon emission (CO_2 and CH_4) across the environmental watering event.

Effect CO_2 emissions (g CO_2 m^{-2} day^{-1})	Wilks lambda value	*F* statistic	*df*	*P*-value
Time	0.059	18.050	8.0	<0.001
Time * zone	0.191	4.753	8.0	0.016
Time * light level	0.105	9.610	8.0	0.001
Time * station(zone)	0.086	2.710	16.0	0.022
Time * light level * zone	0.182	5.043	8.0	0.013
Time * light level * station (zone)	0.297	0.939	16.0	0.547
Effect of CH_4 (g CO_2-e m^{-2} day^{-1})	**Wilks lambda value**	***F* statistic**	***df***	***P*-value**
Time	0.046	23.218	8.0	<0.001
Time * zone	0.040	27.095	8.0	<0.001
Time * light level	0.196	4.606	8.0	0.017
Time * station(zone)	0.016	7.781	16.0	<0.001
Time * light level * zone	0.145	6.632	8.0	0.005
Time * light level * station (zone)	0.162	1.668	16.0	0.148

The summary of the log-transformed repeated measures ANOVA statistics shows significant differences between Time (days), zone (Fringe and Aquatic), station (nested within the Fringe and Aquatic Zone), and Light levels (day + night sampling periods).

to all other phases presumably occurred due to low soil moisture content from the previously drained wetland conditions of Duck Creek North (North Central CMA Report, 2015). Drained conditions allow for higher potential O_2 penetration within the soil profile that increases aerobic microbial carbon mineralization and subsequent CO_2 emissions (Batson et al., 2015; Evans et al., 2016). Previous research noted that drier soil sediments in a lake produced high CO_2 emissions because stored organic carbon within dry sediments was more susceptible to microbial decomposition processes than in wet sediments (Weise et al., 2016).

There were several taxonomic groups present during the Pre phase that may be responsible for higher CO_2 emissions. In total, soil microbial community sequencing produced a sum of 955,540 sequences from each soil core (day + night within the Aquatic Zone) across all four phases of the environmental watering event (average soil microbial samples had 56,208 sequences; **Supplementary Tables S7, S8**). There were no significant differences in alpha diversity among phase, station and light levels (**Supplementary Table S8**); however, the pairwise PERMANOVA showed that the Pre phase of microbial beta diversity varied significantly from both wet phases (During and Post; **Supplementary Table S9**; *t*-value = 1.848–2.095; $p = 0.002$–0.006). There were no significant differences in microbial beta diversity between light level and aquatic stations. Microbial community structure was not expected to change on the short time scale of hours; however, results from the flux data show that there were likely changes in activity (e.g., increased CO_2 in the day compared to night; **Supplementary Figure S1** and **Supplementary Table S10**). Thus, community changes between light and dark sampling might not be expected. However, the repeated day-night samples provide increased sampling density that could potentially be used to help evaluate within-site variability. The results from this study show a higher relative abundance of *Actinobacteria* and *Oscillatoriophycideae* during dry conditions; both of which have functional traits for soil organic carbon decomposition and subsequent CO_2 emissions (**Figures 4**, **5** and **Table 2**). Past research in boreal and arctic peatlands shows members of the *Actinobacteria* can play a significant contribution to two major parts of the carbon cycle: degradation of complex polymers and decomposition of organic matter (Tveit et al., 2013). *Micromonosporaceae*, a family within *Actinobacteria* found during this phase, have been isolated from habitats including freshwater soil sediments and are composed of species that degrade chitin, cellulose, lignin, and pectin (Wang et al., 2013). *Micromonosporaceae* have also been noted to play an important role in the turnover of organic plant material in a mangrove wetland ecosystem (Wang et al., 2013). *Phormidiaceae* bacteria, a family within *Oscillatoriophycideae*, have been found to provide subsurface carbon and nitrogen by breaking down complex organic matter thus making it more easily available for heterotrophic bacteria consumption in lake ecosystems of Africa (Glaring et al., 2015). The higher relative abundance of these taxonomic groups within the microbial communities during the dry Pre phase may therefore be the contributing to the breakdown of organic matter, resulting in higher CO_2 emissions in this floodplain wetland.

CH_4 uptake in dry soil conditions has been linked to CH_4 oxidation at the aerobic–anaerobic interface in surface soils, as well as the oxygenated area surrounding the roots of wetland plants (Cai et al., 2016), both of which could have been occurring at this phase. Further, microbes within the class *Alphaproteobacteria* were also in high relative abundance during this stage and are known to consist of various methanotrophic bacteria that could be responsible for CH_4 uptake during this period of environmental watering (He et al., 2014; Cai et al., 2016). For instance, there was a higher relative abundance of *Methylocystaceae* (a type II methanotroph family; Nazaries et al., 2013) in this phase, which in part drove the differences between the Pre and dry phases in accordance to the SIMPER analyses (**Table 2**).

The association between higher CO_2 emissions and CH_4 uptake during the day compared to night within Pre environmental watering conditions is likely driven by environmental parameters, such as moisture and temperature. CO_2 and CH_4 emissions in the wetland positively correlate with temperature within the study period ($p < 0.001$; **Supplementary Table S11**). Temperatures throughout this experiment during daylight were 68% higher during the day, averaging 22.4°C, compared to 7.25°C at night (**Supplementary Table S12**). Higher diurnal temperature has been associated with increased aerobic microbial enzymatic activity that further contributes to wetland CO_2 emissions (Lovelock, 2008); however, soil microbial communities were not significantly different between day and night (Pseudo F = 1.793; P-perm 0.080). Past research links diurnal patterns of CH_4 emissions to soil temperature, affecting the rates of activity for CH_4-cycling

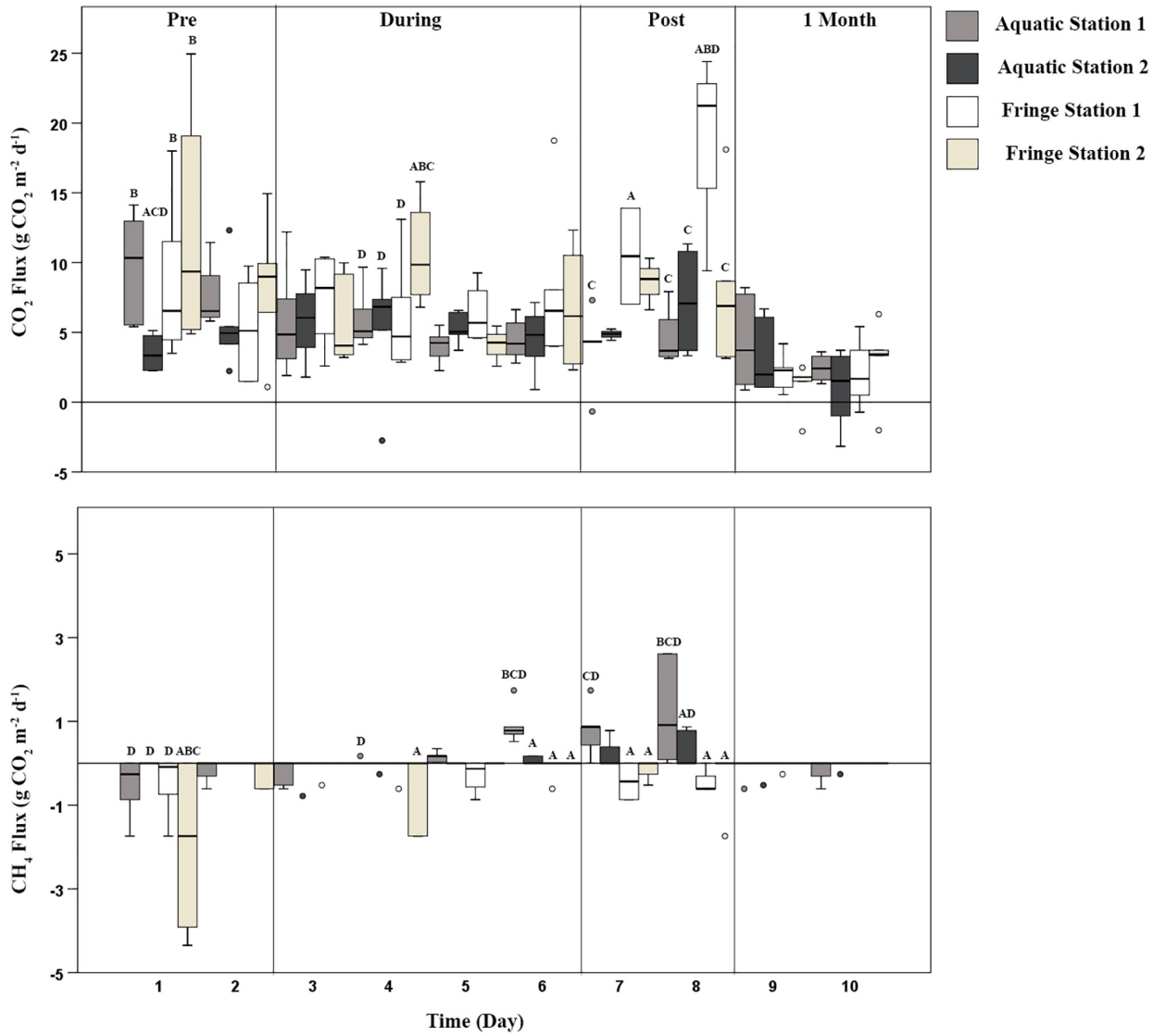

FIGURE 3 | CO_2 (g CO_2 m^{-2} day^{-1}) and CH_4 (g CO_2-e m^{-2} day^{-1}) emissions across the entire watering event. Station significantly altered carbon emissions over time. Time represented the calendar day of measurement (pooled day and night sampling periods). Vertical lines within the figure represent divisions between different phases across time. Pre environmental watering occurred during days 1–2, during environmental watering occurred during days 3–6, post environmental watering occurred during days 7–8, and 1 month after water left the wetland, flux measurements were taken for 2 days (shown here as day 9–10). Two stations were nested within each zone; the Aquatic Station 1 (light gray box), Aquatic Station 2 (darker gray box), Fringe Station 1 (white box), and Fringe Station 2 (light brown box). Letters above bars denote significant variation across each station at that specific time. If Aquatic Station 1 (A), Aquatic Station 2 (B), Fringe Station 1 (C), and Fringe Station 2 (D) were significantly different from one another, the letters corresponding with their significant variation were placed above that station.

bacteria (Le Mer and Roger, 2001; Serrano-Silva et al., 2014). Within Duck Creek North, higher temperatures during the day may have been the reason for the increase in methanotrophic *Methylocystaceae* and subsequent CH_4 uptake (**Table 2** and **Supplementary Table S10**).

During Environmental Watering

The introduction of environmental water played a key role in altering microbial communities and subsequent carbon emissions. Once water was added to the wetland (depths ranging from 27.9–101 mm; **Supplementary Table S12**), the period in which each Aquatic Station was inundated significantly altered CO_2 and CH_4 flux, while Fringe Stations 3 and 4 stayed relatively similar to the Pre watering phase. Aquatic Station 1 received water on day 3; however, there was little to no change in carbon flux until 24 h after inundation (**Figure 3**). These patterns were consistent with Aquatic Station 2, where water arriving during the night of day 5 did not alter CO_2 and CH_4 flux until the night of day 6 (∼24 h after inundation; wetland depth 101 mm; **Supplementary Tables S10, S12**). Similar to the Pre environmental watering phase, daylight CO_2 flux within the "During phase" remained higher in both

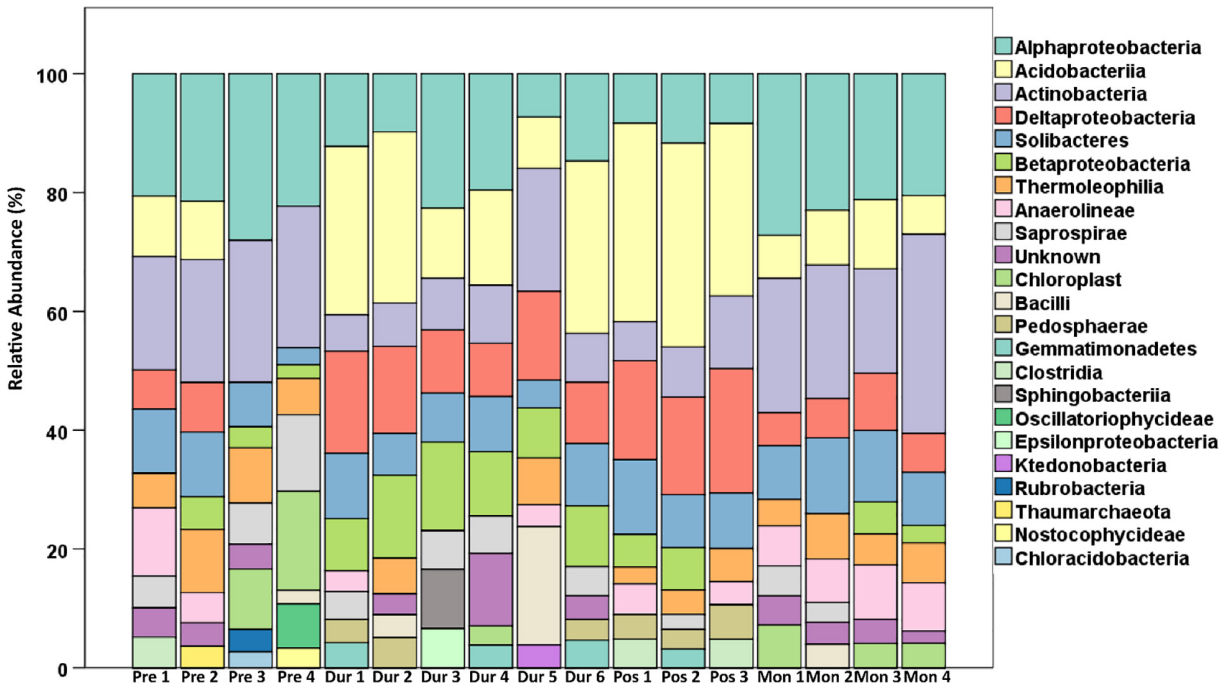

FIGURE 4 | Microbial community composition of the top 10 most abundant classes within each sample. Two soil samples were taken within the Aquatic Zone across day and night sampling for each environmental phase (n = 4 per phase). At the Pre and 1 Month phases (Pre 1–4 and Mon 1–4), there was no water in the wetland, whereas at the During and Post phases (Dur 1–6 and Pos 1–3), soils were inundated. More samples were taken in the During phase (n = 6), as the presence of CH_4 emissions was detected during this phase. Therefore, extra sampling ensured that bacteria producing CH_4 were captured for this experiment. One sample in the Post phase was unable to be sequenced (n = 3).

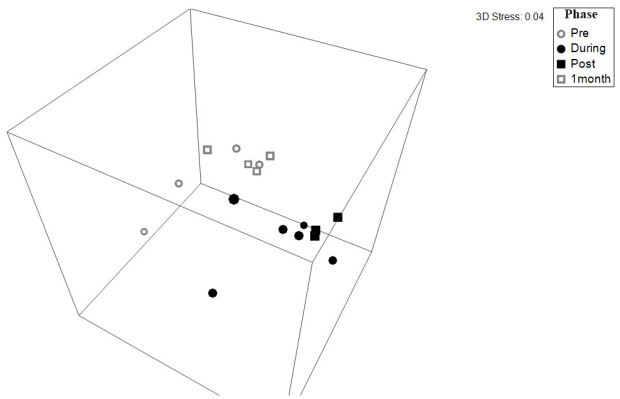

FIGURE 5 | Non-dimensional plot of multidimensional scaling (NMDS) of prokaryotic communities in freshwater wetland soils across each phase of environmental watering, derived from the UNiFRAC matrix of the 16S rRNA gene fragments (stress = 0.04). Points that are closer in the NMDS plot indicate samples with more similar beta-diversity community structure. The pairwise PERMANOVA showed that microbial communities during the "Pre" dry phase (gray) were significantly different from the communities present in the wet phases (black) ($p \leq 0.006$). The 1 Month phase was only marginally insignificant compared to the wet phases ($p \leq 0.081$).

zones compared to night until days 5 and 6 (**Supplementary Figure S1** and **Supplementary Table S10**). After the Aquatic Zone was inundated for more than 24 h at each station, average CO_2 emissions were suppressed by 24%, while average CH_4 emissions doubled compared to Pre environmental watering conditions (**Figure 3** and **Supplementary Table S10**). These results are similar to the 15–49% CH_4 emission increase observed when adding water in reservoirs to an upland boreal forest (Matthews et al., 2005).

The lag in suppressed CO_2 emissions from days 5–6 for both Aquatic Stations could be related to several bacterial families that were suppressed during the wet phases of this experiment, including carbon-degrading *Micromonosporaceae* and *Phormidiaceae* (Wang et al., 2011; Glaring et al., 2015), at the expense of increased relative abundances of *Koribacteraceae* and *Geobacteraceae*. The relative shifts observed in soil microbial communities could be linked to the shifts in metabolic outputs, i.e., fluctuating CO_2 emissions between stations that were nested in the Fringe and Aquatic Zone (**Figure 3**). A similar study investigating microbial responses to inundation in a Victorian floodplain wetland found that leucine aminopeptidase concentrations, an enzyme produced by microbes for carbon degradation, was significantly lower in activity after 1–3 days of inundation (Wilson et al., 2011).

During environmental watering, CO_2 emissions decreased while CH_4 emissions increased, which may be due to the shift between primarily aerobic to primarily anaerobic conditions, thereby also causing a shift in microbial communities and metabolic processes related to CH_4 release (Wilson et al., 2011). Biogeochemical processes influence which microbial

TABLE 2 | The SIMPER table of OTUs driving microbial community differences between phases.

Order/family (class)	Percent (%) average relative abundance			
	Pre v During	**Pre v Post**	**During v 1 Month**	**Post v 1 Month**
Nitrososphaeraceae (*Thaumarchaeota*)	4 v 0.8 (1)	0.04 v 0.01 (1)	0.01 v 0.02 (1)	
Koribacteraceae (*Acidobacteriia*)	1.8 v 13 (7)	0.02 v 0.19 (8)	0.08 v 0.02 (5)	0.15 v 0.02 (7)
Frankiaceae (*Actinobacteria*)	1.6 v 0.05 (2)			
Geodermatophilaceae (*Actinobacteria*)	2.3 v 0.5 (1)	0.01 v 0 (1)	0.003 v 0.02 (1)	
Micromonosporaceae (*Actinobacteria*)	1.2 v 0.04 (1)		<0.001 v 0.01 (1)	
Anaerolinaceae (*Anaerolineae*)	1.4 v 1 (1)	0.02 v 0.01 (1)	0.01 v 0.05 (2)	0.01 v 0.03 (1)
Streptophyta (*Chloroplast*)	4.8 v 1.1 (2)	0.05 v 0.01 (2)		0.01 v 0.006 (1)
Phormidiaceae (*Oscillatoriophycideae*)	0.6 v 0 (1)			
Bacillales (*Bacilli*)	1.4 v 2.3 (1)		0.02 v 0.01 (1)	
Rhodospirillaceae (*Alphaproteobacteria*)	2. 9 v 0.5 (1)	0.04 v 0.01 (2)	0.004 v 0.02 (1)	0.003 v 0.02 (1)
Sphingomonadaceae (*Sphingomonadales*)	2 v 1.2 (1)			
Comamonadaceae (*Betaproteobacteria*)	0.09 v 2 (1)	0.001 v 0.01 (1)	0.02 v 0.003 (1)	
Oxalobacteraceae (*Betaproteobacteria*)	0 v 0.64 (1)			
Myxococcaceae (*Deltaproteobacteria*)	0.09 v 3.5 (2)	0.005 v 0.05 (3)	0.03 v 0.002 (1)	0.04 v 0.004 (3)
Geobacteraceae (*Deltaproteobacteria*)		0.01 v 0.06 (3)	0.005 v 0	0.04 v 0.01 (3)
Kineosporiaceae (*Actinobacteria*)			0.004 v 0.03 (1)	0.005 v 0.03 (1)
Pseudonocardiaceae (*Actinobacteria*)			<0.001 v 0.02 (1)	
Thermomonosporaceae (*Actinobacteria*)			<0.001 v 0.02 (1)	0.005 v 0.02 (1)
Stramenopiles (*Chloroplast*)			<0.001 v 0.01 (1)	0 v0.01 (1)
N1423WL (*Gemmatimonadetes*)			0.006 v 0 (1)	
Acetobacteraceae (*Alphaproteobacteria*)			<0.001 v 0.006 (1)	
Ellin6067 (*Betaproteobacteria*)			0.01 v <0.001 (1)	
Campylobacteraceae (*Epsilonproteobacteria*)			0.005 v 0 (1)	
Acidobacteriaceae (*Acidobacteriia*)				0.006 v 0 (1)
Pseudonocardiaceae (*Actinobacteria*)				0.004 v 0.02 (1)

*The significant pairwise interactions between phases (**Supplementary Table S5**), were each analyzed by SIMPER. The resulting OTUs forming the top 25% cumulative contribution to dissimilarity are presented, collapsed into taxonomic groups with numbers in parentheses showing the number of OTUs within each taxonomic group.*

communities and metabolic processes occur in wetland sediments. Within the surface of the soil profile, aerobic microbial populations gain energy by oxidizing carbon while utilizing O_2 as the terminal electron acceptor (Macreadie et al., 2017; McCloskey et al., 2018). As wetland ecosystems become inundated and wetland soils develop more anoxic zones (due to reduced diffusion of O_2), microbial communities require alternative electron acceptors for respiration processes, which affects carbon mineralization rates (Wiessner et al., 2017). Electron acceptors that are used below the oxic/aerobic interface include nitrogen dioxide (NO_2^-) and nitrate (NO_3^-), followed by nitric oxide (NO) and nitrous oxide (N_2O), oxidized manganese (Mn) compounds, ferric oxides, sulfate (SO_4), and finally CO_2, which results in microbial respiration processes such as fermentation and methanogenesis (Bhaduri et al., 2017). We also saw a relative increase in the abundance and diversity of anaerobic microbial taxa within the soil communities, including *Myxococcaceae*, *Nitrososphaeraceae*, *Koribacteraceae*, *Comamonadaceae*, and *Geobacteraceae*. These taxa suggest that anaerobic microbial respiration processes were involved in fermentation, denitrification, sulfate, and carbon cycling, respectively (Hütsch et al., 2002; King and Weber, 2007; Morita et al., 2011; Zhou et al., 2014; He et al., 2015). Based on the average increase in CH_4 emissions (0.01 ± 0.04 CO_2-e m^{-2} day^{-1}) and decrease in CO_2 emissions (5.18 ± 2.55 g CO_2 m^{-2} day^{-1}) during this phase in the Aquatic Zone compared to Pre environmental watering conditions, we hypothesize that the shift of microbial communities was linked to a decline in redox potential when water was present (i.e., days 5–6; **Supplementary Tables S5, S10**).

Following the probable decrease in redox potential during this phase of environmental watering, *Deltaproteobacteria* became significantly more abundant during the wet phase (**Figure 4** and **Table 2**). These bacteria typically comprised of putative anaerobic bacterial functional groups, such as iron reducers, sulfate reducers, and fermenting bacteria (Rawat et al., 2012). The presence of the *Myxococcaceae* bacterial family suggests the higher potential of sulfate reduction in this wetland ecosystem (Yousefi et al., 2014). Even with the shift to more anaerobic metabolic pathways after watering, methanogenesis was still less competitive than the other pathways. Inhibition of methanogenesis by sulfate reducing bacteria has been documented in wetland ecosystems (Borowski et al., 1996; Valentine and Reeburgh, 2000). Compared to a recent freshwater floodplain wetland study, CH_4 emissions were low in Duck Creek North during high inundation levels, which may be in response to an increased abundance of sulfate reducing bacteria (Batson et al., 2015).

Koribacteraceae also increased in the During phase due their resilient nature in response to fluctuating temperatures (Kielak et al., 2016). A study providing genomic insights into the ecology of *Acidobacteriia* noted the importance of this bacterial class for the turnover of soil organic carbon within damp arctic and boreal environments (Rawat et al., 2012). Furthermore, *Koribacteraceae*, a family of bacteria within the *Acidobacteriia* class, were found to improve conditions for methanogens by providing a carbon substrate through the decay of organic matter, which is required for anaerobic hydrogenotrophic methanogenesis (King and Weber, 2007; Soman et al., 2017). The members within the *Acidobacteriia* bacterial class that were present in both dry and wet phases may be a key group involved in carbon emissions in semi-arid freshwater wetlands, regardless of the inundation level.

Overall, CH_4 fluxes were greater at night during environmental watering across each station and zone (**Figure 3** and **Supplementary Table S10**). The night time peaks averaged 0.006 CH_4 whereas the day CH_4 fluxes averaged −0.01 g CO_2-e m^{-2} day^{-1}, respectively. Drivers of diurnal variation in CH_4 fluxes may be explained by a fluctuation in O_2 levels caused by plant photosynthesis. A study measuring the plant-mediated oxygen supply by wetland vegetation *Phragmites australis* showed significant O_2 declines within the rhizosphere at night (Faußer et al., 2016), thus implying a shift in the aerobic/anaerobic interface to more anaerobic conditions, which better suit methanogenic bacteria (Wagner, 2017). O_2 levels for this experiment were only measured within the water profile; however, patterns during days 3–8 show light DO levels to be 0.5 mg L^{-1} or 40% higher than dark measurements, which may explain the higher CO_2 emissions during those days and higher CH_4 emissions at night during anoxic conditions (**Supplementary Figure S1** and **Supplementary Tables S10, S12**).

Finally, the production of root exudates at night from previous photosynthetic activity during the day may provide labile carbon substrates to methanogens, therefore increasing their CH_4 output at night (Dooling et al., 2018). This slight lag-time of increased root exudates at night compared to the day while vegetation is photosynthesizing has been noted in previous wetland research. For instance, isotopic studies following wetland carbon cycling noted lag times between photosynthate production, root exudates, and finally CH_4 emissions to be between 2 and 24 h depending on the vegetation type (King and Reeburgh, 2002; Ström et al., 2003). A higher abundance in the *Comamonadaceae* family, found in the rhizosphere and specialized to degrade non-aromatic plant exudates (Hütsch et al., 2002), at the "During" phase, further suggests that the decomposition of root exudates increased during this phase. Additional research into the links between wetland vegetative O_2 and root exudates to soil CH_4 emissions is needed to definitively make this connection.

Post Environmental Watering

Carbon flux and microbial communities continued to vary as water receded (averaging 76.8 mm on day 7 and 29.7 mm on day 8; **Supplementary Table S12**) during the Post environmental watering phase. At this phase, increased anoxic conditions due to continual periods of inundation potentially favored methanogenesis and may have resulted in the 46% higher emission rate of CH_4 seen within the Aquatic Zone (0.065 g CO_2-e m^{-2} day^{-1}) compared to the Fringe Zone (−0.035 g CO_2-e m^{-2} day^{-1}). These results are comparable to a past study analyzing marshland soil emission rates under both anoxic (0.007 g CO_2-e day^{-1}) and oxic (0.004 g CO_2-e day^{-1}) conditions that occurred simultaneously with higher counts of methanogenic species and increased CH_4 flux during higher water levels (Wagner, 2017). In this study, CO_2 and CH_4 flux continued to follow a similar pattern within the Aquatic Zone as the water began to leave the floodplain wetland after 2 days. Patterns of higher CO_2 emissions and lower CH_4 emissions during the day compared to night found in the "During" phase also continued throughout the Post environmental watering phase (**Supplementary Figure S1**).

The highest abundance of CH_4 cycling bacteria were present during this phase, including the *Myxococcaceae*, *Nitrososphaeraceae*, *Koribacteraceae*, *Methylocystaceae*, *Hyphomicrobiaceae*, and *Geobacteraceae* families (**Table 2** and **Supplementary Table S13**). *Myxococcaceae*, *Nitrososphaeraceae*, *Methylocystaceae*, and *Hyphomicrobiaceae* microorganisms during this phase may be the reason for a relatively small amount of CH_4 release during the wet phases of this experiment. For instance, anaerobic oxidation of CH_4 occurs when different terminal electron acceptors are used during microbial respiration. *Nitrososphaeraceae* and *Hyphomicrobiaceae* are sulfate and nitrite reducing bacteria thus enhancing the conditions under which anaerobic oxidation can occur (Harrison et al., 2009; Ettwig et al., 2010). However, the presence of *Koribacteraceae* and *Geobacteraceae* bacteria may be the reason for the highest CH_4 release during "Post" environmental watering compared to the other phases of this experiment (**Table 2** and **Supplementary Table S13**). *Geobacteraceae*, for instance, are abundant in areas with aggregates of methanogenic archaea and may enable the rapid conversion of organic matter to CH_4 (Morita et al., 2011). Research shows that *Geobacteraceae* have direct interspecies electron transfer between CH_4-producing *Methanosaetaceae* (Zhang et al., 2017). Although methanogenic microbial communities were not within the top 10 most abundant classes, the highest sequences of methanogenic archaea (*Methanomicrobia* and *Thermoplasmata*) were found within the Post environmental watering phase and may be responsible for the highest CH_4 release at this time period (**Supplementary Table S13**). Despite their low abundance, the microorganisms identified during this phase may play a key role in the carbon flux.

One Month After Environmental Watering

The introduction of environmental water significantly altered the carbon cycling processes in Duck Creek North, even a month after water was last present within the floodplain wetland ecosystem. One month after the water left the floodplain, CO_2 and CH_4 emissions were significantly lower in the Aquatic Zone compared to Pre environmental watering conditions (**Figure 3**, **Supplementary Figure S1**, and **Supplementary Table S6**). Patterns of CO_2 emissions between the different zones and different light levels were not evident at the 1 Month phase;

however, average CH_4 emissions were much lower in the Aquatic Zone compared to the Fringe Zone during this phase (**Figure 3**, **Supplementary Figure S1**, and **Supplementary Table S6**). Lower carbon emissions could be connected with higher plant growth within the Aquatic Zone a month after watering in the degraded wetland ecosystem (**Figure 3**).

The increased vegetation within Duck Creek North at the 1 Month phase has the potential to improve carbon sequestration rates by reducing CO_2 emissions and storing organic carbon matter in plant biomass. Several studies note the importance of wetland plants mediating carbon sequestration processes after restoring vegetative growth. For instance, past research described *Typha* sp. and *Phragmites* sp. dominated wetlands as carbon sinks because these vegetation types photosynthetically assimilated CO_2 from the atmosphere and sequestered this carbon into biomass that eventually became organic matter stored in the wetland soil (Brix, 1993; Rocha et al., 2008; Strachan et al., 2015). Carbon emissions from a restored freshwater wetland were lower in areas with vegetation (3.84 g CO_2-e m^{-2} day^{-1}) compared to areas without vegetation (9.59 g CO_2-e m^{-2} day^{-1}; McNicol et al., 2017). Therefore, lower carbon emissions during the 1 Month phase compared to all other phases of environmental watering may be caused by the increase in vegetation in the aquatic zones of Duck Creek North.

Within Duck Creek North, microbial communities returned to reflect those of the Pre environmental watering phase, suggesting a circular successional change throughout the environmental watering event. The 1 Month phase was not significantly different (t-value 1.569–1.789; p = 0.059–0.081) to the wet phases; however, general trends show similar microbial community abundance between the Pre and 1 Month phases (**Figure 3** and **Table 2**). For instance, relative abundances of *Alphaproteobacteria* and *Actinobacteria* during the Pre and 1 Month phases (5 and 8%; **Table 2**), where higher than *Acidobacteriia* and *Deltaproteobacteria* during the wet phases (10–13% higher; **Figure 3** and **Table 2**).

Despite the overall community succession seen during the environmental watering process, there were several taxonomic groups that were present during the 1 Month phase that were not present prior to watering. During the 1 Month phase, the family *Methylocystaceae* in the *Alphaproteobacteria* class were in higher abundance compared to Pre environmental watering conditions. These *Alphaprotobacteria* have species that are methanotrophs; utilizing methanol or CH_4 as their carbon source (Conrad, 2009). An increase in CH_4 sequestration during the 1 Month phase compared to the other phases of environmental watering may be associated with the increased abundance of *Methylocystaceae* as well as the increase of abundance in *Myxococcaceae* and *Nitrososphaeraceae*. The bacterial class *Actinobacteria* was more abundant in the dry phases, specifically the family *Micromonosporaceae*. Because this microorganism plays an important role in the turnover of organic plant material (Wang et al., 2011), there are implications for higher CO_2 release when they are in higher abundance. However, this bacterial family was less abundant in the 1 Month phase compared to the Pre phase which may be linked with the overall lower CO_2 emissions in the Aquatic Zone and Stations at this time. Bacterial taxa associated with CH_4 cycling, such as *Koribacteraceae* and *Methylocystaceae*, were more abundant in the 1 Month phase compared to the Pre phase. The relative abundance of these bacterial communities was still lower compared to during the wet phases of environmental watering (**Table 2**). Re-wetting has been known to quickly alter microbial abundance in wetland soils (Meisner et al., 2018). However, environmental watering may have permanently altered the microbial community and carbon cycling within this ecosystem, as some community differences were still seen after 1 Month of watering. Further research into the time-frame of microbial community variation would determine the overall effect of environmental watering and carbon emissions.

Global Warming Potential

Pre environmental watering carbon emissions were similar between zones, averaging 6.65 ± 3.67 g CO_2-e m^{-2} day^{-1} in the Aquatic Zone and 8.29 ± 5.73 g CO_2-e m^{-2} day^{-1} in the Fringe Zone. While water was present in the Aquatic Zone in the During and Post environmental watering periods, average carbon emissions decreased and were significantly lower than Pre environmental and Fringe Zone compared to the Aquatic Zone ($p < 0.019$; **Figure 6** and **Supplementary Tables S14, S15**). Past research observed similar patterns of lower carbon emissions when water was present in the aquatic zone of wetland ecosystems (Blodau et al., 2007). Further, the CO_2-e of the Aquatic and Fringe Zone after 1 Month of environmental watering was lower than pre-environmental watering conditions. Increased vegetation after the growing season and subsequent increased carbon sequestration likely caused the overall lower CO_2-e during this phase (Zhou et al., 2009; Pelletier et al., 2015; **Figure 6**). However, the Aquatic zone was still 84% lower in the compared to the Fringe Zone. The underlying drivers of the emissions across each watering event could be related to differing water levels between the zones that influence soil temperature changes, O_2 availability, microbial community composition, and vegetative growth.

Research concerning wetland management for carbon emissions reduction within degraded wetland ecosystems remains unclear as to whether rehabilitation processes, such as environmental watering, improve wetland carbon sequestration, and storage capacity (Morin et al., 2014; Mitsch and Gosselink, 2015). According to the results in this study, Duck Creek North remained a carbon source; however, carbon emissions were significantly reduced after the environmental watering event. Therefore, returning wetland conditions to previous floodplain water levels, in the short term, may reduce the GWP in degraded semi-arid wetlands in Australia. Further, carbon markets allow for carbon credits to be collected for avoided emissions (Vanderklift et al., 2019). The observed average emission reduction of 6.34 to 0.31 within the Aquatic Zone would equate to 22.8 tons of C ha^{-1} $year^{-1}$ or 4.5 car's worth of carbon emissions per ha^{-1} $year^{-1}$ (Vanderklift et al., 2019). Managers would theoretically be able to apply for carbon credits at a rate of $11.90 with a return of $271 ha^{-1} $year^{-1}$ after applying environmental watering practices for carbon emission reduction potential.

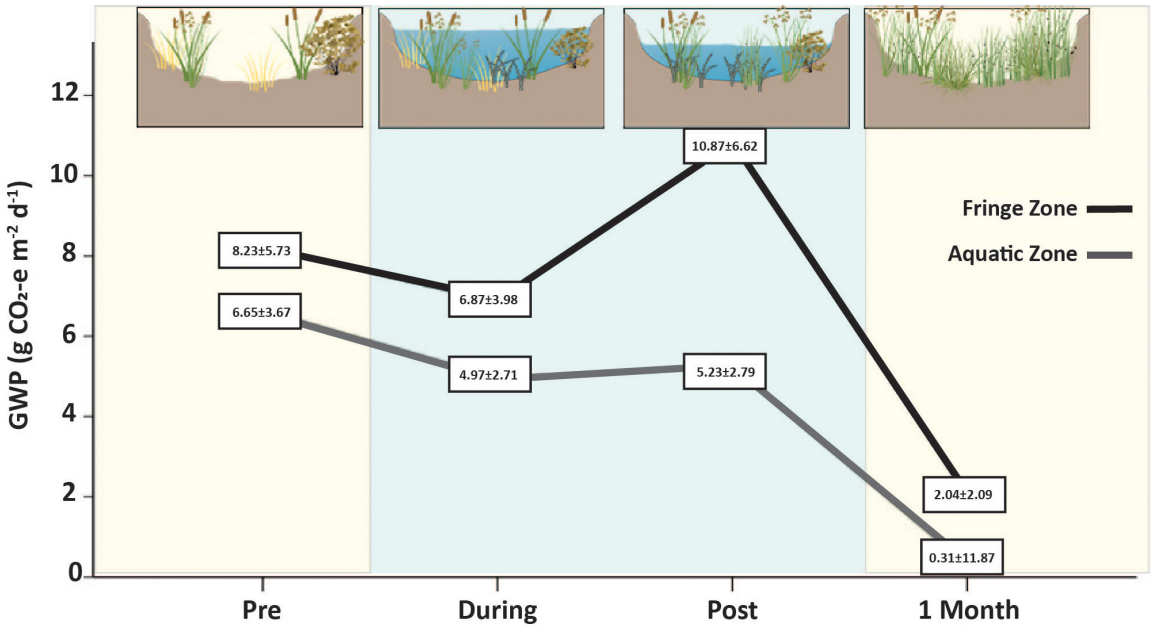

FIGURE 6 | Total carbon emissions/global warming potential (CO_2 + CH_4 g CO_2-e m^{-2} day^{-1}) before (Pre), during (During and Post), and after watering (1 Month). Blue panels signify the presence of water in the wetland ecosystem whereas yellow panels indicate that no water was present at that time. Carbon emissions were 84% lower in the Aquatic Zone (gray line) compared to the Fringe Zone (black line) after the entire watering event. The lower emissions across the entire watering event could be correlated with presence of water in the During and Post phases which altered microbial composition and subsequent carbon emissions in the degraded wetland ecosystem. Higher vegetative growth in the Aquatic Zone compared to the Fringe Zone may have influenced the lower carbon emissions at this time.

Limitations and Future Directions

Continued measurements of carbon stock assessments (i.e., 3–5 years) for this management practice would improve our understanding of the significance of environmental watering for long-term soil carbon storage in low soil carbon accumulation areas of semi-arid Australia. Due to the significant correlation between carbon emissions and temperature in this study, measurements should be taken further into other seasonal watering plans to account for differences of time since inundation, temperature, and day length. The short watering event may have altered this wetland for a longer period of time (i.e., 6, 12, and 18 months) thus, further measurements would capture this change. As the frequency and duration of inundation alters microbial activity and carbon emissions (particularly CH_4 emissions; McComb and Qiu, 1998), further investigation of longer wetting periods should be measured to accurately assess how environmental watering management impacts emission reduction and soil carbon storage in degraded freshwater wetland ecosystems. In this study, temperature and DO were only measured within the water column and at ambient atmospheric levels. Direct measurements of O_2 and temperature within the surface and subsurface soil layers may help further explain the variations of carbon emissions across an entire environmental watering event, as O_2 levels were significantly correlated with CH_4 emissions (**Supplementary Table S11**). Moreover, using targeted functional gene analyses would better link key microbial metabolic functions with greenhouse gas release during various environmental phases (Yarwood, 2018).

CONCLUSION

We found that the environmental watering plan in this semi-arid floodplain wetland lowered carbon emissions while water was present as well as a month after the entire watering event by increasing anoxic conditions and vegetation within the Aquatic Zone of this ecosystem. Environmental watering also significantly altered soil microbial communities, and we hypothesize that the circular succession we detected was linked to shifts in greenhouse gas emissions, thus highlighting the importance of soil microorganisms to wetland management strategies. Changes in diel temperatures and varying water levels could also attribute to altering soil O_2 levels within the wetland, further altering the relative abundance of the microorganisms associated with soil organic carbon breakdown. This research shows that the effect of environmental watering on wetland ecosystem carbon emissions varies according to microclimatic environmental conditions and successive microbial community compositions. Overall, the carbon emission reduction benefits have been gained from the environmental watering program at this wetland ecosystem. Continuing this management practice will likely be required to prevent conditions from returning to Pre environmental watering and to further reduce carbon emissions in Duck Creek North.

Environmental watering is increasingly used for the improvement of water quality, riparian vegetation health, and enhancing fauna habitat and breeding opportunities within

Australian catchments (VEWH 2018–2019). With increasing land-use change, there is greater risk of further loss of wetland carbon storage functionality and associated carbon emissions through wetland degradation. Freshwater wetlands have the ability to provide a sink for the atmospheric carbon pool but if not managed properly, wetlands such as Duck Creek North could become greater sources of CO_2 and CH_4. Difficulties in estimating the net carbon sequestration and storage potential are largely due to the complexity of carbon fluxes and corresponding microorganisms within wetland sediments. This research presents further insights pertaining to soil carbon emission reduction after wetland rehabilitation practices have occurred. These data will be instrumental in conveying efficient strategies for managers and policy makers to applying greenhouse gas emission reduction within semi-arid floodplain wetlands.

DATA AVAILABILITY STATEMENT

This manuscript contains previously unpublished data. The name of the repository and accession number(s) are not available.

AUTHOR CONTRIBUTIONS

KL, PC, ST-T, and PM conceived and planned the experiments. KL, PC, and ST-T carried out the experiments and contributed to the interpretation of the results. KL took the lead in writing the manuscript. All authors provided critical feedback and helped shape the research, analysis, and manuscript.

FUNDING

This research was supported by the North Central Catchment Management Authority, Wimmera Catchment Management Authority, and Deakin University.

ACKNOWLEDGMENTS

Special thanks to Giuditta Bonetti for her assistance with the bioinformatics. We are particularly grateful for the assistance from Sarah Treby and Muvindu Yudhara Liyanapathiranato during data collection and processing.

SUPPLEMENTARY MATERIAL

The Supplementary Material for this article can be found online at: https://www.frontiersin.org/articles/10.3389/fenvs.2020.00008/full#supplementary-material

REFERENCES

Altor, A. E., and Mitsch, W. J. (2008). Methane and carbon dioxide dynamics in wetland mesocosms: effects of hydrology and soils. *Ecol. Appl.* 18, 1307–1320. doi: 10.1890/07-0009.1

Baer, D. S., Paul, J. B., Gupta, M., and O'Keefe, A. (2002). Sensitive absorption measurements in the near-infrared region using off-axis integrated-cavity-output spectroscopy. *Appl. Phys. B* 75, 261–265. doi: 10.1007/s00340-002-0971-z

Baldwin, D. S., Rees, G. N., Wilson, J. S., Colloff, M. J., Whitworth, K. L., Pitman, T. L., et al. (2013). Provisioning of bioavailable carbon between the wet and dry phases in a semi-arid floodplain. *Oecologia* 172, 539–550. doi: 10.1007/s00442-012-2512-8

Batson, J., Noe, G. B., Hupp, C. R., Krauss, K. W., Rybicki, N. B., and Schenk, E. R. (2015). Soil greenhouse gas emissions and carbon budgeting in a short-hydroperiod floodplain wetland. *J. Geophys. Res. G* 120, 77–95. doi: 10.1002/2014JG002817

Bernal, B., and Mitsch, W. J. (2012). Comparing carbon sequestration in temperate freshwater wetland communities. *Glob. Change Biol.* 18, 1636–1647. doi: 10.1111/j.1365-2486.2011.02619.x

Bernal, B., and Mitsch, W. J. (2013). Carbon sequestration in freshwater wetlands in Costa Rica and Botswana. *Biogeochemistry* 115, 77–93. doi: 10.1007/s10533-012-9819-8

Bhaduri, D., Mandal, A., Chakraborty, K., Chatterjee, D., and Dey, R. (2017). Interlinked chemical-biological processes in anoxic waterlogged soil - A review. *Indian J. Agricult. Sci.* 87, 1587–1599.

Blodau, C., Roulet, N. T., Heitmann, T., Stewart, H., Beer, J., Lafleur, P., et al. (2007). Belowground carbon turnover in a temperate ombrotrophic bog. *Glob. Biogeochem. Cycles* 21:GB1021. doi: 10.1029/2005GB002659

Bolyen, E., Rideout, J. R., Dillon, M. R., Bokulich, N. A., Abnet, C., Ghalith, G. A. A. L., et al. (2018). QIIME 2: reproducible, interactive, scalable, and extensible microbiome data science. *PeerJ* 6:e27295v2. doi: 10.7287/peerj.preprints.27295v2

Boon, P. I., Mitchell, A., and Lee, K. (1997). Effects of wetting and drying on methane emissions from ephemeral floodplain wetlands in south-eastern Australia. *Hydrobiologia* 357, 73–87. doi: 10.1023/A:1003126601466

Borowski, W. S., Paull, C. K., and Ussler, W. (1996). Marine pore-water sulfate profiles indicate in situ methane flux from underlying gas hydrate. *Geology* 24, 655–658.

Brix, H. (1993). "Macrophytes-mediated oxygen transfer in wetlands: transport mechanism and rate," in *Constructed Wetlands for Water Quality Improvement*, eds G. A. Moshiri, and A. Arbor (London: Lewis).

Bureau of Meteorology [BOM] (2017). *Average Annual, Seasonal and Monthly Rainfall*. Available at: http://www.bom.gov.au/jsp/ncc/cdio/weatherData/av?p_nccObsCode=136&p_display_type=dailyDataFile&p_startYear=2017&p_c=-1280733113&p_stn_num=080023 (accessed August 20, 2018).

Byrne, M. (2008). Evidence for multiple refugia at different time scales during Pleistocene climatic oscillations in southern Australia inferred from phylogeography. *Q. Sci. Rev.* 27, 2576–2585. doi: 10.1016/j.quascirev.2008.08.032

Cai, Y., Zheng, Y., Bodelier, P. L. E., Conrad, R., and Jia, Z. (2016). Conventional methanotrophs are responsible for atmospheric methane oxidation in paddy soils. *Nat. Commun.* 7:11728. doi: 10.1038/ncomms11728

Callahan, B. J., McMurdie, P. J., Rosen, M. J., Han, A. W., Johnson, A. J. A., and Holmes, S. P. (2016). DADA2: high-resolution sample inference from Illumina amplicon data. *Nat. Methods* 13, 581–583. doi: 10.1038/nmeth.3869<pmid<

Camp Scott Furphy Pty Ltd, (1985). *Camp Scott Furphy Pty Ltd, and Associated Firms. Lower Loddon Flood Plain Management Study: Kerang to Little Murray R. Final Report Volume 1, Report prepared for the Rural Water Commission, Victoria and Lower Loddon Municipalities*. Chatswood: Camp Scott Furphy Pty Ltd.

Caporaso, J. G., Lauber, C. L., Walters, W. A., Berg-Lyons, D., Huntley, J., Fierer, N., et al. (2012). Ultra-high-throughput microbial community analysis on the Illumina HiSeq and MiSeq platforms. *ISME J.* 6, 1621–1624. doi: 10.1038/ismej.2012.8

Carnell, P. E., Windecker, S. M., Brenker, M., Baldock, J., Masque, P., Brunt, K., et al. (2018). Carbon stocks, sequestration, and emissions of wetlands in south eastern Australia. *Glob. Change Biol.* 24, 4173–4184. doi: 10.1111/gcb.14319

Clarke, L., Jiang, K., Akimoto, K., Babiker, M., Blanford, G., Fisher-Vanden, K., et al. (2014). "Assessing transformation pathways," in *Climate Change 2014: Mitigation of Climate Change. Contribution of Working Group III to the Fifth Assessment Report of the Intergovernmental Panel on Climate Change*, eds O. Edenhofer, R. Pichs-Madruga, Y. Sokona, E. Farahani, S. Kadner, K. Seyboth, et al. (Cambridge, MA: Cambridge University Press).

Cole, J. J., Prairie, Y. T., Caraco, N. F., McDowell, W. H., Tranvik, L. J., Striegl, R. G., et al. (2007). Plumbing the global carbon cycle: integrating inland waters into the terrestrial carbon budget. *Ecosystems* 10, 172–185. doi: 10.1007/s10021-006-9013-8

Conacher, A. (2002). A role for geomorphology in integrated catchment management. *Aust. Geogr. Stud.* 40, 179–195. doi: 10.1111/1467-8470.00173

Conrad, R. (2009). The global methane cycle: recent advances in understanding the microbial processes involved. *Environ. Microbiol. Rep.* 1, 285–292. doi: 10.1111/j.1758-2229.2009.00038.x

Cook, D. (2014). *Vegetation Survey, Mapping and Analysis of Wirra-lo Wetland Complex, Benjeroop. A Report Commissioned by the North Central Catchment Management Authority*. Castlemaine: Rakali Ecological Consulting Pty Ltd.

Cosentino, D., Chenu, C., and Le Bissonnais, Y. (2006). Aggregate stability and microbial community dynamics under drying-wetting cycles in a silt loam soil. *Soil Biol. Biochem.* 38, 2053–2062. doi: 10.1016/j.soilbio.2005.12.022

Davidson, N. C. (2014). How much wetland has the world lost? Long-term and recent trends in global wetland area. *Mar. Freshw. Res.* 65, 934–941. doi: 10.1071/MF14173

Denef, K., Six, J., Bossuyt, H., Frey, S. D., Elliott, E. T., Roel, M., et al. (2001). Influence of dry-wet cycles on the interrelationship between aggregate, particulate organic matter, and microbial community dynamics. *Soil Biol. Biochem.* 33, 1599–1611. doi: 10.1016/S0038-0717(01)00076-1

Dooling, G. P., Chapman, P. J., Baird, A. J., Shepherd, M. J., and Kohler, T. (2018). Daytime-Only Measurements Underestimate CH4 Emissions from a Restored Bog. *Ecoscience* 25, 259–270. doi: 10.1080/11956860.2018.1449442

Ettwig, K. F., Butler, M. K., Le Paslier, D., Pelletier, E., Mangenot, S., Kuypers, M. M. M., et al. (2010). Nitrite-driven anaerobic methane oxidation by oxygenic bacteria. *Nature* 464, 543–548. doi: 10.1038/nature08883

Evans, C. D., Renou-Wilson, F., and Strack, M. (2016). The role of waterborne carbon in the greenhouse gas balance of drained and re-wetted peatlands. *Aquatic Sci.* 78, 573–590. doi: 10.1007/s00027-015-0447-y

Faußer, A. C., Dušek, J., Čížková, H., and Kazda, M. (2016). Diurnal dynamics of oxygen and carbon dioxide concentrations in shoots and rhizomes of a perennial in a constructed wetland indicate down-regulation of below ground oxygen consumption. *AOB Plants* 8:lw025. doi: 10.1093/aobpla/plw025

Foulquier, A., Volat, B., Neyra, M., Bornette, G., and Montuelle, B. (2013). Long-term impact of hydrological regime on structure and functions of microbial communities in riverine wetland sediments. *FEMS Microbiol. Ecol.* 85, 211–226. doi: 10.1111/1574-6941.12112

Fromin, N., Pinay, G., Montuelle, B., Landais, D., Ourcival, J. M., Joffre, R., et al. (2010). Impact of seasonal sediment desiccation and rewetting on microbial processes involved in greenhouse gas emissions. *Ecohydrology* 3, 339–348. doi: 10.1002/eco.115

Gerardo-Nieto, O., Vega-Peñaranda, A., Gonzalez-Valencia, R., Alfano-Ojeda, Y., and Thalasso, F. (2019). Continuous measurement of diffusive and ebullitive fluxes of methane in aquatic ecosystems by an open dynamic chamber method. *Environ. Sci. Technol.* 53, 5159–5167. doi: 10.1021/acs.est.9b00425

Glaring, M. A., Vester, J. K., Lylloff, J. E., Al-Soud, W. A., Soørensen, S. J., and Stougaard, P. (2015). Microbial diversity in a permanently cold and alkaline environment in Greenland. *PLoS One* 10:e0124863. doi: 10.1371/journal.pone.0124863

Halverson, L. J., Jones, T. M., and Firestone, M. K. (2000). Release of intracellular solutes by four soil bacteria exposed to dilution stress. *Soil Sci. Soc. Am. J.* 64, 1630–1637. doi: 10.2136/sssaj2000.6451630x

Harrison, B. K., Zhang, H., Berelson, W., and Orphan, V. J. (2009). Variations in archaeal and bacterial diversity associated with the sulfate-methane transition zone in continental margin sediments (Santa Barbara Basin, California). *Appl. Environ. Microbiol.* 75, 1487–1499. doi: 10.1128/AEM.01812-08

He, G. X., Li, K. H., Liu, X. J., Gong, Y. M., and Hu, Y. K. (2014). Fluxes of methane, carbon dioxide and nitrous oxide in an alpine wetland and an alpine grassland of the Tianshan Mountains, China. *J. Arid Land* 6, 717–724. doi: 10.1007/s40333-014-0070-0

He, Z., Geng, S., Cai, C., Liu, S., Liu, Y., Pan, Y., et al. (2015). Anaerobic oxidation of methane coupled to nitrite reduction by Halophilic Marine NC10 bacteria. *Appl. Environ. Microbiol.* 81, 5538–5545. doi: 10.1128/aem.00984-15

Hemes, K. S., Chamberlain, S. D., Eichelmann, E., Knox, S. H., and Baldocchi, D. D. (2018). A biogeochemical compromise: the high methane cost of sequestering carbon in restored Wetlands. *Geophys. Res. Lett.* 45, 6081–6091. doi: 10.1029/2018GL077747

Hütsch, B. W., Augustin, J., and Merbach, W. (2002). Plant rhizodeposition - An important source for carbon turnover in soils. *J. Plant Nutr. Soil Sci.* 165, 479–486. doi: 10.1002/1522-2624(200208)165

Jimenez, K. L., Starr, G., Staudhammer, C. L., Schedlbauer, J. L., Loescher, H. W., Malone, S. L., et al. (2012). Carbon dioxide exchange rates from short- and long-hydroperiod Everglades freshwater marsh. *J. Geophys. Res. G* 117:G04009. doi: 10.1029/2012JG002117

Justine, M. F., Yang, W., Wu, F., Tan, B., Khan, N. M., Zhao, Y., et al. (2015). Biomass stock and carbon sequestration in a chronosequence of Pinus massoniana plantations in the upper reaches of the Yangtze River. *Forests* 6, 3665–3682. doi: 10.3390/f6103665

Kayranli, B., Scholz, M., Mustafa, A., and Hedmark, Å (2010). Carbon storage and fluxes within freshwater wetlands: a critical review. *Wetlands* 30, 111–124. doi: 10.1007/s13157-009-0003-4

Kielak, A. M., Barreto, C. C., Kowalchuk, G. A., van Veen, J. A., and Kuramae, E. E. (2016). The ecology of Acidobacteria: moving beyond genes and genomes. *Front. Microbiol.* 7:744. doi: 10.3389/fmicb.2016.00744

King, G. M., and Weber, C. F. (2007). Distribution, diversity and ecology of aerobic CO-oxidizing bacteria. *Nat. Rev. Microbiol.* 5, 107–118. doi: 10.1038/nrmicro1595

King, J. Y., and Reeburgh, W. S. (2002). A pulse-labeling experiment to determine the contribution of recent plant photosynthates to net methane emission in arctic wet sedge tundra. *Soil Biol. Biochem.* 34, 173–180. doi: 10.1016/S0038-0717(01)00164-X

Lal, R. (2007). Carbon management in agricultural soils. *Mitigat. Adapt. Strateg. Glob. Change* 12, 303–322. doi: 10.1007/s11027-006-9036-7

Lal, R. (2009). Sequestering atmospheric carbon dioxide. *Crit. Rev. Plant Sci.* 28, 90–96. doi: 10.1080/07352680902782711

Le Mer, J., and Roger, P. (2001). Production, oxidation, emission and consumption of methane by soils: a review;[Production, oxydation, emission et consommation de methane par les sols: revue]. *Eur. J. Soil Biol.* 37, 25–50. doi: 10.1016/s1164-5563(01)01067-6

Limpens, J., Berendse, F., Blodau, C., Canadell, J. G., Freeman, C., Holden, J., et al. (2008). Peatlands and the carbon cycle: from local processes to global implications - a synthesis. *Biogeosciences* 5, 1379–1419. doi: 10.5194/bgd-5-1379-2008

Lovelock, C. E. (2008). Soil respiration and belowground carbon allocation in mangrove forests. *Ecosystems* 11:342. doi: 10.1007/s10021-008-9125-4

Ma, W., Alhassan, A. R. M., Wang, Y., and Xhao, J. (2018). Greenhouse gas emissions as influenced by wetland vegetation degradation along a moisture gradient on the eastern Qinghai-Tibet Plateau of North-West China. *Nutr. Cycl. Agroecosyst.* 112, 335–354. doi: 10.1007/s10705-018-9950-6

Macreadie, P. I., Nielsen, D. A., Kelleway, J. J., Atwood, T. B., Seymour, J. R., Petrou, K. C., et al. (2017). Can we manage coastal ecosystems to sequester more blue carbon? *Front. Ecol. Environ.* 15:206–213. doi: 10.1002/fee.1484

Matthews, C. J. D., Joyce, E. M., St. Louis , V. L., Schiff, S. L., Venkiteswaran, J. J., Hall, B. D., et al. (2005). Carbon dioxide and methane production in small reservoirs flooding upland boreal forest. *Ecosystems* 8:267. doi: 10.1007/s10021-005-0005-x

McCloskey, T. A., Smith, C. G., Liu, K. B., Marot, M., and Haller, C. (2018). How could a freshwater swamp produce a chemical signature characteristic of a Saltmarsh? *ACS Earth Space Chem.* 1, 9–20. doi: 10.1021/acsearthspacechem.7b00098

McComb, A., and Qiu, S. (1998). "The effects of drying and reflooding on nutrient release from wetland sediments," in *Wetlands in a Dry Land: Understanding for Management*, ed. W. D. Williams (Canberra: Environment Australia), 147–159.

McKenzie, N. J., Jacquier, D. W., Ashton, L. J., and Cresswell, H. (2000). *Estimation of Soil Properties Using the Atlas of Australian Soils*. Technical Report 11/00, CSIRO Land and Water, Canberra, ACT.

McNicol, G., Sturtevant, C. S., Knox, S. H., Dronova, I., Baldocchi, D. D., and Silver, W. L. (2017). Effects of seasonality, transport pathway, and spatial structure on greenhouse gas fluxes in a restored wetland. *Glob. Change Biol.* 23, 2768–2782. doi: 10.1111/gcb.13580

Meisner, A., Jacquiod, S., Snoek, B. L., Ten Hooven, F. C., and van der Putten, W. H. (2018). Drought legacy effects on the composition of soil fungal and prokaryote communities. *Front. Microbiol.* 9:294. doi: 10.3389/fmicb.2018.00294

Mikha, M. M., Rice, C. W., and Milliken, G. A. (2005). Carbon and nitrogen mineralization as affected by drying and wetting cycles. *Soil Biol. Biochem.* 37, 339–347. doi: 10.1016/j.soilbio.2004.08.003

Miller, A. E., Schimel, J. P., Meixner, T., Sickman, J. O., and Melack, J. M. (2005). Episodic rewetting enhances carbon and nitrogen release from chaparral soils. *Soil Biol. Biochem.* 37, 2195–2204. doi: 10.1016/j.soilbio.2005.03.021

Mitra, S., Wassmann, R., and Vlek, P. L. G. (2005). An appraisal of global wetland area and its organic carbon stock. *Curr. Sci.* 88, 25–35.

Mitsch, W. J., and Gosselink, J. G. (2015). *Wetlands*, 5th Edn. New York, NY: John Wiley and Sons, doi: 10.1017/CBO9781107415324.004

Morillas, L., Durán, J., Rodríguez, A., Roales, J., Gallardo, A., Lovett, G. M., et al. (2015). Nitrogen supply modulates the effect of changes in drying-rewetting frequency on soil C and N cycling and greenhouse gas exchange. *Glob. Change Biol.* 21, 3854–3863. doi: 10.1111/gcb.12956

Morin, T. H., Bohrer, G., Naor-Azrieli, L., Mesi, S., Kenny, W. T., Mitsch, W. J., et al. (2014). The seasonal and diurnal dynamics of methane flux at a created urban wetland. *Ecol. Eng.* 72, 74–83. doi: 10.1016/j.ecoleng.2014.02.002

Morita, M., Malvankar, N. S., Franks, A. E., Summers, Z. M., Giloteaux, L., Rotaru, A. E., et al. (2011). Potential for direct interspecies electron transfer in methanogenic wastewater digester aggregates. *mBio* 2:e00159-11. doi: 10.1128/mBio.00159-11

Moyano, F. E., Manzoni, S., and Chenu, C. (2013). Responses of soil heterotrophic respiration to moisture availability: an exploration of processes and models. *Soil Biol. Biochem.* 59, 72–85. doi: 10.1016/j.soilbio.2013.01.002

Muhr, J., Franke, J., and Borken, W. (2010). Drying-rewetting events reduce C and N losses from a Norway spruce forest floor. *Soil Biol. Biochem.* 42, 1303–1312. doi: 10.1016/j.soilbio.2010.03.024

Musarika, S., Atherton, C. E., Gomersall, T., Wells, M. J., Kaduk, J., Cumming, A. M. J., et al. (2017). Effect of water table management and elevated CO_2 on radish productivity and on CH_4 and CO_2 fluxes from peatlands converted to agriculture. *Sci. Total Environ.* 58, 665–672. doi: 10.1016/j.scitotenv.2017.01.094

Nahlik, A. M., and Fennessy, M. S. (2016). Carbon storage in US wetlands. *Nat. Commun.* 7:13835. doi: 10.1038/ncomms13835

Nahlik, A. M., and Mitsch, W. J. (2011). Methane emissions from tropical freshwater wetlands located in different climatic zones of Costa Rica. *Glob. Change Biol.* 17, 1321–1334. doi: 10.1111/j.1365-2486.2010.02190.x

National Water Commission, (2008). *Australian Water Market Report 2007-2008*. Canberra: National Water Commission.

Nazaries, L., Murrell, J. C., Millard, P., Baggs, L., and Singh, B. K. (2013). Methane, microbes and models: fundamental understanding of the soil methane cycle for future predictions. *Environ. Microbiol.* 15, 2395–2417. doi: 10.1111/1462-2920.12149

Nedrich, S. M., and Burton, G. A. (2017). Indirect effects of climate change on zinc cycling in sediments: the role of changing water levels. *Environ. Toxicol. Chem.* 36, 2456–2464. doi: 10.1002/etc.3783

Neubauer, S. C., and Megonigal, J. P. (2015). Moving beyond global warming potentials to quantify the climatic role of ecosystems. *Ecosystems* 674, 67–89. doi: 10.1007/s10021-015-9879-4

North Central CMA Report (2015). *North Central CMA Report*. Available at: http://www.nccma.vic.gov.au/sites/default/files/publicationsnorth_central_cma_annual_report_2014-2015.pdf (accessed August 28, 2018).

Oertel, C., Matschullat, J., Zurba, K., Zimmermann, F., and Erasmi, S. (2016). Greenhouse gas emissions from soils—A review. *Chem. Geochem.* 76, 327–352. doi: 10.1016/j.chemer.2016.04.002

Olefeldt, D., Euskirchen, E. S., Harden, J., Kane, E., McGuire, A. D., Waldrop, M. P., et al. (2017). A decade of boreal rich fen greenhouse gas fluxes in response to natural and experimental water table variability. *Glob. Change Biol.* 23, 2428–2440. doi: 10.1111/gcb.13612

Page, K. L., and Dalal, R. C. (2011). Contribution of natural and drained wetland systems to carbon stocks, CO_2, N_2O, and CH_4 fluxes: an Australian perspective. *Soil Res.* 49, 377–388. doi: 10.1071/SR11024

Parada, A. E., Needham, D. M., and Fuhrman, J. A. (2016). Every base matters: assessing small subunit rRNA primers for marine microbiomes with mock communities, time series and global field samples. *Environ. Microbiol.* 18, 1403–1414. doi: 10.1111/1462-2920.13023

Pearse, A. L., Barton, J. L., Lester, R. E., Zawadzki, A., and Macreadie, P. I. (2018). Soil organic carbon variability in Australian temperate freshwater wetlands. *Limnol. Oceanogr.* 18, 1403–1414. doi: 10.1002/lno.10735

Peel, M. C., Finlayson, B. L., and McMahon, T. A. (2007). Updated world map of the Köppen-Geiger climate classification. *Hydrol. Earth Syst. Sci.* 11, 1633–1644. doi: 10.5194/hess-11-1633-2007

Pelletier, L., Strachan, I. B., Roulet, N. T., and Garneau, M. (2015). Can boreal peatlands with pools be net sinks for CO_2? *Environ. Res. Lett.* 10:035002. doi: 10.1088/1748-9326/10/3/035002

Poulos, B. (2015). *RNAlater Recipe*. Available at: https://www.protocols.io/view/RNAlater-Recipe-c56y9d (accessed May 17, 2019).

Rasilo, T., Hutchins, R. H. S., Ruiz-González, C., and del Giorgio, P. A. (2017). Transport and transformation of soil-derived CO_2, CH_4 and DOC sustain CO_2 supersaturation in small boreal streams. *Sci. Total Environ.* 579, 902–912. doi: 10.1016/j.scitotenv.2016.10.187

Rawat, S. R., Männistö, M. K., Bromberg, Y., and Häggblom, M. M. (2012). Comparative genomic and physiological analysis provides insights into the role of Acidobacteria in organic carbon utilization in Arctic tundra soils. *FEMS Microbiol. Ecol.* 82, 341–355. doi: 10.1111/j.1574-6941.2012.01381.x

Repo, M. E., Huttunen, J. T., Naumov, A. V., Chichulin, A. V., Lapshina, E. D., Bleuten, W., et al. (2007). Release of CO2 and CH4 from small wetland lakes in western Siberia. *Tellus Ser B* 59, 788–796. doi: 10.1111/j.1600-0889.2007.00301.x

Rocha, A. V., Potts, D. L., and Goulden, M. L. (2008). Standing litter as a driver of interannual CO2exchange variability in a freshwater marsh. *J. Geophys. Res.* 113:G04020. doi: 10.1029/2008JG000713

Rochette, P., Ellert, B., Gregorich, E. G., Desjardins, R. L., Patty, E., Lessard, R., et al. (2011). Description of a dynamic closed chamber for measuring soil respiration and its comparison with other techniques. *Can. J. Soil Sci.* 77, 195–203. doi: 10.4141/s96-110

Schimel, D. (2007). Carbon cycle conundrums. *Proc. Natl. Acad. Sci. U.S.A.* 104, 18353–18354. doi: 10.1073/pnas.0709331104

Schimel, J., Balser, T. C., and Wallenstein, M. (2007). Microbial stress-response physiology and its implications for ecosystem function. *Ecology* 88, 1386–1394. doi: 10.1890/06-0219

Segarra, K. E. A., Schubotz, F., Samarkin, V., Yoshinaga, M. Y., Hinrichs, K.-U., Joye, S. B., et al. (2015). High rates of anaerobic methane oxidation in freshwater wetlands reduce potential atmospheric methane emissions. *Nat. Commun.* 6:7477. doi: 10.1038/ncomms8477

Serrano-Silva, N., Sarria-Guzmán, Y., Dendooven, L., and Luna-Guido, M. (2014). Methanogenesis and methanotrophy in soil: a review. *Pedosphere* 24, 291–307. doi: 10.1016/S1002-0160(14)60016-3

SKM, (2005). *Kerang to Little Murray River Floodplain Management Plan: Assessment of options, report prepared for the North Central Catchment Management Authority by Sinclair Knight Merz*. Melbourne: SKM.

Soman, C., Li, D., Wander, M. M., and Kent, A. D. (2017). Long-term fertilizer and crop-rotation treatments differentially affect soil bacterial community structure. *Plant Soil* 413, 145–159. doi: 10.1007/s11104-016-3083-y

IBM SPSS Inc, (2017). *SPSS Statistics for Windows, version 24.0. IBM Corp. Released 2017*. Armonk, NY: IBM Corp.

St. Louis, V. L., Kelly, C. A., Duchemin, É, Rudd, J. M., and Rosenberg, D. M. (2000). Reservoir surfaces as sources of greenhouse gases to the atmosphere: a global estimate. *Bioscience* 50, 766–775.

Strachan, I. B., Nugent, K. A., Crombie, S., and Bonneville, M. C. (2015). Carbon dioxide and methane exchange at a cool-temperate freshwater marsh. *Environ. Res. Lett.* 10:065006. doi: 10.1088/1748-9326/10/6/065006

Strayer, D. L., and Dudgeon, D. (2010). Freshwater biodiversity conservation: recent progress and future challenges. *J. N. Am. Benthol. Soc.* 29, 344–358. doi: 10.1899/08-171.1

Ström, L., Ekberg, A., Mastepanov, M., and Christensen, T. R. (2003). The effect of vascular plants on carbon turnover and methane emissions from a tundra wetland. *Glob. Change Biol.* 9, 1185–1192. doi: 10.1046/j.1365-2486.2003.00655.x

Sun, Z. G., and Liu, J. S. (2007). Development in study of wetland litter decomposition and its responses to global change. *Shengtai Xuebao* 86, 505–512. doi: 10.1189/jlb.0409230

Tveit, A., Schwacke, R., Svenning, M. M., and Urich, T. (2013). Organic carbon transformations in high-Arctic peat soils: key functions and microorganisms. *ISME J.* 7, 299–311. doi: 10.1038/ismej.2012.99

Valentine, D. L., and Reeburgh, W. S. (2000). New perspectives on anaerobic methane oxidation. *Environ. Microbiol.* 2, 477–484. doi: 10.1046/j.1462-2920.2000.00135.x

Van Huissteden, J., Berrittella, C., Parmentier, F. J. W., Mi, Y., Maximov, T. C., and Dolman, A. J. (2011). Methane emissions from permafrost thaw lakes limited by lake drainage. *Nat. Clim. Change* 2, 119–123. doi: 10.1038/nclimate1101

Vanderklift, M. A., Marcos-Martinez, R., Butler, J. R. A., Coleman, M., Lawrence, A., Prislan, H., et al. (2019). Constraints and opportunities for market-based finance for the restoration and protection of blue carbon ecosystems. *Mar. Policy* 107:103429. doi: 10.1016/j.marpol.2019.02.001

Venterink, H. O., Davidsson, T. E., Kiehl, K., and Leonardson, L. (2002). Impact of drying and re-wetting on N, P and K dynamics in a wetland soil. *Plant Soil* 243:119. doi: 10.1023/A:1019993510737

Wagner, D. (2017). Effect of varying soil water potentials on methanogenesis in aerated marshland soils. *Sci. Rep.* 7:14706. doi: 10.1038/s41598-017-14980-y

Waletzko, E. J., and Mitsch, W. J. (2013). The carbon balance of two riverine wetlands fifteen years after their creation. *Wetlands* 33, 989–999. doi: 10.1007/s13157-013-0457-2

Wang, C., Xu, X. X., Qu, Z., Wang, H. L., Lin, H. P., Xie, Q. Y., et al. (2011). Micromonospora rhizosphaerae sp. nov., isolated from mangrove rhizosphere soil. *Int. J. Syst. Evol. Microbiol.* 61(Pt 2), 320–324. doi: 10.1099/ijs.0.020461-0

Wang, X., Song, C., Sun, X., Wang, J., Zhang, X., and Mao, R. (2013). Soil carbon and nitrogen across wetland types in discontinuous permafrost zone of the Xiao Xing'an Mountains, norWang, X., Song, C., Sun, X., Wang, J., Zhang, X., & Mao, R. (2013). Soil carbon and nitrogen across wetland types in discontinuous permafrost. *Catena* 101, 31–37. doi: 10.1016/j.catena.2012.09.007

Weise, L., Ulrich, A., Moreano, K., Gessler, A., Kayler, Z., Steger, K., et al. (2016). Desiccation and rewetting of lake sediments causes enhanced carbon turnover and shifts in microbial community composition. *FEMS Microbiol. Ecol.* 92:fiw035. doi: 10.1093/femsec/fiw035

Wiessner, A., Kuschk, P., Nguyen, P. M., and Müller, J. A. (2017). The sulfur depot in the rhizosphere of a common wetland plant, Juncus effusus, can support long-term dynamics of inorganic sulfur transformations. *Chemosphere* 184, 375–383. doi: 10.1016/j.chemosphere.2017.06.016

Wilson, J. S., and Baldwin, D. S. (2008). Exploring the "Birch effect" in reservoir sediments: influence of inundation history on aerobic nutrient release. *Chem. Ecol.* 24, 379–386. doi: 10.1080/02757540802497582

Wilson, J. S., Baldwin, D. S., Rees, G. N., and Wilson, B. P. (2011). The effects of short-term inundation on carbon dynamics, microbial community structure and microbial activity in floodplain soil. *River Res. Appl.* 27, 213–225. doi: 10.1002/rra.1352

Xiang, S. R., Doyle, A., Holden, P. A., and Schimel, J. P. (2008). Drying and rewetting effects on C and N mineralization and microbial activity in surface and subsurface California grassland soils. *Soil Biol. Biochem.* 40, 2281–2289. doi: 10.1016/j.soilbio.2008.05.004

Yarwood, S. (2018). The role of wetland microorganisms in plant-litter decomposition and soil organic matter formation: a critical review. *Microbiol. Ecol.* 94:fiy175. doi: 10.1093/femsec/fiy175

Yousefi, A., Allahverdi, A., and Hejazi, P. (2014). Accelerated biodegradation of cured cement paste by Thiobacillus species under simulation condition. *Int. Biodeterior. Biodegrad.* 86, 317–326. doi: 10.1016/j.ibiod.2013.10.008

Zhang, S., Chang, J., Lin, C., Pan, Y., Cui, K., Zhang, X., et al. (2017). Enhancement of methanogenesis via direct interspecies electron transfer between Geobacteraceae and Methanosaetaceae conducted by granular activated carbon. *Bioresour. Technol.* 245(Pt A), 132–137. doi: 10.1016/j.biortech.2017.08.111

Zhou, L., Zhou, G., and Jia, Q. (2009). Annual cycle of CO2 exchange over a reed (Phragmites australis) wetland in Northeast China. *Aquatic Bot.* 91, 91–98. doi: 10.1016/j.aquabot.2009.03.002

Zhou, X. W., Li, S. G., Li, W., Jiang, D. M., Han, K., Wu, Z. H., et al. (2014). Myxobacterial community is a predominant and highly diverse bacterial group in soil niches. *Environ. Microbiol. Rep.* 6, 45–56. doi: 10.1111/1758-2229.12107

Zhu, B., van Dijk, G., Fritz, C., Smolders, A. J. P., Pol, A., Jetten, M. S. M., et al. (2012). Anaerobic oxidization of methane in a minerotrophic peatland: enrichment of nitrite-dependent methane-oxidizing bacteria. *Appl. Environ. Microbiol.* 78, 8657–8665. doi: 10.1128/AEM.02102-12

Conflict of Interest: The authors declare that the research was conducted in the absence of any commercial or financial relationships that could be construed as a potential conflict of interest.

frontiers in Environmental Science

ORIGINAL RESEARCH
published: 12 May 2020
doi: 10.3389/fenvs.2020.00048

A Potential Approach for Enhancing Carbon Sequestration During Peatland Restoration Using Low-Cost, Phenolic-Rich Biomass Supplements

Adel Alshehri[1], Christian Dunn[1], Chris Freeman[1], Sandrine Hugron[2], Timothy G. Jones[1] and Line Rochefort[2]**

[1] Bangor Wetlands Group, Wolfson Carbon Capture Laboratories, School of Natural Science, Brambell Building, Bangor University, Bangor, United Kingdom, [2] Peatland Ecology Research Group (PERG), Centre for Northern Studies (CEN), Université Laval, Quebec City, QC, Canada

OPEN ACCESS

Edited by:
Colin McCarter,
University of Toronto Scarborough, Canada

Reviewed by:
Sébastien Gogo,
University of Orléans, France
Bijendra Man Bajracharya,
University of Waterloo, Canada

***Correspondence:**
Chris Freeman
c.freeman@bangor.ac.uk
Line Rochefort
Line.Rochefort@fsaa.ulaval.ca

Specialty section:
This article was submitted to Biogeochemical Dynamics, a section of the journal Frontiers in Environmental Science

Received: 22 May 2019
Accepted: 08 April 2020
Published: 12 May 2020

Citation:
Alshehri A, Dunn C, Freeman C, Hugron S, Jones TG and Rochefort L (2020) A Potential Approach for Enhancing Carbon Sequestration During Peatland Restoration Using Low-Cost, Phenolic-Rich Biomass Supplements. Front. Environ. Sci. 8:48. doi: 10.3389/fenvs.2020.00048

The addition of phenolic compounds to peatland soils has been proposed as a means of enhancing the suppression of enzymes, reducing the rate of organic matter decomposition and increasing below-ground carbon sequestration. This study evaluated the potential of phenolic enrichment as a peatland restoration strategy by adding wood chips from common tree species to peat substrate and determining the impacts on key components of organic matter decomposition and *Sphagnum* growth. All treatments tended to increase the concentration of phenolics and suppress the activities of β-glucosidase (measured as an indicator enzyme that plays a key role in cellulose decomposition), significantly so with the Spruce (*Picea mariana*) and Cedar (*Thuja occidentalis*) wood chips mixed into the peat. All substrate additions to the peat tended to reduce fluxes of carbon dioxide (CO_2) and significantly more so with surface additions of Spruce and Larch (*Larix laricina*) wood chips. The addition of woodchips *per se* had no detrimental effect on *Sphagnum* growth for any of the treatments. These results indicate that through the addition of phenolic compounds to peatlands, it may be possible to inhibit extracellular enzyme activities in order to reduce the flux of CO_2 from soils to the atmosphere. Thus, organic soil conditioning could reduce the carbon footprint for commercial activities such as *Sphagnum* culture.

Keywords: peatlands, phenolics, hydrolase enzymes, carbon dioxide, *Sphagnum* culture, geoengineering

INTRODUCTION

Peatland ecosystems are freshwater wetlands that accumulate partially decomposed organic material derived from decaying plant matter. Globally, peatlands cover 2.84% of the land surface, but the amount of carbon stored as peat is equivalent to 20% of the world's soil carbon and 60% of the carbon currently in the atmosphere (Joosten, 2016; Xu et al., 2018). Peat forms where the water table is close to the ground surface, creating anaerobic conditions in the soil that are unfavorable

for complete decomposition of plant matter. According to the enzymic latch theory (Freeman et al., 2001), the lack of oxygen prevents the enzyme phenol oxidase from breaking down phenolic compounds, which are released into the soil following plant senescence (Northup et al., 1998; Meier et al., 2008). These compounds are inhibitory to hydrolase enzymes (Freeman et al., 1990; Wetzel, 1992; Tejirian and Xu, 2011), the main agents of decomposition in soils; therefore, their suppressed activity causes organic matter to accumulate.

Large areas of peatlands have been disturbed by drainage and land use conversion for urbanization, forestry, agriculture, and peat extraction (Joosten et al., 2016). The lowered water table in degraded peatlands can allow oxygen ingress "opening" the enzymic latch causing these wetlands to lose their ability to sequester carbon and potentially to become net sources of carbon by oxidation of accumulated peat, having important repercussions for climate change (Paul and Clark, 1989; Laine and Minkkinen, 1996; Waddington et al., 2002; Ramchunder et al., 2009). In extreme dry conditions (particularly in aged *Sphagnum* peat), constraints on decomposing communities from poor water availability can become more important than oxygen constraints (Toberman et al., 2008), however leading structural changes in *Sphagnum* communities to potentially become the dominant determinant of decomposition.

Poikilohydric *Sphagnum* plants can maintain waterlogging in surface peat and their tissues also contain an oxopolysaccharide (Painter, 1983) and phenolic compounds (Rasmussen et al., 1995) that suppress soil heterotroph and extracellular enzyme activity (Verhoeven and Toth, 1995; Freeman et al., 2001), thereby impeding decomposition, although the importance of *Sphagnum* solely derived soluble phenolics are being questioned compared to vascular-plant-derived phenolics. Similarly, microorganisms can be manipulated in peatlands by adding inhibitory phenolics, such as is present in woody plants, which have the potential to reduce the rate of decomposition of soil organic matter (SOM) (Freeman et al., 2012; Fenner and Freeman, 2020) by strengthening the enzymic latch mechanism (Freeman et al., 2001). Woody plants are principle producers of polyphenols (Haslam, 1989). Lignin, a complex polyphenol, can ensure long-term recalcitrance in litter and therefore exert control over fine scale decomposition dynamics (Horner et al., 1988).

In this study, we investigated a new approach for potentially enhancing below-ground carbon storage in restored peatlands—the use of phenolic (i.e., vascular-plant-derived lignin) enrichment as a strategy for strengthening the "enzymic latch mechanism" that exerts a strong influence on controls of the rate of decomposition in peatland soils. For example, this can be achieved by (a) strengthening the enzymic latch by either increasing the abundance of phenolic inhibitors or (b) by increasing the amount of C influenced by the enzymic latch (Freeman et al., 2012). In this study, wood chip fragments from three tree species have been selected to test as phenolic inhibitors to promote C sequestration in the peat soil while also determining the impact on *Sphagnum* growth, according to these hypotheses:

- The addition of coniferous wood chips to peat soil will increase the concentration of polyphenolic compounds. The coniferous wood chips selected represent the three most common trees present in peatlands of North America and are thus a low cost source of phenolics.
- The increase in phenolic compounds will lead to lower hydrolase enzyme activities and reduced CO_2 fluxes.

METHODS

Experimental Design and Implementation of Treatments

To test the effect of exogenous phenolic inhibitors on soil decomposition processes and *Sphagnum papillosum* productivity, a completely randomized design experiment with seven treatments was created using peat mesocosms within a greenhouse at Laval University, Quebec, Canada. The treatments tested were as follows: adding wood chips from three locally abundant tree species, Larch (*Larix laricina*), Spruce (*Picea mariana*), and Cedar (*Thuja occidentalis*), which are all common in Northern American peatlands, at the surface of the peat; mixing woodchips from the three same tree species within the top 10 cm of peat; and no amendment of the peat (baseline comparison). For all of the treatments, fresh *S. papillosum* fragments were added on top of the peat substrate. All treatments were repeated five times for a total of 35 experimental units (EUs).

Each EU was a mesocosm (plastic box) measuring 60 × 40 × 36 cm equipped with a perforated drain and pipe to allow the water table to be maintained at the desired level. Each EU was filled with ∼20 cm of bulk fibric peat (von Post: H3–4) collected from a vacuum extracted peatland. The peatland type was a raised bog from a region of lowland Quebec (46°42′N 71°03′W) where ombrotrophic and peat-accumulating conditions arrived as early as 8,000 years ago, with a stable plant community comprising *Sphagnum* mosses, *Chamaedaphne calyculata* and *Picea mariana* (Lavoie et al., 2012). Mature trees from the three species were harvested in another natural peatland of the same ecoregion (46°46′ N, 71°00′ W) and the trunks (without needles) were processed through a wood chipper to produce chips of 1–2 cm diameter. A layer of ∼2 cm of woodchips (corresponding to a dry weight of 500 g) were either spread on top of the peat ("surface" treatments) or mixed with the top 10 cm of peat ("mixed" treatments). *S. papillosum* was hand collected in fragments of ∼10 cm in a natural peatland of the same ecoregion. *Sphagnum* fragments were spread on top of the amended peat in a ratio of 1:10—i.e., 1 m^2 of *Sphagnum* collected in a natural peatland spread over 10 m^2 of the mesocosms. Each mesocosm was watered twice every week with rainwater to maintain the water table at 5–10 cm below the peat surface. Greenhouses conditions were set at 22°C during the day and 18°C during the night with a constant 75% relative humidity and a photoperiod of 15 h. The experiment took place over a 10 month period (July 2013–May 2014).

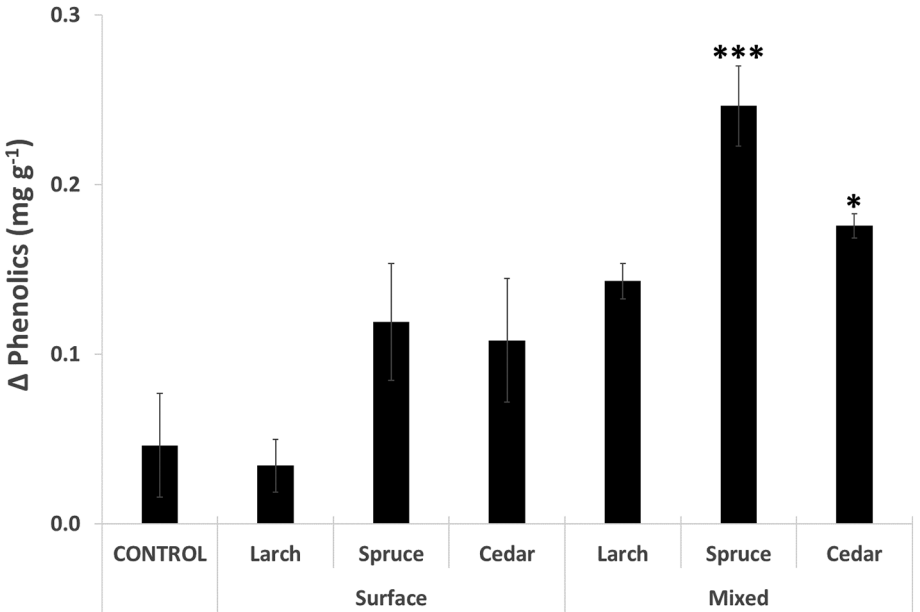

FIGURE 1 | Mean change in concentration of Phenolics over the period September 2013 to July 2014 ($n = 5$). Significance levels: $^{*}p < 0.05$, $^{***}p < 0.001$.

Sampling

Gas flux sampling was carried out using a static headspace technique. The opaque chambers (19 cm height × 13–21 cm width) included a septum for sampling. Each chamber was placed on the peat/*Sphagnum* surface, pressed down gently to create a seal, and sampled after 1 h had elapsed, a time over which headspace CO_2 accumulation remains linear (Freeman et al., 1993). A 20 ml sample of gas was extracted and injected into 12 ml Exetainer vials (Labco, Buckinghamshire, UK). Several samples of air from the greenhouse environment were also collected periodically during the flux analysis to provide the initial background concentration. Soil samples were collected from each EU before and at the end of the experimental period. This was achieved by extracting ∼200 g peat by hand (with plastic gloves) from a depth of 5–10 cm and placing the soil in a sandwich bag, which was then sealed and stored at 4°C. All vials and soil samples were shipped to Bangor University, UK, for analysis.

S. papillosum cover was visually estimated at the end of the experiment. All *Sphagnum* carpets were then collected in each mesocosm, cleaned from any woodchip or peat residues, and weighed for biomass measurements.

Laboratory Analyses

The gas samples collected in the exetainer vials were analyzed using a Varian model 450 gas chromatograph (GC) instrument. The GC system is designed for the analysis of the three main greenhouse gases (CH_4, CO_2, N_2O), being equipped with a methanizer (temperature, 380°C) and flame ionization detector (FID, 125°C) for CO_2 and CH_4 and an electron capture detector (ECD, 300°C) for N_2O. Two milliliters of gas was extracted from the exetainer vials using a CombiPal autosampler (CTC Analytics AG, Zwingen, Switzerland) equipped with a 5 ml syringe and added to the column injector system (100°C). Gases were separated on a 1.83 m × 3.18 mm PoroPak QS 80/100 column (40°C). Oxygen-free nitrogen, at a flowrate of 30 ml min^{-1}, was used as the carrier gas. Gas fluxes were calculated by subtracting the mean values of the greenhouse atmosphere samples from each of the 1 h chamber values and expressing the flux values as mg m^{-2} h^{-1}.

Soil samples were analyzed for conductivity, the concentration of phenolic compounds, and the activity of β-D-glucosidase. Samples were prepared for the analysis of conductivity and phenolics using a water extraction method similar to that described by Chantigny (2003). The soil samples were homogenized, and 5 g was placed in a 50 ml centrifuge tube (Fisher Scientific, Loughborough, UK) with 40 ml of deionized water. The tubes were placed on a KS501 orbital shaker (Ika, Staufen, Germany) at a speed of 300 rpm for 24 h, after which conductivity was measured using a FiveGo conductivity meter (Mettler Toledo, Leicester, UK). Then, the samples were centrifuged at 5,000 rpm for 30 min on a Sorvall ST16R centrifuge (Thermo Fisher, Altricham, UK). The supernatant was filtered through 0.45 μM syringe filters (Phenomenex, Macclesfield, UK) and analyzed for phenolics using a method adapted from Box (1983). One milliliter of the sample, 50 μl of Folin–Ciocalteu phenol reagent (Sigma, Gillingham, UK), and 0.15 ml of Na_2CO_3 (200 g L^{-1}) were added to 1.5-ml microcentrifuge tubes. The process was repeated for calibration standards (0–30 mg L^{-1}) made from phenol (Sigma, Gillingham, UK). After ∼90 min, 300 μl of each sample and standard were transferred to wells of a clear 96-well microplate (Triple Red, Long Crendon, UK), and absorbance was measured at 750 nm on a SpectraMax M2*e* spectrophotometer (Molecular Devices, Wokingham, UK).

Hydrolase enzyme (β-glucosidase) activities were determined by following Dunn et al. (2014). All substrates were obtained from Glycosynth (Warrington, UK), prepared by dissolving in ethylene glycol monomethyl ether (Sigma) and deionized water, and stored at 4°C until required. A standard solution of 1,000 μM 4-methylumbelliferone (MUF)-free acid was prepared using 4-methylumbelliferone sodium salt (Sigma) and a dilution series prepared in 2-ml microcentrifuge tubes in the range of 0–100 μM. Peat soil samples and substrates were placed in an incubator set to the mean temperature of the peat soil in the greenhouses (∼20°C) the day before the assays were undertaken. The peat soil samples were homogenized by hand, and 1 g was placed in six separate stomacher bags (Seward, Worthing, UK), one for each of the five hydrolase enzyme substrates and the standard solution. To each stomacher bag, 7 ml of the appropriate substrate or deionized water (standard solution) was added, and the bags were homogenized in a Stomacher 80 (Seward) for 30 s. The bags were incubated at the mean greenhouse temperature for 60 min (45 min for phosphatase) and 1.5 ml of solution centrifuged at 14,000 rpm. For the substrate solutions, 50 μl of deionized water was pipetted into wells of a 96-well black microplate (Scientific Laboratory Supplies, Yorkshire, UK), followed by 250 μl of supernatant from the substrate bags. For the standards, 50 μl of each MUF-free standard solution was pipetted into the microplate followed by 250 μl of supernatant from the peat/deionized water bag. The microplate was then analyzed by a SpectraMax M2*e* plate, using a fluorescence at 330 nm excitation and 450 nm emission. The instrument creates a calibration curve from the standards to calculate the enzyme concentration of the samples. From these values, the enzyme activities are calculated and expressed as μmol g^{-1} min^{-1}. Peat soil samples were also analyzed for dry weight and organic content by weighing samples in crucibles and following the standard methods detailed in Frogbrook et al. (2009).

Statistical Analyses

First, for the soil parameters, the differential change from 2 to 10 months incubation, thus a period of 8 months, was calculated. The subtraction was made from month 2, rather than month 0, to account for a period of stabilization of the mesocosms following their creation.

The effect of the exogenous phenolic inhibitors on the measured above- and below-ground parameters were determined using the Kruskal-Wallis test for a randomized complete block design and non-normally distributed data. For the soil parameters (conductivity, phenolics, hydrolase enzyme activities, and greenhouse gas fluxes), the analysis was performed in R v3.3.1 and used pairwise comparisons using Dunn's test where significant treatment effects were found. Pearson correlation was used to test for significant relationships between parameters. The effect of the exogenous phenolic inhibitors on *S. papillosum* cover and biomass was analyzed using the MIXED procedure of SAS (SAS Statistical System Software, v. 9.2, SAS Institute Inc., Cary, NC, USA). Following the ANOVAs, protected Fisher's least significant differences (LSDs) were run when a significant difference between treatments was found. Data met the homogeneity and normality assumptions.

RESULTS

Phenolic Content

Over the 10 month incubation period, the concentration of phenolics increased for all 35 EUs, and all but one treatment (Larch, surface) had a higher mean concentration compared to the control (**Figure 1**). There was a significant treatment effect on phenolics ($H = 21.472$, $p < 0.01$), with *post hoc* analysis revealing significantly greater increases in phenolics for the treatments with mixed additions of Spruce (5× greater than control) and Cedar (3.5× greater than control).

Extracellular Hydrolases

In terms of extracellular enzymic activity, the wood chip addition treatments suppressed the activity of the indicator hydrolase enzyme β-glucosidase. The mean activity of the enzyme was lower for all treatments after the 10 month incubation period, with a greater reduction in activity being observed for all six wood chip addition treatments compared to the control (**Figure 2**). There was a significant overall treatment effect ($H = 18.488$, $p < 0.01$), with *post hoc* analysis showing significant reductions in activity for all three mixed wood chip treatments compared to the control. Inversely to the greatest increase in phenolic concentration caused by the Spruce, *mixed* treatment, this same treatment had the greatest suppression of β-glucosidase activity, almost 20× lower compared to the control. The Larch and Cedar mixed wood chip addition treatments reduced the β-glucosidase activity by 5–6× compared to the control.

CO_2

The CO_2 flux data were analyzed in the same way as the phenolic and enzyme data, by calculating the difference from month 2 to 10, to allow time for the soil to stabilize following the initial treatment. The mean CO_2 flux increased slightly in the control treatment with no wood chip additions, but decreased in all of the treatments with wood chips added, with a significant treatment effect (**Figure 3**; $H = 14.26$; $p < 0.05$). *Post hoc* analysis demonstrated that it was the surface and mixed additions of Larch, and surface only addition of Spruce wood chips, that led to statistically significant reductions in the CO_2 flux compared to the control. The initial fluxes of CO_2 showed large spikes and a high degree of variability between the treatments during the initial posttreatment stabilization. This coincided with a period of instrument concerns but may have been a disturbance effect or resulted from an initial flush of labile carbon from the wood chips causing a temporary stimulation of decomposition. There would be some value in further studies of this initial phase with the aim of producing a carbon budget for the entire experiment. CH_4 and N_2O fluxes were also measured, but the variability between and within each treatment was consistently high throughout the experiment, so these data have not been analyzed further.

A significant negative relationship was observed between the mean change in both phenolics concentration and β-glucosidase activity (**Figure 4**; $r = -0.51$, $p < 0.01$).

Vegetation

No significant effect of phenolic enrichment was recorded on *Sphagnum* cover nor biomass. *Sphagnum* productivity was thus

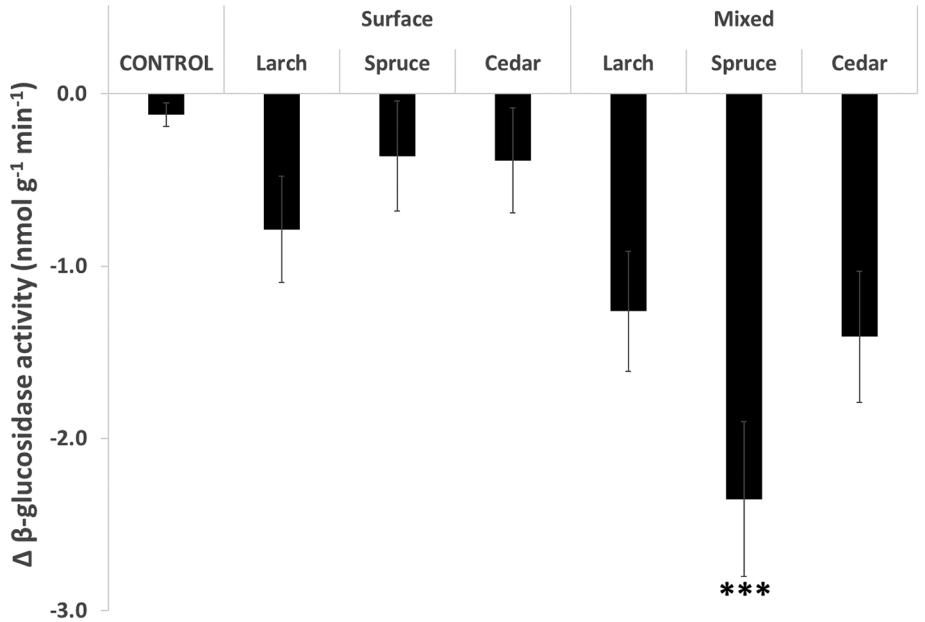

FIGURE 2 | Mean change in activity of β-glucosidase over the period September 2013 to July 2014 ($n = 5$). Significance levels: $^{***}p < 0.001$.

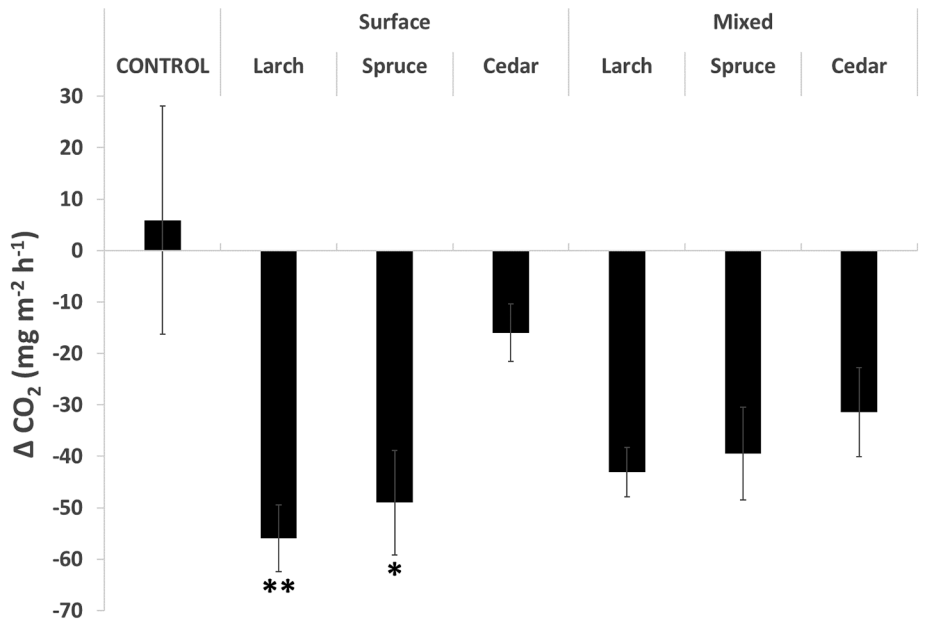

FIGURE 3 | Mean change in CO_2 flux over the period September 2013 to July 2014 ($n = 5$). Significance levels: $^{*}p < 0.05$, $^{**}p < 0.01$.

similar between the control treatment and the treatments with added woodchips.

DISCUSSION

This mesocosm experiment has demonstrated that it is possible to increase the concentration of phenolic compounds and consequently reduce soil enzyme activities and CO_2 emissions during peatland restoration through the addition of exogenous phenolic compounds in the form of wood chips. The work therefore supports proposals in previous studies that phenolic supplements can suppress microbial metabolism and therefore reduce CO_2 fluxes to the atmosphere (Freeman et al., 2012; Fenner and Freeman, 2020), and other studies proposing

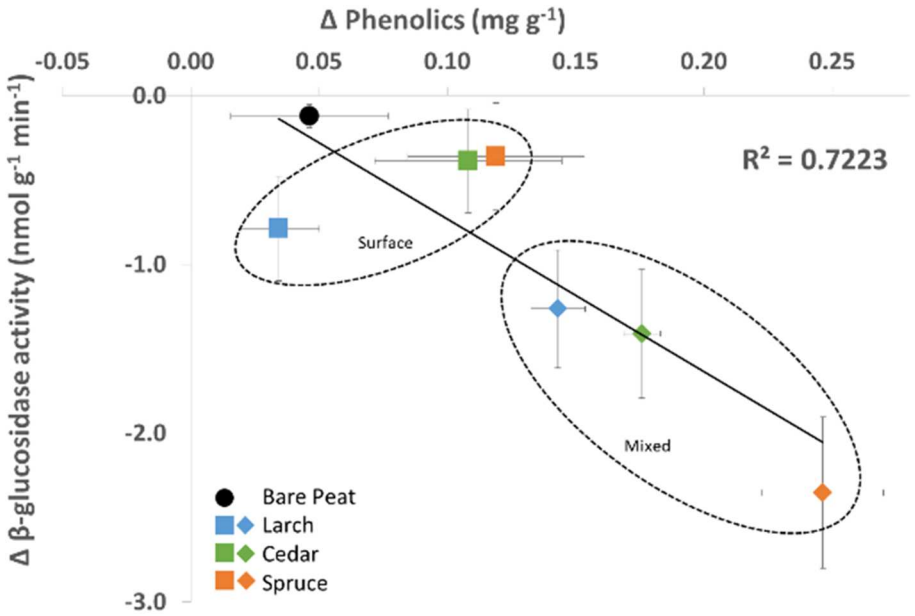

FIGURE 4 | Relationship between mean change in concentration of Phenolics and mean change in β-glucosidase activity over the period September 2013 to July 2014 ($n = 5$).

phenolic content in peat ecosystems can be enhanced by either increased expression of phenolic inhibitors from peatland plants or by enhancement of the enzyme latch by physicochemical modification (Min et al., 2015). However, we acknowledge that the addition of woody materials may initially lead to a short-term increase in CO_2 emissions as any labile materials within that supplement decompose and that there is a risk of temporarily priming decomposition. Clearly, further research would be required (a) to assess this potential risk, (b) to identify sources of wood with minimal labile material content, and (c) to seek further treatments using natural inhibitors that could suppress the metabolism of any labile materials added with the supplements.

The process of mixing the wood chips into the peat profile was found to be particularly effective at increasing phenolics concentration (rather than direct surface application), probably because it increases the surface area of wood chips in contact with soil and causes the dissolved phenolic release from the wood chips to be more widely distributed throughout the soil profile. It should be noted that in terms of *Sphagnum* growth, the presence of woodchips in the soil profile could potentially reduce the availability of water in the capitulum of the plant by reducing the capillary rise of the water to the surface of the peat. The potential detrimental effect of woodchip amendments on upward water movement might be expected to be more important for the surface only added treatment than for the mixed within the surface peat treatment. However, no detrimental effect on *Sphagnum* growth was observed for any of the addition treatments. In this experiment, the presence of woodchips (of any tree species, either at the surface or mixed with the peat) did not impede *Sphagnum* growth, probably because the water table was maintained relatively high (5–10 cm below the surface) and watered twice a week from above simulating regular rain events.

Of the three wood materials used as sources of phenolics, Spruce had the greatest impact in terms of elevating phenolics and suppressing β-glucosidase in the "mixed" treatments only, but Larch had a greater impact more generally in reducing the CO_2 emissions, being effective for both the surface applied and mixed wood chip treatments. Previous laboratory experimental work demonstrated that, on its own, Cedar released ∼3.5 times more phenolics into water than the other two wood types (data not shown); however, in this experiment, it did not significantly decrease β-glucosidase activity or CO_2 emissions and did not increase the phenolics concentration of the peat soil as much as spruce. Clearly, the source of applied phenolics can have a major influence in the success of the approach, and other sources of phenolics should be evaluated for effectiveness. For example, Yoo and Kang (2012) reported that the addition of biochar with high phenolics content could represent a further approach to stabilize soil organic matter (SOM) in terrestrial ecosystems by inhibiting enzyme activities.

CONCLUSION

Our results show that the addition of supplementary phenolic compounds, especially when mixed into the peat soil, is an effective method of enhancing carbon sequestration during peatland restoration, and the enzymic latch might be the reason behind that carbon sequestration. Further research is required including testing the effect of phenolic addition on a larger scale and whether alternative phenolic compounds result in

more inhibition when added to the peat surface or when mixed into the substrate. Longer-term monitoring would also be beneficial, and alternative tree species investigated as a source of wood chips.

DATA AVAILABILITY STATEMENT

All datasets generated for this study are included in the article/supplementary material.

AUTHOR CONTRIBUTIONS

LR and CF conceived the project. CD and LR formulated the experimental design and logistics plan. SH collected field samples. AA conducted the laboratory analysis. AA and TJ analyzed the data and wrote the first draft of the manuscript. All authors contributed to subsequent revisions and refinement of interpretation.

FUNDING

Financial support was provided by the Natural Sciences and Engineering Research Council of Canada (grant no. IRCPJ 282989−2012), the Canadian Sphagnum Peat Moss Association and its members.

ACKNOWLEDGMENTS

We thank Noémie D'Amour and Christiane Dupont for the greenhouse gas and vegetation sampling.

REFERENCES

Box, J. D. (1983). Investigation of the Folin-Ciocalteau phenol reagent for the determination of polyphenolic substances in natural waters. *Water Res.* 17, 511–525. doi: 10.1016/0043-1354(83)90111-2

Chantigny, M. H. (2003). Dissolved and water-extractable organic matter in soils: a review on the influence of land use and management practices. *Geoderma* 113, 357–380. doi: 10.1016/S0016-7061(02)00370-1

Dunn, C., Jones, T. G., Girard, A., and Freeman, C. (2014). Methodologies for extracellular enzyme assays from wetland soils. *Wetlands* 34, 9–17. doi: 10.1007/s13157-013-0475-0

Fenner, N., and Freeman, C. (2020). Woody litter protects carbon stocks during drought. *Nat. Clim. Chang.* 10, 363–369. doi: 10.1038/s41558-020-0727-y

Freeman, C., Fenner, N., and Shirsat, A. H. (2012). Peatland geoengineering: an alternative approach to terrestrial carbon sequestration. *Philos. Trans. R. Soc A* 370, 4404–4421. doi: 10.1098/rsta.2012.0105

Freeman, C., Hawkins, J., Lock, M. A., and Reynolds, B. (1993). "A laboratory perfusion system for the study of biogeochemical responses of wetlands to climatic change." in *Wetlands and Ecotones: Studies on Land-Water Interactions*, eds B. Gopal, A. Hillbricht-Ilkowska, and R. G. Wetzel (New Delhi: National Institute of Ecology), 75–84.

Freeman, C., Lock, M. A., Marxsen, J., and Jones, S. E. (1990). Inhibitory effects of high molecular weight dissolved organic matter upon metabolic processes in biofilms from contrasted rivers and streams. *Freshw. Biol.* 24, 159–166. doi: 10.1111/j.1365-2427.1990.tb00315.x

Freeman, C., Ostle, N., and Kang, H. (2001). An enzymic 'latch' on a global carbon store - a shortage of oxygen locks up carbon in peatlands by restraining a single enzyme. *Nature* 409, 149–149. doi: 10.1038/35051650

Frogbrook, Z. L., Bell, J., Bradley, R. I., Evans, C., Lark, R. M., Reynolds, B., et al. (2009). Quantifying terrestrial carbon stocks: examining the spatial variation in two upland areas in the UK and a comparison to mapped estimates of soil carbon. *Soil Use Manag.* 25, 320–332. doi: 10.1111/j.1475-2743.2009.00232.x

Haslam, E. (1989). *Plant Polyphenols: Vegetable Tannins Revisited*. Cambridge: Cambridge University Press.

Horner, J. D., Gosz, J. R., and Cates, R. G. (1988). The role of carbon-based plant secondary metabolites in decomposition in terrestrial ecosystems. *Am. Nat.* 132, 869–883. doi: 10.1086/284894

Joosten, H. (2016). "Peatlands across the globe," in *Peatland Restoration and Ecosystem Services: Science, Policy and Practice,* eds A. Bonn, T. Allott, M. Evans, H. Joosten, and R. Stoneman (Cambridge: Cambridge University Press), 19–43.

Joosten, H., Sirin, A., Couwenberg, J., Laine, J., and Smith, P. (2016). The role of peatlands in climate regulation. in *Peatland Restoration and Ecosystem Services: Science, Policy and Practice,* eds A. Bonn, T. Allott, M. Evans, H. Joosten, and R. Stoneman (Cambridge: Cambridge University Press), 63–76.

Laine, J., and Minkkinen, K. (1996). Effect of forest drainage on the carbon balance of a mire: a case study. *Scand. J. For. Res.* 11, 307–312. doi: 10.1080/02827589609382940

Lavoie, C., Allard, M., and Duhamel, D. (2012). Deglaciation landforms and C-14 chronology of the Lac Guillaume-Delisle area, eastern Hudson Bay: a report on field evidence. *Geomorphology* s159–160, 142–155. doi: 10.1016/j.geomorph.2012.03.015

Meier, C. L., Suding, K. N., and Bowman, W. D. (2008). Carbon flux from plants to soil: roots are a below-ground source of phenolic secondary compounds in an alpine ecosystem. *J. Ecol.* 96, 421–430. doi: 10.1111/j.1365-2745.2008.01356.x

Min, K., Freeman, C., Kang, H., and Choi, S.-U. (2015). The regulation by phenolic compounds of soil organic matter dynamics under a changing environment. *BioMed Res. Int*. 2015:825098. doi: 10.1155/2015/825098

Northup, R. R., Dahlgren, R. A., and McColl, J. G. (1998). Polyphenols as regulators of plant–litter–soil interactions in northern California's pygmy forest: a positive feedback? *Biogeochemistry* 42, 189–220. doi: 10.1007/978-94-017-2691-7_10

Painter, T. J. (1983). Residues of D-lyxo-5-hexosulopyranuronic acid in Sphagnum holocellulose, and their role in cross-linking. *Carbohydr. Res.* 124, C18–C21. doi: 10.1016/0008-6215(83)88373-6

Paul, E. A., and Clark, F. E. (1989). *Soil Microbiology and Biochemistry*. San Diego, CA: Academic Press Inc.

Ramchunder, S. J., Brown, L. E., and Holden, J. (2009). Environmental effects of drainage, drain-blocking and prescribed vegetation burning in UK upland peatlands. *Prog. Phys. Geogr.* 33, 49–79. doi: 10.1177/0309133309105245

Rasmussen, S., Wolff, C., and Rudolph, H. (1995). Compartmentalization of phenolic constituents in Sphagnum. *Phytochemistry* 38, 35–39. doi: 10.1016/0031-9422(94)00650-I

Tejirian, A., and Xu, F. (2011). Inhibition of enzymatic cellulolysis by phenolic compounds. *Enzyme Microb. Technol.* 48, 239–247. doi: 10.1016/j.enzmictec.2010.11.004

Toberman, H., Freeman, C., Evans, C., Fenner, N., and Artz, R. R. E. (2008). Summer drought decreases soil fungal diversity and associated phenol oxidase activity in upland Calluna heathland soil. *FEMS Microbiol. Ecol.* 66, 426–436 doi: 10.1111/j.1574-6941.2008.00560.x

Verhoeven, J. T. A., and Toth, E. (1995). Decomposition of *Carex* and *Sphagnum* litter in fens: effect of litter quality and inhibition by living tissue homogenates. *Soil Biol. Biochem.* 27, 271–275. doi: 10.1016/0038-0717(94)00183-2

Waddington, J. M., Warner, K. D., and Kennedy, G. W. (2002). Cutover peatlands: a persistent source of atmospheric CO_2. *Global Biogeochem. Cycles* 16:1002. doi: 10.1029/2001GB001398

Wetzel, R. G. (1992). Gradient-dominated ecosystems: sources and regulatory functions of dissolved organic matter in freshwater ecosystems. *Hydrobiologia* 229, 181–198. doi: 10.1007/BF00007000

Xu, J., Morris, P. J., Liu, J., and Holden, J. (2018). PEATMAP: refining estimates of global peatland distribution based on a meta-analysis. *Catena* 160, 134–140. doi: 10.1016/j.catena.2017.09.010

Yoo, G., and Kang, H. (2012). Effects of biochar addition on greenhouse gas emissions and microbial responses in a short-term laboratory experiment. *J. Environ. Qual.* 41, 1193–1202. doi: 10.2134/jeq2011.0157

Conflict of Interest: The authors declare that the research was conducted in the absence of any commercial or financial relationships that could be construed as a potential conflict of interest.

Advantages of publishing in Frontiers

OPEN ACCESS
Articles are free to read for greatest visibility and readership

FAST PUBLICATION
Around 90 days from submission to decision

HIGH QUALITY PEER-REVIEW
Rigorous, collaborative, and constructive peer-review

TRANSPARENT PEER-REVIEW
Editors and reviewers acknowledged by name on published articles

Frontiers
Avenue du Tribunal-Fédéral 34
1005 Lausanne | Switzerland

Visit us: www.frontiersin.org
Contact us: info@frontiersin.org | +41 21 510 17 00

REPRODUCIBILITY OF RESEARCH
Support open data and methods to enhance research reproducibility

DIGITAL PUBLISHING
Articles designed for optimal readership across devices

FOLLOW US
@frontiersin

IMPACT METRICS
Advanced article metrics track visibility across digital media

EXTENSIVE PROMOTION
Marketing and promotion of impactful research

LOOP RESEARCH NETWORK
Our network increases your article's readership